

# **Cell Cultures from Walleye (*Sander vitreus*) for Use in Cell Biology and Virology**

by

**Nguyen Tran Khoi Vo**

A thesis  
presented to the University of Waterloo  
in fulfillment of the  
thesis requirement for the degree of  
Doctor of Philosophy  
in  
Biology

Waterloo, Ontario, Canada, 2014  
© Nguyen Tran Khoi Vo 2014

## **AUTHOR'S DECLARATION**

I hereby declare that I am the sole author of this thesis. This is a true copy of the thesis, including any required final revisions, as accepted by my examiners.

I understand that my thesis may be made electronically available to the public.

## ABSTRACT

This thesis has developed from the walleye, *Sander vitreus* (Mitchill), cell lines (WE) and used them to study viral hemorrhagic septicemia virus (VHSV IVb), which is the causative agent for viral hemorrhagic septicaemia (VHS), and to contribute to the comparative cellular biology and physiology of fish. The outcomes have been organized into six chapters whose major discoveries are abstracted below.

A cell line, WE-cfin11f, with a fibroblast-like morphology was developed from a caudal fin and used to study the intersection of thermobiology of walleye with the thermal requirements for replication of VHSV IVb. WE-cfin11f proliferated from 10 °C to 32 °C and endured as a monolayer for at least a week at 1 °C to 34 °C. WE-cfin11f adopted an epithelial-shape and did not proliferate at 4 °C. Adding VHSV IVb to cultures at 4 °C and 14 °C but not 26 °C led to cytopathic effects (CPE) and virus production. At 4 °C, virus production developed more slowly, but western blotting showed more N protein accumulation. Infecting monolayer cultures at 4 °C for 7 days and then shifting them to 26 °C resulted in the monolayers being broken in small areas by CPE, but with time at 26 °C the monolayers were restored. These results suggest that at 26 °C the VHSV IVb life cycle stages responsible for CPE can be completed but the production of virus and the initiation of infections cannot be accomplished.

A cell line, WE-cfin11e, with an epithelial-like morphology was developed from a caudal fin, characterized as distinct from the fibroblast-like cell line, WE-cfin11f, and compared with WE-cfin11f for susceptibility to VHSV IVb. Immunocytochemistry and confocal microscope were used to localize the intermediate filament protein, vimentin, the tight junction protein, zona occludin (ZO-1), the extracellular matrix protein, collagen I, and the viral protein, G. Although both cell lines contained vimentin, only WE-cfin11e stained for ZO-1 and only WE-cfin11f stained for collagen I. Ascorbic acid increased the accumulation of collagen I and caused the appearance of collagen fibers only in WE-cfin11f cultures. At 14 °C, both cell lines produced VHSV IVb but the infection developed more rapidly in WE-cfin11f. At 4 °C both cell lines became infected with VHSV IVb as judged by the expression of viral proteins, N and G, but only WE-cfin11f produced virus. The results suggest that low temperature can modulate viral tropism.

A cell line, WE-spleen6, has been developed from the stromal layer of primary spleen cell cultures. On conventional plastic, WE-spleen 6 cells had a spindle morphology at low cell density but grew to become epithelial-like at confluency. On the commercial extracellular matrix (ECM), Matrigel, the cells remained spindle shaped and formed lumen-like structures. WE-spleen 6 cells had intermediate filament protein, vimentin and the ECM protein, collagen I, but not smooth muscle  $\alpha$ -actin (SMA) and von Willebrand factor (vWF) and lacked alkaline phosphatase and phagocytic activities. WE-spleen6 was more susceptible to infection with VHSV IVb than a fibroblast cell line from the walleye caudal fin, WE-cfin11f. Viral transcripts and proteins appeared earlier in WE-spleen6 cultures as did cytopathic effect (CPE) and significant virus production. The synthetic double stranded RNA (dsRNA), polyinosinic: polycytidylic acid (pIC), induced the antiviral protein Mx in both cell lines. Treating WE-spleen6 cultures with pIC prior to infection with VHSV IVb inhibited the early accumulation of viral transcripts and proteins and delayed the appearance of CPE and significant viral production. Of particular note, pIC caused the disappearance of viral P protein 2 days post infection. WE-spleen6 should be useful for investigating the impact of VHSV IVb on hematopoietic organs and the actions of pIC on the rhabdovirus life cycle.

A cell line, WEBA, has been developed from the bulbus arteriosus (BA). WEBA produced collagen I, and when held at confluency for days or weeks, spontaneously formed capillary-like tubes. WEBA cells bound fluorescently-labeled *Ulex europaeus* lectin agglutinin I (UEA-1), took up acetylated low density lipoprotein (Ac-LDL), stained for von Willebrand factor (vWF), and produced nitric oxide (NO). The cytoskeleton consisted at least of  $\alpha$ - and  $\beta$ - tubulin, vimentin, and actin, with the actin organized into circumferential bundles. Immunofluorescent staining revealed at least two tight junction proteins, zona occludens -1 (ZO-1) and claudin 3. Together these results suggest that WEBA is an endothelial cell line. Relatively high doses of 2,3, 7,8-tetrachlorodibenzodioxin (TCDD) induced cytochrome P4501A (CYP1A) protein and 7-ethoxyresorufin o-deethylase (EROD) activity in WEBA. As one of the first fish endothelial and BA cell lines, WEBA should be useful in many disciplines in which the teleost cardiovascular system is a focus.

Cell lines and primary cultures from several teleost tissues and species were stained for senescence-associated  $\beta$ -galactosidase (SA  $\beta$ -Gal), revealing four general outcomes. (1) For long-standing fish cell lines that can be considered immortal, little or no SA  $\beta$ -Gal staining was observed, regardless of the culture conditions. (2) For a new walleye cell line from the bulbous arteriosus (WEBA), most cells stained for SA  $\beta$ -Gal even after 40 passages. This suggested that high SA  $\beta$ -Gal activity was a unique property of WEBA, perhaps reflecting their endothelial character, rather than cellular senescence. (3) For cell lines developed from the walleye caudal fin and from somatic cells in rainbow trout coelomic fluid, no SA  $\beta$ -Gal staining was observed in the earliest cultures to over 70 passages later. This suggested that cells from these anatomical sites do not undergo senescence in vitro. (4) By contrast, for cell lines developed from the walleye brain and from somatic cells in rainbow trout milt, most cells in the early stage cultures stained for SA  $\beta$ -Gal, but as these were developed into cell lines, SA  $\beta$ -Gal negative cells became dominant. This suggested that if cellular senescence occurred in vitro, this happened early in these cultures and subsequently a few SA  $\beta$ -Gal negative cells went onto to form the cell line. Overall the presence of SA  $\beta$ -Gal positive cells in cultures could be interpreted in several ways, whereas their absence predicted that in these cultures cells would proliferate indefinitely.

Twenty three cell lines from seven fish species were examined immunocytochemically with the monoclonal antibody (mAb), 6-11B-1, for acetylated  $\alpha$ -tubulin, revealing universal staining of some structures, such as midbodies, but more restricted staining for others, such as primary cilia. The midbody and mitotic spindle stained strongly in all the cell lines. As well as being from two salmonid species, Chinook salmon (*Onchorhynchus tshawytscha*) and rainbow trout (*O. mykiss*), the cell lines were from Pacific herring (*Clupea pallasii*), haddock (*Melanogrammus aeglefinus*), walleye (*Sander vitreus*), fathead minnow (*Pimephales promelas*), and zebrafish (*Danio rerio*). Strong cytoplasmic staining of microtubule networks was observed in only a few cell lines. These were from walleye brain (astroglial-like), spleen (epithelia-like), skin (fibroblastic) and liver (fibroblastic). For the same species, cell lines with an endothelial-like shape from the bulbous arteriosus and epithelial-like shape from the caudal fin and eye retina had no cytoplasmic staining. Primary cilia stained intensely in seven of eight

walleye cell lines and in cell lines from fathead minnow (EPC), zebrafish (ZSSJ), and Pacific herring (PHL). By contrast, few or no primary cilia were observed in cultures of the other twelve cell lines, one from haddock and eleven from salmonids, and in cultures of these cell lines a portion of the cells had weak staining in either the nucleus or cytoplasm. Overall this is the first demonstration of primary cilia in fish cell lines and of cells from a particular taxonomic group, in this case the salmonids, being unable to maintain primary cilia in vitro. In the future, these fish cell lines could be used to study the formation and function of primary cilia, but as well, primary cilia could be a useful marker for characterizing new fish cell lines.

## ACKNOWLEDGEMENTS

This thesis would not have been possible without the following individuals and organizations:

My PhD advisor Dr. Niels C. Bols: Thank you for everything that you have taught me, both in and outside of the lab. Not only are you an esteemed researcher but you are also an incredible human being. I am forever indebted to you for your unparalleled kindness and for your rich decades of scientific knowledge and life experiences. If you read these words, please read my next section because you are also mentioned in its passages.

My former PhD Proposal and Comprehensive Exam committee member and my very first formal academic mentor Dr. Lucy E. J. Lee: Your generosity of giving me the freedom to do literally anything and everything in your laboratory is one of the most precious gifts that I have received to date. Your introduction of me to the art of tissue and cell cultures was the foundation of my doctoral work. Thus this thesis is mine as much as yours. I am utmostly grateful for your continued trust, support, guidance and tolerance of me. Please accept my sincere apologies if I forget any scale bar in my thesis.

My PhD Examining committee members:

Dr. Brian Dixon: I have not officially been a member of your laboratory, at least on the record. But I am grateful to having been treated equally as such. Your “Mi casa es su casa” greeting to me is a dream for every passionate and dedicated graduate student. Thank you for allowing me to participate in your research. I have worked with almost every graduate student in your laboratory during my time at UW, which I consider a blessing. Your continued support will be remembered and greatly appreciated.

Dr. John S. Lumsden (Dept of Pathobiology, OVC, University of Guelph): Thank you for painfully trying to keep up with my demands for more fish and more samples in your laboratory. Your fish pathology knowledge and your guidance throughout my degree are crucial to the completion of my doctoral study.

Dr. James Winton (Western Fisheries Research Center and University of Washington) and Dr. Marc Aucoin (Dept of Chemical Engineering, UW): Thank you for contributing your valuable time and constructive critiques to my thesis.

The past and present Bols and Lee labs' graduate members that I have had the opportunity to know and work with: Dr. Richelle Monaghan: Thank you for your unwavering support and friendship. Your outstanding academic integrity, among many other admirable qualities, is my aspiration. Dr. Marcel Pinheiro: It was pleasant to step into the new lab when everything was ready on the get-go and you made it possible for me. Dr. Phuc Pham: Thank you for your insights, both in and outside of the lab. Dr. Fanxing Zeng: Your genuineness is incredible, seriously! Thank you for sharing your knowledge with me. Sophia Bloch and Robbie Smith: I hope that you are enjoying a new chapter of your life. Ci Chen: Thank you for your help with EROD assays. Billy Martin: Your kind-hearted nature warms my heart. Michael MacLeod: Our mutual friendship was something pleasantly unexpected from my Laurier years but is something I truly value and appreciate. Fates also find themselves in another unexpected precious moment in time when your wedding anniversary also happens to be my birthday. Katelin Spiteri: Knowing that perch and walleye are like cousins, I feel that we share certain strong connections and thank you for introducing me to cheesecakes. Sarah Gignac: There will be ups and downs but I hope that you will have a great time on your PhD journey.

All the past and present undergraduate members of the Bols lab, especially the following individuals lending me their hands and sharing their thoughts with me: Ian Liu, Emily Li, Krista Schleicher, Hina Bandukwala, Patrick Rivers, David VanDelden, Dustin Ammendolia, Aaron Bender, Annie Mak, Eric Kung, Karen Chan, Rodney St. Louis, Jacky Xia, Matt Hass, Patrick Pumputis, Goda Cutajar and Tu Duong + All of the past Lee lab members, especially Mike Mikhaeil. You were my mentees; you are my friends; and I hope that one day we will be colleagues. Thank you for being a good sport and putting up with my daily cheesy song list (“you’ll find us chasing the sun”...) and my spontaneity/craziness. I feel very fortunate and very blessed to know such a select group

of gifted and dedicated students and to have your constant support and your overwhelming interest in my work. Go Walleye!

All the past and present Dixon lab members, for making me feel like the Dixon lab is my second home at UW. Dr. Lital Sever: I honestly do not remember how we met or how everything was started. Everything just happened and the next things I knew were that we were in each other's company everyday, that I spent time watching awesome Avatar episodes and having dinner with your family (Dr. Amit Sever, Noam, Yotam and Neta) and that we have shared publications together. Your impeccable work ethics, contagious passion for research, technical expertise and love for your family are my inspirations.

Members of the Lumsden Lab, especially Dr. Lowia Al-Hussinee and Dr. Alex Reid: Your assistance with walleye care and knowledge is appreciated.

The Faculty and Staff of the Department of Biology at UW for supporting my doctoral research in the forms of Teaching Assistantships and scholarships, enriching my learning day by day and administrative assistance; Graduate Student Associations at UW for Travel grants that allowed me to present my research at (inter)national conferences.

Collaborators & colleagues: Dr. Rob Hanner and Natasha Serrao (U of Guelph), Dr. Niels Lorenzen (Denmark), Dr. Jo-Ann Leong (U.S.A.) and Dr. Theresa Curtis (U.S.A.) for reagents, superior expertise and productive discussions.

NSERC for funding my doctoral research.

My family for their love, trust, care and tolerance of me. My sister, Chi Vo-Quy, and brother, Kha Vo: Thank you for the bond that we share. For this bond that we carry and cherish for the rest of our lives, regardless of the causes and consequences, I hope that we continue listening to and absorbing the wisdom of the elders: “Khôn ngoan đối đáp người ngoài. Gà cùng một mẹ chớ hoài đá nhau” and learn to acquire or continue exercising the act and the power of forgiveness.

## DEDICATION

This thesis is the labour of love and a four-year journey of self-exploration of scientific freedom and self-realization of personal and professional identities. To every purpose, there is an opportunity cost. I have been fortunate enough to have this cost paid for me, both financially and mentally. I am eternally grateful to the following extraordinary individuals, who are my finest teachers and without whom this labor of love and this journey of mine would not have been possible. *[Translation in Vietnamese: Luận án tốt nghiệp Tiến Sĩ này là kết quả của một quá trình lao động cực lực với đầy lòng yêu thương. Luận án này cũng là kết quả của một hành trình dài bốn năm khám phá niềm tự do nghiên cứu khoa học. Mỗi mục đích và mỗi ước mơ đều có một cái giá của riêng nó. Tôi cảm nhận mình thật may mắn vì cái giá mà đáng lý ra bản thân tôi phải tự trả đã được những quý nhân vĩ đại sau đây trả dùm tôi cả về mặt tài chính lẫn cả tinh thần. Đời đời kiếp kiếp này tôi vạn lần biết ơn những tấm gương giáo dục sau đây.]*

In my honest and humble opinion, referring this thesis in its present form to as “labour” perhaps falls a little short from the weight of its meaning. To dedicate this work to the following human extraordinaires, I would like to make it clear, at least in writing, that the work presented here is a modest representation of what I have sought to learn, provoked to question, inspired to tell a story and aspired to accomplish during my doctoral study. *[Translation in Vietnamese: Theo quan điểm trung thực của tôi, so sánh phiên bản hiện tại của luận án tốt nghiệp Tiến Sĩ này với bốn chữ “lao động cực lực” có lẽ hơi thậm xưng. Tôi xin mạn phép được tâm sự là phiên bản này là phiên bản nhỏ bé của những gì tôi học được từ trong phòng thí nghiệm cho đến đường đời. Với vốn liếng và kiến thức như vậy, tôi mới dám mạn phép công hiến luận án tốt nghiệp Tiến Sĩ này cho những quý nhân vĩ đại sau đây.]*

First, I dedicate this labour of love to my parents, Mr. Thang Vo and Mrs. Cuc Thi Thu Tran. You are my rock and you are my light. On behalf of my siblings, I am sincerely sorry but forever thankful for your decades of sacrifice and endurance. Your care is immeasurable. Your love is unconditional. Your kindness, love for your families and

“paying-it-forward” philosophy are your wealth and our guiding lights. Thank you for (quietly) demonstrating to me that forgiveness is the best teacher in this world. My siblings’ lives and mine are forever your gravity debts, which we cannot possibly carry over and pay on your behalf. We can only wish to pay them forward and pass your “debts”/lessons to your grandchildren. For anything in the future that I will do and make you fall ill, I am truly sorry. I promise that these unfortunate events will not take place. But I have faith that, without a heavy heart and a hesitant undivided mind, you did, have and will forgive me, sometimes vocally but usually quietly. Even later in your last breath. And mine. I love you very much. *[Translation in Vietnamese: Đầu tiên, con xin công hiến luận án Tiến Sĩ này cho ba mẹ kính yêu của con: Ông Võ Thắng and Bà Trần Thị Thu Cúc. Ba mẹ là sông, là núi, là hơi thở và là ánh sáng của con. Con xin đại diện chị em con thành thật hối tiếc nhưng mãi mãi biết ơn những năm tháng những thập kỷ chịu đựng và hy sinh của ba mẹ. Sự chăm sóc của ba mẹ không thể đong đếm nổi. Tình thương con của ba mẹ không có sách vở nào viết hết được. Lòng tốt, lòng hiếu thảo, lòng yêu thương với cả hai đại gia đình và triết lý sống tốt và sống có nghĩa thì trời thương là vốn liếng và tài sản của ba mẹ. Những tố chất này cũng là ánh sáng rọi đường của ba mẹ, của chúng con và của những ai thấu hiểu và quý trọng ba mẹ. Con xin cảm ơn ba mẹ đã chứng tỏ cho con thấy tha thứ là bài học hay nhất mà mỗi người chúng ta cần phải học hỏi và tích lũy trong cuộc sống vô thường này. Cuộc đời của chị em con mãi mãi là món nợ không thể trả hết được. Món nợ này cứ như trọng lực: chấp nhận là nó giúp mình thăng bằng để sinh sống, để tồn tại và để đi tiếp, nhưng nó luôn luôn kéo mình xuống bất chấp dù mình có muốn hay không. Chúng con có muốn gánh đỡ món nợ trọng lực của ba mẹ thì cũng không được. Chúng con chỉ có thể kì vọng trao cái gánh nợ này cho các cháu của ba mẹ. Con tin là đây cũng là ước mơ của ba mẹ. Con thương ba mẹ lắm.]*

Second, I dedicate this labour of love to my late, much-missed, much-loved grandfather, or “ông nội” as lovingly called in Vietnamese, Mr. Kiet Vo. I was told that I had inherited many of your charismas; for this, I am grateful for your exceptional genes. Unknowing to me, I, apparently, walk like you, talk like you, laugh like you and have habits like yours. To the people around you, your laughter was infectious; your

impeccable work ethic was infectious; your humility was infectious; your kind-hearted nature was infectious; and your love was infectious. You ARE an inspiration to your grandchildren and great grandchildren, present and forthcoming. I love you and miss you very much.

Third, I dedicate this labour of love to my grandmother, or “bà ngoại” as daringly called in Vietnamese, Mrs. Triem Thi Le. Thank you for showing me the Right and the Wrong since my heavy birth. Thank you for your strict teachings. Thank you for years of patience letting me immerse in the sacred spirits in numerous pagodas and opening my narrow eyesight. I am thankful that you have found your peace with your much-sought devotion to Buddha.

Last, but definitely not the least, I dedicate this labour of love to my PhD advisor and my journey “wingman”, Professor Emeritus Dr. Niels Bols. Before you accepted me into your laboratory, I thought that I could run, that I could make long speeches and that I could write stories. I was very wrong. Thank you for your countless hours showing me how to walk, how to spell alphabet and how to write phrases and sentences. Thank you for allowing me to share a car ride with you almost every second day. Thank you for tirelessly putting up with me, in every sense and aspect, in the last four years. Thank you for your investment in me. It was always pleasing to hear from you or read in your e-mails “Let us buy...”; I always felt like I had made an accomplishment. After just a little over one year into our relationship, you made a shocking deal-breaker declaration: “Nguyen, you and I are such a bad combination. (We both want to learn so much)” (Niels Bols, 2011). Thank you for allowing me to explore my scientific freedom despite your occasional undesired signature “voice raising”. Thank you for your compelling multidimensional storytelling. Every storyteller needs a “muse”. For my story, I (and walleye) am privileged to be your Pinocchio: “You are such a little rascal” (Niels Bols, 2014). Dear Niels: Thank you for allowing me to be part of your research work, your academic career, your teaching philosophy, your daily stories and your tree of life.

## TABLE OF CONTENTS

<b>AUTHOR'S DECLARATION .....</b>	<b>ii</b>
<b>ABSTRACT.....</b>	<b>iii</b>
<b>ACKNOWLEDGEMENTS .....</b>	<b>vii</b>
<b>DEDICATION .....</b>	<b>x</b>
<b>TABLE OF CONTENTS .....</b>	<b>xiii</b>
<b>LIST OF FIGURES.....</b>	<b>xix</b>
<b>LIST TABLES.....</b>	<b>xi</b>
<b>LIST OF ABBREVIATIONS .....</b>	<b>xxiii</b>
<b>CHAPTER 1. General Introduction .....</b>	<b>1</b>
1.1. Fish aquaculture.....	2
1.2. Impact of viral diseases.....	2
1.3. Walleye as a fish model.....	2
1.4. VHS outbreaks in Great Lakes regions.....	4
1.5. VHSV.....	5
1.6. Animal cell cultures.....	9
1.6.1. Animal cell cultures in virology.....	9
1.6.2. Animal cell cultures in comparative cellular biology and physiology.....	10
1.6.2.1. Endothelial cell lines .....	11
1.6.2.2. Cellular senescence .....	12
1.6.2.3. Primary cilia and acetylated $\alpha$ -tubulin.....	13
1.7 Walleye cell lines.....	14
1.8. Objectives .....	16
<b>CHAPTER 2. Development of a walleye cell line and use to study the effects of temperature on infection by viral hemorrhagic septicaemia virus (VHSV) group IVb .....</b>	<b>17</b>
2.1. Introduction.....	18
2.2. Materials and Methods.....	20

2.2.1. Fish.....	20
2.2.2. Preparation of caudal fin primary cell cultures .....	20
2.2.3. Routine maintenance of cell lines .....	21
2.2.4. Routine propagation of VHSV IVb.....	21
2.2.5. General characterization of WE-cfin11f.....	21
2.2.6. Characterizing the thermobiology of the WE-cfin11f cell line.....	22
2.2.7. Characterizing the thermovirology of VHSV IVb in WE-cfin11f.....	24
2.3. Results.....	30
2.3.1. Development and general characterization of WE-cfin11f.....	31
2.3.2. Thermobiology of WE-cfin11f cultures.....	32
2.3.3. Thermovirology of VHSV IVb in WE-cfin11f cultures .....	34
2.4. Discussion .....	44

**CHAPTER 3. Development of a walleye caudal fin epithelial cell line and demonstration that viral haemorrhagic septicemia virus genotype IVb preferentially infects a walleye caudal fin fibroblast cell line especially at 4 °C..... 50**

3.1. Introduction.....	51
3.2. Materials and Methods.....	53
3.2.1. Fish cell lines and virus.....	53
3.2.2. General fluorescent immunocytochemistry procedures.....	53
3.2.3. Development and characterization of WE-cfin11e .....	54
3.2.4. Collagen I expression in WE-cfin11e and WE-cfin11f .....	55
3.2.5. Characterizing the thermobiology of the WE-cfin11e cell line .....	55
3.2.6. Cytopathic effects (CPE).....	55
3.2.7. Western blotting for N protein in VHSV IVb infected cell cultures.....	56
3.2.8. Immunocytochemical staining for G protein in VHSV IVb infected cell cultures .....	56
3.2.9. Evaluating viral production in VHSV IVb infected cell cultures .....	57
3.2.10. Western blotting for Mx in VHSV IVb infected cell cultures .....	57
3.3. Results.....	59
3.3.1. Development and general characterization of WE-cfin11e .....	59

3.3.2. Collagen I expression in WE-cfin11e and WE-cfin11f .....	59
3.3.3. Thermobiology of WE-cfin11e cultures .....	63
3.3.4. VHVS IVb infectious cycle in WE-cfin11e at 14 °C and 4 °C.....	65
3.3.5. VHVS IVB infectious cycle in WE-cfin11e and WE-cfin11f cultures at 4 °C ... .....	65
3.3.6. Mx induction by VHSV IVb in WE-cfin11f and WE-cfin11e cultures at 4 and 14 °C .....	66
3.4. Discussion .....	73

**CHAPTER 4. Development of a walleye spleen stromal cell line sensitive to viral hemorrhagic septicemia virus (VHSV IVb) and to protection by synthetic dsRNA ..**

.....	<b>78</b>
4.1. Introduction.....	79
4.2. Materials and Methods.....	81
4.2.1. Tissue culture supplies, fish and miscellaneous reagents .....	81
4.2.2. Antibodies for cellular and viral proteins.....	81
4.2.3. Development of WE-spleen6 .....	82
4.2.4. Appearance of WE-spleen6 cultures on tissue culture plastic versus matrix gel. .....	82
4.2.5. Alkaline phosphatase and phagocytic activities of WE-spleen6.....	83
4.2.6. Immunocytochemistry for cellular markers .....	83
4.2.7. Other cell lines and viral haemorrhagic septicemia virus group IVb (VHSV IVb) .....	84
4.2.8. Evaluating viral transcripts during VHSV IVb infection cycle in WE cell cultures.....	85
4.2.9. Evaluating viral proteins during VHSV IVb infection cycle in WE cell cultures .....	85
4.2.10. Evaluating CPE during VHSV IVb infection cycle in WE cell cultures .....	86
4.2.11. Evaluating VHSV IVb production in walleye cell cultures .....	86
4.2.12. Monitoring Mx expression through western blotting.....	86
4.3. Results.....	88

4.3.1. Appearance of WE-spleen6 cultures on tissue culture plastic versus Matrigel ...	88
4.3.2. Immunocytochemistry, alkaline phosphatase activity, and phagocytosis of WE-spleen6 .....	88
4.3.3. VHSV IVb infection cycle in WE-spleen6 versus WE-cfin11f.....	92
4.3.4. Mx induction in WE-spleen6 and WE-cfin11f .....	97
4.3.5. Effect of prior exposure to pIC on VHSV IVb infection cycle in WE-spleen6...	99
4.4. Discussion .....	102

**CHAPTER 5. Development of an endothelial cell line from the bulbus arteriosus of walleye..... 105**

5.1. Introduction.....	106
5.2. Materials and Methods.....	108
5.2.1. Tissue culture supplies and fish .....	108
5.2.2. Initiation of BA primary cultures and development of WEBA cell line.....	108
5.2.3. Maintenance of other fish cell cultures .....	109
5.2.4. Cell line authentication by DNA barcoding.....	109
5.2.5. Measurement of cell proliferation and cell size .....	109
5.2.6. General fluorescence microscopy procedures.....	110
5.2.7. Fluorescence microscopy of collagen type I in WEBA cultures .....	110
5.2.8. Phagocytosis, Ac-LDL uptake, and UEA-binding.....	111
5.2.9. Fluorescence microscopy of WEBA for von Willebrand Factor (vWF) .....	112
5.2.10. Fluorescence microscopy of WEBAcytoskeleton.....	112
5.2.11. Fluorescence microscopy of WEBAfor tight junctions .....	113
5.2.12. Nitric oxide (NO) production.....	113
5.2.13. Induction of CYP1A .....	114
5.3. Results.....	116
5.3.1. Development of BA primary cultures into the cell line, WEBA .....	116
5.3.2. Capillary-like tubes .....	119
5.3.3. Collagen type I .....	120

5.3.4. von Willebrand Factor (vWF).....	121
5.3.5. Phagocytosis, Ac-LDL uptake, and UEA-1 binding.....	121
5.3.6. Cytoskeleton.....	121
5.3.7. Tight junction (TJ) proteins .....	124
5.3.8. Nitric oxide (NO) production.....	125
5.3.9. CYP1A induction.....	125
5.4. Discussion.....	128

**CHAPTER 6. Senescence-associated  $\beta$ -galactosidase staining in fish cell lines and primary cultures from several tissues and species, including rainbow trout coelomic fluid and milt ..... 134**

6.1. Introduction.....	135
6.2. Materials and Methods.....	137
6.2.1. Cell lines.....	137
6.2.2. Culture medium and conditions .....	137
6.2.3. Cell line development from solid organs of walleye and rainbow trout .....	137
6.2.4. Cell line development from rainbow trout ovarian fluid (OvF).....	138
6.2.5. Cell line development from rainbow trout milt.....	139
6.2.6. Senescence-associated $\beta$ -galactosidase (SA $\beta$ -Gal) staining.....	139
6.2.7. Periodic Acid-Schiff (PAS) staining.....	140
6.2.8. Comparing cell proliferation in WE-cfin11f and WEBA cultures.....	140
6.3. Results.....	141
6.3.1. SA $\beta$ -Gal staining during cell line development from walleye bulbus arteriosus .....	141
6.3.2. SA $\beta$ -Gal staining during cell line development from other walleye solid organs .....	141
6.3.3. Comparison of PAS staining and growth of two walleye cell lines.....	145
6.3.4. SA $\beta$ -Gal staining for rainbow trout cell lines .....	145
6.3.5. SA $\beta$ -Gal staining during cell line development from rainbow trout OvF ....	145
6.3.6. SA $\beta$ -Gal staining during cell line development from rainbow trout milt.....	149
6.3.7. Staining cultures of cell lines from a range of fish species for SA $\beta$ -Gal.....	151

6.4. Discussion .....	153
-----------------------	-----

**CHAPTER 7. Immunocytochemical demonstration of acetylated  $\alpha$ -tubulin and primary cilia in cell lines from different species, life stages, and organs of fish .. 159**

7.1. Introduction.....	160
7.2. Materials and Methods.....	162
7.2.1. Fish cell lines.....	162
7.2.2. Mammalian cell lines .....	162
7.2.3. Immunofluorescence of acetylated alpha tubulin .....	163
7.2.4. $\alpha$ -tubulin sequence alignment .....	164
7.3. Results.....	165
7.3.1. Primary cilia .....	165
7.3.2. Cytoplasmic staining.....	165
7.3.3. Nuclear staining .....	166
7.4. Discussion .....	176

**CHAPTER 8. General Summary and Future Research ..... 181**

8.1. General Summary .....	182
8.2. Future Research Directions.....	186

**REFERENCES..... 188**

Chapter 1 references.....	188
Chapter 2 references.....	196
Chapter 3 references.....	201
Chapter 4 references.....	205
Chapter 5 references.....	212
Chapter 6 references.....	220
Chapter 7 references.....	224
Chapter 8 references.....	229

## LIST OF FIGURES

<b>Figure 1.1.</b> Diagrammatic representation of RNA genome arrangement of VHSV IVb...	6
<b>Figure 2.1.</b> Development of walleye caudal fin cultures .....	31
<b>Figure 2.2.</b> Growth, viability, and morphology of WE-cfin11f cells at different temperatures.....	33
<b>Figure 2.3.</b> Expression of viral transcripts in WE-cfin11f at various temperatures.....	35
<b>Figure 2.4.</b> Expression of VHSV N protein in infected WE-cfin11f at low temperatures .....	36
<b>Figure 2.5.</b> Cell Viability of WE-cfin11f infected with VHSV IVb at different temperatures.....	39
<b>Figure 2.6.</b> WE-cfin11f supported VHSV IVb production at low temperatures .....	40
<b>Figure 2.7.</b> RT-PCR and Western blot analysis of WE-cfin11f cells infected with VHSV IVb at 26 °C .....	41
<b>Figure 2.8.</b> Observation of cytopathic effects when shifting VHSV IVb-infected WE-cfin11f cultures at 4 °C for 7 days to higher temperatures.....	43
<b>Figure 3.1.</b> Development of the walleye caudal fin epithelial-like cell line WE-cfin11e.. .....	60
<b>Figure 3.2.</b> Immunocytochemical results of cellular markers expressed in WE-cfin11f (A-C) and WE-cfin11e (D-E) .....	61
<b>Figure 3.3.</b> Differences between WE-cfin11e and WE-cfin11f cell lines in their ability to form extracellular collagen I matrix .....	62
<b>Figure 3.4.</b> Effect of temperatures on the growth and morphology of WE-cfin11e cell line.....	64
<b>Figure 3.5.</b> Expression of VHSV IVb N protein in WE-cfin11e cells post infection at 4 °C and 14 °C .....	67
<b>Figure 3.6.</b> Immunofluorescence detection of VHSV G protein in WE-cfin11f and WE-cfin11e infected with VHSV IVb at 4 °C and 14 °C .....	68

<b>Figure 3.7.</b> Viral production in WE-cfin11f and WE-cfin11f at the optimal VHSV infection temperature 14 °C (Panel A) and the winter-like temperature 4 °C (Panel B).....	70
<b>Figure 3.8.</b> Examination of induction of Mx protein in WE-cfin11f and WE-cfin11e cultures infected with VHSV IVb at 4 °C and 14 °C by Western blotting.....	72
<b>Figure 4.1.</b> Morphology of cells in WE-spleen6 cultures .....	89
<b>Figure 4.2.</b> Formation of lumen-like structures by WE-spleen6 cells on Matrigel-coated surface .....	90
<b>Figure 4.3.</b> Immunocytochemical staining of WE-spleen6 cell line.....	91
<b>Figure 4.4.</b> WE-spleen6 cells were more susceptible to VHSV IVb infection than the walleye caudal fin fibroblast WE-cfin11f cell line .....	93
<b>Figure 4.5.</b> WE-spleen6 cell line was more sensitive to VHSV IVb infection than WE-cfin11f cell line .....	95
<b>Figure 4.6.</b> Mx protein induction by a viral mimic pIC and VHSV IVb in WE-spleen6 and WE-cfin11f cell lines by Western blotting.....	98
<b>Figure 4.7.</b> Antiviral effects of pIC against VHSV IVb infection in WE-spleen6 .....	100
<b>Figure 5.1.</b> Cell cultures of walleye bulbus arteriosus and effects of fetal bovine serum on growth of WEBA cell line .....	117
<b>Figure 5.2.</b> Influence of culture confluence level on WEBA cell size.....	118
<b>Figure 5.3.</b> Capillary-like formation in WEBA cultures .....	119
<b>Figure 5.4.</b> Expression of collagen type I in WEBA .....	120
<b>Figure 5.5.</b> WEBA cells demonstrated properties of endothelial cells .....	122
<b>Figure 5.6.</b> Cytoskeletal filament proliferation in WEBA cell line.....	123
<b>Figure 5.7.</b> Immunocytochemistry of tight junction proteins in WEBA cell line.....	124
<b>Figure 5.8.</b> Detection of NO in walleye cells.....	126
<b>Figure 5.9.</b> Induction of CYP1A catalytic activity and protein expression by TCDD .....	127
<b>Figure 6.1.</b> Senescence-associated $\beta$ galactosidase (SA $\beta$ -Gal) staining of cultures of the endothelial cell line WEBA from walleye bulbus arteriosus (A) and of CHSE-214 from chinook salmon (B), RTG-2 from rainbow trout (C) and EPC from fathead minnow (D) .....	142

<b>Figure 6.2.</b> Senescence-associated $\beta$ -Gal staining in early passage cultures of walleye brain (A) and heart (B).....	143
<b>Figure 6.3.</b> Periodic acid Schiff (PAS) staining in WEBA cells.....	146
<b>Figure 6.4.</b> Comparing cell proliferation in cultures of two walleye cell lines under similar growth conditions .....	147
<b>Figure 6.5.</b> Appearance and senescence-associated $\beta$ -Gal staining of primary somatic cell cultures of ovarian fluid (OvF) and of milt from rainbow trout .....	150
<b>Figure 7.1.</b> Examples of mitotic spindles, midbodies and centrioles being stained for acetylated $\alpha$ -tubulin by mAb 6-11B-1 in fish cell lines.....	167
<b>Figure 7.2.</b> Demonstration by mAb 6-11B-1 for primary cilia and cytoplasmic staining in the walleye caudal fin fibroblast WE-cfin11f cell line .....	168
<b>Figure 7.3.</b> Immunocytochemical staining by mAb 6-11B-1 in cell lines from rainbow trout gill (RTgill-W1), Chinook salmon embryo (CHSE-214), walleye brain (WE-brain5), walleye skin (WE-skin11f) and zebrafish spleen (ZSSJ) .....	169
<b>Figure 7.4.</b> Nuclear staining by mAb 6-11B-1 in cell lines from Chinook salmon embryo (CHSE-214) and haddock embryo (HEW).....	171
<b>Figure 7.5.</b> Sequence alignment of amino acids 25-50 of $\alpha$ -tubulin from human, salmonids and zebrafish.....	172

## LIST OF TABLES

<b>Table 1.1.</b> List of fish species identified to be susceptible to VHSV IVb (as of June 2014) .....	7
<b>Table 1.2.</b> Geographic distribution and fish type susceptibility of 4 genotypes of VHSV .....	8
<b>Table 1.3.</b> List of cell lines derived from walleye reported in the literature (as of the creation of new walleye cell lines presented in this thesis, starting date in 2010) .....	15
<b>Table 2.1.</b> Primers used in RT-PCR experiments .....	24
<b>Table 6.1.</b> Senescence-associated $\beta$ -Gal staining in cultures of cell lines from walleye, <i>Sander vitreus</i> .....	144
<b>Table 6.2.</b> Senescence-associated $\beta$ -Gal staining in cultures of cell lines from different tissues of rainbow trout.....	148
<b>Table 6.3.</b> Senescence-associated $\beta$ -Gal staining in cultures of cell lines from other fish species .....	152
<b>Table 7.1.</b> Immunocytochemical staining pattern of acetylated $\alpha$ -tubulin <sup>1</sup> in cell lines from seven fish species .....	173
<b>Table 7.2.</b> Immunocytochemical staining pattern of acetylated $\alpha$ -tubulin <sup>1</sup> in mammalian cell lines .....	175

## LIST OF ABBREVIATIONS

Ac-LDL	Acetylated low density lipoprotein
ANOVA	One-way analysis of variance
ATCC	American Tissue Culture Collection
BA	Bulbus arteriosus
BCA	Bicinchoninic acid
BSA	Bovine serum albumin
CaCo-2	Human colorectal adenocarcinoma epithelial cell line
cDNA	Complementary DNA
CFDA-AM	5'-carboxyfluorescein diacetate acetoxymethyl ester
CHSE-214	Chinook salmon embryonic epithelial cell line
COX1	Cytochrome c oxidase subunit 1
COL-1	Collagen type 1
CYP1A	Cytochrome P4501A
CPE	Cytopathic effects
DAPI	4',6-diamidino-2-phenylindole
DMSO	Dimethyl sulfoxide
dsRNA	Double-stranded DNA
DPBS	Dulbecco's Phosphate Buffer Saline
EC	Endothelial cells
EROD	7-ethoxyresorufin o-deethylase
EPC	Fathead minnow epithelial cell line
FBS	Fetal bovine serum
FHMT	Fathead minnow testicular cell line
GFSk-S1	Goldfish skin fibroblastic cell line
h	Hours
H4IIE	Rat hepatoma cell line
HeLa	Human cervical adenocarcinoma epithelial cell line
HepG2	Human liver carcinoma cell line
HUVEC	Human umbilical vein endothelial cells

HEW	Haddock embryonic fibroblastic cell line
ICC	Immunocytochemistry
IHNV	Infectious hematopoietic necrosis virus
IP	Intraperitoneal
IPNV	Infectious pancreatic necrosis virus
L-15	Leibovitz's L-15
L-15/ex	Simplified Leibovitz's L-15 with L-15 inorganic salts and carbohydrates
MOI	Multiplicity of infection
NO	Nitric oxide
OvF	Ovarian fluid
PBS	Phosphate Buffer Saline
PHL	Pacific herring larval epithelial cell line
PFA	Paraformaldehyde
p.i.	Post infection
pIC	Polyinosinic:polycytidylic acid
P/S	Penicillin Streptomycin solution
qPCR	Quantitative polymerase chain reaction
RFUs	Relative fluorescence units
RTbrain	Rainbow trout brain cell line
RTeeb	Rainbow trout early embryo blastula-stage cell line
RTG-2	Rainbow trout gonadal fibroblastic cell line
RTgill-W1	Rainbow trout gill epithelial cell line
RTgut-GC	Rainbow trout intestinal epithelial cell line
RTH	Rainbow trout heart cell line
RTHDF	Rainbow trout hypodermal fibroblastic cell line
RTL-W1	Rainbow trout liver epithelial cell line
RTmilt5	Rainbow trout milt cell line
RTO-2	Rainbow trout ovary cell line
RTovf1	Rainbow trout ovarian fluid epithelial cell line
RT-PCR	Reverse transcriptase polymerase chain reaction
RTS11	Rainbow trout spleen monocyte/macrophage cell line

RT-Testis	Rainbow trout testicular epithelial cell line
SA $\beta$ -Gal	Senescence-associated $\beta$ -galactosidase
SAPRE	Walleye epithelial cell line derived from the posterior wall of the eye
SDS	Sodium dodecyl sulfate polyacrylamide gel electrophoresis
TC	Tissue culture
TCID <sub>50</sub> /mL	50% Tissue Culture Infectious Dose per mL
Tmb	Tilapia bulbus arteriosus endothelial cell line
UG	University of Guelph
UEA-1	<i>Ulex europaeus</i> lectin agglutinin I
UILT	Upper incipient lethal temperature
vWF	von Willebrand factor
UW	University of Waterloo
WDSV	Walleye dermal sarcoma virus
WE	Walleye
WE-afin8e	Walleye anal fin epithelial-like cell line
WEBA	Walleye bulbus arteriosus endothelial cell line
WE-brain3	Walleye brain astroglial-like cell line 3
WE-brain5	Walleye brain astroglial-like cell line 5
WE-cfin11e	Walleye caudal fin epithelial-like cell line
WE-cfin11f	Walleye caudal fin fibroblastic cell line
WE-heart1	Walleye heart cell line 1
WE-heart6	Walleye heart cell line 6
WE-spleen6	Walleye spleen stromal cell line
WE-skin11f	Walleye skin fibroblastic cell line
VHS	Viral hemorrhagic septicemia
VHSV IVb	Viral hemorrhagic septicemia virus group IVb
VSV	Vesicular stomatitis virus
ZEB2J	Zebrafish embryo blastula-stage epithelial cell line
ZO-1	Zona occludens -1
ZSSJ	Zebrafish spleen stromal cell line

# **CHAPTER 1.**

## **General Introduction**

### **1.1. Fish aquaculture**

Aquaculture has been reported to generate annual revenue of 6.6 billion dollars for the Canadian economy (Canadian Aquaculture Industry Alliance, 2012). For farmed marine fish, salmonids have always been the most important for Canada and in the competitive international market account for 70% of Canada's total aquaculture production and 81% of overall commercial value (FOC, 2008). In fact Canada is ranked fourth among the salmon producers of the world (FOC, 2008). The top freshwater cultured fish in Canada is the rainbow trout. Among the freshwater species being considered for aquaculture is walleye, *Sander vitreus* (formerly known as *Stizostedion vitreum vitreum*) (FOC, 2008).

### **1.2. Impact of viral diseases**

Infectious diseases are a serious concern to fisheries and aquaculture. Although bacterial and parasitic infections often have chronic effects, mass fish kills in natural habitats and in fry and fingerling stocks in aquaculture facilities are more likely associated with viral infections (Heppell et al., 1997). While antibiotic treatments successfully minimize and even prevent certain common types of bacterial and fungal infections, vaccination has shown some promises in coping with viral infections in farmed fish. Unfortunately, this vaccination process still requires strict safety regulations and good investments in research, pharmaceutical development, and labour: factors which account for the limited number of commercially available vaccine products. Given the importance of Canadian aquaculture provides to its national economy, it is important to develop an excellent aquaculture program that improves the health of emerging aquaculture species such as walleye. One indispensable diagnostic tool when studying viral diseases in fish is the availability of permissible fish cell cultures.

### **1.3. Walleye as a fish model**

Walleye, or also known as pickerel or yellow pike by local fishermen, is a fish species of great commercial value (Scott and Crossman, 1973). They are popular sport and highly prized food fish that are widely stocked in Canada and the Northern regions of the U.S. (Summerfelt et al., 2010). Walleye is the most important fish species to the \$2.5-

billion recreational fishery in Ontario; Lake Erie is the biggest commercial fishery for walleye (Canada's Department of Fisheries and Oceans, 2007). Currently walleye is the official fish of two Canadian provinces (Saskatchewan, Manitoba) and four U.S.A. states (Minnesota, South Dakota, Ohio and Vermont). Unfortunately, the populations of wild walleye are declining; thus walleye fry are produced, stocked, and released into the wild waters to supplement the annual shortage (Kerr, 2008). Despite an intensive effort in enhancement of walleye fry stockings, production of food-size walleye is still falling behind. As a result, walleye have been considered for aquaculture in North America. So far, Canada is leading in taking initiatives in farming walleye and its major market is the United States, where walleye aquaculture is still limited.

Walleye belong to the genus *Sander* of the family *Percidae*, which includes the ecotoxicologically and economically important yellow perch (*Perca flavescens*). This latter species has been used to evaluate the toxicity of chemotherapeutic agents such as hydrogen peroxide (Clayton and Summerfelt, 1996; Tort et al., 2002), naturally occurring biological waste such as nitrite (Madison and Wang, 2006), and environmental contaminants such as chlorpyrifos (Phillips et al., 2003). Moreover, walleye have long been a species of interest for research in parasitic and viral diseases. Like other freshwater fish, walleye are prone to infections by external protozoa such as *Ichthyophthirius multifiliis* and *Trichodina spp.* (Summerfelt, 2000) and obligate intracellular pathogens such as microsporidia (Sutherland et al., 2004). Walleye are also susceptible to viral infections that lead to non-fatal diseases such as lymphocystis, epidermal hyperplasia, and dermal sarcoma (Summerfelt, 2000). Dermal sarcoma is a type of skin tumour that is particularly associated with walleye and caused by walleye dermal sarcoma virus (WDSV). In fact, WDSV, a piscine retrovirus, is probably the most intensively studied virus in walleye (Bowser et al., 1997; Rovnak et al., 2007; Zhang and Martineau, 1999). There had been no known viral infections that resulted in high mortality in walleye, as briefly reviewed by Summerfelt in 2000. However, infectious pancreatic necrosis virus (IPNV) and infectious hematopoietic necrosis virus (IHNV) have been detected and isolated from walleye in the past (Summerfelt, 2006). Recently, an epizootic viral disease caused by viral hemorrhagic septicemia virus genotype IVb (VHSV IVb) arose in the Great Lakes in 2003 and caused a considerable death rate in

populations of walleye and other freshwater fish. The first report on VHSV-affected walleye appeared in 2006, a year after the first Canadian report of VHSV outbreak in the Great Lakes regions. Recently, walleye could experimentally been demonstrated to show VHS pathology by VHSV IVb (Grice et al., 2014).

#### **1.4. VHS outbreaks in Great Lakes regions**

Recently massive die-offs of many freshwater fish have been documented in the Great Lakes and have been attributed to viral hemorrhagic septicemia (VHS). VHS is characterized by pathological symptoms including, but not limited to, severe hemorrhaging of internal organs, epidermal petechiae and exophthalmia and is caused by viral hemorrhagic septicemia virus (VHSV). A new genotypically distinct variant of VHSV subtype IV has been identified in the Great Lakes regions and is referred to as VHSV IVb. This new strain shares high sequence similarities to VHSV subtype IVa that was previously isolated from marine fish in Asia and on the West coast of North America. VHSV IVb was first isolated from a few dead mummichog (*Fundulus heteroclitus*), stickleback (*Gasterosteus aculeatus aculeatus*), and striped bass (*Morone saxatilis*) in New Brunswick in 2000-2002 (Gagné et al., 2007). The first Great Lakes VHS outbreak was reported with muskellunge (*Esox masquinongy*) from Lake St. Clair in Michigan, USA in 2003 (Elsayed et al., 2006). The first Canadian VHS outbreak was reported two years later; the infected species was freshwater drum (*Aplodinotus grunniens*) from Bay of Quinte of Lake Ontario (Lumsden et al., 2007). This particular Great Lake variant appears to have a broad range of host susceptibility (Table 1.1).

To date, nearly all fish that have been challenged with VHSV IVb have shown some degree of susceptibility (Table 1.1). Although VHSV IVb mostly infects freshwater fish, Kim and Faisal (2010b) showed that Atlantic salmon (*Salmo salar*), an anadromous fish, was slightly susceptible to VHSV IVb after intraperitoneal (IP) injection. On the other hand, while Chinook salmon was susceptible to VHSV IVb in both wild (U.S. Office of the Federal Register, 2008) and experimental settings (Kurath et al., 2009), Kim and Faisal (2010b) found a contradictory result. When they intraperitoneally inoculated VHSV IVb into juvenile Chinook salmon, all ten experimentally challenged fish recovered from infection and none of them showed any typical pathological signs after 28

days post-infection (p.i.). Kim and Faisal (2010b) did not further elaborate on this observation. Infectivity by VHSV IVb might be modulated by the age of the fish. Only adult fish were observed and documented during Great Lakes VHS die offs (Kim and Faisal, 2010b). However, Kim and Faisal (2010c) found that juvenile muskellunge was highly susceptible to VHSV IVb that was isolated from infected adult muskellunge. Interestingly, their results demonstrated that waterborne infection caused mortality earlier (on day 3 p.i.) than IP infection (on day 5 p.i.). Nevertheless, their results were in some agreement with other studies in that VHSV IVb is more pathogenic to muskellunge and largemouth bass than most salmonids (Kin and Faisal, 2010a; Kim and Faisal, 2010b). One salmonid species exception is lake herring (*Coregonus artedii*), which was found to be significantly more susceptible to VHSV IVb than muskellunge (Weeks et al., 2011). Walleye are moderately susceptible to VHSV IVb while muskellunge are one of the most susceptible and salmonids are the least susceptible (Grice, 2012). It should also be noted that different fish species responded differently to VHSV IVb in terms of onset of pathological signs, degree and severity of hemorrhage, as well as survival period until death (Kim and Faisal, 2010a; Kim and Faisal, 2010b).

## 1.5. VHSV

VHSV belongs to the genus *Novirhabdovirus* of the family *Rhabdoviridae* (Kuzmin et al., 2009). A well-known example of this family is the rabies virus; however, the prototypical and most intensively studied rhabdovirus is vesicular stomatitis virus (VSV) thanks to the easy manipulation of producing VSV in vitro (Licata and Harty, 2003). In addition to VHSV, two other important fish novirhabdoviruses are infectious hematopoietic necrosis virus (IHNV) and snakehead rhabdovirus (SHRV).

VHSV is a negative-sense single-stranded RNA virus of 180 nm in length and 60 nm in diameter (Tordo et al., 2004; WFRC, 2008). The RNA genome of this enveloped and bullet-shaped virus contains about 11 kilobases (kb) that comprise six genes (Ammayappan and Vakharia, 2009) (Figure 1). Its gene arrangement is 3'-N-P-M-G-NV-L-5' (Ammayappan and Vakharia, 2009). Five genes code for structural proteins that are required to form infectious virions (Ammayappan and Vakharia, 2009; WFRC, 2008).

The other gene, denoted as “NV”, codes for a non-structural protein whose function is still unknown (Ammayappan and Vakharia, 2009; WFRC, 2008). There are four genotypes and group IVb is mainly associated with VHS outbreaks in the Great Lakes (Table 1.2.)

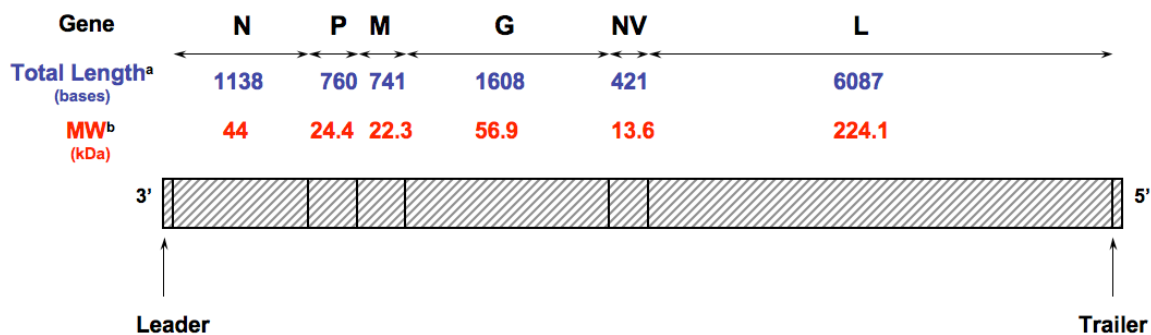


**Figure 1.1. Diagrammatic representation of RNA genome arrangement of VHSV IVb.** The genome is mapped from 3' to 5' direction. Relative lengths of genes are approximated and not up to the exact scale. <sup>a</sup>Total length of nucleotide sequence of each viral gene is in bases. Between two genes is a gene junction, indicated by a straight black vertical line. <sup>b</sup>Molecular weights (MW) of the final protein products are in kDa. N = nucleoprotein; P = phosphoprotein; M = matrix protein; G = glycoprotein; NV = non-virion protein; L = large polymerase (adapted from Ammayappan and Vakharia, 2009).

**Table 1.1. List of fish species identified to be susceptible to VHSV IVb** (as of June 2014). Infected species #1-31 (adult fish) reported were from the wild habitats (under non-experimental settings, i.e. natural cause of infection). Some of them have been experimentally challenged with VHSV IVb infection (mostly by IP infection, some cases with waterborne infection) and similar results were obtained except for Chinook salmon (species #11) (see Kim and Faisal, 2010b). Infected species #32-44 were experimentally found to be susceptible to VHSV IVb.

No.	Common name	Scientific name	Reference
1	Striped bass	<i>Morone saxatilis</i>	
2	Mummichog	<i>Fundulus heteroclitus</i>	Gagné et al., 2007
3	3-spined stickleback	<i>Gasterosteus aculeatus</i> <i>aculeatus</i>	
4	Brown trout	<i>Salmo trutta</i>	
5	Black crappie	<i>Pomoxis nigromaculatus</i>	
6	Bluegill	<i>Lepomis macrochirus</i>	
7	Bluntnose minnow	<i>Pimephales notatus</i>	
8	Brown bullhead	<i>Ictalurus nebulosus</i>	
9	Burbot	<i>Lota lota</i>	
10	Channel catfish	<i>Ictalurus punctatus</i>	
11	Chinook salmon	<i>Oncorhynchus tshawytscha</i>	
12	Emerald shiner	<i>Notropis atherinoides</i>	
13	Spottail shiner	<i>Notropis hudsonius</i>	
14	Gizzard shad	<i>Dorosoma cepedianum</i>	
15	Lake whitefish	<i>Coregonus clupeaformis</i>	
16	Largemouth bass	<i>Micropterus salmoides</i>	
17	Muskellunge	<i>Esox masquinongy</i>	U.S. Office of the Federal Register, 2008
18	Shorthead redhorse	<i>Moxostoma macrolepidotum</i>	
19	Northern Pike	<i>Esox lucius</i>	
20	Pumpkinseed	<i>Lepomis gibbosus</i>	
21	Rainbow trout	<i>Onchorhynchus mykiss</i>	
22	Rock bass	<i>Ambloplites rupestris</i>	
23	Round goby	<i>Neogobius melanostomus</i>	
24	Silver redhorse	<i>Moxostoma anisurum</i>	
25	Smallmouth bass	<i>Micropterus dolomieu</i>	
26	Freshwater drum	<i>Aplodinotus grunniens</i>	
27	Trout-Perch	<i>Percopsis omiscomaycus</i>	
28	Walleye	<i>Sander vitreus</i>	
29	White bass	<i>Morone chrysops</i>	
30	White perch	<i>Morone americana</i>	
31	Yellow perch	<i>Perca flavescens</i>	
32	Fathead minnow	<i>Pimephales promelas</i>	Al-Hussinee et al., 2010
33	Lake trout	<i>Salvelinus namaycush</i>	
34	Brook trout	<i>Salvelinus fontinalis</i>	Kim and Faisal, 2010b
35	Atlantic Salmon	<i>Salmo salar</i>	
36	Coho salmon	<i>Oncorhynchus kisutch</i>	

37	Lake herring	<i>Coregonus artedi</i>	Weeks et al., 2011
38	Pacific herring	<i>Clupea pallasii</i>	Emmenegger et al., 2013
39	Zebrafish	<i>Danio rerio</i>	Hope et al., 2009
40	Golden shiner	<i>Notemigonus crysoleucas</i>	Cornwell et al., 2013a
41	Koi Carp	<i>Cyprinus carpio L.</i>	Cornwell et al., 2013b
42	Japanese fluvial sculpin	<i>Cottus pollux</i>	
43	Japanese rice fish	<i>Oryzias latipes</i>	Ito and Olesen, 2013
44	Yoshinobori	<i>Rhinogobius sp.</i>	

**Table 1.2. Geographic distribution and fish type susceptibility of 4 genotypes of VHSV (adapted from Kuzmin et al., 2009 and WFRC, 2008)**

<b>Genotype</b>	<b>Geographic location(s)</b>	<b>Affected fish type</b>
Ia	Europe	Farmed trouts
Ib	Baltic Sea, North Sea, Skagerrak, Kattegat, English channel	Marine fish
II	Baltic Sea	Marine fish
III	North Sea (British Isles), Skagerrak, Kattegat	Marine fish
IVa	Pacific coast of North America, Japan, Korea	Marine fish
IVb	Great Lakes regions	Freshwater fish

## **1.6. Animal cell cultures**

The placing of cells from multicellular organisms into a manufactured vessel, such as a petri dish or flask, in order to grow and experiment on the cells independent of the organism is the essence of in vitro biology. The strength of the in vitro or cell culture approach is that cellular phenomenon can be studied a controlled environment, independent of the complexities of systemic controls. Animal cell cultures can be classified as two basic types (Bols et al., 2005). Primary cultures are initiated directly from an animal and usually are used within a few days of preparation. When primary cultures are subcultivated, this begins a cell line. Some cell lines can only go through a limited number of subcultivations or population doublings. These are termed finite cell lines and classic examples are human skin fibroblasts (Hayflick, 2005). Other cell lines can be grown indefinitely or continuously. Most fish cell lines appear to be continuous (Bols et al. 2005). The first fish cell lines were developed for virology (Wolf, 1988).

### **1.6.1. Animal cell cultures in virology**

Cell lines have been invaluable for studying animal viruses. Five general areas can be identified. Firstly, cell lines are needed to produce sufficient virus to characterize the biophysical and biochemical properties of a virus. Examples of such characterization include describing viral genome, proteins and structure. Secondly, cell cultures are needed to study the single-cell reproductive cycle of virus. This would include understanding the molecular events involved in the entry, replication, assembly and release of viruses. Thirdly, cell lines can contribute to preventing and controlling viral diseases by being a source of viruses for vaccines and an experimental system for developing antiviral drugs. Fourthly, in some cases, cell lines can advance an understanding of viral pathogenesis. For example, the use of neuronal cell lines to study neurological damage of the poliovirus in humans. Thus for studying the species and tissue-specific pathogenicity of a virus at the cellular and molecular level, cell culture systems from the species and/or cell types of interest are needed. Finally, cell lines are powerful diagnostic tools.

Cell lines contribute to the diagnosis of viral infections in at least four fundamental ways. Firstly, the characterization of new viruses usually only can be done using cell

cultures. Secondly, cell lines allow the development of diagnostic reagents. For example, they can be used to produce viral proteins for the purpose of generating antibodies to be used in ELISA assays for the detection of viruses. Thirdly, cell cultures can reveal an infectious virus. Fourthly, cell lines continue to be one of the best methods for quantifying the concentration of infectious virus present in a tissue sample.

For animal virology a range of cell lines needs to be available. This is because not all cell lines support the replication of any given virus. In vivo the type of cells that will sustain the replication of a specific virus is related to the host range and tissue tropism of the virus. Therefore, whether a particular cell line will support the replication of a particular virus will depend on several factors. These include the species from which the cell line is derived, the lineage of the cell, and the degree of differentiation. For a single species, humans, thousands of cell lines are available. Yet, no single cell culture system is susceptible to all viruses and there is a need to search for additional sensitive cell lines for detecting unknown and /or currently non-cultivable viral agents.

### **1.6.2. Animal cell cultures in comparative cellular biology and physiology**

Mammalian cell cultures and cell lines have been exploited to study a variety of cellular phenomena for over the past century. They can include, but not limited to, the descriptions of the morphology, organization, properties and ultrastructure of particular cell types and their constituents, the characterization of their cellular and biochemical processes and their biotechnological uses in making monoclonal antibodies, recombinant proteins and creating mutant clones. A classical example of use of cell cultures to study cell biology is the groundbreaking discovery of dendritic cells, which are key regulators of the innate and adaptive immunity, by the late Nobel Laureate Professor Ralph Steinman.

With the increasing efforts to develop cell lines from fish (Bols et al., 2005), an emerging area of research might be termed comparative cellular biology and physiology. This discipline would determine the degree to which knowledge of cells and cellular process of mammals can be applied to the cells and cellular processes of lower vertebrates. The most understood vertebrate cells will always be from mammals because of the primacy of medical research. Understanding the cells and cellular processes in fish

can help in understanding fish diseases and how to promote fish health in aquaculture, but also give insights into the evolution of cellular processes. Three potential areas where comparative cellular biology and physiology could be established are endothelial cell biology, cellular senescence, and primary cilia. These three are briefly reviewed below.

### **1.6.2.1 Endothelial cell lines**

With a few exceptions, most fish cell lines have been described as either epithelial-like or fibroblast-like (Bols et al., 2005), whereas for mammals, endothelial cell primary cultures and lines have been developed for multiple research purposes. The endothelium is the layer of cells that lines the blood vessels of the circulatory system. The essential function is to maintain blood vessel permeability but the endothelium is also described as having secretory, synthetic, metabolic and immunological functions (Cines et al., 1998). In human medicine several families of viruses have been found to impair the endothelium and an interplay between the virus, the endothelium and the immune system can be responsible for viral pathologies, such as coagulopathy, haemorrhagic abnormalities, plasma leakage, and thrombocytopenia (Sirkiatkhachorn & Spiropoulou, 2014). Additionally some viruses, such as Ebola, directly infect endothelial cells. Some pathological symptoms of VHS in different species of fish include external and internal haemorrhages and thrombocytopenia (Grice et al., 2014; Wolf 1988).

Both primary cultures and cell lines of endothelial cells have proven invaluable for studying the mammalian cardiovascular system. One of the most frequently used culture systems has been human umbilical vein endothelial cells (HUVEC) (Cines et al., 1998). HUVEC have been popular because the umbilical vein can be obtained easily and is large, allowing many ECs to be isolated and put into primary culture. In some cases, mammalian EC have been deliberately immortalized (Ades et al., 1992) and in others they have spontaneously immortalized into cell lines (Takahashi et al. 1990). These cell lines often retain different subsets of endothelial cell properties and have been very useful research tools (Unger et al. 2002). One marker is von Willebrand factor (vWF). Only endothelial cells and megakaryocytes synthesize vWF, which in endothelial cells is stored in rod shaped granules about 3  $\mu\text{m}$  long known as Weibel-Palade bodies (Wagner et al.,

1982). Also known as factor VIII-related antigen, vWF is a large glycoprotein that participates in blood clotting by promoting the adhesion of platelets to the subendothelial matrix but is also involved in maintaining blood tissue barriers (Yosef & Uboqu, 2013). Another marker is endothelial nitric oxide synthase (eNOS) (Blecharz et al., 2014). This enzyme catalyzes the formation of nitric oxide (NO) from L-arginine. NO regulates vascular pressure by causing the relaxation of smooth muscle cells that surround blood vessels (Desjardins & Balligand, 2006).

#### **1.6.2.2 Cellular senescence**

One triumph of cell culture has been the identification approximately 50 years ago of the phenomenon of cellular senescence. Hayflick (1965) found that human skin fibroblasts underwent 50-60 population doublings in vitro and before the cells stopped growing and became what has been termed senescent. Cellular senescence is the entry of cells into an irreversible non-dividing state that cannot be overcome even upon treatment with mitogenic stimuli (Ohtani & Hara, 2013) and is considered important to several physiological processes. The foremost of these is aging, and human skin fibroblast cell lines have become a popular model for studying aging in vitro. Indeed, cellular senescence is thought to contribute to the degenerative pathologies of aging. Yet cellular senescence can also be considered beneficial, being a tumour suppressive or an anticancer mechanism by preventing the growth of cells at risk of undergoing transformation into tumour cells (Rodier & Campisi, 2011). Paradoxically, cellular senescence might also be involved in tumour promotion (Rodier & Campisi, 2011). Senescent cells can secrete multiple factors, with interleukin 8 being just one example, to stimulate the growth and migration of surrounding weakly malignant cells. This behaviour is termed the senescence-associated secretory phenotype (SASP). Again, SASP might also be beneficial: the factors secreted can promote tissue repair. Finally, some have suggested recently that cellular senescence can be an antiviral mechanism (Reddel, 2010).

Surprisingly cellular senescence has yet to be demonstrated in fish cell cultures, although recently primary cultures from a short-lived species has been studied (Graf et al., 2013). Nearly all fish cell lines have grown continuously, with no signs of growth

arrest. However, one of the common markers that is used for identifying senescent cells in mammalian cell cultures has rarely been examined with fish cell lines. This is senescence-associated  $\beta$ -galactosidase (SA  $\beta$ -Gal) (Dimri et al., 1995). The underlying biochemical and cellular basis for the correlation between SA  $\beta$ -Gal and cellular senescence has been a matter of debate (Hwang et al., 2009; Lee et al., 2006; Severino et al., 2000). SA  $\beta$ -Gal has been found not due to a variant form of the enzyme or a paralog but due to the lysosomal  $\beta$ -galactosidase that although optimally active at pH 4.0, can be detected at pH 6.0 in senescent cells but not in non senescent cells (Kurz et al., 2000). Thus for some cell cultures, the detection of SA  $\beta$ -Gal is a surrogate marker for an increase in lysosome number or activity (Lee et al., 2006). Despite this question about the meaning of the marker, cells can easily be tested for SA  $\beta$ -Gal through cytochemical staining (Debacq et al., 2009) and a wide number of mammalian primary cultures and cell lines, and even in vivo, have been tested and might be considered as part of their characterization.

### **1.6.2.3 Primary cilia and acetylated $\alpha$ -tubulin**

The primary cilium is one of several kinds of cilia that can occur on the cells of vertebrates. A unique aspect of the primary cilium is that practically each cell in the body of vertebrates appears to have one primary cilium (Satir et al., 2010). The common structural organization of cilia is the axoneme. The axoneme is the cytoskeleton of the cilia and is composed of 9 microtubule doublets. Some cilia have an additional microtubule pair and this organization is referred to as the 9 + 2 structure. Primary cilia on the other hand have a 9 + 0 structure. Usually the 9 + 2 arrangement means the cilia are motile. An example of these is the multiple cilia found on the surface of the respiratory epithelium of mammals. By contrast, the primary cilium is immotile. The primary cilium is considered a sensory organelle that contains specific receptors and relays signals from receptors into the cell and is essential for development (Guemez-Gamboa et al., 2014).

The main proteins of the cilia are microtubules, which make up the axoneme. The microtubules are filamentous structures made up of dimers of the globular proteins,  $\alpha$ - and  $\beta$ - tubulin. Besides cilia, microtubules make up the eukaryotic cell cytoskeleton and

several other structures. The tubulins are subject to post-translation modifications, such as phosphorylation and acetylation. Acetylated  $\alpha$ -tubulin is particularly abundant in primary cilia. A commercial monoclonal antibody (mAb 6-11B-1) to acetylated  $\alpha$ -tubulin has been widely used to detect primary cilia in mammalian cell cultures (Piperno et al., 1987). The mAb also stains other cellular structures, including the cytoskeleton in a few cell type (Piperno et al., 1987). One function proposed for acetylated  $\alpha$ -tubulin is to stabilize microtubules by bundling them (Sadoul et al., 2011).

Cilium biology and acetylated  $\alpha$ -tubulin have been the focus of study in the virology of mammals but not fish. The interaction between viruses, such as influenza, and the motile cilia on respiratory surfaces has long been studied (Hamlin & Harford, 1952). However to date primary cilia/virus interaction has yet to be reported. In human bronchial epithelial cell cultures, the deacetylation of  $\alpha$ -tubulin increased the release of influenza A virus from infected cells (Husain & Harrod, 2011). Herpes simplex virus 1 stimulated the acetylation of  $\alpha$ -tubulin in human MRC cells; the acetylated  $\alpha$ -tubulin interacted with heat-shock protein 90 (HSP 90) to mediate viral capsids nuclear translocation (Zhong et al., 2014). Probably the involvement of acetylated  $\alpha$ -tubulin in the infectious cycle of many more viruses remains to be discovered.

### **1.7. Walleye cell lines**

VHSV IVb has yet to be studied in vitro using walleye cells. Although cell lines have been developed from walleye, no cell lines from normal walleye tissue appear to be available currently. Six walleye-derived cell lines (WF, WF-2, WC-1, W12, WO and We-2) have been reported during more than 30 years of intermittent research (Wolf and Mann, 1980; Kelly et al., 1980; Kelly et al., 1983; Wilensky and Bowser, 2005), but none of them are available from the American Type Culture Collection (ATCC®). WF-2 was developed from a walleye fry by Bruce Calnek (Cornell University). Unfortunately, WF-2 was recently reported to have been cross-contaminated with a bluegill cell line (Sansom et al., 2013). Other walleye cell lines might have been lost or were not available. Thus new cell models from walleye are sought for studying viral pathogens such as VHSV IVb that is now reported to infect walleye.

To study the pathogenicity of VHSV IVb in walleye cells, cell lines from relevant tissues were considered and sought. Inasmuch as fish novirhabdoviruses preferentially enter and inhabit the fin bases first at the very early stage of infection (Harmache et al., 2006) and VHSV IVb antigens are detected in the fins of experimentally infected walleye (Grice et al., 2014), fin cell lines would be desirable to potentially study the early phases of VHSV IVb infection in walleye. In addition, a walleye endothelial cell line would be useful because the endothelium is one of the most important tissues affected in VHS (Al-Hussinee et al., 2010; Brudeseth et al., 2005; Lumsden et al., 2007) and endothelial disruption is likely one of the possible causes of the characteristic hemorrhages seen in fish with VHS, whether directly or indirectly caused by VHSV. A walleye cell line from hemopoietic organs would be also of interest as VHSV has been found to affect head kidney and spleen tissues of infected fish (Al-Hussinee et al., 2010; Evensen et al., 1994; Olson et al., 2013).

**Table 1.3. List of cell lines derived from walleye reported in the literature** (as of the creation of new walleye cell lines presented in this thesis, starting date in 2010)

<b>Cell line designation</b>	<b>Tissue of origin</b>	<b>Cell Morphology</b>	<b>Reference</b>
WF	embryo	n.r.	Wolf and Mann (1980)
WF-2	whole fry	Fibroblastic	Wolf and Mann (1980)
We-2	embryo	n.r.	Kelly et al. (1983)
WO	ovary	n.r.	Kelly et al. (1983)
WC-1	Dermal tumour	Fibroblastic	Kelly et al. (1980)
W12	Dermal tumour	Fibroblastic	Zhang and Martineau (1999)

n.r. = not reported

## 1.8. Objectives

The thesis had two overarching objectives with three sub-objectives under each.

### A. Can cell lines be developed from walleye and used to study viral hemorrhagic septicemia virus (VHSV IVb)?

1. Does the thermobiology of walleye cells match the thermovirology of VHSV IVb?
2. Does temperature modulate the cellular tropism of VHSV IVb for walleye cells?
3. Can a cell line be developed to study the antiviral actions of dsRNA on VHSV IVb?

### B. Can cell lines from walleye be used to contribute to comparative cellular biology and physiology of vertebrates?

1. Can an endothelial cell line be developed for the first time from the bulbus arteriosus?
2. Can senescence-associated  $\beta$ -galactosidase (SA  $\beta$ -Gal) be used to identify the development of cellular senescence in cell cultures from walleye and other fish?
3. Do cell lines from walleye and other fish have acetylated  $\alpha$ -tubulin-containing structures, such as primary cilia?

## **CHAPTER 2.**

### **Development of a walleye cell line and use to study the effects of temperature on infection by viral hemorrhagic septicaemia virus (VHSV) group IVb\***

\* This chapter is a slightly revised version of the publication by Vo NTK et al. (2014). Development of a walleye cell line and use to study the effects of temperature on infection by viral hemorrhagic septicaemia virus (VHSV) group IVb. *J. Fish. Dis.* (In Press) doi:10.1111/jfd.12208 (Online November 21, 2013). The revisions centre on the origin of viral transcripts seen by RT-PCR within a few hours of infection and with heat-killed virus. The source of these transcripts had been speculated upon in the Materials and Methods and now additional conjecture about their origin is added to this paragraph. As well, three statements in the Results, and one sentence each in the Discussion and Figure legend 2.7 have been slightly modified so that no conclusions are drawn from the appearance of low transcript levels early in an infection.

## 2.1. INTRODUCTION

Although a well studied parameter for many aspects of fish biology, temperature in viral disease development is more complex and difficult to study because critical temperatures need to be known, separately and together, for two biological entities, fish and virus. An example of a relatively new combination is viral hemorrhagic septicaemia virus (VHSV) and walleye (*Sander vitreus*). VHSV is a rhabdovirus with 6 genes, N, P, M, G, NV and L, and causes the disease viral hemorrhagic septicaemia (VHS) (Purcell et al., 2012). Over the last decade, a unique VHSmV genotype, IVb, has appeared and spread in the Great Lakes region, causing mortality in a wide range of freshwater fish, including walleye (Al-Hussinee et al., 2011; Kim & Faisal, 2011). Walleye is likely the most widely stocked and important commercial and recreational freshwater fish species in North America (Fenton et al., 1996; Summerfelt, 2005). Knowing more about the role of temperature in the biology of VHS can help in developing strategies to restrict VHS spread and to understand VHSV IVb-associated fish kills (Goodwin & Merry, 2011; Eckerlin et al., 2011; VHSV Expert Panel and Working Group, 2010).

The influence of temperature on fish at the cellular level (i.e. cellular thermobiology) may be studied using in vitro experiments (e.g. using cell lines) (Bols et al., 1992). Fish cell lines can be conveniently incubated at different temperatures and their responses can be used to define three temperature ranges: zones of endurance, proliferation, and resistance (lethality) (Bols et al., 1992). These were meant to parallel the tolerance, growth and resistance zones of fish. The upper incipient lethal temperature (UILT) defines the upper boundary between tolerance and resistance (Beitinger et al., 2000). For a given species, cell cultures usually survive temperatures slightly higher than fish's UILT (Bols et al., 1992). Systematic studies on the response of cell lines from walleye to different temperatures have yet to be done because although a few walleye cell lines (WF, WF-2, WC-1, W12, WO, and We-2) have been described in the literature (Wolf & Mann, 1980; Kelly et al., 1980; Kelly et al., 1983; Wilensky & Bowser, 2005), these cell lines appear to have been lost. Their original characterization did suggest that proliferation was optimal at between 20-25 °C (Kelly et al., 1980; Wilensky & Bowser, 2005), but the responses to more extreme temperatures remain to be studied.

For the influence of temperature on viral diseases, the effect of temperature on the inert extracellular virion and on the replication cycle of the virus must be considered, which might be termed the thermovirology of a virus. In the case of extracellular VHSV IVb, the virion remained infective for weeks to months at 4 °C but rapidly lost infectivity at temperatures above 26 °C (Pham et al., 2011; Hawley & Garver, 2008). In the case of intracellular VHSV IVb, virus was produced at three temperatures in fathead minnow (*Pimephales promelas*) cell cultures: 10 °C, which appeared to be the lowest temperature examined, 15 °C, which was optimal, and 20 °C, which was the highest temperature to support viral replication (Winton et al., 2007).

In the current study, a walleye caudal fin cell line, WE-cfin11f, has been developed and used to define the thermobiology of walleye cells and to study how this intersects with the thermovirology of VHSV IVb. For the first time, VHSV is shown to be produced at 4 °C, which is in the lower resistance zone for walleye cells.

## **2.2. MATERIALS AND METHODS**

### **2.2.1. Fish**

Juvenile walleye of the Bay of Quinte stock were obtained from the White Lake Fish Culture Station of the Ontario Ministry of Natural Resources and maintained at 12°C at the Fish Pathology Laboratory at the University of Guelph (UG). One individual, approximately 16 cm in length, was euthanized with an overdose of 50 mgL<sup>-1</sup> benzocaine (Sigma) at UG and kept on ice for the 30 minute trip to the University of Waterloo (UW) where primary cell cultures were initiated. Fish were maintained and used according to the guidelines of the Canadian Council of Animal Care (CCAC) and the UG Animal Care Committee (UGACC).

### **2.2.2. Preparation of caudal fin primary cell cultures**

In a laminar flow hood the caudal fin was removed and cut into small fragments (explants). The explants were rinsed 5 times in Dulbecco's Phosphate Buffered Saline (DPBS, Cellgro) with antibiotics (200 U mL<sup>-1</sup> penicillin and 200 µg mL<sup>-1</sup> streptomycin, Thermo Scientific) and then transferred into plastic tissue culture vessels with Leibovitz L-15 medium (Hyclone, Thermo Scientific). The L-15 was supplemented with 10% fetal bovine serum (FBS, Sigma) and the above antibiotics. The tissue culture vessels were incubated at room temperature. As early as 30 h later, cells were migrating out of tissue explants and over the polystyrene growth surface. In 6-well tissue culture plates (BD Falcon), confluent monolayers were achieved as early as 3 days but subcultivation was not done until 3 weeks later. Subcultivation or passaging was done with Tryple (Invitrogen) and usually involved transferring the contents of a confluent vessel into two new vessels (1:2 split). During the early passaging, fibroblasts detached more rapidly than the epithelial cells and cultures enriched with either fibroblasts or epithelial cells were obtained. One culture with predominantly fibroblast-shaped cells was chosen for further propagation and was called the WE-cfin11f cell line.

### **2.2.3. Routine maintenance of cell lines**

In addition to WE-cfin11f, the EPC (epithelioma papulosum cyprini) cell line was used. EPC has commonly been used to propagate VHSV IVb (Al-Hussinee et al., 2010) and recently has been identified as being from fathead minnow (Winton et al., 2010). The cell lines were grown routinely in L-15 with 10-15% FBS in 25-cm<sup>2</sup> polystyrene flasks (BD Falcon) at 20-26°C. Subcultivation or passaging was done with TrypLE, which is a trypsin replacement enzyme manufactured by Invitrogen. TrypLE was used precisely as recommended by the manufacturer except all solutions and manipulations were done at room temperature.

### **2.2.4. Routine propagation of VHSV IVb**

The VHSV IVb was CEFAS strain U13653 originally isolated from infected freshwater drum (*Aplodinotus grunniens*) from Lake Ontario in 2005 (Lumsden et al., 2007) and was routinely propagated on confluent cultures of EPC in L-15 with 2% FBS. After 10 days post-infection (p.i.) at 14 °C, EPC monolayers were completely lysed and the medium was collected and centrifuged at 4500 × g for 5 min at 4 °C. The supernatant was syringe-filtered through 0.2-µm membranes (Pall Corporation), aliquoted and stored at -80 °C as previously described (Pham et al., 2011). As described previously (Pham et al., 2011), aliquots were titred for VHSV on EPC and expressed as tissue culture infectious dose TCID<sub>50</sub> mL<sup>-1</sup>.

### **2.2.5. General characterization of WE-cfin11f**

WE-cfin11f was passaged at approximately 1:2 every week and cryopreserved at a range of passage levels. Cryopreservation was done in L-15 with 10 % FBS and 10 % dimethyl sulfoxide (DMSO) (Sigma) as described for fish cell lines in general (Bols & Lee, 1994). Briefly, pellets of approximately 5 × 10<sup>6</sup> cells were resuspended in 1 mL of ice-cold cryopreservation medium and frozen in the gas phase of liquid nitrogen overnight and then fully immersed in the liquid nitrogen for long-term storage.

WE-cfin11f was authenticated as walleye by DNA barcoding for cytochrome c oxidase subunit 1 (COX1) gene. This was performed at the Biodiversity Institute of Ontario (Guelph, ON, Canada) using a PCR primer cocktail designed for teleosts as

previously described for fish cell lines in particular (Kawano et al., 2010; Sansom et al., 2013). Briefly cells were placed on indicating FTA<sup>R</sup> cards and DNA extracted according to the manufactures instructions (Whatman<sup>R</sup>, Piscataway, NJ, USA). Subsequent steps were done as described previously (Cooper et al., 2007) with a PCR primer cocktail developed for fishes (Ivanova et al., 2007). A 655 bp region of the walleye COX1 gene was sequenced. DNA sequence was compared and matched to the species identification in both Barcode of Life Data (BOLD) (Ratnasingham & Hebert, 2007) (<http://www.barcodinglife.org>) as well as the NCBI BLAST databases (<http://www.ncbi.nlm.nih.gov/BLAST>). The WE-cfin11f samples were run along with samples of the putative walleye cell line WF-2. WE-cfin11f was confirmed to be walleye while WF-2 was found to be bluegill sunfish (*Lepomis macrochirus*) (Sansom et al., 2013).

WE-cfin11f cultures were stained with May-Grünwald/Giemsa to evaluate the organization and shape of cells within cultures and with the “Senescence Cells Histochemical Staining Kit” (Sigma) to detect senescence-associated  $\beta$ -galactosidase (SA  $\beta$ -Gal) Activity. SA  $\beta$ -Gal activity was done as described previously for a rainbow trout (*Oncorhynchus mykiss*) cell line (Kawano et al., 2010) and yielded blue/green coloring within positive cells. Early passaged walleye heart cell cultures were used as positive controls.

#### **2.2.6. Characterizing the thermobiology of the WE-cfin11f cell line**

The first step in characterizing the thermobiology of WE-cfin11f was to grow cells in L-15 with 10 % FBS at room temperature in flasks until confluent monolayers formed and then to incubate the flasks at different temperatures and to monitor the integrity of the monolayer over a week by phase contrast microscopy. The temperatures at which the monolayer remained intact were defined as being in the endurance zone and were from 1 to 32 °C. For temperatures, inside the endurance zone, cell proliferation was measured as described in the section below entitled ‘proliferation zone’. For temperatures within the endurance zone at which proliferation did not occur, the ability of cells to persist was measured as defined in the section entitled ‘lower resistance zone’. For temperatures

outside the endurance zone, cell viability was evaluated as described below in the section entitled ‘upper lethal zone’.

#### Proliferation zone

WE-cfin11f cells in L-15 with 10 % FBS were added to 12-well plates at  $5 \times 10^4$  cells per well and allowed to attach overnight at 20 °C. At this point 6 wells were counted to establish the zero time reference value. The remaining plates were then incubated at 10, 14, 20, 26 or 32 °C. For each temperature, six wells were counted on days 2, 5 and 8 with a Z2 Coulter particle counter (Beckman Coulter, Brea, CA). The numbers of cells were expressed as a percentage of the cells at time zero.

#### Lower resistance zone

The ability of WE-cfin11f cells to persist at low temperatures was evaluated by first plating them in L-15 with 10 % FBS in 12-well plates but unlike for proliferation, at the much higher density of  $3.5 \times 10^5$  cells per well. After being incubated overnight at 20 °C, the cells had attached and formed a nearly confluent monolayer. At this point 4 wells were counted to establish the zero time reference value. The remaining plates were then placed at 1 or 4 °C and incubated for up to a month without changing the medium. The numbers of cells in wells were counted with the Coulter counter on days 7, 14 and 28. The numbers of cells were expressed as a percentage of the cells at time zero.

#### Upper lethal zone

The survival of WE-cfin11f at 37 °C was evaluated by phase contrast microscopy observations and by evaluating cell viability with the indicator dye, Alamar Blue® (Invitrogen). Cells in L-15 with 10 % FBS were put into 24-well plates at  $1.5 \times 10^5$  cells per well and allowed to attach overnight at 20 °C. The plates were then put at 37 °C and evaluated immediately and then periodically over the next 20 h. For Alamar Blue, which indicates cellular metabolism, the method of use was done as described previously in step-by-step detail (Dayeh et al., 2003) and just recently updated (Dayeh et al., 2013). Living cells reduce Alamar Blue to a fluorescent product that is measured with a fluorescence plate reader as relative fluorescence units (RFUs). The RFUs were

expressed as a percentage of the RFUs recorded in wells immediately upon being shifted to 37 °C.

### 2.2.7. Characterizing the thermovirology of VHSV IVb in WE-cfin11f

The general steps for infecting cultures are described here, and subsequent sections detail the viral titre, the specific culture vessel used, and the p.i. exposure conditions and times. WE-cfin11f cells were seeded into vessels and allowed to attach overnight at 26 °C. Vessels were then placed at 1, 4, 14, 20 or 26 °C for 24 h prior to exposure to VHSV IVb in L-15 with 2 % FBS at these temperatures for 2 h. Viral exposure was terminated by removing the medium, washing the vessels with PBS, and adding L-15 with 2 % FBS.

**Table 2.1. Primers used in RT-PCR experiments**

Primer	Primer sequence (5'→3')	Product length (bps)	Annealing temperature (°C)	Reference
VHSV-IV-N	F - AGGACCCCAGACTGTGCAAGC R - TCCGCCTGGCTGACTCAACA	605	65	Pham et al., 2013
VHSV-IV-P	F - AGGAGAACGGGAAGAAGACCGACA R - TCCAACCTCCGCCTTGATTGCCT	311	53	Pham et al., 2013
VHSV-IV-M	F - TCAACCATCCTGACGGAAGGCA R - TGATCAGGGTTTTGCTCCGGGT	217	53	Pham et al., 2013
VHSV-IV-G	F - CCCCGAACCTTCCTGCATCTGG R - CCCGTCAGTGTGTGTCTATCCG	738	65	Pham et al., 2013
VHSV-IV-Nv	F - ACCCAAGCAACTACCTCAACTGTGA R - AGAGTCCAGGATCCGACGGTCT	228	65	Pham et al., 2013
VHSV-IV-L	F - TGAGAGTGGGACAAGAAAGCTGGGA R - GCACACGCTGTCCATCCTTGTC	512	65	Pham et al., 2013
$\beta$ -actin	F - ATCGTGGGGCGCCCCAGGCACC R - CTCCTTAATGTACGCACGATTTC	514	53	Brubacher et al., 2000

### Detecting viral transcripts by RT-PCR

Cultures of WE-cfin11f in 25-cm<sup>2</sup> flasks were infected with VHSV IVb at 10<sup>7</sup> TCID<sub>50</sub> mL<sup>-1</sup> (or at MOI of 10) and analyzed at various times afterwards by reverse-transcription polymerase chain reaction (RT-PCR) for transcripts of all 6 VHSV genes: N, P, M, G, Nv and L. The primers are listed in Table 1; the primers and the methods were as described recently for rainbow trout cell lines infected with either VHSV IVa or IVb (Pham et al., 2013). The methods are presented in more detail below.

For RNA extraction, cells were collected by trypsinization and washed with 5 mL of ice-cold PBS. The cell pellets were resuspended into 100 µL of D-PBS and transferred to a microcentrifuge tube. The tubes were spun at 3000 × g for 3 minutes to pellet the cells and PBS was removed from the pellet. To lyse cells the pellets were pipette-mixed 5 times in 350 µL of RTK-lysis buffer from the E.Z.N.A. Total RNA Kit I (Omega Bio-Tek). The tubes were allowed a 30 minute incubation period on ice then the cell lysis suspension was frozen at -80 °C until all RNA samples were collected. The RNA extraction was done according to manufacturer's specifications using the Total RNA Kit I (Omega Bio-Tek). RNA was eluted with 40-50 µL of DEPC-treated water.

For cDNA synthesis, 1000 ng of total RNA from each sample was added to a 12.6-µL reaction where it was treated with DNase I at 37 °C for 30 minutes. DNase I was subsequently inactivated by adding 2.6 µL of EDTA and then heating to 70 °C for 10 minutes. Next a cDNA synthesis reaction was done according to the manufactures specifications using the Revert Aid H Minus First Strand cDNA Synthesis Kit (Thermo Scientific). The cDNA synthesis reaction program (25 °C for 10 min, 42 °C for 60 min, 70 °C for 10 min and hold at 4 °C) was carried out using an Eppendorf Mastercycler thermocycler. cDNA was diluted with 25 µL of DEPC-treated water prior to being used as template in PCR, which was done in PCR tubes in a 25-µL reaction.

PCR reagents from Thermo Scientific were used. Each tube contained: 3 µL of cDNA template, 2.5 µL of Taq buffer with KCl, 0.2 mM of each dNTP, 1.5 mM MgCl<sub>2</sub>, 0.625 units Taq DNA polymerase, 0.5 µM of forward primer and 0.5 µM of reverse primer. As previously described by Pham et al. (2013). The PCR program carried out by the Eppendorf Mastercycler thermocycler was as follows: initial denature at 95 °C for 3 min,

denature for 1 min at 94 °C, anneal for 45 sec, extend at 72 °C for 45 sec, repeat the three previous steps for 35 cycles and final extension at 72 °C for 7 min. PCR products were resolved on a 1% agarose gel with Gel Red (1:10,000, v/v) at 80 V for 45 min. The agarose gels were visualized under UV transillumination in an Alpha Innotech fluorchem 8000 imager connected to AlphaImagerHP software.

Controls were cultures that had not been exposed to VHSV IVb or had been exposed to VHSV IVb that had been heated at 65 °C for 60 min in order to kill the virus. For cultures receiving heat-killed virus, transcripts were occasionally detected. These are thought not to be products of the culture and of indicating the start of a viral infection for the following reasons. The transcripts were seen only in some experiments with heat-killed virus, and when they did appear, only variable subsets of the six viral transcripts appeared and their intensity did not increase with time post infection.

The origin of these PCR products is a matter of speculation. They could represent viral transcripts that were in the virus preparation and have been either taken up by cells or stuck to the surface of cells, so despite the rinsing of cultures, these viral RNAs were extracted. The PCR products might also represent priming from viral genomic RNA. Despite the cultures having been rinsed after a period of exposure to the virus, some virus might have remained in cultures adsorbed to cells or to culture surface. When RNA was extracted from cultures, viral genomic RNA along with viral mRNA would have been isolated together with cellular RNAs. From this total RNA, cDNA was synthesized, using oligoDT primers for first strand synthesis, which should have ensured only mRNA was copied. However internal poly(A) priming of genomic RNA might have generated cDNAs. An additional complexity is the very recent discovery about another rhabdovirus, vesicular stomatitis virus (VSV) (Shimizu et al., 2014). Surprisingly for a non-retroviral RNA virus, VSV DNA was found in cells upon infection of some human primary cultures and cell lines (Shimizu et al., 2014). The VSV DNA was single-stranded and corresponded to the viral genes but with the opposite polarity to the coding sequence and was found in the cytoplasm in a non-integrated form. Whether such events occur with VHSV IVb and walleye cells and contribute to the suspicious PCR products of this thesis is unknown. Overall the simplest way to avoid the problem of these PCR products in the future would be to use a lower MOI or purified virus so that washing

cultures leaves behind only cells and viruses associated with cells. Yet the cause of the problem might be interesting to explore in the future because processes with biological meaning might be revealed. However, at this time, these methodological complexities have led to the RT-PCR data being treated conservatively: only bands that have obviously increased in intensity over time are interpreted as representing viral RNA synthesis.

#### Detecting viral N protein by western blotting

Cultures of WE-cfin11f in 25-cm<sup>2</sup> flasks were infected with VHSV IVb at 10<sup>7</sup> TCID<sub>50</sub> mL<sup>-1</sup> (or at MOI of 10), and at various times afterwards protein cell lysates prepared. The lysates were electrophoresed and western blotting was performed to detect the N protein among the separated polypeptides. Previously, the procedures have been described in detail (DeWitte-Orr et al., 2007). Briefly the cell lysates were prepared with 1% (w/v) NP-40 lysis buffer containing protease inhibitor cocktail (Qiagen). Protein concentrations were determined by Bicinchoninic Acid (BCA) protein assays (ThermoFisher) as instructed by the manufacturer. Sodium dodecyl sulphate polyacrylamide gel electrophoresis (SDS- PAGE) was performed in a mini-PROTEAN<sup>R</sup> Tetra Cell (Bio-Rad, Mississauga, ON). Polypeptides were electro-transferred overnight at 4 °C at 23 V with a Bio-Rad mini-Trans Blot cell to nitrocellulose membrane (Bio-Rad). Equal loading was demonstrated with a 0.1% Ponceau S stain in 5% (w/v) acetic acid. The membrane was probed with a mouse monoclonal antibody (IP5B11) for VHSV N protein (Lorenzen et al., 1988). IP5B11 was used at 1:600 as described previously (Tafalla et al., 2008; Pham et al., 2013). For detecting a reference cellular protein, a rabbit polyclonal anti-actin antibody (Sigma) was used at 1:400. The secondary antibodies were either goat anti-mouse IgG or goat anti-rabbit IgG conjugated to alkaline phosphatase (Sigma) used at 1:20,000. Protein bands were detected by NBT/BCIP substrate reaction.

#### Cytopathic effect (CPE)

The potential of WE-cfin11f cultures to succumb to the CPE of VHSV IVb was examined at different temperatures. A range of MOI was tested, including a very high

MOI of 175 to 1 (equivalent to  $10^8$  TCID<sub>50</sub> mL<sup>-1</sup>), because the interest was in defining the temperatures at which damage could or could not take place. As a high MOI can possibly block infection due to auto-interference, a MOI as small as 0.002 to 1 was also tested. A low pH, such as 6.5 or less, can block the spread of VHSV between cells and impede the development of CPE (Mas et al., 2004). Therefore, the pH of the culture medium, L-15 with 2 % FBS, in which cells were exposed to the virus and maintained p.i. for CPE development, was noted. At temperatures of 4, 14 and 26 °C, L-15 with 2 % FBS had a pH of 7.1. With cells for 24 h, the pH of the medium was 7.3. With cells for 14 days either at 4 °C or 14 °C, pH of the medium was 7.0. After 14 days post VHSV IVb infection at both 4 °C and 14 °C, pH of the conditioned medium was 7.1.

CPE was monitored as a change in cell morphology and attachment through phase contrast microscopy observations and by evaluating the loss of cell viability with the indicator dyes, Alamar Blue® (Invitrogen) and 5'-carboxyfluorescein diacetate acetoxymethyl ester (CFDA-AM, Molecular probes). CFDA AM provides a measure of cell membrane integrity and like Alamar Blue is recorded as RFUs (Dayeh et al., 2013). The two dyes were used as detailed by Dayeh et al. (2013) and more specifically for CPE due to VHSV IVb as described by Pham et al. (2013). WE-cfin11f cells in L-15 with 10 % FBS were added to 24-well plates at  $1 \times 10^5$  cells per well and allowed to attach for two days at 26 °C. The medium was removed and wells received L-15 with 2 % FBS and ten-fold serial dilutions of VHSV IVb stock with a viral titre of  $1.33 \times 10^8$  TCID<sub>50</sub> mL<sup>-1</sup>. The plates were then incubated at 1, 4, 14, 20, and 26 °C and observed periodically by phase contrast microscopy for up to 35 days. Cell viability was evaluated in 3 wells for each different viral titre after 14 days. The RFUs were expressed as a percentage of the RFUs in control wells without virus.

#### Measuring production of viral titre

Medium from WE-cfin11f cultures that had been exposed to VHSV IVb at  $10^7$  TCID<sub>50</sub> mL<sup>-1</sup> (or at MOI of 10) in 6-well plates for 2 h was titred on EPC for VHSV IVb in order to determine the capacity of the walleye cells to produce infectious virus at different temperatures for up to 28 days. Medium from 3 replicate wells for each p.i. condition was collected and centrifuged at  $500 \times g$  for 4 min at 4 °C. The supernatants

were then transferred to new collection tubes and ten-fold serial dilutions were prepared in L-15 with 2% FBS. Each dilution for each culture conditions was applied to 6 wells with monolayers of EPC in 96-well plates. The plates were incubated at 14 °C for 14 days and then observed by phase contrast microscopy and scored for CPE. Viral titres were as expressed as TCID<sub>50</sub> mL<sup>-1</sup>.

#### Shifting cultures infected at 4 °C into the proliferation zone

WE-cfin11f cultures in 25-cm<sup>2</sup> flasks were exposed to 10<sup>7</sup> TCID<sub>50</sub> mL<sup>-1</sup> VHSV IVb for 2 h at 4 °C and after rinsing left at 4 °C or shifted to either 14 or 26 °C. These cultures were examined by phase contrast microscopy for CPE at various times for up to 35 days p.i.. Medium from some cultures was collected at 14 days p.i. and titred as described above.

## 2.3. RESULTS

### 2.3.1. Development and general characterization of WE-cfin11f

Although both epithelial and fibroblast-like cells migrated out from caudal fin explants (Fig 2.1A), TrypLE treatment preferentially detached fibroblasts, leading to the continuous propagation of cultures with predominantly fibroblast-shaped cells (Fig 2.1B). This is the WE-cfin11f cell line. WE-cfin11f required fetal bovine serum (FBS) for growth (data not shown) and was maintained routinely in L-15 with 10 % FBS at room temperature and subcultured with trypsin. WE-cfin11f has now been passaged 60 times over 2.5 years. During this time the cultures consistently had cells with a fibroblastic morphology (Fig. 1B) that at confluency had parallel alignment but in older confluent cultures long bipolar cells appeared intertwined on top of the monolayer (Fig. 2.1C-D). In early passage cultures no staining for SA  $\beta$ -Gal was seen with WE-cfin11f, whereas a walleye heart culture stained strongly (Fig. 2.1E-F). WE-cfin11f was successfully cryopreserved at a wide range of passage levels. The cell line was confirmed as walleye by DNA barcoding: sequencing of a 655 bp region of the cytochrome c oxidase I gene, followed by sequence alignment analysis with the NCBI BLAST search engine, returned a 100% match for *S. vitreus* cytochrome c oxidase subunit I (Accession No EU524375).

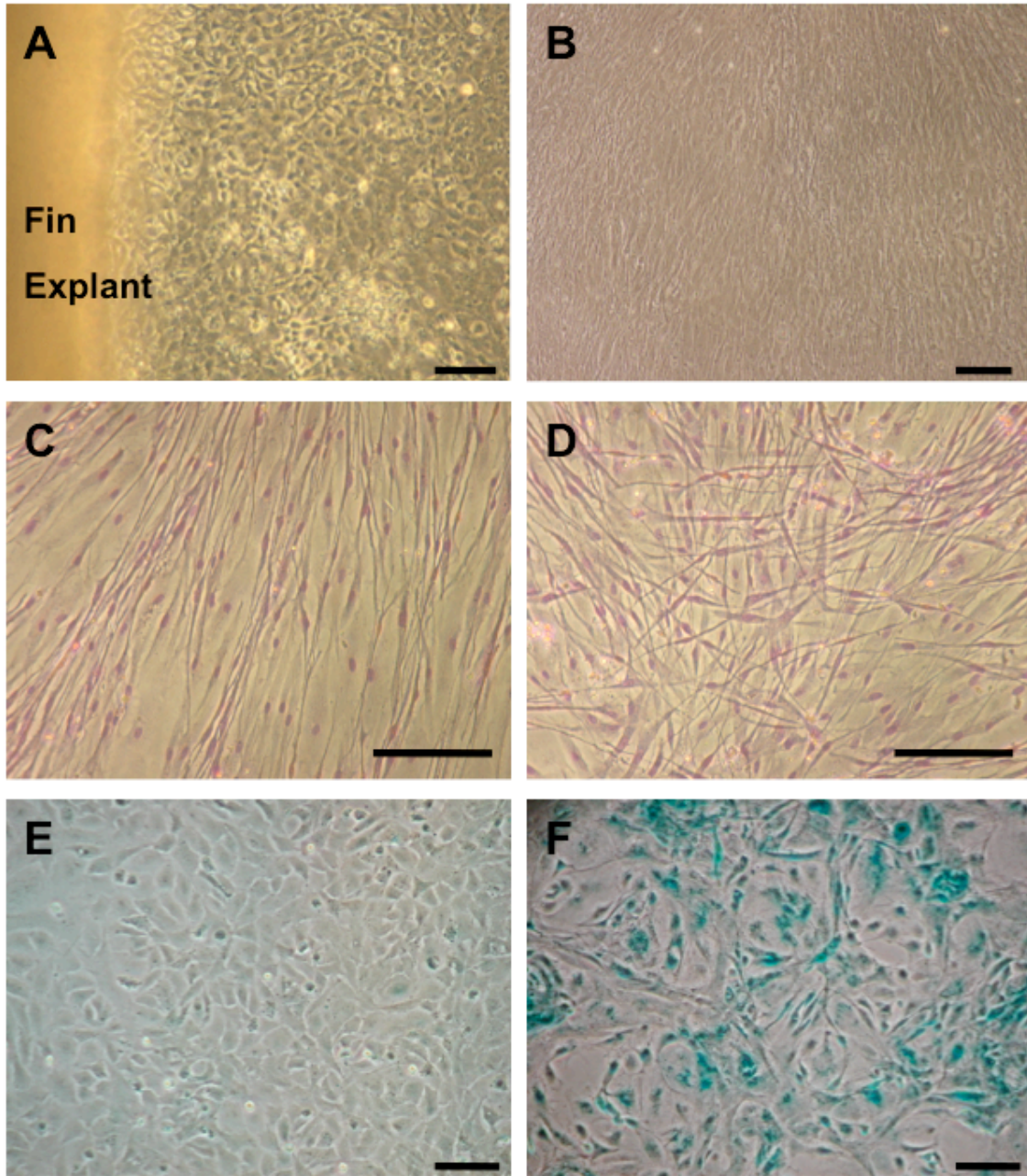


**Figure 2.1. Development of walleye caudal fin cultures.** (A) Epithelial and fibroblastic cells migrated directly out of the fin explants after 2 days in cultures. (B) Morphology of the walleye caudal fin fibroblastic cell line WE-cfin11f at passage 30 at 26 °C. Giemsa-stained cultures showed organization of cells in parallel alignment (C) or intertwined fashion (D). Senescent-associated  $\beta$ -galactosidase staining was negative in WE-cfin11f at passage 5 (E) and positive in walleye heart culture at passage 4 (F). Scale bar = 100  $\mu$ m.

### **2.3.2. Thermobiology of WE-cfin11f cultures**

When monolayers of WE-cfin11f cultures were established at room temperature and then shifted to temperatures from 1 °C to 37 °C, the monolayers remained adherent to the plastic growth surface for at least 7 days at temperatures from 1 °C to 32 °C. This is referred to as the endurance zone. Temperatures above 32 °C are referred to as the upper lethal zone. The endurance zone has been divided into the lower resistance zone and the proliferation zone.

#### Proliferation zone

Within the endurance zone, the temperatures at which cells in WE-cfin11f cultures maintained a fibroblast-like shape and proliferated were defined as the proliferation zone. The lower limit of this zone was not precisely defined because only 4 and 10 °C were studied and not temperatures in between. Yet as mentioned later, cells in cultures at 4 °C adopted an epithelial-like morphology and failed to grow (Fig 2.2A). By contrast at 10 °C the cells maintained a fibroblast-like morphology and increased slightly in number over 7 days (data not shown). At the upper limit, 32 °C, the fibroblast morphology was maintained for at least 7 days and cell number increased slightly over the first 3 days but appeared to decline back to the starting value by 8 days (Fig 2.2B). Cell proliferation was optimal at 20 °C and 26 °C but could occur even at 14 °C (Fig 2.2B).

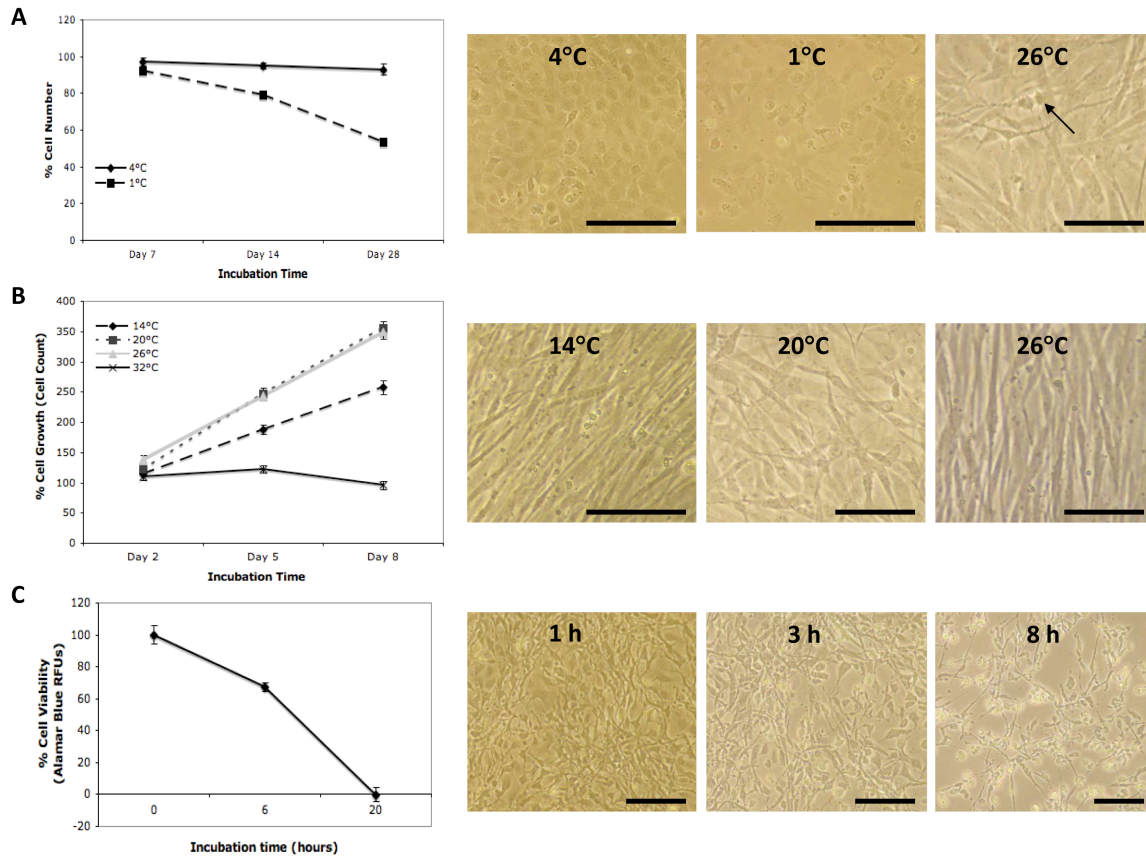


**Figure 2.2. Growth, viability, and morphology of WE-cfin11f cells at different temperatures.** In row A cultures at 1 and 4 °C were examined for cell number (graph) and photographed after 14 days (4 °C & 1 °C). Mitotic figures disappear from cultures with time at these temperatures and to illustrate a mitotic figure (arrow) the photograph of a culture at room temperature is presented on the far right. In row B cultures at 14, 20, and 26 °C were examined for cell number (graph) and photographed after 14 days (14 °C, 20 °C & 26 °C). In both row A and B, cell number was determined in 4 and 6 wells of 6 well plate respectively with a Z2 Coulter counter, expressed as a % of the starting values for graphical presentation, and subject to one-way analysis of variances (ANOVA). If the ANOVA was significant, Dunnett’s test was performed to find values significantly different from the time zero values and these are marked on the graphs with an asterisk. In row C, cultures at 37 °C were examined for viability with Alamar Blue (graph) up to 20 h and photographed at 1 h, 3 h and 8 h. For each time point, RFUs from Alamar Blue were recorded for 8 wells in a 96 well plate, expressed as a % of the starting values for the graphical presentation, and subject to ANOVA and Dunnett’s post test. In all cases a p-level <0.05 was considered as significantly different. Statistical analyses were done using GraphPad InStat (version 3.00 for Windows 95, GraphPad Software, San Diego California USA, [www.graphpad.com](http://www.graphpad.com)). Scale bar = 100 μm.

### Upper lethal zone

At temperatures above 34 °C, cultures deteriorated in less than 7 days, and the higher the incubation temperature the more rapid was the deterioration. Within 1 h at 37 °C, the boundaries of cells began to draw away from one another and by 8 h, most cells had string-like morphologies and were detaching from the plastic growth surface (Fig 2.2C). By 20 h at 37 °C, cell viability had been completely lost as measured with Alamar Blue, which evaluates cellular energy metabolism (Fig 2.2C).

### Lower resistance zone

Over 2 weeks at 1 °C and 4 °C, cell number remained largely unchanged, but the cells adopted an epithelial-like morphology (Fig 2.2A) and mitotic figures disappeared. For further 2 weeks at these temperatures cell number remained steady for 4 °C cultures but declined for cultures at 1 °C (Fig 2.2A). As the WE-cfin11f cells at these temperatures neither died quickly nor proliferated, these temperatures are referred to as the lower resistance zone rather than the lower lethal zone.

### **2.3.3. Thermovirology of VHSV IVb in WE-cfin11f cultures**

The walleye cell cultures were infected with VHSV IVb at temperatures in the proliferation zone (10 to 32 °C), the upper lethal zone (>32 °C) and the lower resistance zone ( $\leq 4$  °C). Cultures were monitored for all 6 viral mRNAs by RT-PCR, the N protein by western blotting, cytopathic effect (CPE) by microscopy and viability dyes, and viral production, expressed as TCID<sub>50</sub>.

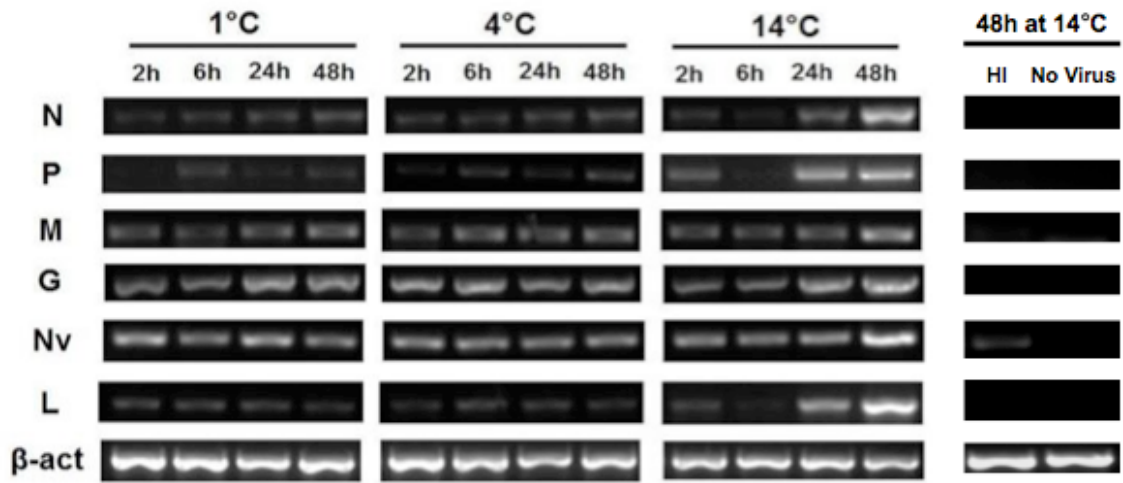


**Figure 2.3. Expression of viral transcripts in WE-cfin11f at various temperatures.** Cultures of WE-cfin11f at 1 °C, 4 °C, or 14 °C were infected with VHSV IVb at  $10^7$  TCID<sub>50</sub> mL<sup>-1</sup> (or at MOI of 10) and RNA collected 2 h, 6 h, 24 h, and 48 h p.i. Control WE-cfin11f cultures received either heat inactivated (HI) VHSV IVb or no virus and RNA collected 48 h later. cDNA was synthesized and amplification of viral transcripts was done by RT-PCR. β-actin (β-act) was used as an internal control.

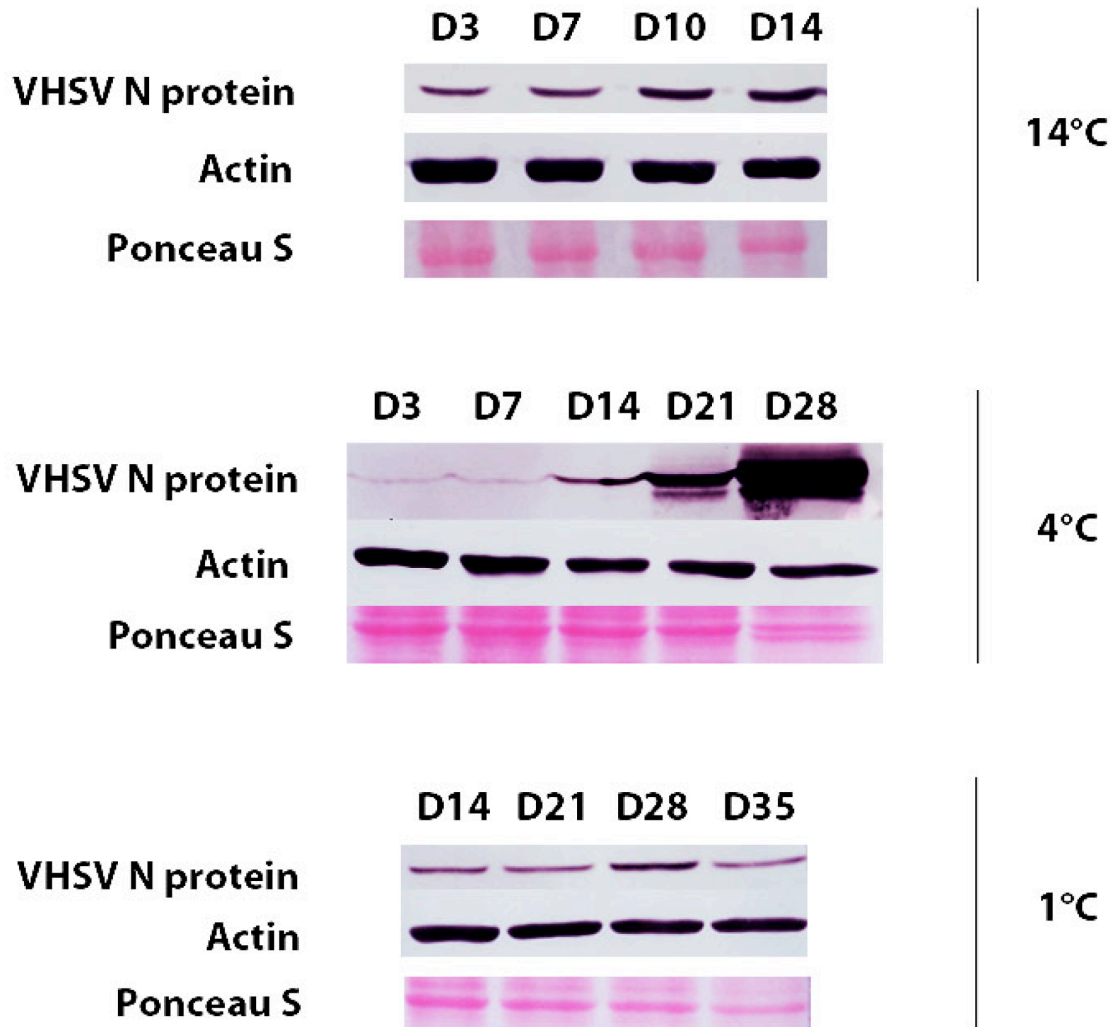


**Figure 2.4. Expression of VHSV N protein in infected WE-cfin11f at low temperatures.** WE-cfin11f cells were infected with VHSV IVb at  $10^7$  TCID<sub>50</sub> mL<sup>-1</sup> (or at MOI of 10) at 14 °C, 4 °C, or 1 °C. Cells were collected on selected days p.i. and lysed in 1% NP-40 protein lysis buffer. Protein samples were equally loaded onto the 12% denaturing polyacrylamide gels. After proteins were transferred onto nitrocellulose membranes, the blots were blocked in 5% skim milk in TBS-T and probed with mouse monoclonal IgG against VHSV N protein and subsequently goat-anti mouse IgG conjugated with alkaline phosphatase. The protein bands were detected with NBT/BCIP substrates.

### Infection in the proliferation zone

In the proliferation zone, productive infections occurred at 14 °C but not at 26 °C. Generally VHSV propagation is found to be optimal in cell cultures at 14 °C (VHSV Expert Panel and Working Group), and 14 °C was optimal for the combination of VHSV IVb and WE-cfin11f. By contrast, 26 °C was optimal for WE-cfin11f growth but a productive VHSV IVb infection was not established at this temperature.

At 14 °C bands representing all six viral mRNAs became prominent by 48 h (Fig 2.3). The N protein became evident as early 3 days p.i. and accumulated slightly over the next 11 days (Fig 2.4). Further time points could not be examined for N protein because the cultures began to be destroyed by viral CPE. When cultures had been inoculated with various TCID<sub>50</sub>s of VHSV IVb and incubated for 14 days at temperatures within the proliferation zone, the proportion of viable cells depended on the TCID<sub>50</sub> and the incubation temperature. Cultures receiving 10<sup>3</sup> to 10<sup>6</sup> TCID<sub>50</sub> and incubated at 14 and 20 °C had viable cells but cultures getting 10<sup>8</sup> TCID<sub>50</sub> had none, as measured with the indicator dyes, Alamar Blue (Fig 2.5A) and CFDA AM (Fig 2.5B). By contrast no loss in cell viability was seen in cultures receiving up to 10<sup>8</sup> TCID<sub>50</sub> and incubated for 14 days at 26°C (Fig 2.5). At 14 °C, cultures produce virus with the viral titre reaching a maximum at 14 days p.i. (Fig 2.6A). As viral titre becomes high, the monolayer of WE-cfin11f becomes destroyed (Fig 2.6B).

At 26 °C, VHSV IVb transcripts were detected inconsistently at 2 h and never at 48 h p.i., and this inconsistency suggests these transcripts were inconclusive evidence for the entry of the virus and expression of viral genes. N protein could not be detected in cell lysates from cultures 7 days p.i. at 26 °C (Fig 2.7). Together, these results suggest that VHSV IVb fails to enter the cells and begin replication at 26 °C.

### Infection in the upper lethal zone

At 37 °C, the cultures deteriorated quickly (Fig 2.2C). Sufficient RNA for RT-PCR could be collected for the first 2 h at 37 °C but not for later periods. For this 2-h period, the viral transcripts were seen only sometimes and not all six at the same time, suggesting that they have not risen from an infection at 37 °C.

### Infection in the lower resistance zone

In WE-cfin11f cultures at 1 °C, N protein was detected. The N protein was monitored by Western blotting but was seen inconsistently in the first 14 days p.i. so analysis was concentrated on cultures at later time points. Over the period of 14 to 35 days p.i. at 1 °C, the N protein band was seen consistently but the intensity of the band was relatively constant (Fig 2.4). In cultures at 1 °C no signs of CPE were seen in the first 2 weeks. At later time points a few cells began to shrivel and lyse, but this also happened in cultures without virus, so any cell death could be due either to low temperature, virus or both. When infected and continuously incubated at 1 °C, WE-cfin11f cultures failed to release infectious VHSV IVb over 35 days (data not shown).

At 4 °C, N protein was detected as early as 3 days p.i.. The intensity of the N protein band increased dramatically during the 4<sup>th</sup> week p.i. (Fig 2.4). CPE developed over 2 weeks at the highest infectious dose, but generally CPE developed much slower at 4 °C than at 14 °C. At 4 °C WE-cfin11f cultures produced and released VHSV IVb. However, these processes were slower in cultures at 4 °C than at 14 °C (Fig 2.6A). Ultimately the same amount of virus was produced but this took 28 days p.i. at 4 °C and just 14 days p.i. at 14 °C (Fig 2.6).

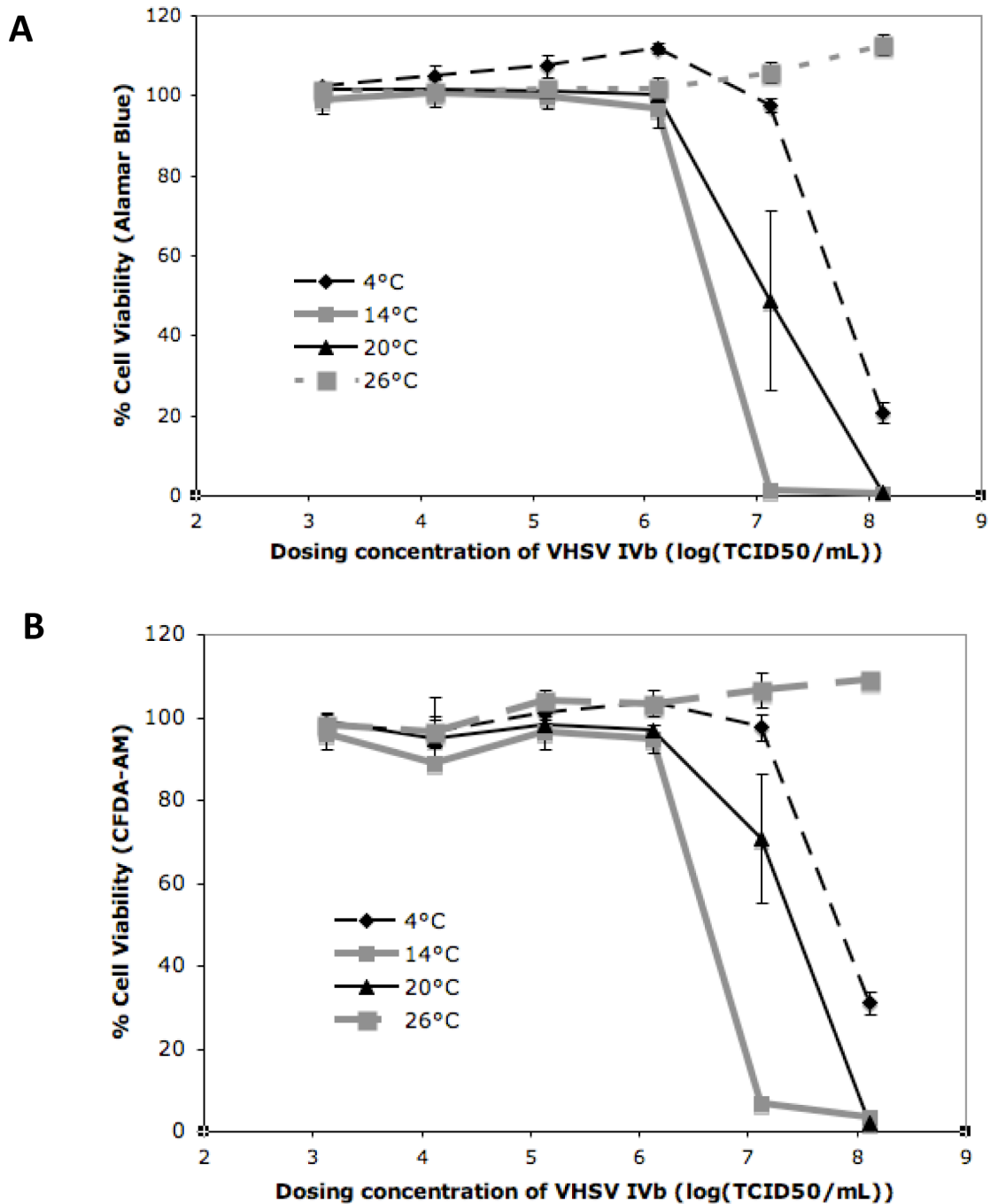


**Figure 2.5. Cell Viability of WE-cfin11f infected with VHSV IVb at different temperatures.** Cells were seeded in 24-well plates and inoculated with VHSV IVb at different titres. Infected cultures (n=3) were incubated at either 4 °C, 14 °C, 20 °C or 26 °C for 14 days. Cell viabilities were determined by Alamar Blue (A) and CFDA-AM (B) fluorescent dyes which measured as relative fluorescence units (RFUs) of infected cultures compared to non-infected control cultures. Each point is the mean % from the control and the bars are the standard deviation.

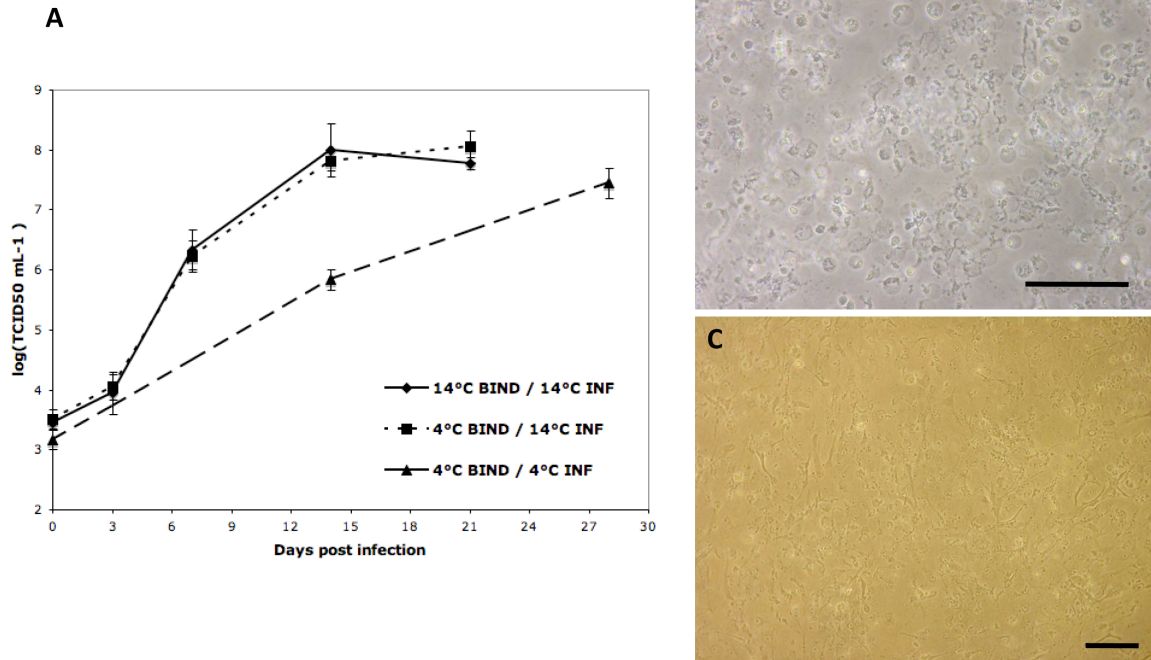


**Figure 2.6. WE-cfin11f supported VHSV IVb production at low temperatures.** VHSV IVb were allowed to “bind” to WE-cfin11f cultures in 6-well plates for 2 h at 4 °C or 14 °C. Then the non-binding viral particles were washed off. Cultures were then incubated at 14 °C for up to 21 days or at 4 °C for up to 28 days. Conditioned media from triplicate wells were collected on selected days and titred on EPC cultures to enumerate the number of viral particles produced and released (A). Each point is the mean and the bars are the standard deviation. Cytopathic effects of infected cultures at 14 °C on day 8 (B) or at 4 °C on day 28 (C). Scale bar = 100 μm.

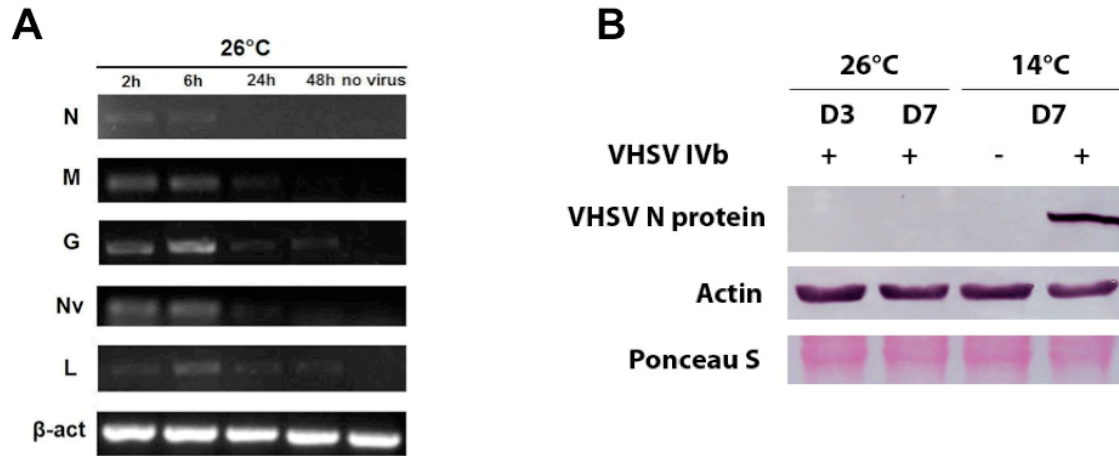


**Figure 2.7. RT-PCR and Western blot analysis of WE-cfin11f cells infected with VHSV IVb at 26 °C.** Cells were infected with VHSV IVb at 26 °C and total RNA or protein was extracted for RT-PCR or Western blotting analysis, respectively.

### Shifting cultures infected at 4 °C into the proliferation zone

WE-cfin11f cultures were exposed to VHSV IVb for 2 h at 4 °C and after rinsing shifted either to 14 °C or 26 °C and monitored for CPE and viral production. CPE developed in the cultures shifted to 14 °C but not in cultures transferred to 26 °C. VHSV IVb was produced in cultures shifted to 14 °C but not in cultures moved to 26 °C. Viral production was similar in cultures shifted to 14 °C as in cultures continuously incubated at 14 °C (Fig 2.6 & 2.8).

Cultures were exposed to VHSV IVb for 2 h at 4 °C, rinsed, and incubated further at 4 °C for 1, 2, 3 or 7 days before being shifted to 14 °C or 26 °C. Again cultures moved to 14 °C developed CPE and produced virus over the next two weeks, and again cultures moved to 26 °C failed to produce virus.

The development of CPE was more complex for shifts to 26 °C. For cultures shifted after 1 to 3 days at 4 °C, no CPE developed during a 3-week incubation at 26 °C. However, if the cultures had been at 4 °C for 7 days before the shift, spots of CPE appeared in the monolayer 5 days after the shift (Fig 2.8). Yet for cultures that had not been shifted (control cultures) and continued to be incubated at 4 °C, CPE did not develop in 5 days. With longer incubations, the control cultures and shifted cultures behaved contrastingly. In cultures continuously incubated at 4 °C (control cultures), CPE did develop over the next 3 weeks. Yet for cultures shifted to 26 °C, the areas of CPE began to be filled in with apparently healthy cells and disappeared over 3 weeks. Thus the CPE was transient at 26 °C and cultures infected at 4 °C appeared to recover by incubation at 26 °C.

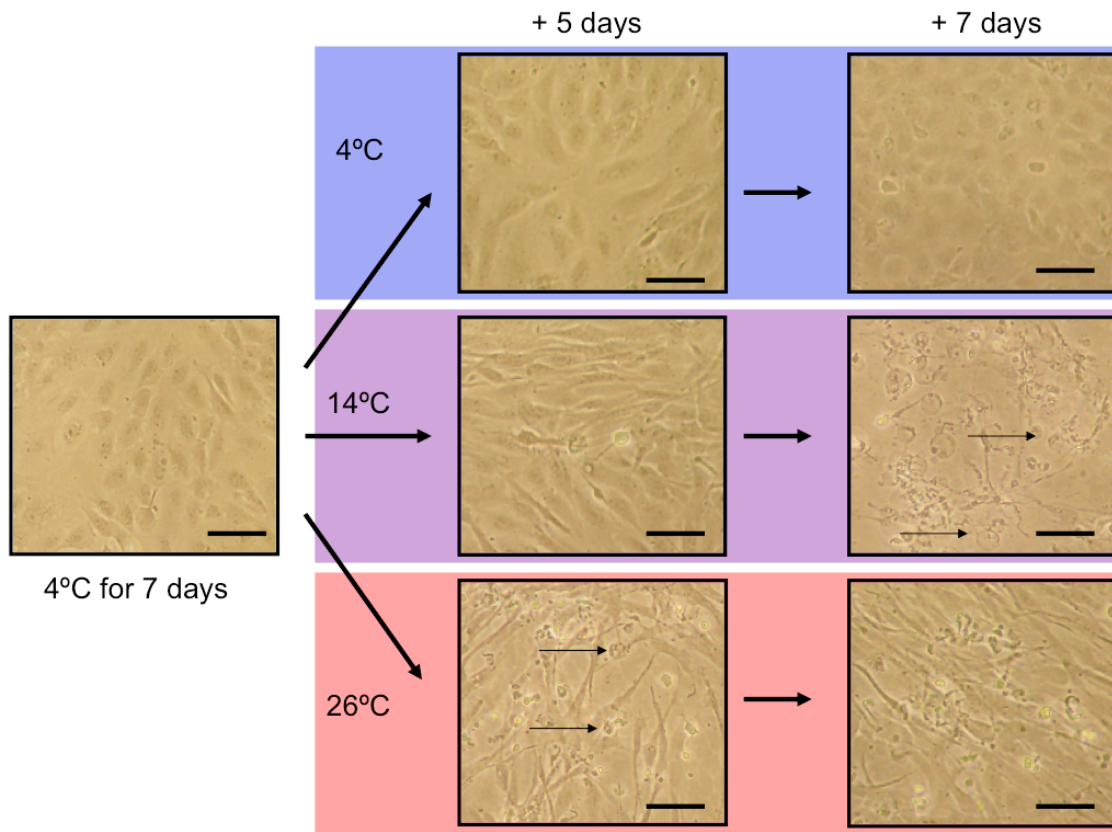


**Figure 2.8. Observation of cytopathic effects when shifting VHSV IVb-infected WE-cfin11f cultures at 4 °C for 7 days to higher temperatures.** Phase micrographs of cultures at 4 °C, 14 °C and 26 °C were taken after 5 days and then additional 7 days after the temperature shift. Scale bar = 50  $\mu$ m.

## 2.4. DISCUSSION

A cell line, WE-cfin11f, with a fibroblast-like morphology has been developed from the caudal fin of walleye. Cultures of WE-cfin11f did not stain for senescence-associated  $\beta$ -galactosidase and have been maintained for over 2.5 years through 60 passages. Thus like cell lines from many teleost species, WE-cfin11f appear to be capable of indefinite growth (Bols et al., 2005; Graf et al., 2013). WE-cfin11f was confirmed as derived from walleye by amplifying and sequencing a 655 bp region of the mitochondrial COX1 gene (Ward et al., 2009). However, of the walleye cell lines that have been described in the literature, only WF-2 (Wilensky & Bowser, 2005) could be obtained and tested in this manner and was not found to be from walleye (Sansom et al., 2013). Thus WE-cfin11f is perhaps the only walleye cell line currently existing. In this study WE-cfin11f have been used to investigate possible relationships between the thermobiology of walleye and thermal requirements of VHSV IVb.

### **Thermobiology of walleye cells and walleye**

The behaviour of walleye cell cultures at different temperatures broadly reflected the thermobiology of the walleye fish. The WE-cfin11f cell cultures proliferated from at least 10 °C to 32 °C, which was therefore defined as the proliferation zone. For walleye, the optimal temperature for fertilization has been reported at between 6-12 °C; the optimal temperature for early development, from 9-15 °C (Colby et al., 1979; Hokanson, 1977; Kerr et al., 1997). Thus walleye cells likely are capable of proliferating at a few degrees lower than 10 °C. At the other extreme walleye have been reported to grow at temperatures slightly above 30°C (Colby et al., 1979). For the WE-cfin11f cell cultures, the best proliferation occurred at 20 °C and 26 °C. For juvenile walleye, the temperature range for optimum growth was observed to be 19 °C to 25 °C (Colby et al., 1997), and the physiological optimum temperature for walleye has been reported to be 22.6 °C (Hokanson, 1977). Thus culturing walleye cells at room temperature is both convenient and physiologically optimal.

At temperatures above and below the proliferation zone, the behaviour of the WE-cfin11f cell cultures reflected observations made by others with walleye. The WE-cfin11f

cell cultures died in less than 7 days when incubated at temperatures above 34 °C, which was thus defined as the upper lethal zone. Accordingly the upper incipient lethal temperature for walleye has been reported to be 33-34 °C (Wilson and Nagler, 2006). At 1°C and 4°C WE-cfin11f did not proliferate but adopted an epithelial shape and remained attached to the growth surface for at least 14 days. Temperatures at 1- 4 °C were here defined as the lower resistance zone. Walleye growth did not occur at temperatures below 5 °C, but walleye have been reported to survive, begin spawning behaviour, and spawn at temperatures as low as 0 °C, 1.1 °C, and 3.4 °C respectively (Colby et al., 1979; Kerr et al., 1997).

### **Thermovirology of VHSV IVb**

How virions alone respond to temperature could be considered the viruses' inherent thermovirology and might be thought of having two aspects. One would be the temperature at which virions could be maintained for long periods and remain infectious. For VHSV IV, infectious virions were still detected after storage for a month at 4 °C and a week at 26 °C (Hawley & Garver, 2008; Pham et al., 2011). The other aspect would be how each viral protein functions at different temperatures in test-tube assays, such as enzymatic measurements of viral RNA-dependent RNA polymerase activity. For the RNA polymerase of VHSV I, activity was detectable at 0 °C, optimal at 15 °C, and virtually absent at 24 °C (McAllister & Wagner, 1977). Having being discussed separately for walleye cells and for VHSV IV, the critical temperatures will now be considered for the two together in infected cultures.

### **Thermovirology of VHSV IVb infecting WE-cfin11f cultures**

The thermobiology of walleye cells intersected in complex ways with the thermovirology of VHSV IVb infecting walleye cells. Productive infections developed most rapidly in the lower region of the walleye cell proliferation zone, and slowly in the lower resistance zone. No infections occurred at the optimal temperature for the cells or in the upper lethal zone.

### Infecting cultures in the proliferation zone

WE-cfin11f cultures produced VHSV IVb in the lower range of the proliferation zone, at 10-14 °C, but not at the optimal walleye cell growth temperature, 26 °C. Regardless of the species of fish or cell cultures that had been infected, VHSV production has been found to be optimal from 10 to 14 °C. When VHSV I or IVb were injected intraperitoneally into several different species, infections were optimal at 9-12 °C (Goodwin & Merry, 2011; Kim & Faisal, 2011), although for the injection of olive flounder (*Paralichthys olivaceus*), with VHSV IVa mortality occurred at 15 °C (Avunje et al., 2013). For cell cultures, slightly higher temperatures, 12-14 °C, have been reported for optimal VHSV production (Kim & Faisal, 2011). Regardless of the fish species from which the cell cultures were derived, the temperatures optimal for virus production would support cell proliferation but be below the optimal temperatures for proliferation in vitro.

The results with WE-cfin11f add to the body of literature that reports VHSV infections normally fail to be established at temperatures above 20 °C, both in vivo and in vitro. When VHSV I or IVb were injected intraperitoneally into several different fish species, the upper limit for infections was at 18-20 °C (Goodwin & Merry, 2011; Kim & Faisal, 2011). Similar temperature restrictions were reported for cell cultures, although the limiting temperature appeared slightly higher (Kim & Faisal, 2011). In an epithelial cell line, EPC from fathead minnow, the production of wild-type VHSV I was reduced significantly at 20 °C and absent at 23 °C and 25 °C (de Kinklein et al., 1980). With WE-cfin11f and VHSV IVb, no CPE developed and no virus was produced at 26 °C.

As 20-26 °C is optimal for the walleye cells, the failure of an infection to establish at 26 °C appears more attributable to thermal properties of the virus than the cells. The G protein is one candidate for a heat sensitive viral protein that is critical in determining the upper temperature limit of an infection. The G protein is required for viral entry and in another fish rhabdovirus the G protein folded differently at 27 °C (Cain et al., 1999). Host cell thermal properties might just reinforce the upper temperature limit set by the virus, but how the host did this would depend on the temperature requirements of the fish. For fish like walleye, a temperature of 26 °C might allow the best expression of cellular antiviral mechanisms, which would impede the establishment of an infection.

For coldwater fish, like rainbow trout, a temperature of 26 °C impairs cellular functions (Mosser et al., 1986), which could inhibit the establishment of an infection.

#### Infecting cultures in the upper lethal zone

At 37 °C, small fractions of the virus (Pham et al., 2011), and of the WE-cfin11f cells survived for approximately a day, but VHSV IVb was unable to infect WE-cfin11f cultures. A temperature of 37 °C would be in the lethal zone or thermal resistance zone for walleye (Wilson & Nagler, 2006), which means some fish would be able to survive a few hours. The results with WE-cfin11f suggest that VHSV IVb infection of walleye would not be initiated during a brief period in the lethal zone.

#### Infecting cultures in the lower resistance zone

This seems to be the first exploration into the infection of cells with VHSV at temperatures in the 4 °C and below range. At 1 °C and 4 °C, VHSV IVb appeared to enter WE-cfin11f because western blotting detected the viral N protein. At 4 °C WE-cfin11f cultures clearly underwent CPE and produced VHSV IVb. One other fish rhabdovirus, infectious hematopoietic necrosis virus (IHNV), has been reported to be produced in piscine cell cultures at 4 °C (Araki et al., 1994). Relative to 14 °C, the development of CPE and production of virus was slow at 4 °C. The likely explanation for this is the general slowing of fish cell metabolism at 4 °C. At 1 °C the viral life cycle was slowed more than at 4 °C: over the time frame of 4 weeks at 1 °C less N protein accumulated and CPE was difficult to detect because control cultures started to deteriorate as the incubation period at 1 °C was increased beyond 4 weeks. Walleye are unlikely to be continuously exposed to water at 1 °C. Therefore, whether the completion of the VHSV IVb life cycle can be completed at 1 °C after having been initiated at 1 °C has been left unanswered.

Although VHSV IVb was produced at 4 °C, albeit more slowly, the relative magnitude of N protein accumulation at 4 °C versus 14 °C suggests different kinetics of the virus-host cell interactions at the two temperatures. Over 28 days, cultures at 4 °C accumulated much more intracellular N protein than cultures at 14 °C. This is likely because cells in 14 °C cultures started dying much earlier than cells in 4 °C cultures. The

earlier death at 14 °C might be attributed to cells at 14 °C better expressing the mechanism of cell death induced by the virus, such as apoptosis (Björklund et al., 1997). Alternatively, later stages of the viral life cycle, like budding of new virus particles, might have been slowed relatively more at 4 °C compared to viral RNA and protein synthesis. A temperature of 4 °C might hereby synchronize the viral life cycle in cultures, causing the accumulation of more cells with viruses in the late stages of development.

#### Shifting cultures infected at 4 °C to 26 °C

Defining the thermal zones makes possible experiments where cultures are infected in one zone and shifted to other zones in order to understand how at the cellular level walleye and VHSV IVb might interact during thermal changes. Although many experimental combinations are possible, only one was explored here to illustrate the approach and resembles recent experiments done with VHSV IVb and several fish species, including bluegill (Goodwin & Merry, 2011; Goodwin et al., 2012). After infections at permissive temperatures, WE-cfin11f cells or fish were shifted to non-permissive temperatures. When bluegill were infected at 15 °C and moved to 25 °C, some fish died while others survived and after 28 days still had copies of the viral genome (Goodwin et al., 2012).

When VHSV IVb infected WE-cfin11f cultures at 4 °C were shifted after 7 days but not fewer days to 26 °C, CPE developed within 5 days at 26 °C. By contrast, CPE did not appear over the same time span for infected cultures continuously incubated at 4 °C. The results suggest that at 26 °C the viral life cycle could progress to the stage that causes CPE and does so more rapidly than at 4 °C. The development of CPE at 26 °C cannot have been due to virus remaining attached and infectious on the plastic tissue culture vessel (Pham et al., 2011) because as mentioned earlier, infections could not be established at 26 °C. For the same reason, the infection was not sustained in cultures at 26 °C and the spots of CPE did not spread. Instead over time the progeny of non-infected cells were able to migrate into the areas of CPE, restoring the monolayer at 26 °C. Thus cultures infected at 4 °C could be ‘cured’ by incubation at 26 °C.

The data thus suggest some scenarios on how VHSV IVb infected walleye might respond to rising temperatures. At 4 °C VHSV IVb infection would develop slowly and possibly end up in clinical disease. Early in the infection, walleye might be 'cured' by a shift to 26 °C. Later in the infection, the shift to 26 °C might have pathological consequences and the walleye shifted to 26 °C might or might not recover from the virally induced cell death, depending on the tissue(s) and number of cells involved. In the context of spring fish kills, the rapid virally induced death of cells might contribute along with other physiological stresses associated with rapidly rising temperatures to the killing of fish. In the future, WE-cfin11f cultures can be used in these types of experiments to help understand how temperature changes influence the establishment and pathology of VHSV IVb infections in walleye.

## **CHAPTER 3.**

**Development of a walleye caudal fin epithelial cell line and demonstration that viral haemorrhagic septicemia virus genotype IVb preferentially infects a walleye caudal fin fibroblast cell line especially at 4 °C**

### 3.1. INTRODUCTION

Understanding the interactions between viral haemorrhagic septicaemia virus genotype IVb (VHSV IVb), walleye, *Sander vitreus* (Mitchill), and temperature are of practical concern and of basic research interest. VHSV IVb is a relatively new rhabdovirus to the Great Lakes region of North America and is the causative agent of viral haemorrhagic septicaemia (VHS) and responsible for several fish kills (Lumsden et al., 2007). Walleye, *Sander vitreus* Mitchell, is one of the most widely stocked and important commercial and recreational freshwater fish species in North America (Fenton et al. 1996) and has been found in VHSV IVb-associated mortality events in the Great Lakes watershed (Grice et al., 2014). Temperature appears to influence the susceptibility of fish to VHSV. When Pacific herring were exposed to VHSV IVa at 8, 11, and 15 °C, mortalities were highest at the lowest temperature (Goodwin & Merry, 2011; Hersberger et al., 2013). The fish kills associated with VHSV IVb were most common during periods of fluctuating temperature, late winter and spring (Lumsden et al., 2007). Winter temperatures, such as 4 °C, are perhaps the least examined temperatures with respect to fish viral diseases and the most difficult to study, but can be studied conveniently with fish cell lines (Vo et al., 2014).

One interesting source of cell lines for studying fish viruses is the caudal fin. Fins are sites of viral entry, replication and shedding (Dorson & Torhy, 1993; Quillet et al., 2001; Harmache et al., 2006) and have been proposed as biopsy sites for detecting VHSV IVb (Cornwell et al., 2013). Fins are anatomically complex, with multiple cell types from several tissues organized into skeletal elements (fin rays) covered by skin (Becerra et al. 1983). A recent study of herring larvae suggested that during VHSV IVa infection viral tropism transitioned from skin epithelial cells to fibroblasts (Lovy et al., 2012). Having fin cell lines of different lineages would allow the cellular events of a viral infection in this organ to be explored, including viral tropism and the influence of temperature. Recently, a walleye caudal fin cell line (WE-cfin11f) was described that had a fibroblast shape and was susceptible to VHSV IVb (Vo et al., 2014). Here the development of an epithelial cell line (WE-cfin11e) from the walleye caudal fin is described and WE-cfin11f characterized further as having the properties of fibroblasts and distinct from WE-

cfin11e. Like WE-cfin11f, WE-cfin11e supported VHSV IVb infection at 14 °C, but at 4 °C VHSV IVb was produced only in the fibroblasts. Low temperature appeared to be modulating viral tropism.

## **3.2. MATERIALS AND METHODS**

### **3.2.1. Fish cell lines and virus**

Three fish cell lines were used. WE-cfin11e has an epithelial shape and was developed from primary cell cultures from the caudal fin of the same fish from which a cell line, WE-cfin11f, with a fibroblast shape was developed (Vo et al., 2014). The fish was a juvenile walleye of the Bay of Quinte stock and was obtained and handled as described as described previously (Vo et al., 2014). The fathead minnow cell line, EPC, was used to propagate the virus (Winton et al., 2010). Cell lines were maintained routinely at 26 °C in L-15 medium (Hyclone) with 5 % to 15% fetal bovine serum (FBS, Hyclone) (Curtis et al., 2013; Vo et al., 2014). The virus was VHSV IVb (CEFAS strain U13653) and was propagated and titred as described previously (Pham et al., 2011; Pham et al., 2013).

### **3.2.2. General fluorescent immunocytochemistry procedures**

Walleye cell lines were examined for several cellular markers, and after viral infection, for G protein by immunocytochemistry procedures used that had some common steps, beginning with culturing in slide flasks. An immunocytochemical procedure similar to that recently described by Gignac et al. (2014) was used. Prior to fixation, the slide flask cultures were rinsed several times in phosphate buffered saline (PBS). Fixation was ice-cold absolute methanol for 20 min at 4 °C, followed by a quick wash in PBS to rehydrate cells, and incubation for 1 h in a blocking buffer (BB) (10% goat serum, 3% bovine serum albumin and 0.1 % Triton X-100 in PBS). At this point some flask cultures received primary antibody, whereas others received secondary antibody directly and were controls for nonspecific staining. Details of the primary antibodies, their dilution in BB, and their application conditions are described in the sections below. The secondary antibodies were Alexa Fluor 488®-conjugated goat anti-rabbit for polyclonal primary antibodies and Alexa Fluor 488®-conjugated goat anti-mouse IgG for monoclonal primary antibodies. The secondary antibodies (1:1000 in PBS) were applied to flask cultures after they had been washed with PBS three times with rocking and incubated for 1 h. Cultures were then washed several times with PBS,

allowed to dry, and mounted in Fluoroshield medium containing DAPI. Fluorescence images were taken with the Zeiss LSM 510 laser-scanning microscope and confocal images were acquired and analyzed using a ZEN lite 2011 software. Fluorescence staining was never observed in flask cultures to which only secondary antibody had been applied.

### **3.2.3. Development and characterization of WE-cfin11e**

When TrypLE was applied to caudal fin primary cells cultures, fibroblasts were detached first, allowing them to be removed and leaving behind epithelial cell-enriched cultures that were serially sub-cultivated to give rise to WE-cfin11e. Previously the development of WE-cfin11e was described as part of a paper in which many vertebrate cell lines were compared for their suitability to be used in a portable impedance based toxicity sensor (Curtis et al., 2013). WE-cfin11e was a superior cell line for that purpose but was not characterized further and so is characterized here.

A Nikon inverted phase contrast microscope was used to observe the organization of cells within cultures before and after being fixed and stained with May-Grünwald Giemsa. For the later, confluent cultures in flasks were washed twice with PBS and fixed with methanol/acetone (1:1) for 20 minutes. After the fixative was removed, each flask was incubated with 10 mL of May-Grünwald solution (EMD Milipore) for 3 min and then subsequently with 10 mL of 1:50 (v/v) Giemsa solution (EMD Milipore) in deionized water for 10 min. The flask was washed with deionized water two times and then allowed to air dry before being observed.

WE-cfin11e and WE-cfin11f were examined for the intermediate filament protein, vimentin, and the tight junction protein, zonula occludens-1 (ZO-1). For vimentin a mouse monoclonal antibody (mAb) to porcine vimentin (clone V9) was obtained from Sigma-Aldrich (St Louis, MO) and was used overnight at a 1: 200 dilution. For ZO-1, a rabbit polyclonal antibody to human ZO-1 (Z-R1) was purchased (Invitrogen, Burlington, ON) and applied to cells overnight at a 1:200 dilution.

#### **3.2.4. Collagen I expression in WE-cfin11e and WE-cfin11f**

WEBA cells were seeded in 4-well chamber slides at approximately  $1.5 \times 10^5$  cells per well and allowed to grow overnight at 26 °C. The next day wells received L-15 with 5 % FBS with (100 µg/ml) and without ascorbic acid (Sigma-Aldrich). The cultures were incubated at 26 °C, and every three days for up to two weeks, the medium in each well was removed and replaced with fresh volumes of the appropriate medium. An affinity purified rabbit polyclonal antibodies against salmon collagen I (Cedarlane, Burlington, ON) was used at 1:400 dilution for 1 h.

#### **3.2.5. Characterizing the thermobiology of the WE-cfin11e cell line**

Characterizing the thermobiology of WE-cfin11e was done as described in detail previously for WE-cfin11f (Vo et al., 2014). The temperature range that supported the accumulation of cells in cultures was the proliferation zone. The rapid death of cells at temperatures above 34 °C was the upper lethal zone, whereas the continued persistence of cell monolayers at 4 °C and below was the resistance zone.

#### **3.2.6. Cytopathic Effects (CPE)**

The potential of WE-cfin11e cultures to succumb to the CPE of VHSV IVb was examined at 4 and 14 °C. A range of MOI was tested, including a very high MOI of 175 to 1, because the interest was in determining whether damage could or could not take place at 4 °C. As a high MOI can possibly block infection due to auto-interference, a MOI as small as 0.002 to 1 was also tested. A low pH, such as 6.5 or less, can block the spread of VHSV between cells and impede the development of CPE (Mas et al., 2004). Therefore, the pH of the culture medium, L-15 with 2 % FBS, in which cells were exposed to the virus and maintained post infection for CPE development, was noted. At temperatures of 4, 14 and 26 °C, L-15 with 2 % FBS had a pH of 7.1. With cells for 24 h, the pH of the medium was 7.3. With cells for 14 days either at 4 °C or 14 °C, pH of the medium was 7.0-7.1. After 14 days post VHSV IVb infection at either 4 °C or 14 °C, pH of the conditioned medium was 7.1.

CPE was monitored as a change in cell morphology and attachment through phase contrast microscopy observations and by evaluating a change in metabolism with the

indicator dye, Alamar Blue® (Invitrogen). Alamar Blue was used as detailed by Dayeh et al. (2013) and more specifically for CPE due to VHSV IVb as described by Pham et al. (2013) and the results recorded as RFUs. WE-cfin11f cells in L-15 with 10 % FBS were added to 24-well plates at  $1 \times 10^5$  cells per well and allowed to attach for two days at 26 °C. The medium was removed and wells received L-15 with 2 % FBS and ten-fold serial dilutions of VHSV IVb stock with a viral titre of  $1.33 \times 10^8$  TCID<sub>50</sub> mL<sup>-1</sup>. The plates were then incubated at 4 and 14 °C and observed periodically by phase contrast microscopy for up to 35 days. After 14 days, metabolism was evaluated with Alamar Blue in 3 wells for each different viral titre. The RFUs were expressed as a percentage of the RFUs in control wells without virus.

### **3.2.7. Western blotting for N protein in VHSV IVb infected cell cultures**

Confluent 75-cm<sup>2</sup> flasks of WE-cfin11e or WE-cfin11f were incubated at 4 or 14 °C for 24 h before being infected with VHSV IVb at MOI of 20:1 and 10:1, respectively, in L-15 with 2 % FBS for up to 28 days. Cell lysates were prepared, subject to SDS-PAGE electrophoresis, and electro-transferred to blotting membranes. Primary antibodies include mAb IP5B11 (used at 1:600) recognizing VHSV N protein (Lorenzen et al., 1988) and was obtained from Dr. N. Lorenzen (Aarhus University, Aarhus, Denmark) or affinity-purified rabbit polyclonal anti-actin (used at 1:400) and purchased from Sigma. Secondary antibody was alkaline phosphatase goat anti-mouse IgG (Sigma) and NBT/BCIP reaction was used to develop the protein bands. Details of western blotting procedures and the source of relevant reagents have been described (Vo et al. 2014).

### **3.2.8. Immunocytochemical staining for G protein in VHSV IVb infected cell cultures**

WE-cfin11e and WE-cfin11f were seeded and allowed to grow to confluency in Nunc slide flasks. Cultures were allowed to acclimatize at 4 °C or 14 °C for 24 h and then were infected with VHSV IVb at MOI of 20:1 for WE-cfin11e and MOI of 10:1 for WE-cfin11f in L-15 with 2 % FBS at 4 °C or 14 °C for 2 h. Cells were washed 3 times with ice-cold PBS and then kept in three mL of fresh 2 % FBS at 4 °C or 14 °C. Virus was not added to the control slide flasks. Virus challenges lasted up to 21 days p.i. for 14 °C

infection and up to 35 days p.i. for 4 °C infection. A similar immunofluorescence approach to the above procedure was used. On selected days p.i., slide flasks were washed with PBS, fixed with ice-cold 3 % (w/v) paraformaldehyde (Sigma) in PBS for 20 min at 4 °C, permeabilized with 0.1 % (v/v) Triton X-100 (Sigma) for 10 min and incubated with the blocking buffer consisting of 3 % BSA, 10 % goat serum and 0.1 % (v/v) Triton X-100 in PBS at room temperature for an hour. Then the cultures were incubated with mAb IP1N11 diluted at 1:100 in the same blocking buffer overnight at 4 °C. The mAb IP1N11 was developed by and obtained from Dr. N. Lorenzen (Aarhus University, Aarhus, Denmark) and detected VHSV G protein (Lorenzen et al., 1988). Alexa Fluor 488 goat anti-mouse IgG secondary antibody (Invitrogen) was used at 1:1000. Slides were mounted in Fluoroshield mounting medium with DAPI. Confocal images were obtained with the Zeiss LSM 510 laser scanning microscope and were acquired and analyzed using a ZEN lite 2011 software.

### **3.2.9. Evaluating viral production in VHSV IVb infected cell cultures**

WE-cfin11e and WE-cfin11f were plated in 6-well plates overnight at room temperature. Cultures were allowed to acclimatize at 4 °C or 14 °C for another 24 h prior to being inoculated with  $10^7$  TCID<sub>50</sub> mL<sup>-1</sup> VHSV IVb (or equivalently at at MOI of 20:1 for WE-cfin11e and MOI of 10:1 for WE-cfin11f) at 4 °C or 14 °C for 2 h, washed three times with ice-cold D-PBS and then incubated in 4 mL of L-15 with 2 % FBS at 4 °C or 14 °C for up to 28 days. On selected days p.i., the conditioned media from triplicate wells at each temperature were collected and tittered on EPC cultures in TCID<sub>50</sub> assays using 96-well-plates described by Pham et al. (2011). Viral titers were as expressed in logarithmic values of tissue culture infectious dose TCID<sub>50</sub> mL<sup>-1</sup>.

### **3.2.10. Western blotting for Mx in VHSV IVb infected cell cultures**

Western blotting was used to evaluate Mx expression in cultures of WE-cfin11e and WE-cfin11f after infection with VHSV IVb at MOI of 20:1 and 10:1, respectively, in L-15 with 2 % FBS and incubation at either 4 or 14 °C. Cell lysates were prepared, subjected to SDS-PAGE, electro-transferred to nitrocellulose membranes, and probed for Mx with the rabbit polyclonal anti-rainbow trout Mx at 1:2000 as described in detail

previously (DeWitte-Orr et al., 2007). Secondary antibody was alkaline phosphatase-conjugated goat anti-rabbit IgG (Sigma) used at 1:20,000.

### **3.3. RESULTS**

#### **3.3.1. Development and general characterization of WE-cfin11e**

As observed previously (Vo et al., 2014), primary cultures of the walleye caudal fin had both epithelial-like and fibroblast-like cells. In some cultures, the epithelial-like cells predominated (Fig 3.1A). When these were sub-cultivated with TrypLE, fibroblasts detached first and could be discarded. Longer TrypLE treatments detached the epithelial-like cells, allowing them to be passaged and leading to the new cultures with just epithelial shaped cells (Fig 3.1B). These cultures have been serially passaged over 40 times over 4 years and retained their epithelial shape (Fig 3.1C-D). They are referred to as WE-cfin11e and were compared with the fibroblast cell line, WE-cfin11f, for features that had yet to be examined in WE-cfin11f.

Although both cell lines stained for the intermediate filament protein, vimentin (Fig 3.2A,D), they differed starkly in the expression of the tight junction protein, zonula occludens-1 (ZO-1). ZO-1 localized to the cell boundaries of WE-cfin11e but was absent from WE-cfin11f (Fig 3.2C, F).

#### **3.3.2. Collagen I expression in WE-cfin11e and WE-cfin11f**

The two cell lines differed in their expression of collagen I as revealed through immunocytochemical staining with an antibody to salmon collagen I. Strong but diffuse staining was observed in the cytoplasm of WE-cfin11f cells (Fig 3.3A) and presumably represented the precursor procollagen type I. In contrast, WE-cfin11e did not stain (Fig 3.3C). When the two cell lines had been maintained for two weeks in medium with ascorbic acid (100 µg/mL), two very different responses were seen. In WE-cfin11f cultures, a dense network of extracellular fibers stained for collagen I (Fig 3.3B). By contrast, little staining was seen in WE-cfin11e cultures, although some tiny “sprouts” of stain were seen occasionally on top of the cell monolayer (Fig 3.3D).

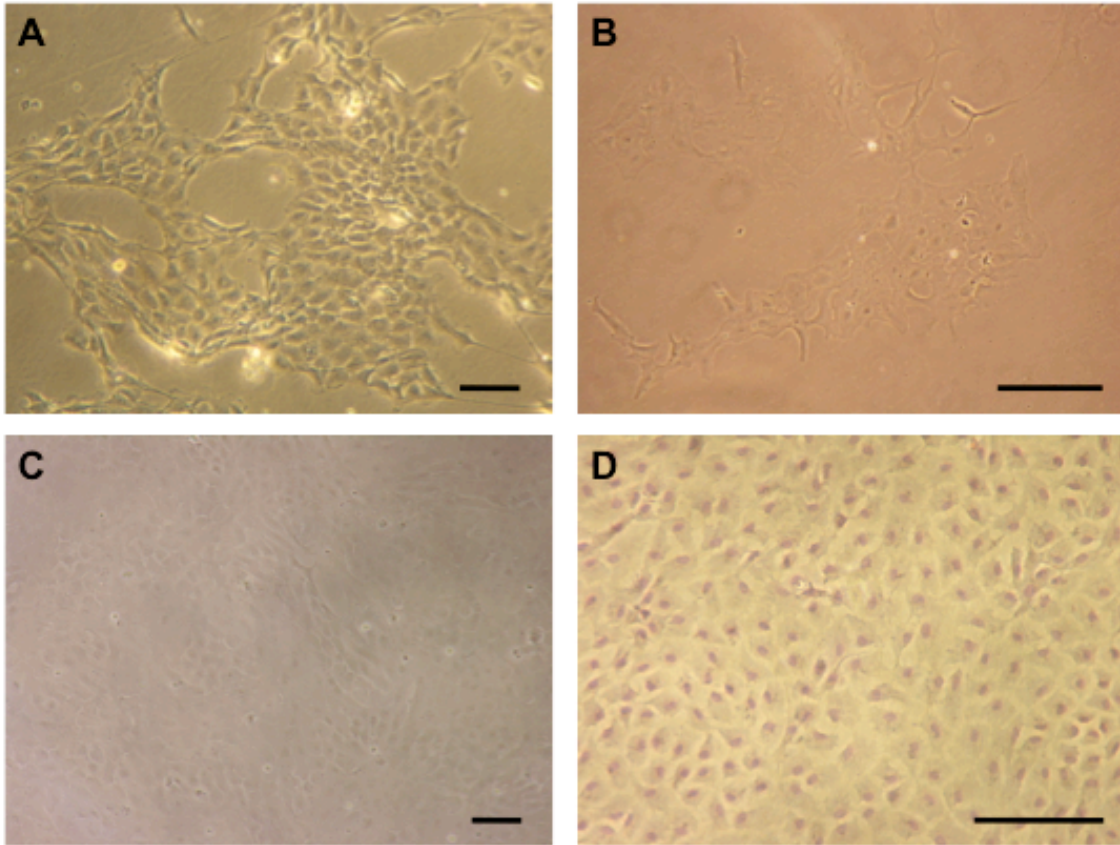


**Figure 3.1. Development of the walleye caudal fin epithelial-like cell line WE-cfin11e.** A. Caudal fin epithelial cells in the primary cultures. B. Phase contrast of the early passaged caudal fin epithelial-like cultures at a low cell density. C. Phase contrast of the confluent monolayer of WE-cfin11e cell line. D. May-Grunwald Giemsa staining of the WE-cfin11e confluent culture. Scale bar = 100 μm.

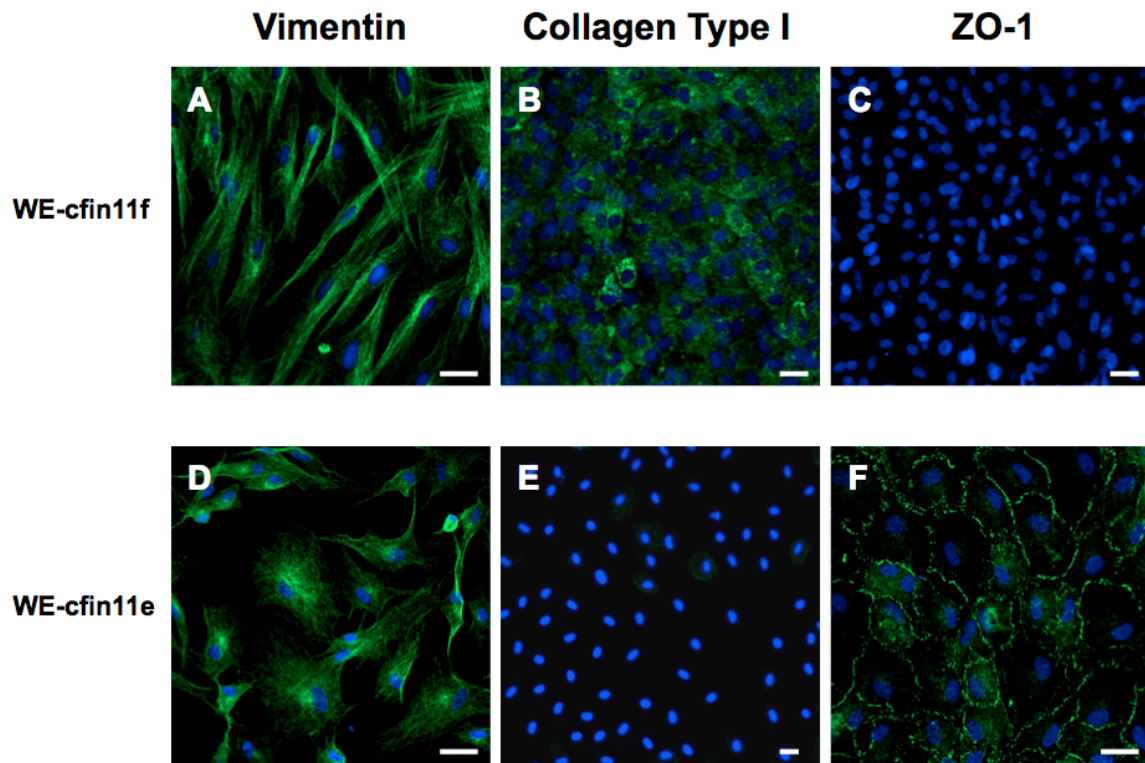


**Figure 3.2. Immunocytochemical results of cellular markers expressed in WE-cfin11f (A-C) and WE-cfin11e (D-E).** The methanol-fixed cells were probed with a mouse monoclonal anti-vimentin (A, D) or a rabbit polyclonal anti-collagen type I (B, E); or the paraformaldehyde-fixed cells were probed a rabbit polyclonal anti-ZO-1 (C, F). Subsequently all cultures were immunofluorescently probed with goat anti-rabbit or anti-mouse secondary antibodies conjugated with Alexa Fluor 488 (green). Cells were then counterstained with DAPI (blue) to visualize the cell nuclei. Samples were examined under the Zeiss LSM 510 laser scanning microscope and confocal images were acquired and analyzed using a ZEN lite 2011 software. Scale bar = 20  $\mu$ m.

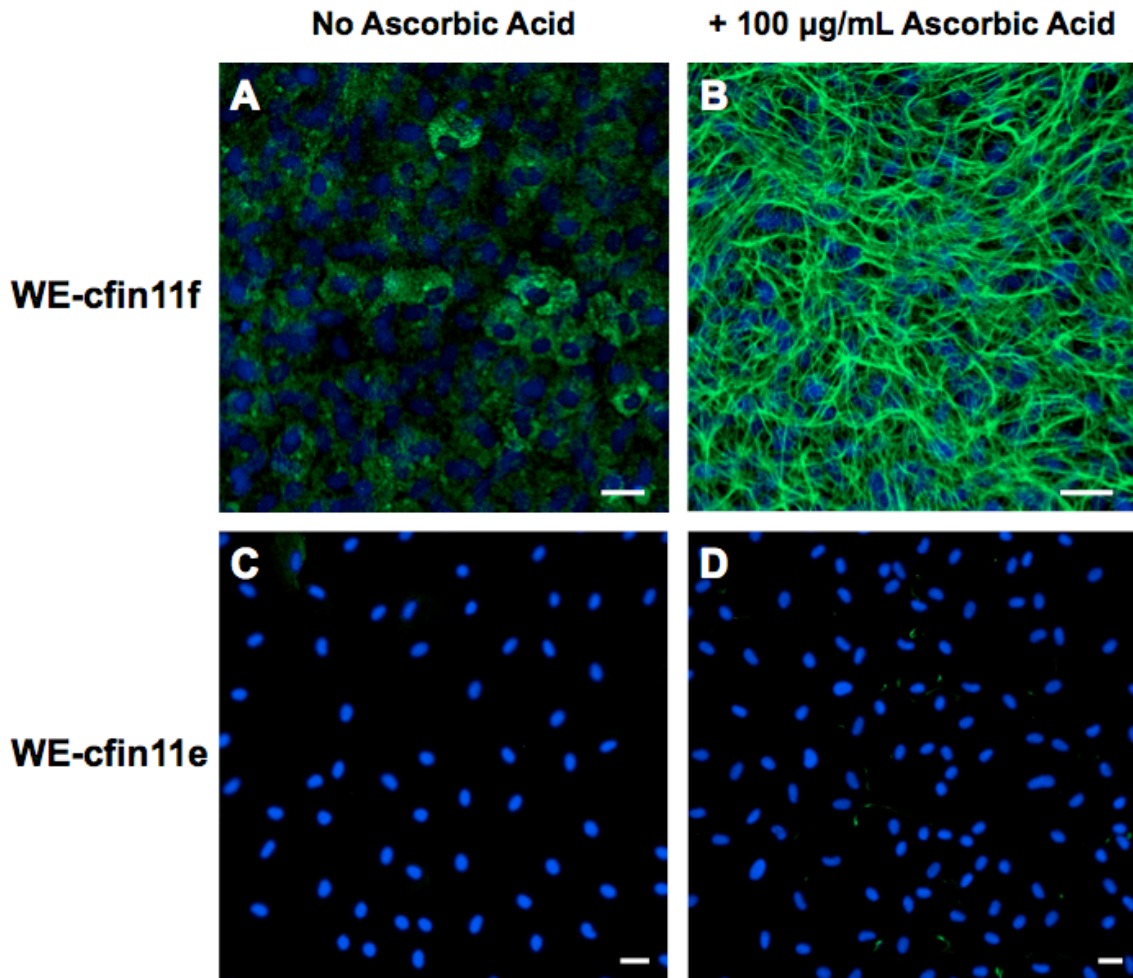


**Figure 3.3. Differences between WE-cfin11e and WE-cfin11f cell lines in their ability to form extracellular collagen I matrix.** Ascorbic acid was used to promote the formation of extracellular collagen I (COL I) matrix. WE-cfin11f (A-B) and WE-cfin11e (C-D) were treated with 100  $\mu\text{g}/\text{mL}$  ascorbic acid in L-15 with 5 % FBS at 26 °C for two weeks. Immunofluorescence was performed to detect COL-1. Primary antibody was affinity-purified rabbit polyclonal anti-salmon COL-1 used at 1:400. Secondary antibody was Alexa Fluor 488 (green)-conjugated goat anti-rabbit IgG used at 1:1000. Samples were examined under the Zeiss LSM 510 laser scanning microscope and confocal images were acquired and analyzed using a ZEN lite 2011 software. Scale bar = 20  $\mu\text{m}$ .

### **3.3.3. Thermobiology of WE-cfin11e cultures**

The thermobiology of the two cell lines was very similar. The upper lethal zone was the same, both cell lines died upon incubation for a week or more at temperatures above 34 °C. The proliferation zone was also the same. Like WE-cfin11f (Vo et al., 2014), WE-cfin11e grew at 14-32 °C, with 26 °C appearing optimal (Fig 3.4). However, the cell lines responded subtly different in the lower resistance zone, which was 4 °C and below (Vo et al., 2014). Like WE-cfin11f, WE-cfin11e cultures persisted for weeks at 4 °C without a decline in cell number (Fig 3.4A). However, while WE-cfin11e retained their epithelial shape (Fig 3.4B), the WE-cfin11f lost their fibroblast shape at 4 °C and became epithelial like (Vo et al., 2014).

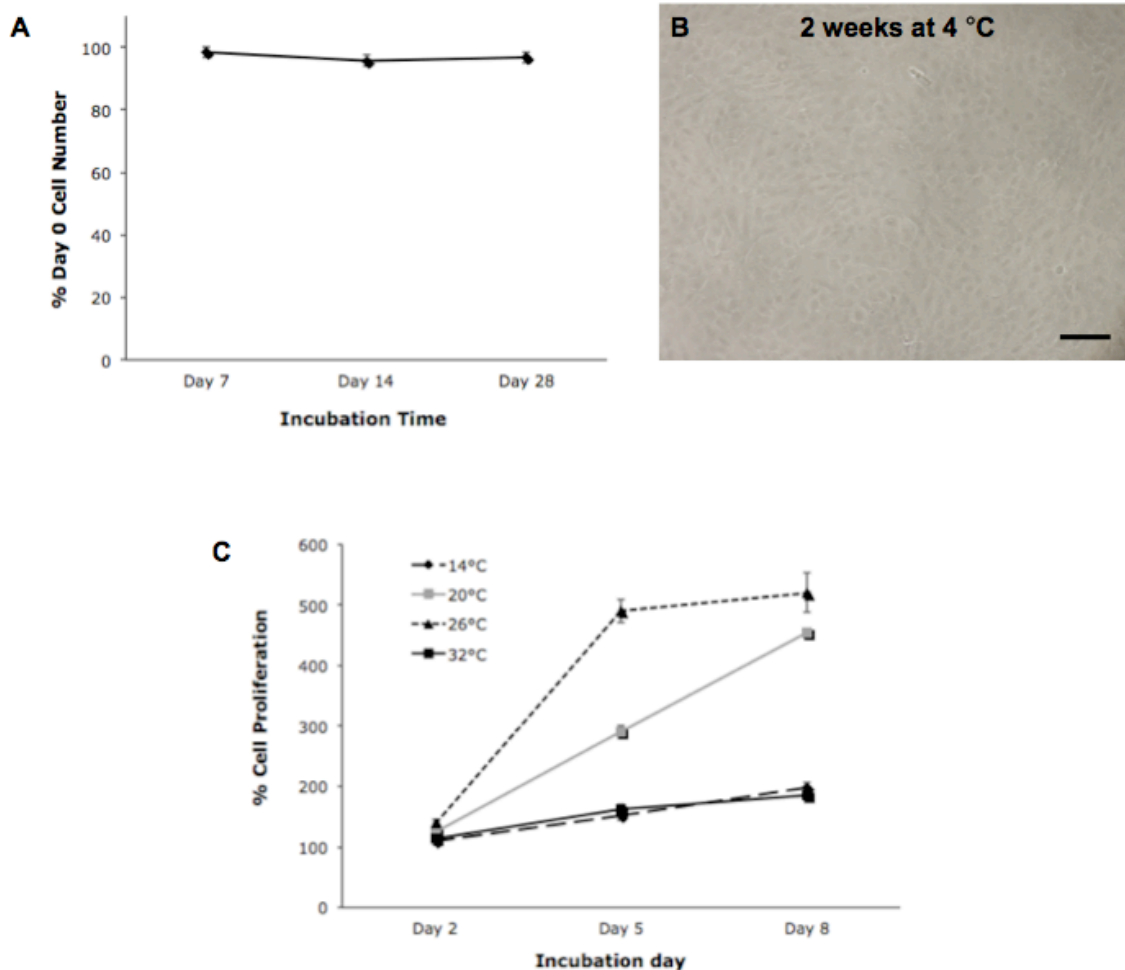


**Figure 3.4. Effect of temperatures on the growth and morphology of WE-cfin11e cell line.** WE-cfin11e could survive and maintain its cell number (A) and epithelial morphology at 4 °C (B). Cell proliferation could occur at the temperatures from 14-32 °C (C). Cell counts were determined by performing cell counts in four-six well replicates of six-well plates with the automated Z2 Coulter particle counter. For the graphical presentation, cell numbers were expressed as a % of initial cell count. Scale bar = 100  $\mu$ m.

#### **3.3.4. VHSV IVb infectious cycle in WE-cfin11e at 14 °C and 4 °C**

WE-cfin11e cultures at 14 °C and 4 °C become infected with VHSV IVb but the infectious cycle was delayed at 4 °C. With cultures at 14 °C and with the highest MOI, foci of CPE were seen as early as 10 days p.i. By 14 days the destruction of the monolayer had been nearly completed and metabolism as measured with Alamar Blue had been reduced by 99 % by 14 days. By contrast, no CPE was visible in cultures infected and kept at 4 °C for 35 days. However, in WE-cfin11e cultures that had received the highest MOI and incubated at 4 °C for 14 days metabolism was diminished. Alamar Blue readings were approximately 30 % of the values in cultures at 4 °C without the virus. Western blotting detected the expression of the viral N protein by 3 days p.i. at 14 °C but was first observed 28 days p.i. at 4 °C (Fig 3.5). When cultures were examined by immunocytochemistry for viral G protein, clusters of infected cells were seen at 10 days p.i. infection at 14 °C but not until day 35 at 4 °C (Fig 3.6). Virus was produced over 3 weeks at 14 °C but at 4 °C virus production by WE-cfin11f cultures was slight or absent (Fig 3.7).

#### **3.3.5. VHSV IVb infectious cycle in WE-cfin11e and WE-cfin11f cultures at 4 °C**

VHSV IVb infected both WE-cfin11e and WE-cfin11f cultures at 4 °C, but at this temperature the virus was produced only in WE-cfin11f cultures. By western blotting, the N protein was detected by 28 days p.i. in WE-cfin11e cultures at 4 °C (Fig 3.5) but had been seen as early as 3 days p.i. in WE-cfin11f at 4 °C (Vo et al., 2014). By immunocytochemistry for G protein, areas of infected cells within cell monolayers were seen as early as 18 days p.i. in WE-cfin11f but not until day 35 in WE-cfin11e (Fig 3.6). Foci of CPE started to appear in WE-cfin11f cultures by 7 days p.i. at 4 °C but never appeared in WE-cfin11e cultures over 35 days at 4 °C. At 4 °C, WE-cfin11f had produced significant virus by 28 days p.i., albeit less than produced by 21 days p.i. at 14 °C (Fig 3.7A). By contrast, during the same time frame, WE-cfin11e produced little or no virus (Fig 3.7B).

### **3.3.6. Mx induction by VHSV IVb in WE-cfin11f and WE-cfin11e cultures at 4 and 14 °C**

As revealed by western blotting, VHSV IVb induced the antiviral protein Mx in cultures at 14 °C but not at 4 °C. At 14 °C, induction was seen as early as 3 days p.i. in WE-cfin11f and 7 days p.i. in WE-cfin11e (Fig 3.8). By contrast, induction was not seen in 28 days p.i. in cultures of either cell line at 4 °C (Fig 3.8).

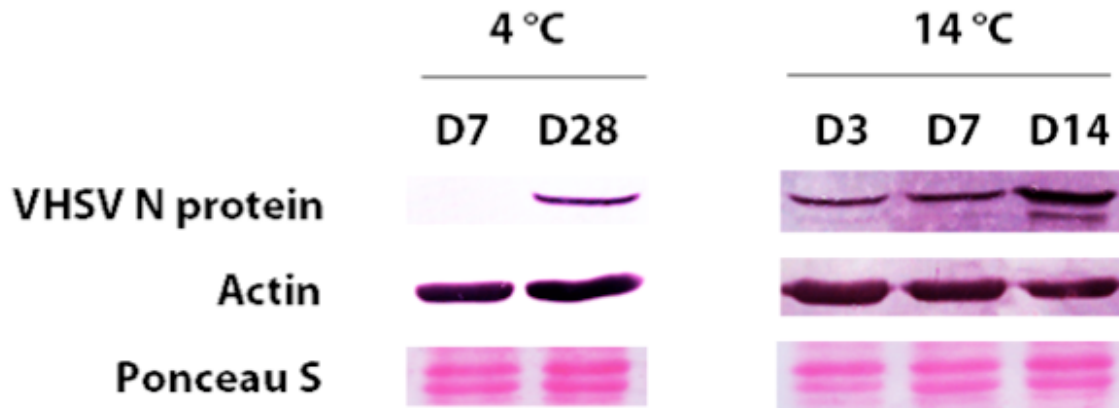
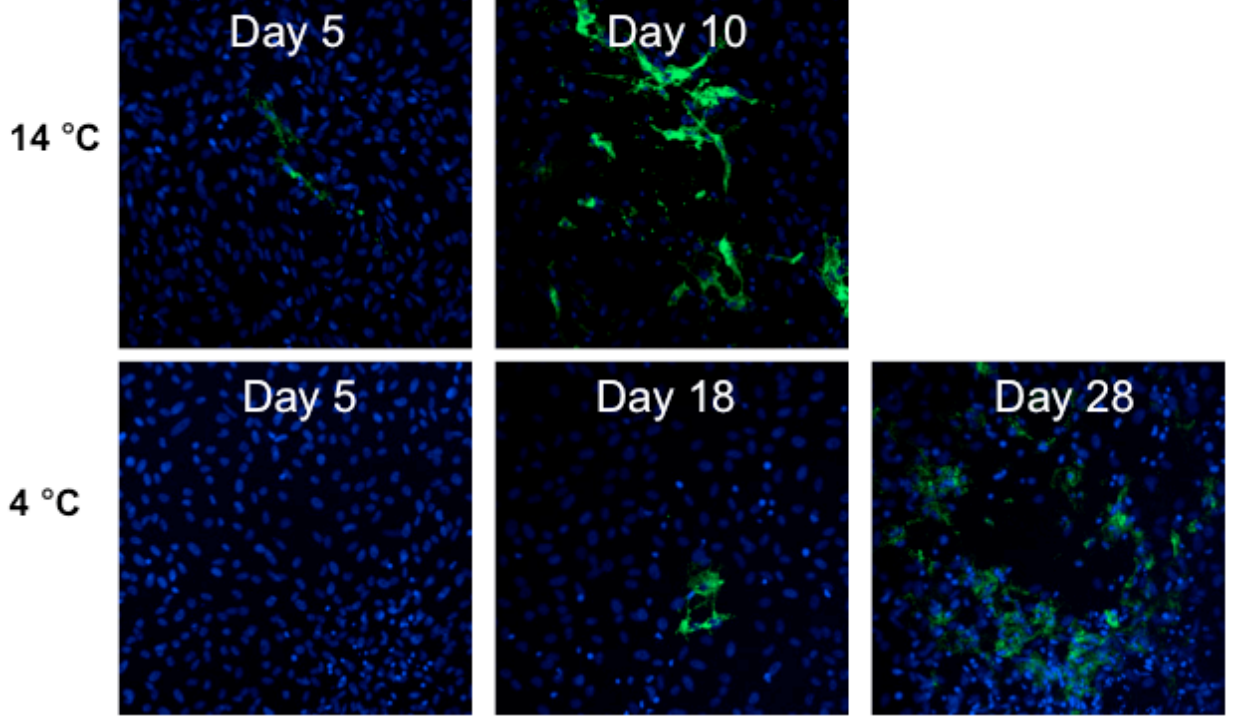


**Figure 3.5. Expression of VHSV IVb N protein in WE-cfin11e cells post infection at 4 °C and 14 °C.** Confluent 75 cm<sup>2</sup> flask cultures in L-15 with 2 % FBS were incubated overnight at either 4 °C or 14 °C prior to the introduction of the VHSV IVb at a MOI of 20:1 for 2 h. Afterwards the medium, which had the virus, was removed and the monolayer rinsed with PBS and incubated further at either 4 °C or 14 °C. At different times (days) post infection, protein lysates were prepared from cultures and analyzed by western blotting as described in the Materials and Methods with the mAb (clone IP5B11) to VHSV N. Actin was used as an internal control.

**WE-cfin11f**



**WE-cfin11e**

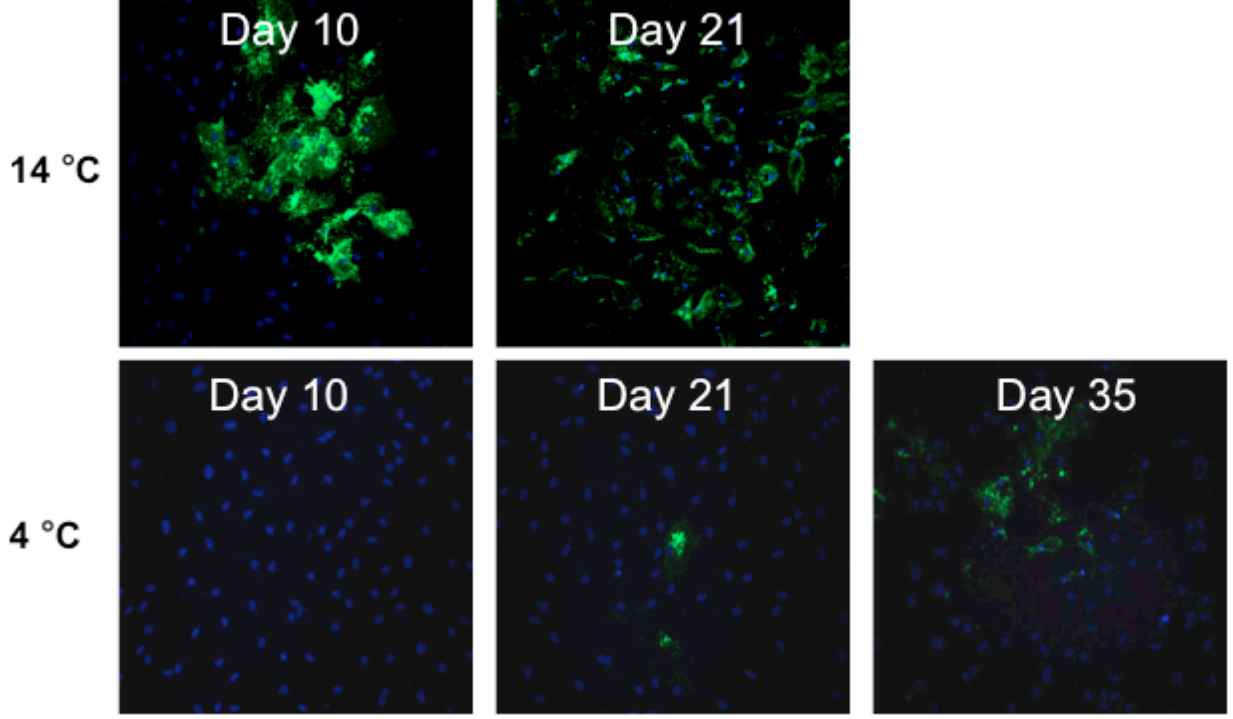


**Figure 3.6. Immunofluorescence detection of VHSV G protein in WE-cfin11f and WE-cfin11e infected with VHSV IVb at 4 °C and 14 °C.** After being allowed to be kept at either 14 °C or 4 °C overnight prior to viral infection challenges, confluent cultures in Nunc polystyrene slide flasks were incubated with VHSV IVb in L-15 with 2% FBS for 2 h at either 14 °C or 4 °C, washed with PBS to remove free unbound viral particles and incubated in fresh L-15 with 2% FBS either at 14 °C for up to 21 days p.i. or at 4 °C for up to 35 days p.i.. On selected days, slide flasks were removed from temperature-controlled incubators and cultures were fixed with 3% paraformaldehyde, blocked with 3% BSA, 10% goat serum and 0.1 % Triton X-100, probed with mouse monoclonal anti-VHSV G protein primary antibody (clone IP1H3) at 1:100. Goat anti-mouse IgG secondary antibody conjugated with Alexa Fluor 488 (green) was used at 1:1000. Cells were counterstained with DAPI (blue) to visualize the cell nuclei. Samples were examined under the Zeiss LSM 510 laser scanning microscope and confocal images were acquired and analyzed using a ZEN lite 2011 software.

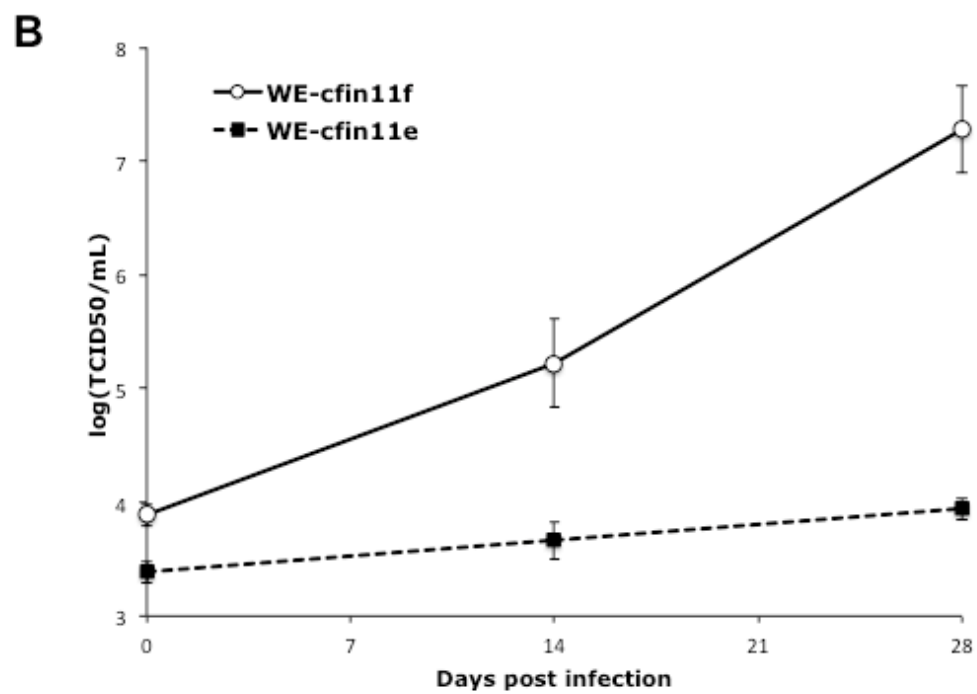
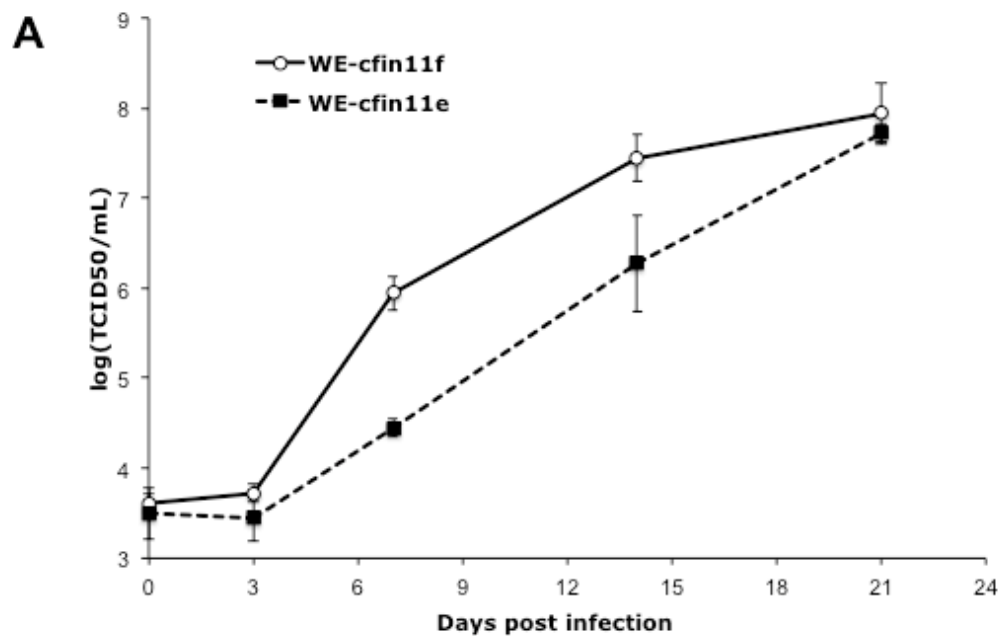


**Figure 3.7. Viral production in WE-cfin11f and WE-cfin11f at the optimal VHSV infection temperature 14 °C (Panel A) and the winter-like temperature 4 °C (Panel B).** Confluent cultures in triplicate wells of six-well plates were allowed to be kept at either 14 °C or 4 °C overnight prior to viral infection challenges. Cells were incubated with VHSV IVb in L-15 with 2% FBS for 2 h at either 14 °C or 4 °C. Subsequently, free unbound viral particles were washed off with PBS and the cultures were replenished with fresh L-15 with 2% FBS and kept either at 14 °C for up to 21 days or at 4 °C for up to 28 days. If the VHSV particles are produced, they only become infectious after being released from the infected cells into the extracellular space or, in in vitro, the conditioned media. Thus, to determine the virus concentration, on selected days the conditioned media in triplicate wells were collected and titred on VHSV-permissible EPC cell cultures in TCID50 assays using 96-well microplates and cytopathic effect scoring format as previously described and demonstrated by Pham et al. (2011) and Vo et al. (2014). The resulting viral titer values were logarithmically transformed. Each data point on the graphs is the mean of log values from triplicates and the bars are standard deviations.

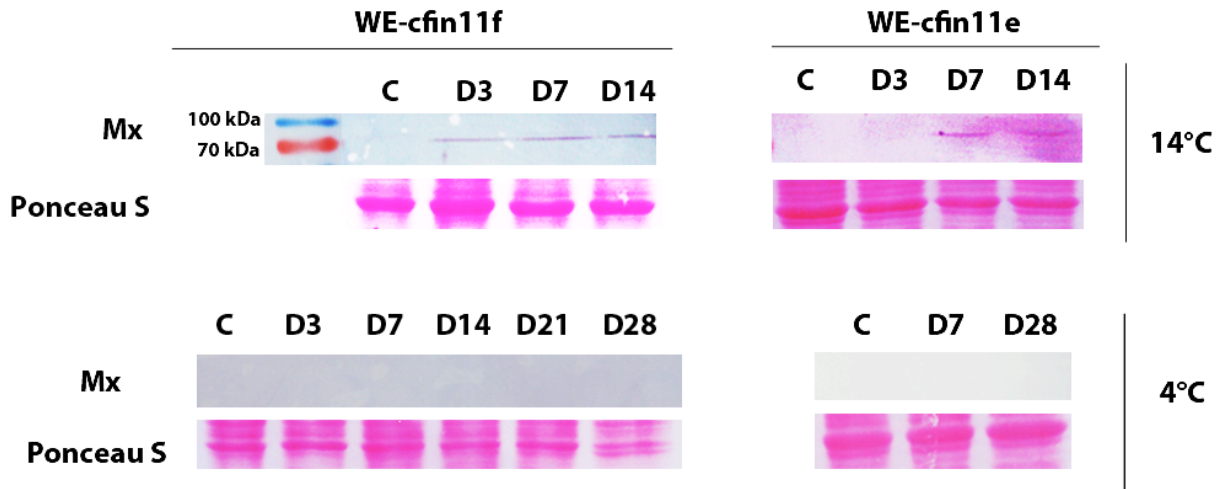


**Figure 3.8. Examination of induction of Mx protein in WE-cfn11f and WE-cfn11e cultures infected with VHSV IVb at 4 °C and 14 °C by Western blotting.** Confluent cultures in 75-cm<sup>2</sup> flasks were incubated with VHSV IVb in L-15 with 2% FBS for 2 h at either 14 °C or 4 °C, washed with PBS and kept in fresh L-15 with 2% FBS either at 14 °C for up to 14 days p.i. or at 4 °C for up to 28 days p.i.. Control cultures did not receive virus. Western blotting procedures were followed accordingly as described in the Materials and Methods. The primary antibody used was rabbit polyclonal anti-rainbow trout Mx antisera used at 1:2000. The secondary antibody was alkaline phosphatase-conjugated goat anti-rabbit IgG used at 1:20,000. Protein bands were detected by NBT/BCIP substrate reactions.

### 3.4. DISCUSSION

An epithelial-like cell line, WE-cfin11e, has been developed from the same primary cell culture of the walleye caudal fin that gave rise to the previously reported fibroblast-like cell line, WE-cfin11f (Vo et al., 2014), and under nearly all culture conditions, the two cell lines retained their characteristic cellular shape. Generally in primary cell cultures of fish fins, the predominant cell types are fibroblasts and epithelial cells (Mauger et al., 2009), but for the goldfish fin, these two cell shapes transiently changed from one to the other in primary cultures (Mauger et al., 2009). However, once WE-cfin11e had been established, the cells were always epithelial-like when cultured at 26 °C and below in L-15 with 5 % FBS. This was true for up to at least 40 passages and after cryopreservation. Thus the two cell lines usually had distinctly different shapes, but one culture condition was an exception. At 4 °C WE-cfin11f lost their fibroblast shape and became epithelial-like (Vo et al., 2014).

These two cell lines appear to represent distinct cellular components of the multiple cell types in the fish caudal fin, fibroblasts and epithelial cells. Biochemical markers that are definitive for fibroblasts are elusive (Krenning et al., 2010), but the presence of collagen I in WE-cfin11f supports describing them as fibroblasts. Furthermore WE-cfin11f responded to ascorbic acid and organized collagen I into extracellular fibers. Ascorbic acid is well known for stimulating the synthesis and matrix deposition of collagen I in human skin fibroblast cultures (Chan et al., 1990) and has been shown to promote collagen fiber formation in a goldfish skin cell line (Lee et al., 1997). The lack of zonula occludens-1 (ZO-1) staining in WE-cfin11f cells is also consistent with the cells being fibroblasts, although ZO-1 has been reported in fibroblasts in a few exceptional cases, such as in the nucleoli of corneal fibroblasts (Benezra et al., 2007). Most commonly, ZO-1 is found at the periphery of the epithelium and endothelium where cells make contact and acts as a scaffolding protein for intercellular junctions, including tight junctions, with additional roles in signal transduction and gene regulation emerging (Bauer et al., 2010). WE-cfin11e stained prominently for ZO-1 around the boundaries of cells in contact with each other. Thus for WE-cfin11e, the presence of ZO-1 staining and absence of collagen I supports the description of them as epithelial.

Both WE-cfin11e and WE-cfin11f stained strongly for vimentin, revealing fibrous cytoplasmic networks that appeared more tangled in WE-cfin11e. Vimentin expression is usually restricted to mesenchymal cells in mammals but seems to have a more complex tissue distribution in teleosts (Mauger et al., 2009; Garcia et al., 2005). Recently another instance of both epithelial and fibroblast cell lines from the same fish species staining for vimentin have been reported (Higaki et al., 2013).

Whether fish epithelial cell lines, such as WE-cfin11e, can express fully functional tight junctions (TJs) remains to be determined. Curtis et al. (2013) examined WE-cfin11e cultures by electric cell-substrate impedance sensing (ECIS) and found that as cultures were maintained as monolayers impedance/resistance increased over time. As ECIS is thought to monitor current passing between the cells, tight junctions forming and acting as a barrier could contribute to impedance/resistance. However, WE-cfin11e did not stain for other TJ proteins, claudins 3 and 5 and occludin. Thus any formation of sealing TJ would have to involve other claudins because claudins belong a large family of proteins (Lal-Nag & Morin, 2009).

Except for the change in shape for WE-cfin11f at 4 °C, the two cell lines had a very similar cellular thermobiology (Vo et al., 2014). At the temperatures above 34 °C, cells in cultures of both cell lines died; at 14 to 32 °C, both cell lines proliferated. At 4 °C, cultures of both cell lines showed neither cell proliferation nor cell death but persisted as stable viable monolayers for at least 5 weeks.

At 14 °C, VHSV IVb infected both cell lines, but infection proceeded slower in WE-cfin11e cultures. Previously, WE-cfin11f were shown to be infected at this temperature (Vo et al., 2014), and generally 14 °C is considered to be at or near optimal for VHSV production (Winton et al., 2010). Immunocytochemical staining for G protein revealed infected cells as early as 5 days in WE-cfin11f cultures and not until 10 days in WE-cfin11e. Likewise CPE started as early as 5 days in WE-cfin11f cultures but did not begin until after 10 days in WE-cfin11e cultures. The significant production of infectious virus became evident after 7 days in WE-cfin11e cultures but later in WE-cfin11f cultures. Ultimately, the amount of virus produced after 3 weeks of infection was similar in both cultures, despite the early stages of infection developing faster in WE-cfin11f.

The ability of fibroblasts to support relatively faster VHSV IVb replication than that of epithelial cells is supported by *in vivo* observations, but causes of this predilection are open to speculation. When rainbow trout and walleye were infected with VHSV Ia and IVb, respectively, through waterborne exposure, the skin was highly immunopositive for the virus, mainly in dermal fibroblasts (Grice et al., 2014; Montero et al., 2011). In the future, the extracellular matrix (ECM) and tight junction proteins might be investigated for their possible contribution to differences in the susceptibility of the WE-cfin11f and WE-cfin11e. Fibronectin has been proposed to be the receptor or co-receptor for VHSV and other fish rhabdoviruses (Albertini et al., 2012; Bearzotti et al., 1999). Collagen I binds fibronectin and triggers fibronectin fibril formation (Dzamba et al., 1993). Perhaps in WE-cfin11f cultures collagen I enhances the ability of fibronectin to act as a VHSV IVb receptor. Alternatively the tight junction proteins in WE-cfin11e might slow completion of the VHSV IVb life cycle. ZO-1 has been found to associate with viral proteins in Dengue virus infections (Ellencrona et al., 2009), and at least one tight junction protein has been to inhibit viral entry (Wilkins et al., 2013).

The preferential replication of VHSV IVb in fibroblasts over epithelial cells is more pronounced when the infection occurs at 4 °C. At this infection temperature, both walleye cell lines supported VHSV IVb entry but relative to 14 °C, the progress of the viral life cycle was slowed. Entry and the beginning of the viral life cycle was revealed in cultures at 4 °C by the appearance of N protein in western blots of cell extracts and of cells positive for G protein in immunocytochemistry of cell monolayers. The infection was impeded as shown by the delay at 4 °C in the accumulation of viral proteins, development of CPE, and the production of virus. The delay could be due to the effect of low temperature on cellular and/or viral processes. A general cellular explanation for the slow progression of the viral life cycle – at 4 °C would be the overall slowing of anabolism. A specific cellular mechanism such as a stronger induction of antiviral mechanisms at 4 °C seems unlikely. Mx would be an example of an antiviral mechanism that inhibits fish rhabdoviruses (Caipang et al., 2003), but VHSV IVb failed to induced Mx in the walleye cell lines at 4 °C, although induction occurred in both cell lines at 14 °C. A possible viral mechanism could revolve around the G protein. The inhibition of VHSV infection by low pH has been attributed partially to the failure of the G protein to

acquire the correct confirmation at the cell surface for the virus to spread between cells (Mas et al., 2004). Perhaps low temperature impedes the acquisition of the active conformation in G protein.

Low temperature (4 °C) impaired the progression of the VHSV IVb life cycle more severely in the caudal fin epithelial cells than the fibroblasts. By 28 days at 4 °C, WE-cfin11f ultimately underwent CPE and produced VHSV IVb (Vo et al., 2014) but WE-cfin11e did not, even at up to 35 days p.i.. Possibly this reflects a more severe reduction in anabolism at 4 °C in fish epithelial cells than in fibroblasts. A precedent for epithelial cells and fibroblasts responding differently to low temperatures has been reported for human skin cell cultures: epithelial cells grew better at temperatures below 37 °C than fibroblasts (Jensen & Therkelsen, 1981). In contrast to a general response to low temperatures, specific cellular process(s) required for the completion of the virus life cycle might be more impaired by the cold in WE-cfin11e than in WEcfin11f. These might be steps related to the final assembly and egress of the virus. For example the viral G protein needs to be glycosylated in endoplasmic reticulum/Golgi complex and transported to the cell surface (Jayakar et al., 2004). Fibroblasts might be expected to have a greater capacity for glycosylation and protein secretion than epithelial cells and perhaps at low temperatures fibroblasts might still have some capacity to carry out these processes. The results imply that that low temperature modulates the tissue tropism of VHSV IVb, which would be the first hint of such a phenomenon in fish virology.

Whether VHSV IVb infection can occur *in vivo* at 4 °C is open to speculation. In this *in vitro* study at a high moi, fibroblasts but not epithelial cells produced VHSV IVb at 4 °C. If temperature influences tropism in this manner *in vivo*, this could be contributing to VHS outbreaks in early spring. In the fall, infection could begin in a few fish as a small epithelial lesion that would produce a small amount of virus before being halted by dropping temperatures. The virus could move to the dermis, where over winter the virus would be slowly produced by fibroblasts. Although infected, the epithelium would remain intact because of the low temperature and virus from the fibroblasts would accumulate in connective tissue. When spring came and water warmed, the viral life cycle would be completed in the epithelial cells, destroying the epithelial barrier, releasing the virus that had accumulated in the dermis over winter. The burst of virus

shed into water would infect other individuals that would be aggregating for spawning and cause a fish kill.

## **CHAPTER 4.**

**Development of a walleye spleen stromal cell line sensitive to viral hemorrhagic septicemia virus (VHSV IVb) and to protection by synthetic dsRNA**

#### 4.1. INTRODUCTION

Having cell lines from walleye, *Sander vitreus*, would help researchers acquire information that would be useful to fisheries and aquaculture managers. Walleye is often described as the most widely stocked and important commercial and recreational freshwater fish species in North America (Fenton et al 1996; Summerfelt, 2005), but few walleye cell lines are available (Vo et al., 2014). The emergence in the North American Great Lakes region of VHSV IVb and the death of fish due to viral hemorrhagic septicaemia (VHS) has complicated the management and aquaculture of walleye (Grice et al., 2014; Lumsden et al., 2007). The information that could be obtained with cell lines would include the detection of the virus, an understanding of the mechanism underlying the pathology of VHS and insights into potential treatments.

The pathology of VHS can be complex but commonly lesions are observed in hematopoietic tissues, such as the head kidney and spleen (Smail & Snow, 2011). Vertebrate hematopoietic tissues are made up of hematopoietic stem cells/progenitors within a stroma. The stroma consists an extracellular matrix (ECM) and stromal cells and provides the microenvironment to support hematopoiesis and to facilitate the initiation of an adaptive immune response by concentrating the antigen and lymphocytes (Kain & Owens, 2013). The stromal cells include endothelial cells, fibroblasts, smooth muscle cells, fibroblastic reticular cells (FRCs), and in some species myofibroblasts (Balaogh et al., 2008; Charbord et al., 2002). Fibroblastic reticular cells (FRCs) are a type of fibroblast in secondary lymphoid organs, like the spleen, and in mammals are targets of many viruses (Mueller & Germain, 2009). Myofibroblasts are found in many tissues and express smooth muscle  $\alpha$ -actin (SAM), synthesize collagen, and may be multipotent (El-Helou et al., 2012; Strakova et al., 2008) and in the spleen they attract and guide lymphocytes to the white pulp (Briard et al., 2005; Steiniger et al., 2001).

Many stromal cell lines have been developed from the spleens of rodents and humans (Despars & O'Neil, 2006) and a few from fish (Ganassin & Bols, 1999). These have supported hematopoiesis to varying degrees, have had different morphologies, and have been designated as belonging to several different mesenchymal lineages. The spleen stromal cell lines have been described as cobblestone, spindle shaped, mixed, endothelial-like, fibroblast-like and epithelial-like (Charbord et al., 2002; Ganassin & Bols, 1999;

Despars & O'Neill, 2006; Piersma et al., 1984; Pietrangeli et al., 1988; Tsuchiyama et al., 1995; Xing et al., 2009; Yanai et al., 1989). Some spleen stromal cell lines of mice are mesenchymal stem cells (MSC) with the potential to differentiate into different mesodermal cell lineages (Pevsner-Fischer et al., 2011; Sagi et al., 2012).

One potential antiviral treatment for fish is the viral mimic, polyinosinic-polycytidylic acid (pIC) (Eaton, 1990; Kim et al., 2014), which is a synthetic double stranded RNA (dsRNA). Multiple antiviral mechanisms are triggered by pIC in vertebrates (Sadler & Williams, 2008), with perhaps the antiviral Mx proteins being most studied in fish (Ngaard et al., 2000). In both fish and fish cell lines pIC induces Mx (Jensen et al., 2002; DeWitte-Orr et al., 2007). Mx proteins are members of the dynamin large GTPase family and have been shown to interfere with the replication of several classes of viruses, but most often single stranded RNA viruses (Verhelst et al., 2013). The mechanism of Mx action appears to vary with the virus but broadly speaking the antiviral Mx activities can be classified as inhibition of viral RNA transcription and protein synthesis, nucleocapsid transportation, and the viral polymerase complex (Lin et al., 2005; Verhelst et al., 2013).

In this report a stromal cell line (WE-spleen6) has been obtained from the walleye spleen and found to be more sensitive to VHSV IVb than a fibroblast cell line (WE-cfin11f) from the walleye caudal fin. Exposure of WE-spleen6 to pIC induced Mx and delayed progression of the VHSV IVb infection cycle, with viral phosphoprotein P being particularly targeted.

## **4.2. MATERIALS AND METHODS**

### **4.2.1. Tissue culture supplies, fish and miscellaneous reagents**

The basal medium Leibovitz's L-15 and fetal bovine serum were from Hyclone (ThermoFisher Scientific, Burlington, ON). Penicillin and streptomycin (P/S) for supplementing L-15 and dimethyl sulfoxide (DMSO) for cryopreservation were purchased from Sigma (St Louis, MO). Other tissue culture supplies were purchased through VWR International (Mississauga, ON) and included trypsin (Lonza) for subcultivation or passaging, 12.5-cm<sup>2</sup>, 25-cm<sup>2</sup> and 75-cm<sup>2</sup> flasks (BD Falcon), 4-chamber slides (BD Falcon) and slide flasks (Nunc). The fish were juvenile walleye of the Bay of Quinte Stock and obtained and handled as described previously (Vo et al., 2014). Sigma was the source of the cytochemical kit for alkaline phosphatase (Sigma 85L3R), 4'-6-damino-2-phenylindole (DAPI), and the synthetic double-stranded RNA (dsRNA), polyinosinic-polycytidylic acid (pIC). Latex beads (0.93 ± 0.1 µm in diameter, 2.7 % solid in water) were purchased from Polysciences Inc. (Warrington, PA).

### **4.2.2. Antibodies for cellular and viral proteins**

Antibodies were bought to detect four cellular proteins: collagen type I (COL-1), von Willebrand Factor (vWF), vimentin and smooth muscle  $\alpha$ -actin ( $\alpha$ -SMA). For COL-1, an affinity-purified rabbit polyclonal antibody that had been raised against salmon COL-I was purchased from Cedarlane (Burlington, ON). For vWF, an affinity-purified rabbit polyclonal antibody that had been raised against human vWF was procured from Sigma-Aldrich. The mouse monoclonal antibodies (mAb) to vimentin (clone V9) and  $\alpha$ -SMA (clone 1A4) were also purchased from Sigma-Aldrich.

The rabbit polyclonal antibody to rainbow trout Mx was acquired from Dr. J. Leong (Hawaii Institute of Marine Biology, O'ahu, HI) and originally described by Trobridge et al. (1997). Mouse mAb to VHSV proteins were obtained from Dr. N. Lorenzen (Aarhus University, Aarhus, Denmark). These were IP5B11 for N protein, IP1H3 for G protein, and IPIC6 for P protein (Lorenzen et al., 1988).

The appropriate secondary antibodies for use with the above primary antibodies in indirect immunofluorescence staining and western blotting were obtained from Life Technologies (Carlsbad, CA) and Sigma-Aldrich, respectively. These were Alexa Fluor

488-conjugated goat anti-rabbit or anti-mouse IgG secondary antibodies for immunocytochemistry. For the western blotting, the secondary antibody was alkaline phosphatase-conjugated goat anti-rabbit or mouse IgG.

#### **4.2.3. Development of WE-spleen6**

Walleye spleen primary cultures were initiated by explant outgrowth as described previously for zebrafish spleen (Xing et al., 2009). The spleen was cut into small fragments and incubated in L-15 with 15% FBS and 1% P/S in 25-cm<sup>2</sup> or 12.5-cm<sup>2</sup> flasks at 26 °C. Over a period of several weeks, cells of different morphologies migrated out of the spleen fragments and onto the tissue culture plastic. In some of the flask cultures, phase bright and non-adherent cells accumulated in the medium and are interpreted as progeny arising from hematopoietic stem cells within the monolayer undergoing hematopoiesis as previously described in details for rainbow trout spleen hematopoietic cultures (Ganassin and Bols, 1996). From one of these flasks that had become nearly confluent, the cell line, WE-spleen6, was developed by subcultivating the flask with trypsin. The cells were added to two new flasks. Subsequently, these grew to confluency and were passaged again at a 1 to 2 ratio. Non-adherent progeny cells no longer appeared in cultures after a few passages. WE-spleen6 has been maintained for over three years through approximately forty passages at 1 to 2 subcultivation and cryopreserved successfully at several passage levels. The cryopreservative was 10 % DMSO in the growth medium; storage was done in liquid nitrogen.

#### **4.2.4. Appearance of WE-spleen6 cultures on tissue culture plastic versus matrix gel**

The cellular morphology of WE-spleen6 cultures on conventional tissue culture plastic and Matrigel was examined by observing them periodically with an inverted phase contrast microscope. Matrigel (BD 35423) was from BD Biosciences (Mississauga, ON) and the surface of wells in 24 well tissue cultures plates was coated with Matrigel according to the manufacturer's instructions. Matrigel is a commercial, soluble extract of basement membrane proteins from a mouse tumour (EHS) and thought to contain angiogenic as well as other factors (Kleinman et al., 2005).

#### **4.2.5. Alkaline phosphatase and phagocytic activities of WE-spleen6**

A histochemical kit for monitoring alkaline phosphatase (AP) activity was used according to the manufacturer's instructions and as used previously to characterize a zebrafish spleen cell line (Xing et al., 1999). WE-spleen6 cells were plated onto sterile microscopic slides in humidified Petri dishes or into 25-cm<sup>2</sup> flasks. The cells were fixed in a citrate-buffered acetone solution for 30 seconds and washed for 45 seconds with deionized water. Immediately following this wash cells were exposed to an AS-MX phosphate alkaline solution mixed with a diazonium salt solution for 30 minutes. After several washes with deionized water, cells were counterstained in Mayer's hematoxylin solution for 10 minutes. A final wash in tap water removed excess stain. AP was seen as pink granular coloring within cells and mummichog embryonic cells were a positive control.

Phagocytic activity was monitored in cultures plated in 12.5-cm<sup>2</sup> flasks. Cells were incubated with latex beads at 1:1000 in the normal growth medium at 26 °C. After 24 h, the cultures were washed with PBS five times to remove the floating and unphagocytized beads. Phagocytic activity was evaluated by examining whether cells had internalized beads under the inverted phase contrast microscope.

#### **4.2.6. Immunocytochemistry for cellular markers**

Fluorescence immunocytochemistry was used to evaluate the cell line for several cellular markers with antibodies described in an early section of the Materials and Methods. Approximately  $1 \times 10^5$  cells were seeded in 4-chamber slides and incubated at 26 °C. Briefly, cells were washed with PBS three times and fixed with 3% paraformaldehyde (PFA, Sigma) for vWF and  $\alpha$ -SMA staining or ice-cold absolute methanol for vimentin and collagen I staining for 20 min at 4 °C, followed by a permeabilization step with 0.1% Triton X-100 in PBS for 10 min. Cultures were then incubated with blocking buffer (10% goat serum, 3% bovine serum albumin and 0.1 % Triton X-100 in PBS) for 1 h at room temperature. Cells were then incubated with primary antibodies diluted in blocking buffer as follows: 1:400 rabbit anti-salmon COL-1 for 1 h, 1:200 rabbit anti-human vWF for 1.5 h, 1:200 mouse mAb anti- $\alpha$ -SMA (clone 1A4) overnight, 1:200 mouse mAb anti-porcine vimentin (clone V9) overnight.

Overnight incubations were done at 4 °C and 1-h or 1.5-h incubations were done at room temperature. Some cultures were incubated with blocking buffer without primary antibodies as controls for nonspecific binding. After incubation with the primary antibody or blocking buffer alone, cultures were washed with PBS three times with rocking and subsequently incubated with Alexa Fluor 488®- conjugated goat anti-rabbit or anti-mouse IgG secondary antibodies (1:1000 in PBS) for 1 h. Cultures were then washed with PBS three times, allowed to air-dry and mounted in Flourosshield medium with DAPI. Fluorescence were examined and images were taken with the Zeiss LSM 510 laser scanning microscope and confocal images were acquired and analyzed using a ZEN lite 2011 software. Fluorescence staining was never observed in cultures to which only secondary antibody had been applied.

#### **4.2.7. Other cell lines and viral haemorrhagic septicemia virus group IVb (VHSV IVb)**

Three other walleye (WE) cell lines were studied and for routine propagation of the virus, the fathead minnow cell line, EPC, (Winton et al., 2010) was used. WE-cfin11f, WE-cfin11e and WE-skin11f were developed and grown as described previously (Vo et al., 2014) and in chapters 3 and 6 in the thesis. The VHSV IVb was CEFAS strain U13653 isolated from infected freshwater drum (*Aplodinotus grunniens*) from Lake Ontario in 2005 (Lumsden et al., 2007). Virus stocks were routinely prepared on the confluent EPC cultures as previously described by Vo et al. (2014) and Pham et al. (2011). For VHSV infection the infection medium was always L-15 with 2% FBS and the infection temperature was always 14 °C, unless otherwise specified. Approximately 10 days post-infection (p.i.), EPC monolayers were completely destroyed and the cell lysates were collected and centrifuged at  $4500 \times g$  for 5 min at 4 °C. The supernatants were syringe-filtered through 0.2- $\mu\text{m}$  membranes (Pall Corporation), aliquotted and stored at -80 °C. Subsequently viral titers of the stock were determined by serially diluting viral stock aliquots and inoculating on EPC in the tissue culture infectious dose TCID<sub>50</sub> assays (as previously described in details by Pham et al., 2011) and expressed as TCID<sub>50</sub> mL<sup>-1</sup>. The viral titers were usually determined to be  $1 \times 10^8 - 2.15 \times 10^8$  TCID<sub>50</sub> mL<sup>-1</sup>.

#### **4.2.8. Evaluating viral transcripts during VHSV IVb infection cycle in WE cell cultures**

Cultures of WE-spleen6 and WE-cfin11f in 25-cm<sup>2</sup> flasks were infected with VHSV IVb at MOI of 1 or 10 and analyzed at various times afterwards by reverse-transcription polymerase chain reaction (RT-PCR) for transcripts of all six VHSV genes: N, P, M, G, Nv and L. The methods were performed as described in details recently (Pham et al., 2013; Vo et al., 2014). RNA was extracted with the Total RNA Kit I (Omega Bio-Tek); cDNA was synthesized with the Revert Aid H Minus First Strand cDNA Synthesis Kit (Thermo Scientific); and viral gene amplification was done with recombinant *Taq* DNA polymerase (Fermentas). The primers were as published in Pham et al. (2013) and are listed in Table 2.1.

#### **4.2.9. Evaluating viral proteins during VHSV IVb infection cycle in WE cell cultures**

Western blotting was used to monitor cultures of WE- spleen6 and WE-cfin11f for viral proteins, N and P, at various time points after infection with 10<sup>7</sup> TCID<sub>50</sub> mL<sup>-1</sup> VHSV IVb (or equivalently at MOI of 10). Cell lysates were prepared, subjected to SDS-PAGE, and electro-transferred to nitrocellulose membranes as described previously (Vo et al., 2014; Pham et al., 2013). The membranes were probed for N protein with mAb IP5B11 at 1:600 and for P proteins with mAb IP1C6 at 1:600. The WE-cfin11f cultures were maintained in L-15 with 2 % FBS at 14 °C and examined at 1, 2, and 7 days p.i.. WE-spleen6 cultures began to undergo significant CPE at 3 days p.i. at 14 °C so for WE-spleen6 cultures only days 1 and 2 were examined. Additionally examination was made of WE-spleen6 cultures after first being dosed for 24 h with 1 µg/mL pIC before being infected with 10<sup>7</sup> TCID<sub>50</sub> mL<sup>-1</sup> VHSV IVb (or equivalently at MOI of 10). In this case lysates could be prepared from cultures after 1, 2 and 3 days p.i.

Viral proteins, N and G, were monitored by indirect immunofluorescence staining of WE-spleen6 and WE-cfin11f cultures in Nunc slide flasks 1 day p.i. with mAb IP5B11 for N protein and 2 days p.i. with mAb IP1H3 for G protein. Both mAb's were diluted at 1:100 and used as described in the section on immunocytochemistry of cellular markers. As controls for nonspecific binding, some cultures were incubated with blocking buffer without primary antibodies before the application of the secondary antibody, Alexa Fluor

488®- conjugated goat anti-mouse IgG secondary antibody (1:1000 in PBS). Fluorescence staining was never observed in these cultures.

#### **4.2.10. Evaluating CPE during VHSV IVb infection cycle in WE cell cultures**

The susceptibility of walleye cells to the cytopathic effect (CPE) of VHSV IVb was compared between two cell lines, WE-spleen6 and WE-cfin11f. Tests were done over a range of MOI from a very large one of 175 to 1 to a small one of 0.002 to 1. As a low pH, such as 6.5 or less, can block the spread of VHSV between cells and impede the development of CPE (Mas et al., 2004), pH was measured in L-15 with 2 % FBS, which was the medium in which cells were exposed to the virus and maintained post infection for CPE development. With cells of either cell line for 24 h, the medium at 14 °C had a pH of 7.3.

The cytopathic effect (CPE) was observed in cultures of WE-spleen6 and WE-cfin11f after being infected with  $10^7$  TCID<sub>50</sub> mL<sup>-1</sup> of VHSV IVb. CPE was monitored as a change in cell morphology and cell detachment/lysis through phase contrast microscopic observations and by evaluating the loss of cell viability with the indicator dyes, Alamar Blue® (Invitrogen). This indicator dye provides a measure of cellular metabolism and is recorded as RFUs (Dayeh et al., 2013). The RFUs for virally infected cultures were expressed as a percentage of the RFUs in control wells without virus.

#### **4.2.11. Evaluating VHSV IVb production in walleye cell cultures**

Viral titres were measured in cultures of WE-spleen6 and WE-cfin11f after infection with  $10^7$  TCID<sub>50</sub> mL<sup>-1</sup> of VHSV IVb (or equivalently at MOI of 10). The infection was allowed to proceed for 14 days at 14 °C in L-15 with 2 % FBS. Titres were obtained at day 0 and days 3, 7, 10 and 14 p.i. as described in detail by Vo et al. (2014) for WE-cfin11f and the results expressed as log (TCID<sub>50</sub> mL<sup>-1</sup>).

#### **4.2.12. Monitoring Mx expression through western blotting**

Mx expression was evaluated in cultures of several walleye cell lines after receiving no additions (the controls) and after being dosed with either pIC or VHSV IVb or both. Confluent cultures of WE-spleen6, WE-cfin11f, WE-cfin11e, and WE-skin11f in 75-cm<sup>2</sup>

flasks received 1  $\mu\text{g}/\text{mL}$  of pIC in L-15 with 2 % FBS and were incubated for 24 h at 26 °C before the preparation of cell lysates. For VHSV infection, cultures of WE-spleen6 and WE-cfin11f were infected with  $10^7$  TCID<sub>50</sub> mL<sup>-1</sup> of VHSV IVb (or equivalently at MOI of 10) in L-15 with 2 % FBS and incubated at 14 °C. For WE-cfin11f, the VHSV infections were terminated at 1, 2, 7, and 10 days p.i.. For WE-spleen6, the VHSV infections were for 1 and 2 days p.i. only because viral lysis of the cultures prevented further time points from being examined. Additionally, some WE-spleen6 cultures received  $10^7$  TCID<sub>50</sub> mL<sup>-1</sup> after first being dosed with 1  $\mu\text{g}/\text{mL}$  pIC for 24 h. These cultures were monitored by western blotting at 1, 2 and 3 days pi. Cell lysates were prepared, subjected to SDS-PAGE, electro-transferred to nitrocellulose membranes, and probed for Mx with the rabbit polyclonal anti-rainbow trout Mx at 1:2000 as described in details previously (DeWitte-Orr et al., 2007).

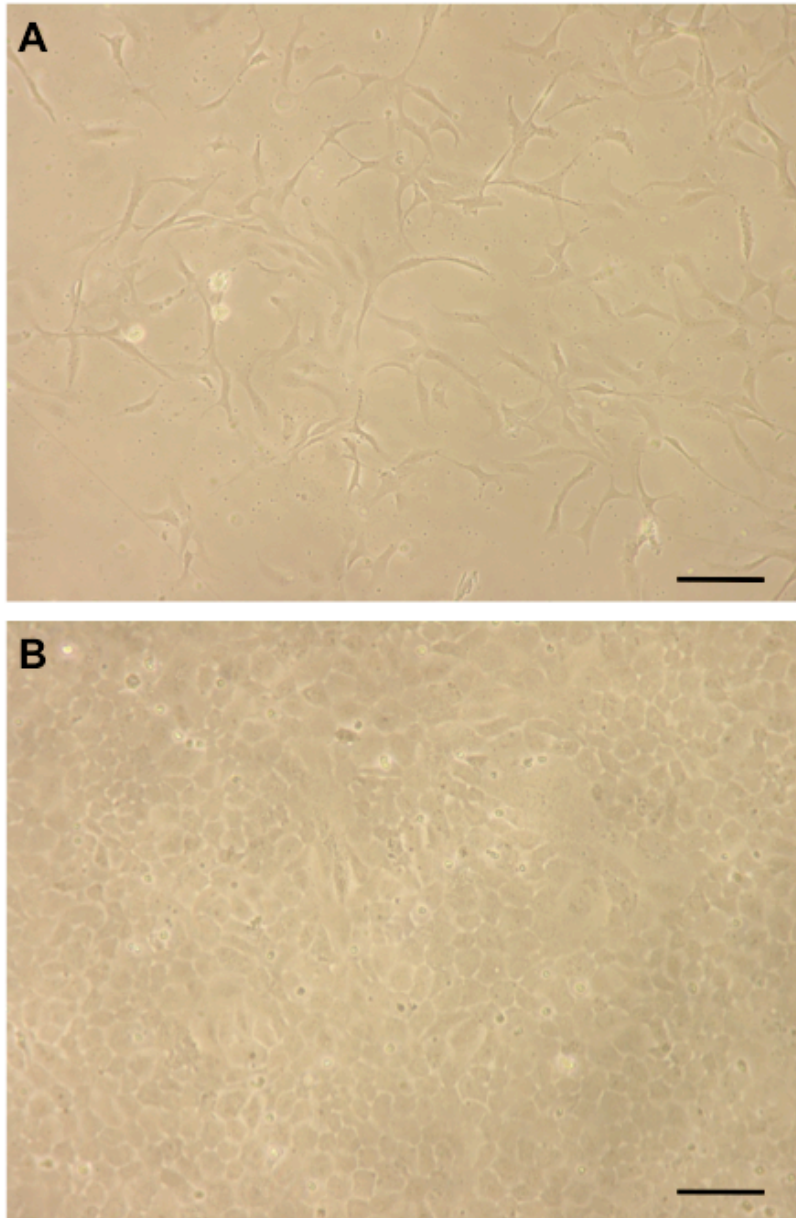
### **4.3. RESULTS**

#### **4.3.1. Appearance of WE-spleen6 cultures on tissue culture plastic versus Matrigel**

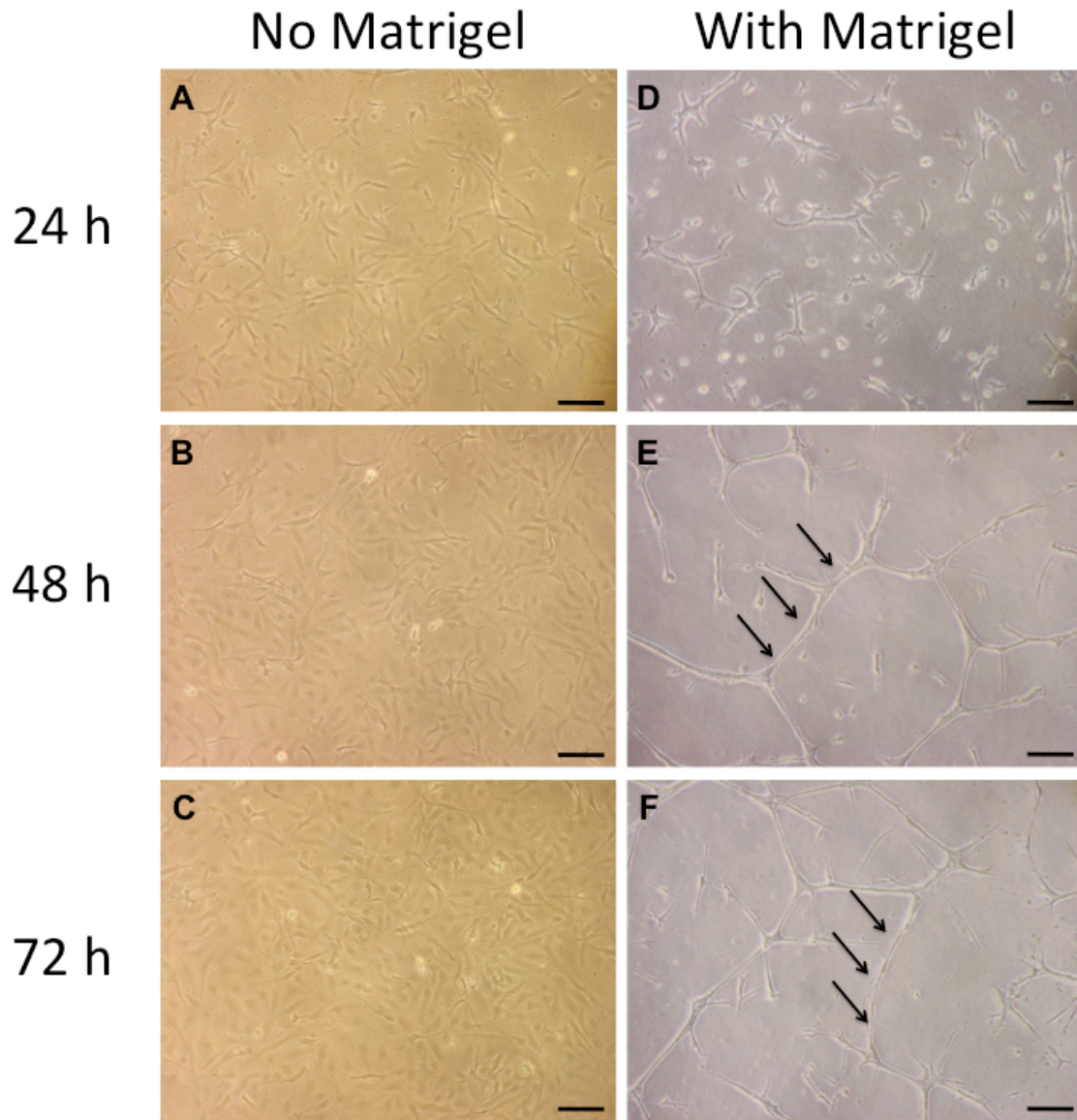
The cellular morphology varied in WE-spleen6 cultures from initiation at low density through growth to become a confluent monolayer (Fig 4.1). The cells had a spindle shape at low density but at confluency they became more flattened and wider and might be best described as epithelial-like (Fig 4.1). Also when the monolayer confluence is reached, in contrast to the walleye caudal fin and skin fibroblast cell lines, WE-cfin11f and WE-skin11f, the WE-spleen6 cells did not overgrow on top of one another. After a few hours on Matrigel the WE-spleen6 cells were spindle-shaped and randomly distributed over the surface. Over the next few days the cells redistributed themselves and became organized into lumen-like structures (Fig 4.2).

#### **4.3.2. Immunocytochemistry, alkaline phosphatase activity, and phagocytosis of WE-spleen6**

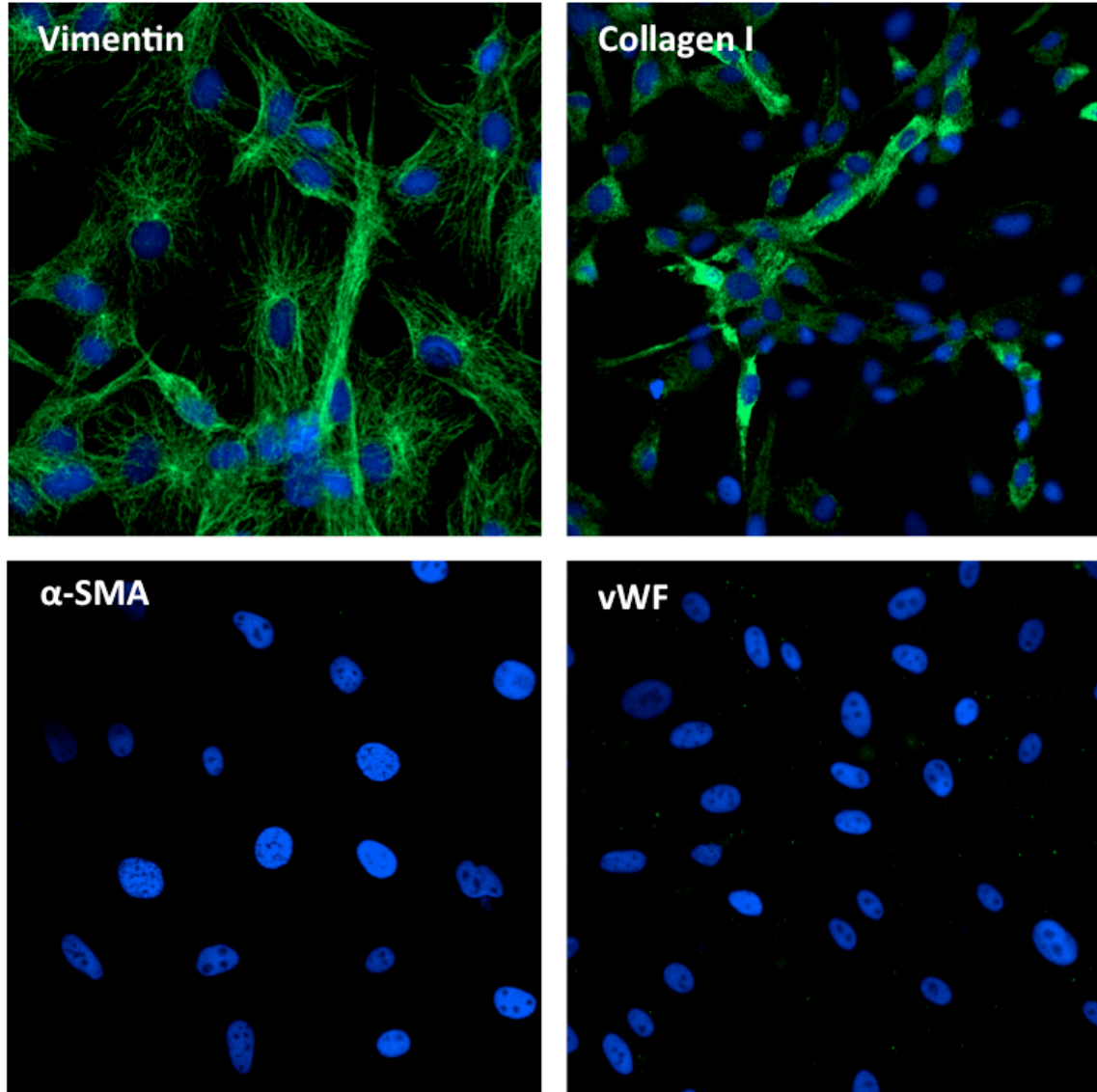
WE-spleen6 cells stained positive for the intermediate filament protein, vimentin, revealing a tangled network of cytoplasmic fibers (Fig 4.3). The WE-spleen6 cultures were also positive for collagen I, with the staining being primarily cytoplasmic (Fig 4.3). WE-spleen6 cells did not stain for the myofibroblast marker,  $\alpha$ -SMA, and the endothelial marker, vWF (Fig 4.3). WE-spleen6 did not stain for alkaline phosphatase (AP) activity and had little ability to phagocytize latex beads (data not shown).



**Figure 4.1. Morphology of cells in WE-spleen6 cultures.** Cells had spindle shape in cultures at a low cell density and became more epithelial-like when cultures reached confluence. Scale bar = 100  $\mu\text{m}$ .



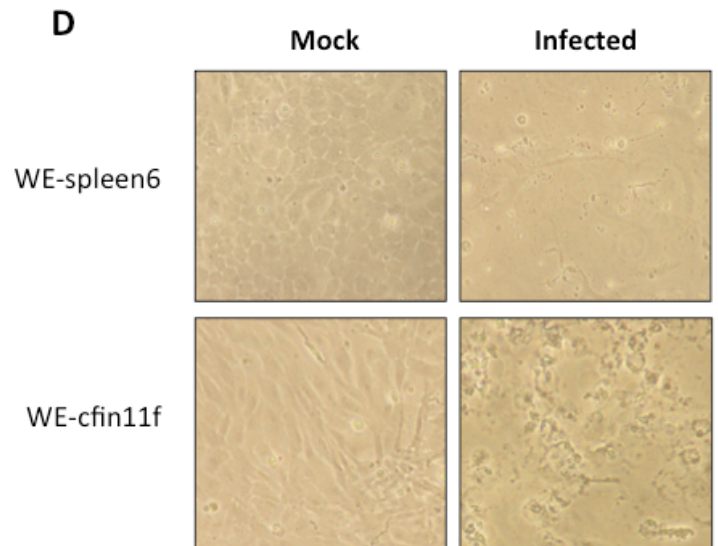
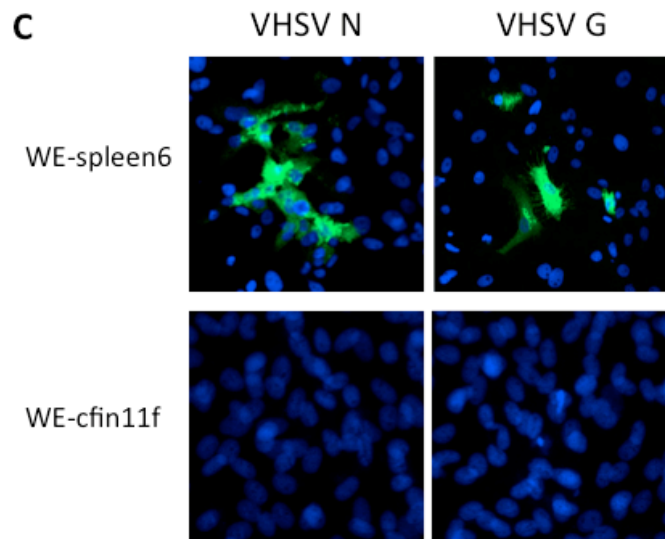
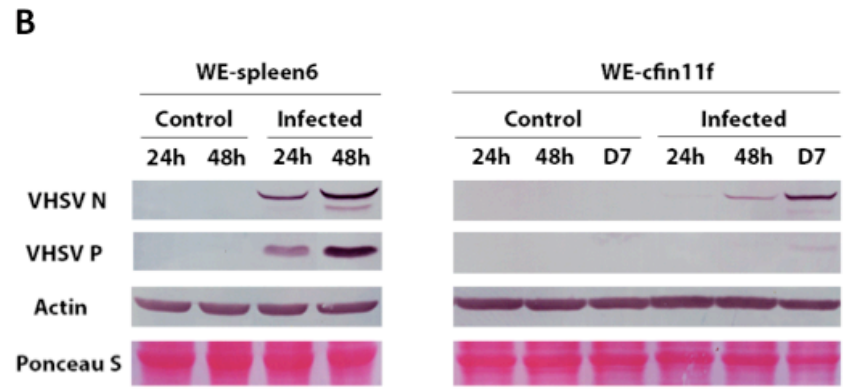
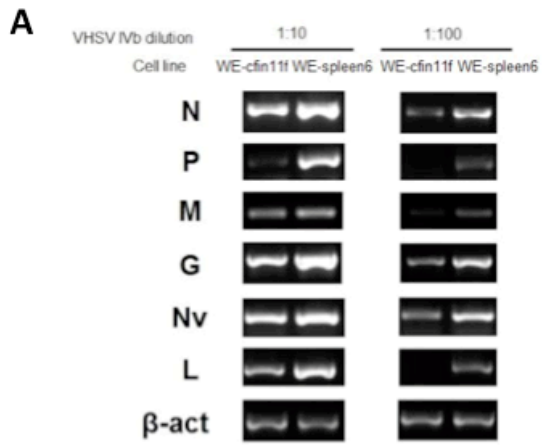
**Figure 4.2. Formation of lumen-like structures by WE-spleen6 cells on Matrigel-coated surface.** On the uncoated (A-C) or pre-coated-with-Matrigel (D-F) triplicate culture wells in 24-well plates,  $5 \times 10^4$  cells per well were seeded in L-15 with 10% FBS. Representative pictures of the cultures were taken at 24 h (A,D), 48 h (B, E), and 72 h (C, F) time points. Lumen-like structures are indicated by arrows. Scale bar = 100  $\mu$ m.



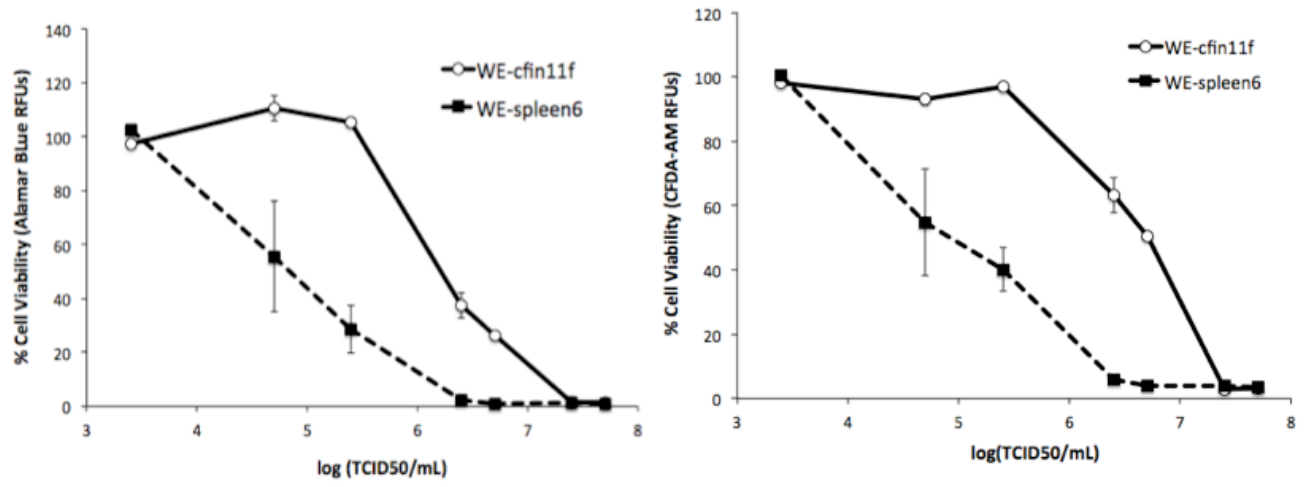
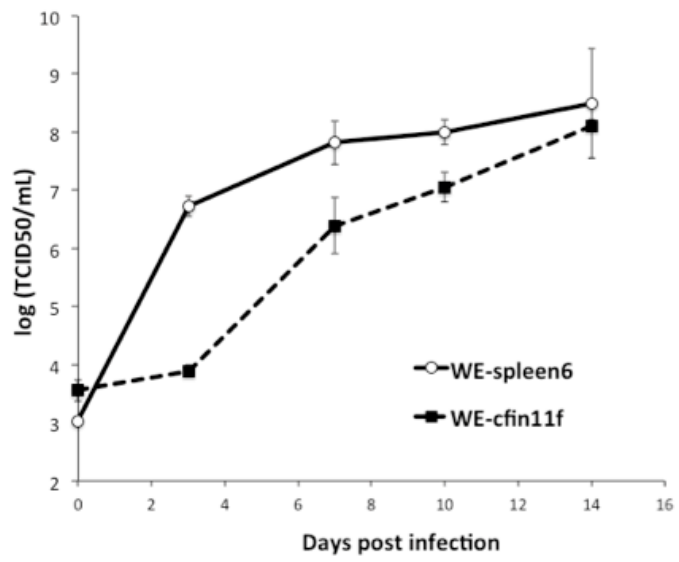
**Figure 4.3. Immunocytochemical staining of WE-spleen6 cell line.** Using monoclonal and polyclonal antibodies (see Materials and Methods) via indirect immunofluorescence in combination with confocal microscopy, polypeptide expression of vimentin, collagen I, von Willebrand factor (vWF) and  $\alpha$ -smooth muscle actin ( $\alpha$ -SMA) in WE-spleen6 was studied. The fluorophore Alexa Fluor 488 (green) was conjugated with the secondary antibody and its fluorescence indicated the presence of the detected protein of interest in the cells. DAPI (blue) was used to counterstain the cell nuclei. Confocal images were taken with the Zeiss LSM 510 laser scanning microscope and acquired and analyzed using a ZEN lite 2011 software. Vimentin and collagen I, but not vWF and  $\alpha$ -SMA, were detected in WE-spleen6.

### **4.3.3. VHSV IVb infection cycle in WE-spleen6 versus WE-cfin11f**

Several measures of the VHSV IVb infectious cycle suggest that infection proceeded more rapidly in WE-spleen6 than in WE-cfin11f cultures. As judged by RT-PCR, transcript levels were higher at 24 h pi in WE-spleen6 (Fig 4.4A); control samples (no virus and no reverse transcriptase addition) showed no detection of viral transcripts (data not shown). Viral polypeptides, N, P and G, appeared earlier in WE-spleen6 cultures. N and P were detected in western blots as early as 1 day p.i. in WE-spleen6 but in WE-cfin11f N and P were not seen respectively until 2 and 7 days p.i. (Fig 4.4B). Cells that immunocytochemically stained for N or G appeared earlier in cultures of WE-spleen6 than in WE-cfin11f (Fig 4.4C). CPE (Fig 4.4D) were observed first in WE-spleen6, appearing around day 2 p.i. but not until day 7 for WE-cfin11f. The greater sensitivity of WE-spleen6 versus WE-cfin11f cultures to killing by VHSV IVb was illustrated by dosing with different amounts of virus and monitoring cell viability with a cell viability fluorescent dye Alamar Blue after 14 days p.i.. In cultures that received 5 log(TCID<sub>50</sub>/ml) no loss of viability was seen for WE-cfin11f, whereas viability had been reduced by approximately 50 % in WE-spleen6 (Fig 4.5A). The amount of virus produced by the two cell lines was similar after 14 p.i. but significant virus production began earlier in WE-spleen6 cultures, being seen as early as after 3 days p.i. (Fig 4.5B).



**Figure 4.4. WE-spleen6 cells were more susceptible to VHSV IVb infection than the walleye caudal fin fibroblast WE-cfin11f cell line.** VHSV infection was always done in L-15 with 2% FBS at 14 °C. (A) Expression of viral transcripts in VHSV IVb-infected WE-spleen6 and WE-cfin11f cell lines by RT-PCR. Briefly, both cell lines were challenged with 1:10 or 1:100 dilution of VHSV IVb stocks ( $10^8$  TCID<sub>50</sub>/mL) (or equivalently at MOI of 1 or 10); total cellular RNA contents were extracted 24 h p.i.; cDNA was synthesized; viral transcripts were amplified by RT-PCR using previously characterized primers (see Pham et al., 2013; Vo et al., 2014; Table 2.1). (B) Detection of viral N and P proteins in VHSV IVb-infected WE-spleen6 and WE-cfin11f cultures by Western blotting. Briefly, both cell lines were infected with  $10^7$  TCID<sub>50</sub>/mL of VHSV IVb. Total protein contents were extracted on selected time points, equally separated on SDS-PAGE gels and electro-transferred onto the nitrocellulose membranes. Ponceau S staining was used to ensure effective protein transferring and equal loading. Membranes were blocked with 5% skim milk, probed with mAb IP5B11 for VHSV N protein or mAb IP1C6 for VHSV P protein or rabbit polyclonal anti-actin antibody and then subsequently probed with alkaline phosphatase-conjugated goat anti-mouse or anti-rabbit IgG antibodies. Protein bands were developed with NBT/BCIP substrates. (C) Detection of viral N and G proteins in VHSV IVb-infected WE-spleen6 and WE-cfin11f cultures by indirect immunofluorescence and confocal microscopy. Briefly, both cell lines were infected with  $10^7$  TCID<sub>50</sub>/mL of VHSV IVb in Nunc slide flasks. Detection of VHSV N protein was performed with mAb IP5B11 one day p.i.; detection of VHSV G proteins was performed with mAb IP1H3 two days p.i.. Alexa Fluor 488 (green) was the fluorophore conjugated with the secondary antibody and DAPI (blue) was used to counterstain the cell nuclei. Confocal images were taken with the Zeiss LSM 510 laser scanning microscope and acquired and analyzed using a ZEN lite 2011 software. (D) Cell monolayers were completely destroyed for on day 14 p.i. for WE-cfin11f and WE-spleen on day 5 p.i. for WE-spleen6.

**A****B**

**Figure 4.5. WE-spleen6 cell line was more sensitive to VHSV IVb infection than WE-cfin11f cell line.** (A) Cell viabilities were evaluated by two cell viability fluorescent dyes, Alamar Blue (left panel) and CFDA-AM (right panel). Briefly, cells in four well replicates were seeded in 24-well plates, infected with a series of dilutions of VHSV IVb stock ( $10^8$  TCID<sub>50</sub>/mL) at 14 °C for 14 days and then subject to Alamar Blue and CFDA-AM cell viability assays. Fluorescence was measured in relative fluorescence units (RFUs) with excitation/emission wavelengths at 530nm/590nm for Alamar Blue and 485nm/530nm for CFDA-AM. Values were expressed as percent of average RFUs of the non-infected control cultures with standard error bars. (B) Enumeration of viral loads in VHSV IVb-infected WE-spleen6 and WE-cfin11f cultures by TCID<sub>50</sub> assays. Briefly, both cell lines in triplicate wells of 6-well plates were infected with  $10^7$  TCID<sub>50</sub>/mL of VHSV IVb for 2 h, washed with PBS three times and incubated in fresh L-15 with 2% FBS. On selected days, conditioned media containing new viral progenies produced by infected walleye cells were collected, syringed filtered, and titred on VHSV-permissible reporter EPC cultures. Viral titres were expressed in logarithmic values as log(TCID<sub>50</sub>/mL) with standard deviations.

#### **4.3.4. Mx induction in WE-spleen6 and WE-cfin11f**

Western blotting was used to monitor expression of the antiviral protein, Mx, in WE-spleen6 and WE-cfin11f cultures to which had been added either pIC or VHSV IVb and compared to control cultures. In cultures of both cell lines with 1 µg/ml of pIC for 24 h but not in control cultures, a strong band was apparent at approximately 70 kDA (Fig 4.6A), which is the molecular weight of relatively conserved Mx isoforms among fish families (Trobridge et al., 1997). Although not shown, pIC also induced Mx after 24 h in two other walleye cell lines, WE-cfin11e and WE-skin11f. In contrast to the rapid onset of Mx induction with pIC, Mx induction by VHSV IVb was detectable after 3 days p.i. (chapter 3) and was also apparent in WE-cfin11f cultures after 7 days p.i. in this study (Fig 4.6B). Mx induction by VHSV IVb was also detected in infected WE-cfin11e (chapter 3) and WE-skin11f cultures (data not shown). In contrast, for WE-spleen6 cultures, VHSV IVb had not induced Mx by 2 days p.i. (Fig 4.6B), albeit active viral transcription activities and significant viral protein production and as CPE developed rapidly at later time points, further examination could not be done.

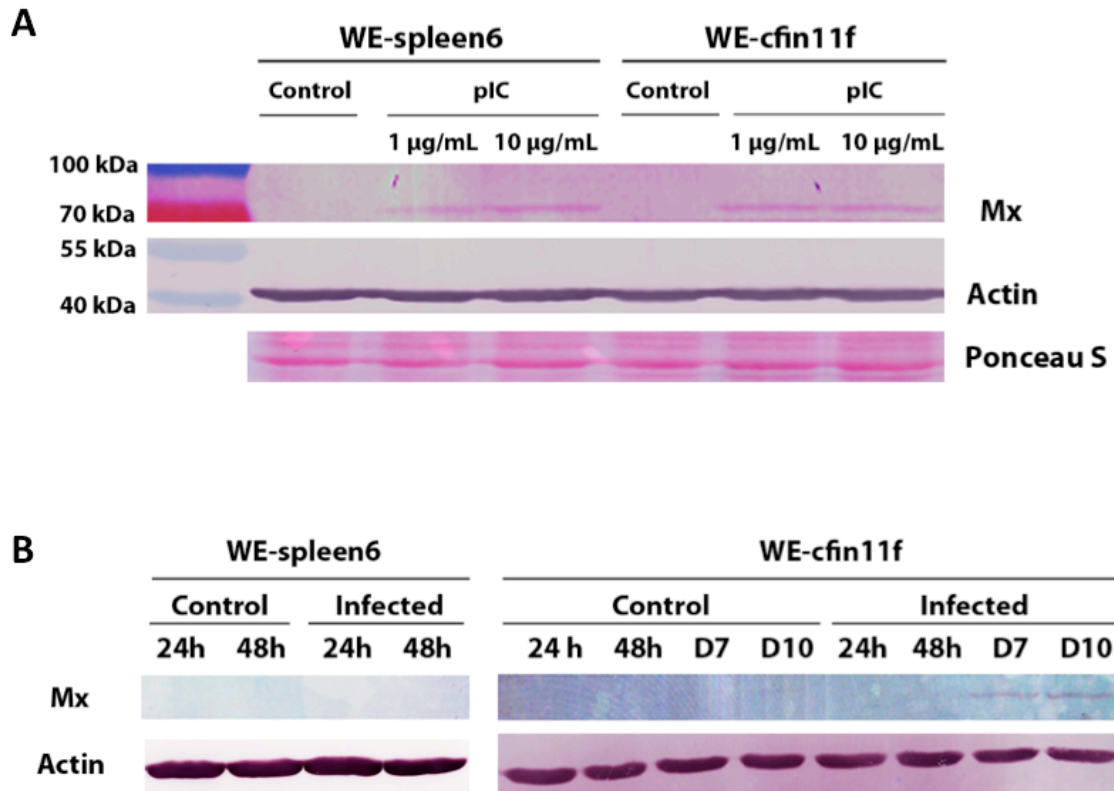


**Figure 4.6. Mx protein induction by a viral mimic pIC and VHSV IVb in WE-spleen6 and WE-cfin11f cell lines by Western blotting.** Both cell lines were (A) treated with 1  $\mu$ g/mL and 10  $\mu$ g/mL pIC in L-15 with 2% FBS at 26 °C for 24 h or (B) infected with  $10^7$  TCID<sub>50</sub>/mL of VHSV IVb (or at MOI of 10) at 14 °C for up to 10 days. Total protein contents were extracted, equally loaded and electrophoretically separated on SDS-PAGE gels and transferred onto the nitrocellulose membranes. Ponceau S was used to ensure equal loading and effective protein transferring. The protein blots were blocked with 5% skim milk, probed with rabbit polyclonal anti-Mx antisera at 1:2000 or affinity-purified rabbit polyclonal anti-actin antibody at 1:400 and then with alkaline phosphatase-conjugated goat anti-rabbit IgG secondary antibodies at 1:20,000. Protein bands were developed with NBT/BCIP reactions. Actin was used as a internal control.

#### **4.3.5. Effect of prior exposure to pIC on VHSV IVb infection cycle in WE-spleen6**

The progression of the VHSV IVb life cycle was impaired in WE-spleen cultures in which 1 µg/ml pIC had been present for 24 h prior to the addition of virus and maintained in the culture during the course of the subsequent viral infection. As detected by RT-PCR, levels of all six VHSV IVb transcripts seemed lower in the presence of pIC, (Fig 4.7A). Without pIC, the viral proteins N and P accumulated over 3 days p.i. as detected in western blots (Fig 4.7B). In the presence of pIC, the level of N protein remained steady, while the level of P declined, almost being barely detectable after 3 days p.i. (Fig 4.7B). Mx induction persisted and its protein production perhaps accumulated further over 3 days p.i. (Fig 4.7B). Cell viability as measured with Alamar Blue was higher at 3 days p.i. in cultures that had been dosed with pIC before the addition of virus (Fig 4.7C). Although virus was produced over 9 days p.i. in control cultures, little virus was produced over 9 days in cultures with pIC (Fig 4.7D). Collectively, these results suggest that treatment of cultures with pIC prior to infection with VHSV IVb impeded viral RNA and protein synthesis, viral-induced cell death, and viral production.

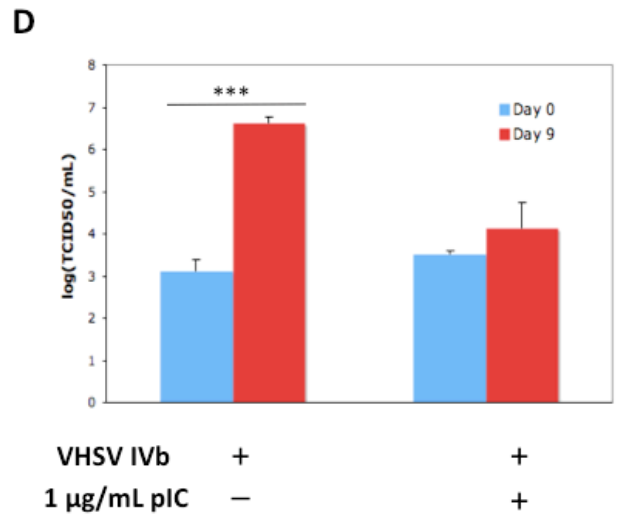
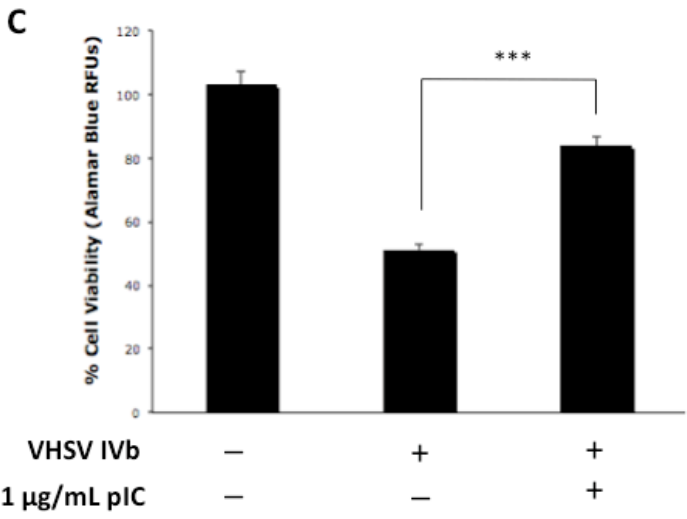
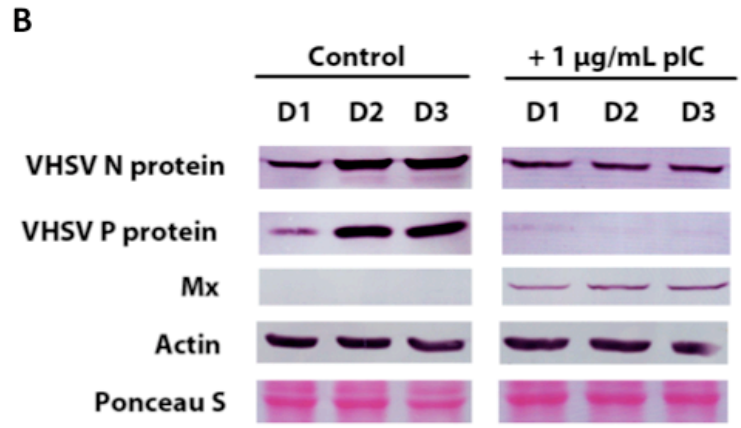
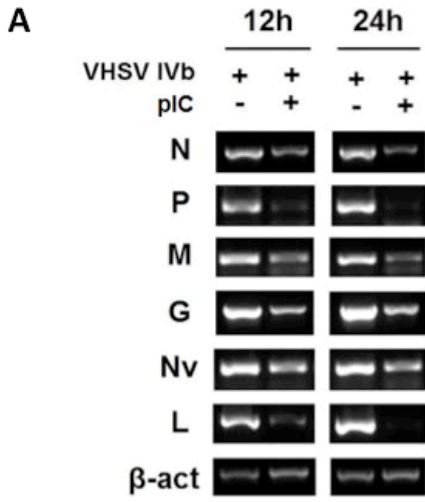


**Figure 4.7. Antiviral effects of pIC against VHSV IVb infection in WE-spleen6.** VHSV infection was always done in L-15 with 2% FBS at 14 °C. (A) Effects of pIC on the expression of viral transcripts. Briefly, cultures untreated or pre-treated with 1 µg/mL of pIC for 24 h were subsequently infected with  $10^7$  TCID<sub>50</sub>/mL of VHSV IVb (or at MOI of 10) and total RNA was isolated 12 h and 24 h p.i.. RT-PCR was performed. β-actin was used as an internal control. No viral transcripts were detected in the mock samples (“no virus and no pIC” controls and “pIC alone” controls). (B) Effects of pIC on the levels of VHSV and antiviral Mx proteins. Briefly, cultures untreated or pre-treated with 1 µg/mL of pIC for 24 h were subsequently infected with  $10^7$  TCID<sub>50</sub>/mL of VHSV IVb and total proteins were extracted from 1, 2 and 3 days p.i.. Protein samples were equally loaded and electrophoretically separated on SDS-PAGE gels and transferred to the protein blots. Equal loading and successful transfers were confirmed with Ponceau S staining. After being blocked in 5% skim milk, the protein blots were incubated with mAb IP5B11 for detecting VHSV N protein or mAb IP1C6 for detecting VHSV P protein or rabbit polyclonal anti-Mx for detecting the antiviral Mx protein or rabbit polyclonal anti-actin antibody for detecting the internal control actin and then subsequently probed with alkaline phosphatase-conjugated goat anti-mouse or anti-rabbit IgG antibodies. Protein bands were developed with NBT/BCIP substrates. (C) Effect of pIC on the cell viability of VHSV IVb-infected WE-spleen6 cultures. Briefly, cells were equally seeded in 24-well plates overnight and each treatment group had 4 well replicates. The first group received no pIC and no virus. The second group received 1 µg/mL of pIC. The third group received  $10^7$  TCID<sub>50</sub>/mL of VHSV IVb. The last group were pre-treated with 1 µg/mL of pIC for 24 h and then exposed to  $10^7$  TCID<sub>50</sub>/mL of VHSV IVb in the presence of 1 µg/mL of pIC. Cell viabilities were measured with Alamar Blue 3 days p.i.. Fluorescence was measured as relative fluorescence units (RFUs). For the graphical presentation, values were expressed as percent of the mean RFU of “no pIC and no virus” controls with standard deviations. (D) Effect of pIC on the VHSV production in WE-spleen6 cultures. Briefly, cells were equally seeded to a confluent level in triplicate wells of 6-well plates. Cultures untreated or pre-treated with 1 µg/mL of pIC for 24 h were subsequently infected with  $10^7$  TCID<sub>50</sub>/mL of VHSV IVb for 2 h, washed with PBS and incubated in new L-15 with 2% FBS. Conditioned media was collected on day 0 and day 9 p.i., serially diluted and titred on VHSV-permissible reporter EPC cultures. Viral titres were expressed in logarithmic values as log(TCID50/mL) with standard deviations. Values were subject to ANOVA and Dunnett’s post test statistical analyses using GraphPad InStat (version 3.00 for Windows 95, GraphPad Software, San Diego California USA, [www.graphpad.com](http://www.graphpad.com)). A p-level < 0.05 was considered as significantly different. \*\*\* indicates p-values < 0.001.

#### 4.4. DISCUSSION

WE-spleen6 expresses markers for several mesenchymal lineages but whether WE-spleen6 represents a particular cell type or is a mesenchymal stem cell line (MSC) capable of differentiating into several lineages is still open to question. WE-spleen6 stained for collagen type I, which is considered a general marker for spleen stromal cells (Zheng et al., 2010). Although WE-spleen6 stained for vimentin, this does not restrict the cells to a particular lineage because vimentin has a complex distribution in fish tissues (Markl & Franke, 1988) and is expressed in mammals in fibroblasts, endothelial cells, and smooth muscle cells (Tang, 2008). The poor phagocytosis of WE-spleen6 would be consistent with them being fibroblastic reticular cells (FRC) (Garnett et al., 1982) or scavenger endothelial cells (Sorensen et al., 2012), but scavenger endothelial cells are not noted in the fish spleen (Sorensen et al., 2012). The formation of lumen-like structures on Matrigel suggests that WE-spleen6 could represent endothelial cells or myofibroblasts. Matrigel has been observed to support the development in vitro of capillary-like structures by many endothelial-cell lines from rodents and humans (Bouis et al., 2001) and recently the formation of lumen-like structures by rat myofibroblasts (El-Helou et al., 2012). However, WE-spleen6 cells did not stain for an endothelial cell marker, vWF, or for a myofibroblast marker,  $\alpha$ -SMA. Alternatively, the lumen-like structures might represent networks that mammalian FRCs form in vitro and in vivo (Fletcher et al., 2011). Commonly alkaline phosphatase activity together with  $\alpha$ -SMA expression indicates FRC (Mueller & Germain, 2009; Weiss, 1991). However, unlike several cell lines from the fish spleen (Ganassin & Bols, 1999; Zing et al., 2009), WE-spleen6 did not stain for AP. However, within the vertebrate spleen several populations of FRCs are being identified (Alvarenga & Marti, 2014): in fish some are AP positive and some are not (Press et al., 1994). Thus WE-spleen6 might still represent a general population of stromal cells or a specific population of FRCs.

With further characterization, WE-spleen6 could be used to study the pathogenesis of VHSV. Whether the virus targets the stroma, hematopoietic cells or both to cause the lesions in hematopoietic tissue of VHSV IV infected fish could be explored. This might be done by initiating co-cultures of blood cells and WE-spleen6 and evaluating the ability

of the cell line to support myelopoiesis, lymphopoiesis or erythropoiesis in the presence or absence of the virus. As FRCs influence the trafficking and activation of lymphocytes and the quality and intensity of mammalian immune responses (Alvarenga & Marti, 2014; Ng et al., 2012), WE-spleen6 could be used in co-cultures with dendritic cells and lymphocytes to explore in vitro how VHSV IV might modulate the start of an immune response.

WE-spleen6 appeared more susceptible to VHSV IVb than other walleye cells lines, which is a property that should make the cell line useful for detecting the virus in tissue extracts and for investigating viral susceptibility. The greater vulnerability was seen as the earlier appearance of viral proteins, CPE and significant virus production in WE-spleen6. The susceptibility could be due to WE-spleen6 having a more robust expression of proteins or processes that support the viral life cycle and/or less robust expression of antiviral mechanisms. Rhabdoviruses interact with a spectrum of host proteins (Gulereia et al., 2011). One group of antiviral proteins is Mx. Mx proteins belong to the dynamin-like GTPases (Haller et al., 2007) and are inducible in fish and fish cell lines by synthetic dsRNA, polyinosinic: polycytidylic acid (pIC) (DeWitte-Orr et al., 2007; Lockhart et al., 2004).

WE-spleen6 has been used to demonstrate that walleye have inducible Mx and seem to be particularly sensitive to pIC. This has been done with walleye cell lines and a polyclonal antibody that had been generated against rainbow trout Mx (Trobridge et al., 1997). The antibody has been used successfully in the past to evaluate Mx in salmonid cell lines (Trobridge et al., 1997; DeWitte-Orr et al., 2007). Although not detecting halibut Mx (Bergan & Robertsen, 2004), the antibody detected a polypeptide at the appropriate size (~ 70 kDa) for Mx in walleye cells. This is likely because the Mx proteins are highly conserved in vertebrates. As in most studies with fish cell lines in which Mx expression was monitored through western blotting (DeWitte-Orr et al., 2007; Lin et al., 2005), the signal in untreated or control cultures was very weak or non-existent in walleye cell lines. However, in all four walleye cell lines examined, pIC induced a strong Mx band. In several reports on fish cell lines, the induction of Mx protein is achieved with 50 µg/ml of pIC (DeWitte-Orr et al., 2007; Lin et al., 2005; Trobridge et al., 1997). By contrast Mx induction in the walleye cell lines could be seen at as low as 1

$\mu\text{g/ml}$  pIC, suggesting that walleye might be relatively more sensitive to dsRNA than other fish species.

The synthetic dsRNA, pIC, slowed progression of the viral infectious cycle in WE-spleen6, and appeared to do this by reducing the level of P and altering the ratio between N and P proteins. The accumulation of viral mRNA, viral proteins, dead cells, and viruses was impeded in cultures that had been first treated with first treated with pIC at 1  $\mu\text{g/ml}$  for 24 h before being infected with VHSV IVb. Whereas N was still evident in VHSV IVb infected cultures that had pIC, P was barely detectable in western blots. In the rhabdovirus life cycle, P has multiple actions that appear to be exerted by P acting as a N-specific chaperone (Mondal et al., 2012). The P/N interactions are crucial for two events in the viral replication cycle (Mondal et al., 2012) and for these the molar ratio between P and N is critical (Green et al., 2000). The P/N interaction keeps N in a form that allows encapsidation of the viral genome and recruits viral RNA-dependent RNA polymerase to the nucleoprotein complex (Mondal et al., 2012). The reduction in P levels could have arisen in several ways because in fish dsRNA induces many antiviral proteins, including interferons and interferon-induced genes, such as Mx (Robertsen, 2008). The actions of Mx on fish viruses have been found to vary (Lester et al., 2012; Kibenge et al., 2005). For hirame rhabdovirus (HIRRV) and VHSV, Japanese flounder Mx reduced the level of G and N transcripts over time, suggesting that Mx impaired the transcription of viral subgenomic mRNAs (Caipang et al., 2003). However, Mx had little impact on N protein synthesis for infectious hematopoietic necrosis virus (IHNV) (Trobridge et al., 1997).

In the future pIC might be considered as a therapeutic agent in walleye aquaculture. For several fish cell lines pIC has been shown to induce an antiviral state against a few fish viruses (Trobridge et al., 1997; Jensen et al., 2002; Jensen & Robertsen, 2002; Saint-Jean & Perez-Prieto, 2006). Recently, pIC was found to protect the Japanese flounder from VHSV (Kim et al., 2014).

## **CHAPTER 5.**

**Development of an endothelial cell line from the bulbus arteriosus of walleye**

## 5.1. INTRODUCTION

Studying the teleost cardiovascular system can contribute to understanding the evolution of the vertebrate circulatory system and provide practical information on the diseases and toxicology of both fish and mammals. An example of relevance to medicine is the description of atherosclerosis in salmon and possible insights this provides for the human disease (Farrell et al., 1986). Examples of direct significance to teleost health are the discoveries that several fish viruses have a tropism for the endothelial cells lining the luminal surface of the cardiovascular system (Aamelfot et al., 2013) and that during aquaculture some species develop cardiovascular abnormalities (Pombo et al., 2012). Significant to the health of both mammals and fish is the correlation between exposure to environmental contaminants, such as dioxin-like compounds, and the development of cardiovascular disease (Humblot et al., 2008; Garrick et al., 2005; 2006).

Endothelial cells (EC) are a key cellular component of many cardiovascular diseases and for mammals are commonly studied *in vitro* as primary cultures or cell lines. Primary cultures of human umbilical vein endothelial cells (HUVEC) have been used intensively in pathophysiology (Cines et al., 1998). EC lines have been obtained by different immortalization procedures (Ades et al., 1992) but also have developed spontaneously (Takahashi et al. 1990). These cell lines retain different subsets of endothelial cell properties and are a valuable research resource (Unger et al. 2002).

By contrast, teleost endothelial cells have been studied *in vitro* only rarely. Primary cultures were prepared first over a decade ago from the rete mirabilis of eels (*Anguilla* spp.) (Garrick, 2000) and have been used in toxicology and cell biology (Garrick et al., 2005; 2006; Huang et al., 2006). Yet a teleost endothelial cell line been reported only recently. Polyoma middle T antigen was used to develop an immortal rainbow trout heart cell line (RTH) (Luque et al., 2014). RTH has a cobblestone morphology and underwent phagocytosis but was not examined for other classic markers of endothelial cells such as internalization of acetylated low density lipoprotein (Ac-LDL) and expression of von Willebrand factor (vWF). Possibly another source of fish endothelial cell lines is the bulbus atherosus (BA). The BA is a regulatory conduit for blood flow from the ventricle to the gills and has been considered a subsidiary chamber of the teleost heart (Grimes et

al., 2006). The chamber is lined with endothelial cells surround by smooth muscle (Benjamin et al., 1983; Icardo, 2013; Leknes, 2009). The literature contains no formal description of cell lines from this organ (Bols & Lee, 1991), although one (Tmb) from tilapia was noted in passing (Lewis & Marks, 1985) and has recently been used to measure osmotolerance (Gardell et al., 2014).

Likely the most widely stocked and important commercial and recreational freshwater fish species in North America is *Sander vitreus* (Mitchill) or walleye (WE) (Fenton et al 1996). WE aquaculture has also begun (Summerfelt, 2005). Thus there is a need for cell lines to study at the cellular level the physiology and diseases of this species. However, the few WE cell lines developed in the past appear to have been lost. Recently, the caudal fin of *S. vitreus* was explored as a cell line source, and a fibroblast cell line (WE-cfin11f) (Vo et al., 2014) and an epithelial-like one (WE-cfin11e) (Curtis et al., 2013) were described.

In this report the development and characterization of an endothelial cell line (WEBA) from the bulbus arteriosus (BA) of walleye (WE) is described. WEBA has several endothelial properties, including UEA-1 binding, Ac-LDL uptake, nitric oxide (NO) production, and vWF expression, and responds to 2,3, 7,8-tetrachlorodibenzodioxin (TCDD) with the induction of cytochrome P4501A (CYP1A).

## **5.2. MATERIALS AND METHODS**

### **5.2.1. Tissue culture supplies and fish**

The basal medium Leibovitz's L-15 and fetal bovine serum were from Hyclone (ThermoFisher Scientific, Burlington, ON). Penicillin and streptomycin (P/S) for supplementing L-15 and dimethyl sulfoxide (DMSO) for cryopreservation were purchased from Sigma-Aldrich (St Louis, MO). Other tissue culture supplies were purchased through VWR International (Mississauga, ON) and included trypsin (Lonza) for subcultivation or passaging, 12.5-cm<sup>2</sup>, 25-cm<sup>2</sup> and 75-cm<sup>2</sup> flasks (BD Falcon), 4-chamber slides (BD Falcon) and slide flasks (Nunc). The fish were juvenile walleye of the Bay of Quinte Stock and obtained and handled as described previously (Vo et al., 2014).

### **5.2.2. Initiation of BA primary cultures and development of WEBA cell line**

In the laminar flow hood, a whole bulbus arteriosus (BA) was removed from the heart of the fish and placed in a sterile plastic Petri dish containing Ca<sup>2+</sup> and Mg<sup>2+</sup>-free Dulbecco's phosphate buffered saline solution (DPBS, Cellgro) with 200 U/mL penicillin, 200 µg/mL streptomycin, and 0.5 µg/mL amphotericin B. The BA was cut into smaller pieces that were then rinsed with DPBS with antibiotics/antimycotics twice prior to being transferred into 25-cm<sup>2</sup> culture flasks for initiation of primary cultures. BA primary cultures were initially kept at 20 °C in L-15 medium with 10% fetal bovine serum (FBS, Hyclone), 200 U/mL penicillin, and 200 µg/mL streptomycin. Media change was done daily during the first three days and then every three-five days. The first passage was performed on the BA primary cultures with TrypLE after approximately a month in cultures. Subsequent subculturing successfully resulted in the continuous propagation of cobblestone-shaped cells that eventually gave rise to the WEBA cell line. May-Grunwald Giemsa staining was performed to examine the organization and morphology of the cells, All chemicals were purchased from Sigma Aldrich, unless otherwise specified.

### **5.2.3. Maintenance of other fish cell cultures**

Rainbow trout liver epithelial (RTL-W1) cell line (Lee et al., 1993) were maintained in L-15 with 5% FBS. Walleye fin fibroblastic (WE-cfin11f) (Vo et al., 2014) and epithelial (WE-cfin11e) (Curtis et al., 2013) cell lines were established from caudal fins of juvenile walleye and grown in L-15 with 10% and 5% FBS, respectively. Rainbow trout and walleye cells were subcultured by trypsin on a weekly basis and kept at 20 °C and 26 °C for routine maintenance, respectively.

### **5.2.4. Cell line authentication by DNA barcoding**

The same procedure was followed as previously described for the walleye fin fibroblast cell line WE-cfin11f (Vo et al., 2014). DNA barcoding was based on amplification of cytochrome c oxidase subunit 1 (COX1) gene using a PCR primer cocktail designed for teleosts (Copper et al., 2007; Ivanova et al., 2007) as previously described for fish cell lines in particular (Sansom et al., 2013). A 655-bp region of the walleye COX1 gene was sequenced. DNA sequence was compared and matched to the species identification in both the Barcode of Life Data (BOLD) (Ratnasingham & Hebert 2007) ([http:// www.barcodinglife.org](http://www.barcodinglife.org)) as well as the NCBI BLAST databases (<http://www.ncbi.nlm.nih.gov/BLAST>). The WEBA samples were run along with samples from the walleye fin fibroblast WE-cfin11f cell line. Both cell lines were confirmed to be from *S. vitreus*.

### **5.2.5. Measurement of cell proliferation and cell size**

Cell number in cultures with different FBS concentrations was monitored with a Coulter counter (Vo et al., 2014). Approximately  $8 \times 10^4$  cells in triplicates were seeded per well in 6-well plates. The next day 3 well cultures were used to establish day 0 cell count. Cultures were then changed to L-15 with 2 %, 5 %, 15 % or 20 % FBS and incubated at 26 °C during the course of the experiment. Cell counts were done on Days 2, 4 and 7.

Cell size was monitored in WEBA cultures as cells grew from sub-confluent to confluency in L15 with 15 % FBS. Approximately  $1 \times 10^5$  WEBA cells were seeded per 12.5-cm<sup>2</sup> flask in L-15 with 15% FBS. Cell concentrations and diameters were

determined in triplicates by the handheld automated cell counter Scepter (Millipore, Mississauga, ON, Canada) on days 0, 2, 5 and 9.

#### **5.2.6. General fluorescence microscopy procedures**

Regardless of the cellular component being targeted for visualization, the procedures for fluorescence microscopy had some common steps, beginning with culturing in Nunc slide flasks. Prior to fixation, cultures were rinsed several times in phosphate buffered saline (PBS). With a few exceptions, fixation was 3% paraformaldehyde (PFA) for 20 min at 4 °C. This was followed with 0.1% Triton X-100 in PBS for 10 min to permeabilize cells. For collagen I, vimentin, and zona occluden-1 (ZO-1), fixation was achieved using ice-cold absolute methanol for 20 min at 4 °C. After fixation, cultures were washed in PBS to rehydrate cells and incubated for 1 h in a blocking buffer (BB): 10% goat serum, 3% bovine serum albumin and 0.1 % Triton X-100 in PBS. At this point some flask cultures received primary antibody, whereas others received secondary antibody directly and were controls for nonspecific staining. Details of the primary antibodies, their dilution in BB, and their application conditions are described in the sections below. The secondary antibodies were Alexa Fluor 488®-conjugated goat anti-rabbit for polyclonal primary antibodies and Alexa Fluor 488®-conjugated goat anti-mouse IgG for monoclonal primary antibodies. The secondary antibodies (1:1000 in PBS) were applied to flask cultures after they had been washed with PBS three times with rocking and incubated for 1 h. Cultures were then washed five times with PBS, allowed to dry, and mounted in Fluoroshield medium containing DAPI. Fluorescence images were taken with the Zeiss LSM 510 laser-scanning microscope and confocal images were acquired and analyzed using a ZEN lite 2011 software. Fluorescence staining was never observed in flask cultures to which only secondary antibody had been applied.

#### **5.2.7. Fluorescence microscopy of collagen type I in WEBA cultures**

WEBA cells were seeded into Nunc slide flasks at approximately  $5 \times 10^5$  cells per flask and allowed to grow at 26 °C for up to 2 days prior to fixation and staining. An

affinity purified rabbit polyclonal antibody against salmon collagen I (Cedarlane, Burlington, ON) was used at 1:400 dilution for 1 h.

#### **5.2.8. Phagocytosis, Ac-LDL uptake, and UEA-binding**

The internalization of polystyrene beads by fish cells in monolayer cultures was monitored with a Nikon inverted phase contrast microscope. Polysciences Inc. (Warrington, PA) was the source of polystyrene carboxylated modified beads (2.0  $\mu\text{m} \pm 0.1 \mu\text{m}$  in diameter, 2.5 % solid in water). Each confluent culture in a 25-cm<sup>2</sup> flask received 4 mL of 1:1000 beads in L-15 with 10% FBS and was incubated at room temperature. After overnight incubations, monolayers were washed vigorously with PBS and observed and photographed.

The binding of fluorescently-labeled *Ulex europaeus* agglutinin I (UEA-1) to WEBA cells was examined. After  $5 \times 10^5$  cells were seeded in Nunc slide flasks for 2 days at 26 °C, cells were washed twice with PBS, fixed in 2% PFA for 20 minutes, washed quickly once with PBS and then incubated with 100  $\mu\text{g}/\text{mL}$  of FITC-conjugated UEA-1 for 1 h at room temperature and then overnight at 4 °C. Cultures were washed three times with PBS, allowed to air-dry and then mounted in Fluoroshield medium containing DAPI. Fluorescence images were taken with the Zeiss LSM 510 laser scanning microscope and confocal images were acquired and analyzed using a ZEN lite 2011 software.

The uptake of acetylated low-density lipoprotein (AcLDL) was monitored in WEBA. WEBA were seeded at  $1.25 \times 10^6$  cells in each of two 25-cm<sup>2</sup> Falcon flasks and allowed to incubate at 26 °C for 2 days. One flask was a control flask and the other flask was added 50  $\mu\text{g}/\text{mL}$  of acetylated low-density lipoprotein conjugated with a fluorophore 1,1'-dioctadecyl-3,3,3',3'-tetramethyl-indocarbocyanine perchlorate (Dil AcLDL) probes (Molecular Probes). The treated flask was wrapped with aluminum foil to prevent fluorescence bleaching. Both control and treated flasks were then incubated at 26°C for 22 hours. Cultures were rinsed with PBS five times to remove excess probes before observing cells under the epifluorescence inverted microscope. To prepare cells for FACS analysis, cells were trypsinized and transferred into 5-mL round-bottom culture

tubes (Falcon). Tubes were centrifuged at  $500 \times g$  for 4 minutes and cells were washed with PBS once before being re-suspended in 500  $\mu$ L of DPBS. Dil AcLDL-positive cells were sorted and detected by a FACSVantage SE flow cytometer (BD Biosciences).

#### **5.2.9. Fluorescence microscopy of WEBA for von Willebrand Factor (vWF)**

An affinity-purified rabbit polyclonal antibody that had been raised against human vWF was obtained from Sigma-Aldrich. The antibody was used at a 1:200 dilution for 1.5 h on confluent WEBA cultures.

#### **5.2.10. Fluorescence microscopy of WEBAcytoskeleton**

Sigma-Aldrich (St Louis, MO) was the source of monoclonal antibodies (mAb) and affinity-purified rabbit polyclonal antibodies to several cytoskeletal proteins and of fluorescein isothiocyanate (FITC)-labeled phalloidin for filamentous actin. The mAbs to microfilament proteins were clone EA-53 to rabbit sarcomeric  $\alpha$ -actinin and clone 1A4 to the N-terminal decapeptide of  $\alpha$ -smooth muscle actin ( $\alpha$ -SMA). For intermediate filament proteins, rabbit polyclonal antibody to chicken desmin and mAb to porcine vimentin (clone V9) were used. For tubulins, staining was done with mAbs to sea urchin  $\alpha$ -tubulin (clone B-5-1-2) and to bovine  $\beta$ -tubulin (clone AA2).

WEBA cells were examined in near confluent and confluent cultures in Nunc slide flasks at 26 °C. The vimentin mAb (clone V9) was used overnight at a 1: 200 dilution. The desmin polyclonal antibody was used for 1 h at a 1:200 dilution. The mAb to  $\alpha$ -tubulin was used at 1:2500 dilution; the mAb to  $\beta$ -tubulin, at a 1:1000. The mAbs to  $\alpha$ -SMA and  $\alpha$ -actinin were diluted 1 to 200 and 1 to 800 respectively.

For filamentous actin, cultures were rinsed with PBS, fixed with 3% PFA for 20 min at 4 °C, permeabilized with 0.1% Triton X-100 in PBS for 10 min at 4°C, and incubated with 50  $\mu$ g/mL FITC-phalloidin in PBS for 45 min at room temperature. Cultures were then rinsed, air dried, mounted in Fluoroshield, and imaged as described above under the general fluorescence microscopy section.

### **5.2.11. Fluorescence microscopy of WEBA for tight junctions**

WEBA cells were seeded into Nunc slide flasks at approximately  $5 \times 10^5$  cells per flask and allowed to grow for 7 days at 26 °C to form a close-fitting monolayer prior to fixation and staining. Polyclonal antibodies were obtained against two tight junction proteins: human ZO -1 (Z-R1) and mouse claudin 3 (Z23.JM) (Invitrogen, Burlington, ON). For ZO-1, the antibody was applied overnight at a 1:200 dilution; for claudin 3, the antibody was applied overnight at a 1:100 dilution.

### **5.2.12. Nitric oxide (NO) production**

A fluorescence microscopy method was used to examine WEBA and the walleye fin epithelial and fibroblast cell lines, WE-cfin11e and WE-cfin11f respectively for intracellular nitric oxide (NO). The method used 4,5 diaminofluorescein diacetate (DAF-2DA) and aldehyde fixation and was developed by Sugimoto et al. (2000). The principle is that DAF-2DA is taken up by living cells and hydrolyzed by esterases to 4, 5-diaminofluorescein (DAF-2) that complexes with NO (Kojima et al., 1998). When cultures were fixed with paraformaldehyde or glutaraldehyde, cells with NO-DAF-2 complexes fluoresce intensely and can be visualized with a fluorescence or confocal microscope. For this technique, cells were plated in Nunc slide flasks in the conventional growth medium and once the cultures became confluent, they received DAF-2DA (Calbiochem). The cultures were incubated with 5  $\mu$ M DAF-2DA in the conventional growth medium at 26 °C for 30-45 minutes. Cultures were then washed once with DPBS and subsequently fixed with 2% PFA for 3 min. Slides flasks were then washed with DPBS once. Control cultures received 0.5 % DMSO and showed no auto-fluorescence. Fluorescence was examined under the Zeiss LSM 510 laser scanning microscope and confocal images were acquired and analyzed using a ZEN lite 2011 software.

As nitric oxide synthase (NOS) is the most common source of NO, several experiments were done to test the effect of modulating NOS activity on WEBA fluorescence. Acetylcholine was used as an NO stimulator and N<sup>G</sup>-monomethyl-L-arginine (*L-NMMA*) was used as a pan NOS inhibitor. Here WEBA were treated with 1  $\mu$ M acetylcholine (Sigma) and 5  $\mu$ M DAF-2DA in the presence or absence of 1 mM *L-NMMA* (Sigma) in the conventional medium at 26 °C for 45 minutes. For cultures with

the inhibitor L-NMMA, cells were pre-treated with the inhibitor for 30 min before acetylcholine and DAF-2DA were added into the medium. Cells were also starved of the NOS substrate, arginine. For this, cells were maintained in L-15/ex, which has basal salts, galactose, and pyruvate only (Schirmer et al., 1997). Cells were evenly seeded in three Nunc slide flasks in L-15 with 10% FBS. Once confluent, one culture was replenished in the same conventional growth medium. The other two cultures were washed with DPBS three times. One of these two cultures was then kept in L15/ex while the other was in L15/ex with 10% FBS. After 3 days at 26 °C, cultures received DAF-2DA for 30 minutes prior to being fixed in paraformaldehyde as described above.

### **5.2.13. Induction of CYP1A**

The induction of CYP1A after treatment of cell cultures with 2,3,7,8-tetrachlorodibenzo-p-dioxin (TCDD) was monitored at the catalytic level as 7-ethoxyresorufin-O-deethylase (EROD) activity and at the protein level through western blotting.

The induction of EROD activity was done in 96 well tissue culture plates. The induction protocols, measurement of EROD activity, and calculation of EC50s for induction were done as described previously in detail in a step by step manner (Ganassin et al., 2000).

For western blotting confluent 75-cm<sup>2</sup> flasks of WEBA cells were exposed to 97.6 to 1562 pM of TCDD in L-15 with 5% FBS for 24 h at 26 °C. Control flasks received 0.5 % DMSO vehicle solvent in the same growth medium. Briefly, cell lysis was performed in 1% (w/v) NP-40 lysis buffer with protease inhibitor cocktail (Qiagen). Protein concentrations were determined by bicinchoninic acid (BCA) protein assays (Pierce, Thermo Fisher). Proteins were separated on 12 % polyacrylamide resolving gel and electrophoresis was performed at 120 V for 1.5 h. Proteins were then electrophoretically transferred onto nitrocellulose membranes (Bio-Rad) at 150 mA for 2 h. Mouse monoclonal anti-CYP1A fish (Cedarlane, Burlington, ON, Canada) was used as primary antibody at 1:3000 for 2 h in 5% skim milk blocking buffer with TBS-T. Goat anti-mouse IgG antibody conjugated with alkaline phosphatase (Sigma) was used as a secondary

antibody at 1:20,000 for 1 h. Protein bands were developed with NBT/BCIP substrate reaction.

### **5.3. RESULTS**

#### **5.3.1. Development of BA primary cultures into the cell line, WEBA**

When small fragments of BA were incubated in L-15 with 10 % FBS for several weeks at room temperature, cobblestone- and spindle-shaped cells migrated out of the fragments onto the polystyrene growth surface (Fig 5.1A). At this point the primary culture had many BA fragments surrounded by adherent cells, predominantly spindle-shaped cells, and was treated with TrypLE for several minutes to detach most of the spread cells, although some tissue fragments were inadvertently dislodged as well. The resulting suspension was added to new flasks in L-15/10% FBS and incubated at room temperature, which were the culture conditions used to take the cells from primary cultures through to a cell line. In the flasks the cells grew to completely cover the growth surfaces. TrypLE was used to sub-cultivate one of these monolayers into two new flasks, which themselves became confluent over several weeks. With passaging, tissue fragments and spindle-shaped cells were lost and cultures took on a very uniform appearance (Fig 5.1B). By passage 5, all cultures were comprised of mostly cobblestone cells; these are now referred to as WEBA.

WEBA cultures have been maintained for over 3 years in L-15 with 10-15% FBS through a cycle of growth to confluency followed by an approximately 1 to 2 split to new flasks. After 24 h of 1:2 splitting, WEBA cells in the underconfluent culture tended to have a larger and more polygonal shape when spread out on the plastic surface and a bigger cell diameter after being trypsinized and in suspension (Fig 5.2A,C). As the cells grew to a confluent monolayer, cells in the monolayer were more cobblestone-like and generally smaller in size, both on the plastic surface and in suspension (Fig 5.2B-C). WEBA was cryopreserved at several passage levels, and upon thawing, cell viability, as judged by the Trypan Blue exclusion test, was 80-95%. The cells attached and spread onto polystyrene growth surfaces and grew to form monolayers of cobblestone-shaped cells.

WEBA were robust, surviving a range of culture conditions but grew slowly. When cultured in DMEM medium with 10% FBS equilibrated at 5 % CO<sub>2</sub>, the cells' cobblestone morphology was also evident and bore a striking resemblance to that of mammalian endothelial cells (Fig 5.1C). Increasing the % of the FBS supplement from 2

to 20 % increased the number of cells produced over time (Fig 5.1D) but cultures could be maintained for at least a month in L-15 alone. WEBA cultures showed a similar temperature growth and tolerance profile to that of walleye caudal fin fibroblastic cell line WE-cfin11f. For routine maintenance, WEBA was subcultured every 12 days at 26 °C, which is the optimal growth temperature for walleye cells (Vo et al., 2014).

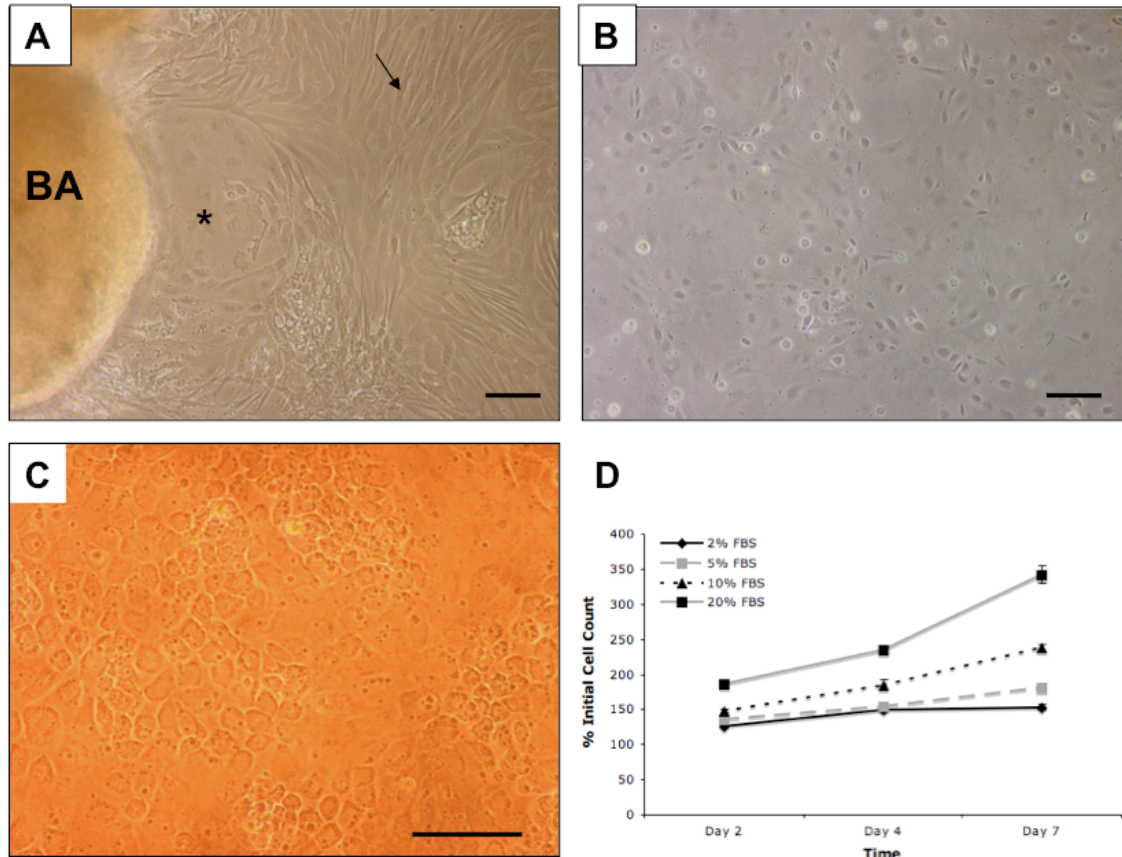


**Figure 5.1. Cell cultures of walleye bulbus arteriosus and effects of fetal bovine serum on growth of WEBA cell line.** (A) Explant outgrowth of bulbus arteriosus (BA) yielded primary cultures with epithelial-like (\*) and fibroblastic cells (arrows). (B) Subculturing these cells with trypsin-like TrypLE for multiple passages in L-15 with 10% FBS resulted in homogenous cultures with a cobblestone morphology. These cells gave rise to WEBA cell line. (C) WEBA cells' cobblestone morphology that was reminiscent of mammalian endothelial cells was more evident when cells were cultured in DMEM with 10% FBS. (D) Influence of increased FBS concentrations on cell proliferation. Cells in triplicate wells were kept in L-15 with 2, 5, 10, 20 % FBS. Cell counts were performed with Coulter counter and expressed as % initial cell count. Scale bar = 100  $\mu$ m.

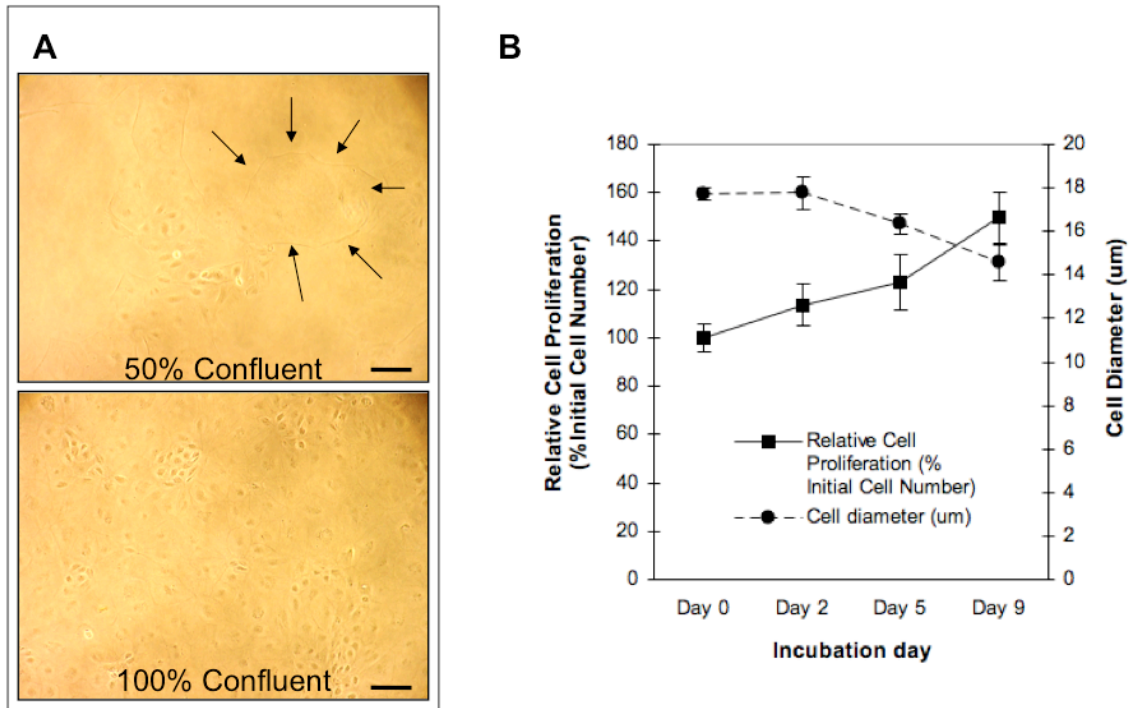


**Figure 5.2. Influence of culture confluence level on WEBA cell size.** (A) Underconfluent WEBA cultures had larger and more polygonal cells (arrows); confluent WEBA cells had relatively smaller and more cobblestone-shaped cells. (B) Cell diameter decreased over time when WEBA cultures grew from underconfluent to confluent levels. Average cell counts and diameters (from triplicates) were determined by the automated cell counter Scepter. Scale bar = 100  $\mu$ m.

### 5.3.2. Capillary-like tubes

After WEBA cultures had formed a confluent cobblestone monolayer, some cells protruded on top of the monolayer (Fig 5.3A) after several days and developed a second growth pattern that would eventually form an intricate capillary-like tube network after about a month (Fig 5.3B). Additionally, when cultures were seeded at high cell density in L-15 with 10 % FBS, sprouting processes and capillary-like tubes formed as early as 24 h after the medium had been changed to L-15 (Fig 5.3C). Overall, these protruding cells were strikingly reminiscent of sprouting processes, which commonly occurred in post-confluent mammalian endothelial cell cultures (Schwartz, 1978; Cotta-Pereira et al., 1980).

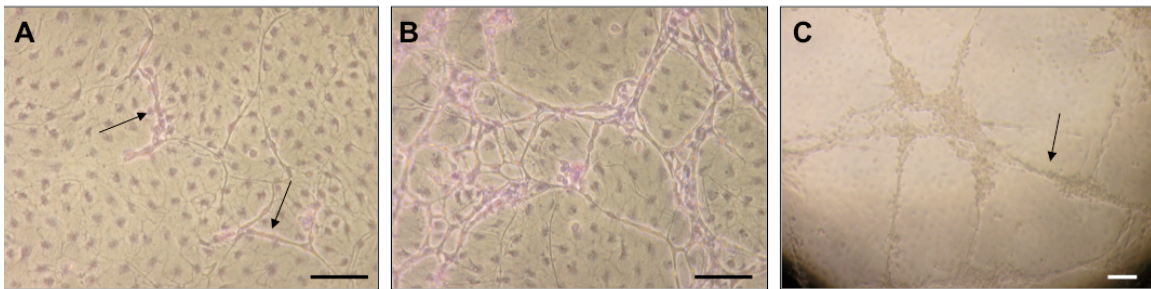


**Figure 5.3. Capillary-like formation in WEBA cultures.** When WEBA cultures reached confluence, sprouting processes formed in several days (A) and a capillary-like network could be established after at least a month (B). In both panels A and B, cultures were stained with May-Grunwald Giemsa to enhance the visualization of the cell morphology and organization. (C) Capillary-like network could be rapidly induced after overnight seeding high cell density in L-15/FBS followed by 24 h media change to serum-free L-15 alone. Scale bar = 100  $\mu$ m.

### 5.3.3. Collagen type I

WEBA cultures stained for collagen type I. Immunocytochemistry revealed staining in the cytoplasm, presumably representing procollagen type I, and in extracellular spaces as collagen fibrils (Fig 5.4A). Interestingly, collagen fibrils formed without exogenous supplements such as ascorbic acid (Fig 5.4B-C), which is usually required for the maturation of collagen and formation of extracellular collagen fiber matrix.

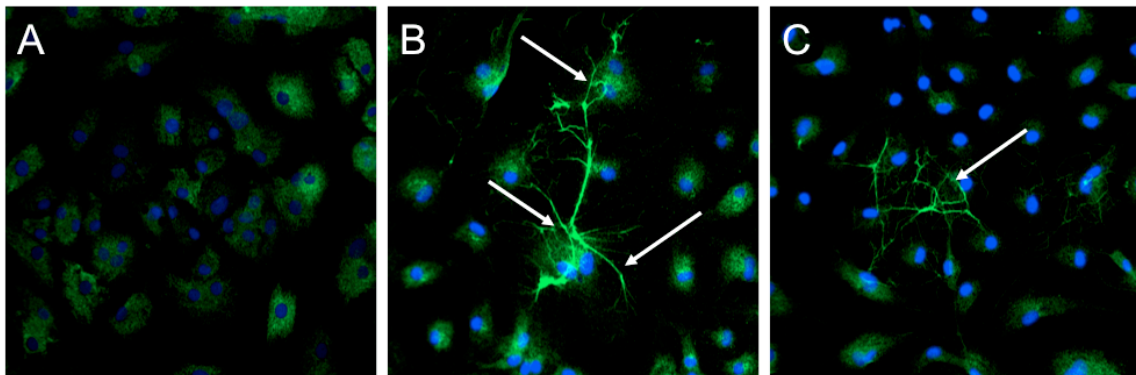


**Figure 5.4. Expression of collagen type I in WEBA.** (A) WEBA cultures that were seeded at confluence level were immunochemically stained for intracellular type I procollagen using affinity purified polyclonal anti-salmon COL-1 antibody. (B-C) Collagen type I fibers could form in the extracellular space on day 4 post cell seeding (E-F). These cultures were subsequently probed with anti-salmon COL-1 antibodies. Alexa Fluor 488-conjugated goat anti-rabbit secondary antibody was used; thus Alexa Fluor 488 (green) represents type I (pro)collagen. DAPI (blue) was used as a counterstain for the cell nuclei.

#### **5.3.4. von Willebrand Factor (vWF)**

The cytoplasm of WEBA cells stained for vWF (Fig 5.5A, left panel). By contrast, the walleye fin epithelial cell line, WE-cfin11e, did not (Fig 5.5A, right panel). Another cell line, WE-spleen6, also did not stain (data shown in chapter 3).

#### **5.3.5. Phagocytosis, Ac-LDL uptake, and UEA-1 binding**

WEBA cells internalized polystyrene beads (2  $\mu\text{m}$ ). This phagocytosis was not uniform with some cells internalizing many more beads than other cells (Fig 5.5B). Fluorescently labeled acetylated low density lipoprotein (Ac-LDL) was taken up by WEBA cells (Fig 5.5C) and fluorescently-labeled *Ulex europaeus* agglutinin I (UEA-1) bound to WEBA cells (Fig 5.5D).

#### **5.3.6. Cytoskeleton**

The cytoskeleton of WEBA had microfilaments and microtubules and the intermediate filament protein, vimentin. Phalloidin, which stains filamentous actin, revealed stress fibers and circumferential actin filaments (Fig 5.6A-C), the latter being especially noticeable in confluent WEBA cultures (Fig 5.6C). Immunofluorescent staining revealed neither smooth muscle  $\alpha$ -actin nor sarcomeric actinin in WEBA (Fig 5.6D-E). However, antibodies to  $\alpha$ -tubulin and  $\beta$ -tubulin showed a complex network of microtubules (Fig 5.6F-G). Vimentin was detected by immunofluorescent staining (Fig 5.6H), but another intermediate filament protein, desmin was not (Fig 5.6I).

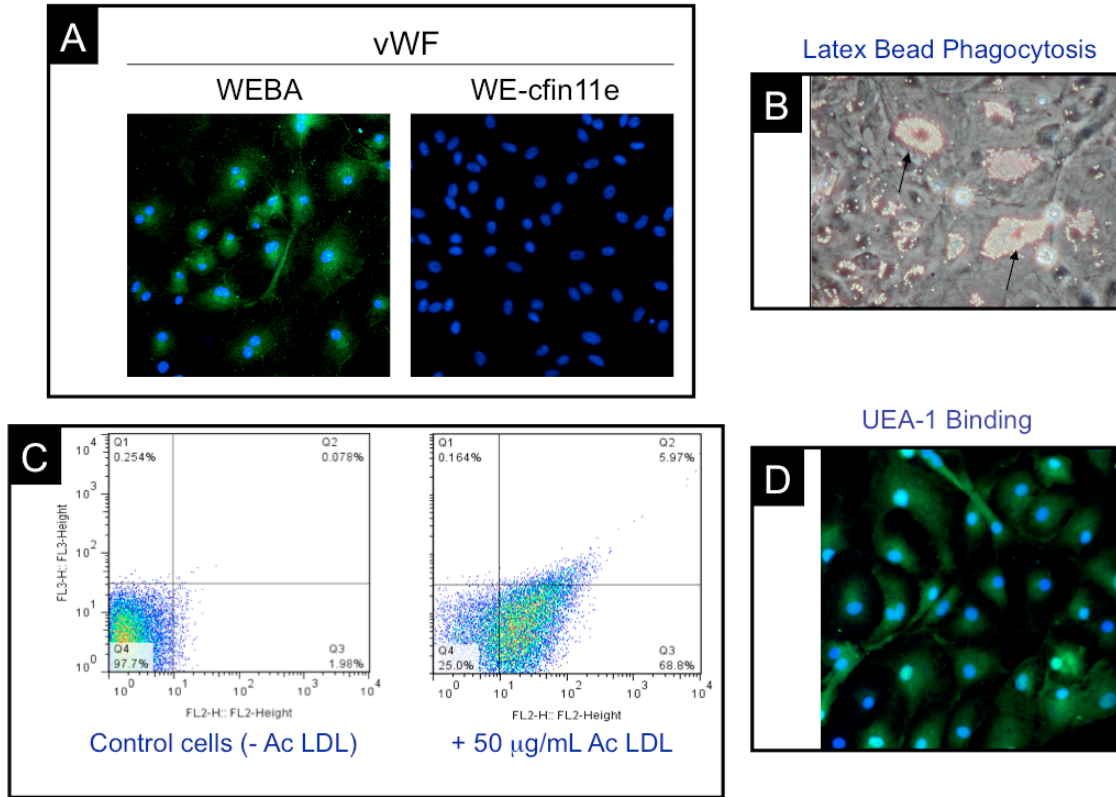


**Figure 5.5. WEBA cells demonstrated properties of endothelial cells.** (A) WEBA were immunopositive for vWF by rabbit affinity-purified polyclonal anti-vWF antibody whereas WE-cfin11e was not. Green (Alexa Fluor 488) represents vWF and blue (DAPI) represents cell nucleus. (B) WEBA phagocytized 2- $\mu\text{m}$  polystyrene beads (arrows). (C) Flow cytometric analysis showed that WEBA took up Ac-LDL fluorescently labelled with Dil fluorochrome. Quarant 3 represents the cell population with Dil-Ac-LDL particles. (D) WEBA cells express receptors with affinity for UEA-1 (green). Cells were counterstained with DAPI (blue) for the cell nuclei.

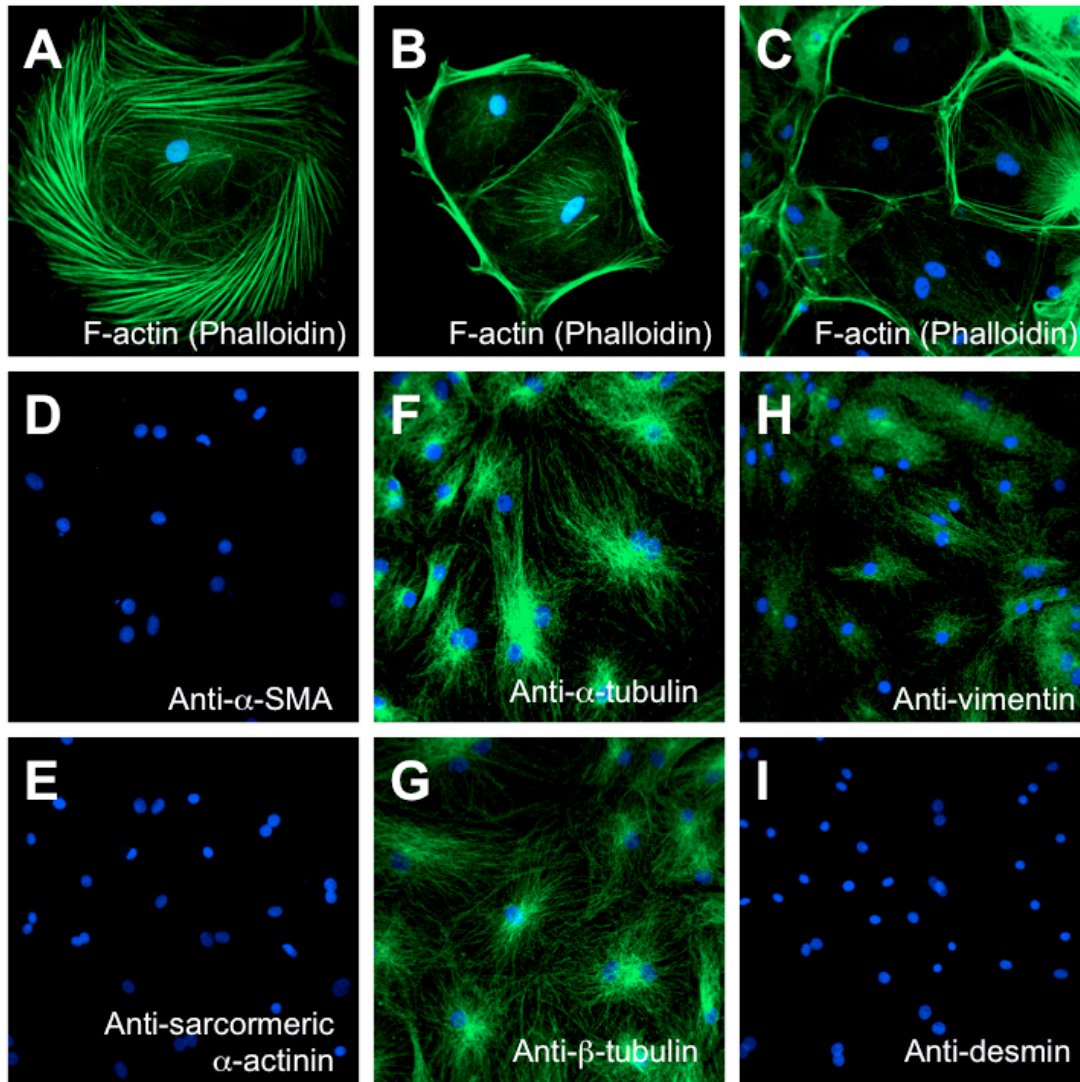


**Figure 5.6. Cytoskeletal filament prolife in WEBA cell line.** (A-C) F-actin was visualized by FITC-phalloidin. By indirect immunofluorescence, WEBA cells were probed with antibodies for  $\alpha$ -smooth muscle actin (D), sarcomeric  $\alpha$ -actinin (E),  $\alpha$ -tubulin (F),  $\beta$ -tubulin (G), vimentin (H) and desmin (I). Alexa Fluor 488 (green)-conjugated secondary antibody was used. DAPI (blue) was used as a counterstain for the cell nuclei. For a complete immunocytochemistry protocol, please refer to the Materials and Methods section.

### 5.3.7. Tight junction (TJ) proteins

WEBA stained strongly for two tight junction proteins: zona occludens-1 (ZO-1) and claudin 3. Staining for ZO-1 was strong only at the cell periphery where cell-to-cell contacts were established (Fig 5.7). By contrast, probing cells with polyclonal affinity-purified anti-claudin 3 showed a weak staining at the cell-to-cell contacts and also some cytoplasmic staining (Fig 5.7).

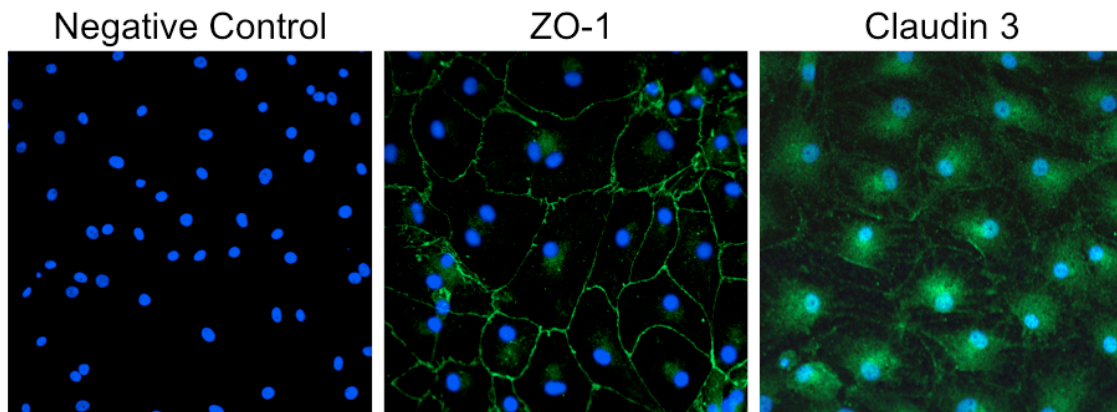


**Figure 5.7. Immunocytochemistry of tight junction proteins in WEBA cell line.** WEBA cells were probed with rabbit polyclonal affinity purified anti-ZO-1 and anti-claudin 3 primary antibodies. Cultures without primary antibodies acted as negative controls. Alexa Fluor 488 (green)-conjugated goat anti-rabbit IgG secondary antibody was used. DAPI (blue) was used as a counterstain for the cell nuclei.

### 5.3.8. Nitric oxide (NO) production

Cells in WEBA cultures stained intensely with DAF-2 whereas cells in cultures of WE-cfin11e not all (Fig 5.8). WE-cfin11f stained weakly (not shown). The intensity of DAF-2 staining in WEBA cultures was unchanged by the addition of a potential stimulator, acetylcholine, and of a potential inhibitor, *L-NMMA*, of *NOS* (not shown). When starved of arginine by being incubated for 3 days in L15/ex with 10 % FBS, WEBA cells showed a slight diminishment in DAF-2 fluorescence (Fig 5.8). When starved of arginine and nitrite by being incubated for 3 days in L15/ex, WEBA continued to be stained with DAF-2 but the fluorescence was further diminished (Fig 5.8).

### 5.3.9. CYP1A induction

In WEBA TCDD induced P4501A, as revealed in a catalytic measure of P4501A, EROD activity, and in western blots for the protein. Without TCDD, EROD activity and P4501A protein were undetectable or barely detectable (Fig 5.9A-B). After WEBA had been exposed to TCDD for 24 h, 100 pM TCDD and higher induced both EROD activity and P4501A protein (Fig 5.9A-B). By contrast, much lower TCDD concentrations induced EROD activity and P4501A in the rainbow trout liver epithelial cell line, RTL-W1 (Fig 5.9C).  $EC_{50}$  values for the induction of EROD for WEBA and RTL-W1 were calculated to be 226.4 and 8.7 pM, respectively. Also the maximal EROD activity was approximately 7 fold higher in RTL-W1. Thus WEBA responded to TCDD but was less sensitive than other TCDD responsive fish cell lines.

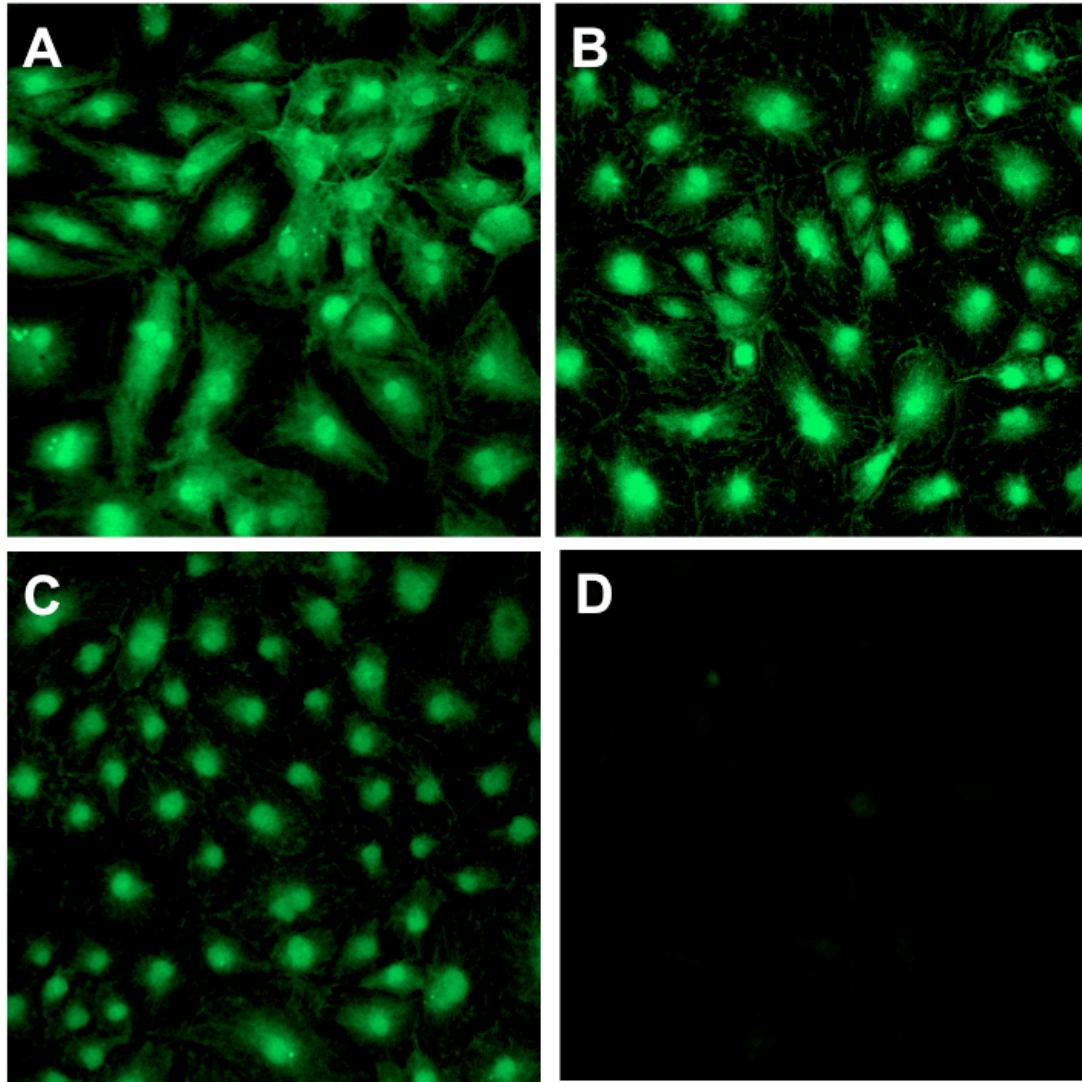


**Figure 5.8. Detection of NO in walleye cells.** Cultures of WEBA (a, b, & c) and of WE-cfin1e (d) were incubated with 4,5 diaminofluorescein diacetate (DAF-2DA), fixed in paraformaldehyde and examined by confocal microscopy. Prior to the addition of DAF-2DA, WEBA had been incubated for 3 days in L-15 with 10 % FBS (A), L-15/ex with 10 % FBS (B) and L-15/ex (C). WE-cfin1c had been in L-15 with 10 % FBS (D).

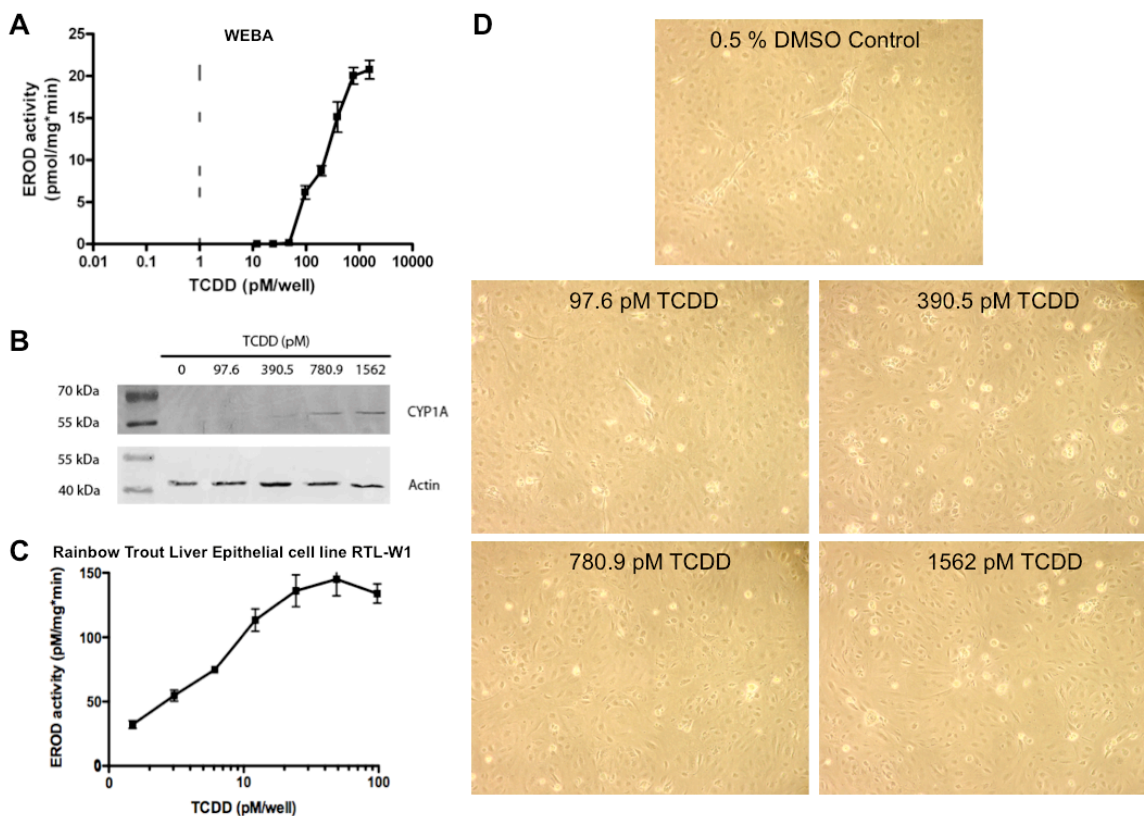


**Figure 5.9. Induction of CYP1A catalytic activity and protein expression by TCDD.** (A) CYP1A catalytic activity was measured by EROD assays. Dose response curve of TCDD-induced EROD activity in the WEBA cell line. (B) Western blotting analysis showing the dose-dependent induction of CYP1A protein by TCDD. Actin was used as a housekeeping protein. (C) Dose response curve of TCDD-induced EROD activity in the RTL-W1 cell line, which was used as a positive control for comparison purposes. (D) Morphological changes of WEBA cells in exposure to increasing concentrations of TCDD.

## **5.4. DISCUSSION**

A cell line has been developed from the walleye (WE) bulbus arteriosus (BA) and is designated WEBA. WEBA had similar growth properties to recently isolated WE caudal fin fibroblast (WE-cfin11f) (Vo et al., 2014) and epithelial (WE-cfin11e) cell lines (Curtis et al., 2013). Like the caudal fin cell lines, WEBA grew well in L-15 supplemented with FBS at room temperature, has been maintained for over 3 years, through approximately 40 passages, was cryopreserved, and was confirmed as walleye by amplifying and sequencing a 655-bp region of the mitochondrial COX1 gene (Ward et al., 2009). These WE cell lines are likely the only ones currently available from this species because previous ones have been lost or misidentified (Sansom et al., 2013; Vo et al., 2014). WEBA joins Tmb from tilapia as the only cell lines from the BA (Gardell et al., 2014; Lewis & Marks, 1985). Both have cobblestone morphologies, but as documented below, WEBA has been characterized for several more properties, and all point to an endothelial origin for WEBA.

### **Capillary-like tubes**

WEBA were able to spontaneously form capillary-like tubes and produce collagen I. Spontaneous angiogenesis in vitro has been observed with mammalian endothelial cell (EC) that had been kept in confluent cultures for up to four weeks (Vernon et al., 1995) and with a rainbow trout pronephric stroma cell line (TPS) that had been confluent for over five months (Diago et al., 2000). Signs of capillary formation could be seen as early as a few days in over confluent WEBA cultures. The much longer time frame for TPS might be because EC are slowly produced from just a few EC precursors in the stroma cell line (Diago et al., 2000).

### **Collagen I**

WEBA produced collagen I and this might have contributed to the spontaneous angiogenesis in vitro. For mammalian EC, collagen I seems to initiate angiogenic sprouting (Cotta-Pereira et al., 1980; Davis & Senger, 2005). A clone of bovine aorta endothelial cells (BAEC) that synthesized and organized collagen I into cables supported

the arrangement of the cells into networks resembling capillary beds, whereas a clone of BAEC that did not synthesize collagen I did not make capillary networks (Vernon et al., 1995). In the future WEBA should be useful for investigating the role of collagen I in angiogenesis and for studying collagen synthesis in the BA, where collagen regulates bulbus compliance (Icardo et al., 2000).

### **UEA-1 binding, Ac-LDL uptake and phagocytic capacity**

Although endothelial cells have remarkable heterogeneity (Aird, 2007), several properties have reliably identified mammalian cells in culture as endothelial (Craig et al., 1998) and these characteristics were evident in WEBA cultures. WEBA cells bound fluorescently-labeled *Ulex europaeus* lectin agglutinin I (UEA-1) and took up fluorescently-labeled acetylated low density lipoprotein (Ac-LDL). UEA-1 binding suggests  $\alpha$ -L-fucosyl glycoproteins characteristic of the endothelial cell surface (Jackson et al., 1990; Hormia et al., 1983); Ac-LDL uptake suggests the presence of scavenger receptors (PrabhusDas et al., 2014; Voyta et al., 1984). Previously, ac-LDL uptake has been demonstrated in cod endocardial endothelial cells (Sorensen et al., 1998). Phagocytosis has been a less consistent marker of endothelial cells (Ryan, 1988). For several fish species, cardiac endothelial cells internalized particles but the extent depended on the species (Nakamura & Shimozawa, 1994). On the other hand, scavenger endothelial cells of the teleost heart have been reported to rarely phagocytize particles  $> 0.5 \mu\text{m}$  (Sorensen et al., 2012). Yet HUVEC engulfed polystyrene microspheres up to  $1.0 \mu\text{m}$  in diameter, although this varied with the proliferative state of cultures (Zauner et al., 2001). In WEBA cultures some cells became engorged with polystyrene beads ( $2 \mu\text{m}$ ) but others had only a few. Whether this represents differences in cell cycle stages or different endothelial cell populations remains to be investigated.

### **von Willebrand Factor (vWF)**

WEBA but not WE-cfin11e cells stained for von Willebrand Factor (vWF) or Factor VIII-related antigen with a commercial polyclonal antibody to human vWF. Previously this antibody detected vWF in endothelial cells of zebrafish arteries and veins (Carrillo et al., 2010). In mammals vWF is synthesized by megakaryocytes and endothelial cells and

is considered an excellent marker for endothelial cells in culture (Craig et al., 1998). The vWF often localizes to unique storage organelles, Weibel-Palade Bodies (WPB), in mammalian endothelial cells (Wagner et al., 1982) but sometimes is described as being associated with cytoplasmic granules, endoplasmic reticulum, and Golgi region (Dorovini-Zis & Huynh, 1992; Reidy et al., 1989). Staining for vWF also has been noted as being perinuclear (Dorovini-Zis & Huynh, 1992; Craig et al., 1998; Sahm & Seifert, 2000) and in one case nuclear (Camalxaman et al., 2013). In fish, electron dense organelles resembling WPB have been seen by transmission electron microscopy (TEM) (Boyd et al., 1980; Ferri & Sesso, 1983), but they have yet to be shown to contain vWF. The staining for vWF in WEBA was largely cytoplasmic, possibly in granules and the ER. WEBA is the first fish cell line to be shown to express vWF.

### **Cytoskeleton**

Although the WEBA cytoskeleton was made up of microfilaments, vimentin, and microtubules like most vertebrate cells, some cytoskeletal features were more characteristic of EC than other cell types and might be important to the functioning of the BA endothelium. Circumferential actin bundles are thought to facilitate the barrier function of the endothelium (Schnittler et al., 2014) and were especially abundant in confluent WEBA cultures. The tissue distribution of intermediate filament proteins in teleost is perhaps more complex than in mammals (Markl, 1991) but vimentin has been seen in at least blood vessel endothelial cells of the mosquito fish (Arena et al., 1995). In mammals vimentin is the only intermediate protein of EC and has been thought to help the endothelium withstand the mechanical forces of blood flow (Schnittler et al., 1998) and to participate in angiogenic sprout formation (Kwak et al., 2012). Microtubules have a significant role in maintaining and supporting capillary tubes (Bayless et al., 2004; Kim et al., 2013) and tubulin modifications can contribute to endothelial dysfunction (Hirase & Node, 2012).

### **Tight junction (TJ) proteins**

WEBA cells expressed at least two tight junction (TJ) proteins: zona occludens-1 (ZO-1) and claudin-3. TJs are made up of several protein families, including zona

occludens, claudins and occludin, and perform a barrier function, regulating the movement of solute between adjacent cells (Runkle & Mu, 2014). Although only recently becoming a research focus (Jeong et al., 2008), teleost TJs appear to have the same general structural composition as the TJs of mammals (Zhang et al., 2012; Baltzegar et al., 2013). However, fish cell lines have rarely, if ever, been inspected for these proteins. In WEBA, ZO-1 and claudin 3 were found at the cell perimeters but claudin 3 also stained in the cytoplasm. Cytoplasmic staining of claudins has been noted before and been attributed to high claudin turnover rate (reviewed by Findley and Koval, 2010) or partly subject to differential regulatory components of mitogen-activated protein kinase (MAPK) pathways (Chen et al., 2000).

For mammals, different endothelial cell lines often express variable subsets of the TJ proteins (Neuhaus et al., 2008; Song & Patcher, 2003; Watanabe et al., 2013), but immunofluorescent staining revealed the presence of ZO-1 and claudin-3 in WEBA but not claudin-5 and occludin. Whether the failure to detect occludin and claudin-5 reflects the inability of the antibodies to detect the walleye orthologs of these proteins or a true lack of their expression in WEBA remains to be determined. Previous *in vivo* examination of zebrafish found expression of ZO-1 in brain endothelial cells (Jeong et al., 2008) and of claudin-3 in the endocardium (Zhang et al., 2012). Thus the pattern of TJ protein expression is suggestive of an endothelial origin for WEBA.

### **Nitric oxide (NO) production**

The demonstration of NO in WEBA is a first for a fish cell line and might reflect a characteristic feature of bulbus arteriosus (BA) cells. *In vivo* studies with fluorescent indicators localized NO specifically to the BA within the cardiovascular system of zebrafish (Grimes et al., 2006; Lepiller et al., 2007). In this case the NO might have been in precursors to smooth muscle cells of the BA (Grimes et al., 2006). Yet, as discussed earlier WEBA had characteristics of endothelial cells and did not express  $\alpha$ -smooth muscle actin (SMA). Perhaps endothelial cells also contribute to the NO in the BA. Yet endothelial nitric oxide synthase (eNOS) would not likely be the source of the NO that causes DAF-2 to fluoresce in WEBA cells. This is because teleost endothelial cells are thought to lack NOS (Donald & Broughton, 2005) and because in the current study,

neither NOS inhibitors nor arginine starvation significantly changed the fluorescence staining of WEBA cells. Spontaneous fluorescence of DAF-2 has been observed (Gan et al., 2012), but such a phenomenon cannot account for the selectivity of the fluorescence in walleye cells: WEBA stained intensely and WEcfm-11e not at all.

An alternative source for NO in WEBA could be the reduction of nitrite [NO<sub>2</sub><sup>-</sup>]. Nitrite would be in the FBS of cell cultures. Inasmuch as WEBA continued to fluoresce despite 3 days without FBS, the intracellular nitrite pool in WEBA would have to be relatively stable. Several proteins reduce nitrite to NO, including myoglobin, xanthine oxidoreductase, aldehyde oxidase and carbonic anhydrase (Hendgen-Cotta et al., 2014; Omar & Webb, 2014). One or more of these might be preferentially expressed in WEBA. Possibly this could be myoglobin because expression of this protein has been seen in teleost endothelial cells (Helbo et al., 2013). As nitrite reduction and NO are important in regulating and protecting the vertebrate cardiovascular system (Omar & Webb, 2014; Sandvik et al., 2012; Tota et al., 2005), WEBA might be convenient for investigating this in teleost cardiovascular physiology at the cellular level.

### **CYP1A induction**

TCDD, the most potent polychlorinated dibenzo-p-dioxin (Elonen et al., 1998), induced CYP1A in WEBA but did so at a much higher TCDD concentration (3-10 times) and with less maximal EROD activity than TCDD did in rainbow trout liver and pituitary cell lines (Bols et al., 1999; Tom et al., 2001). TCDD toxicity varies considerably among freshwater fish species and the salmonids are considered the most sensitive group (Elonen et al., 1998). Walleye might be a more tolerant species, although this species has yet to be exposed to TCDD experimentally. However, the fact that WEBA responded to TCDD whereas the caudal fin cell lines did not fits the suggestion that the endothelium is a common toxicological target for TCDD in fish and mammals (Garrick et al., 2005; Guiney et al., 1997; Kopf et al., 2010). WEBA might be useful for studying at the cellular level the sensitivity of walleye to TCDD and how TCDD could cause endothelial dysfunction in fish.

## **Summary**

As one of the first fish cell lines to be documented as endothelial and to be characterized from the bulbus arteriosus (BA), WEBA should be useful for studying many aspects of the teleost endothelium in general and the BA in particular and for evaluating how viruses and toxicants impact the fish circulatory system.

## **CHAPTER 6.**

**Senescence-associated  $\beta$ -galactosidase staining in fish cell lines and primary cultures from several tissues and species, including rainbow trout coelomic fluid and milt**

## 6.1. INTRODUCTION

Characterizing piscine cell cultures and cell lines, especially for features that allow them to be better compared with their mammalian counterparts, improves their value as research tools. Yet fish cell line characterization is often impeded by the lack of commercial antibodies to detect teleost orthologs of proteins that in mammals have proven useful for distinguishing structural characteristics and physiological states of different cell types. By contrast, enzyme activities can be assayed broadly across a phylum and be powerful biomarkers in the case of some enzymes, such as senescence associated  $\beta$ -galactosidase (SA  $\beta$ -Gal). SA  $\beta$ -Gal activity is measured easily in animal cell cultures by in situ staining and potentially identifies senescent cells (Dimri et al., 1995; Debacq-Chainiaux et al., 2009).

In mammals SA  $\beta$ -Gal activity is used to monitor replicative senescence in vitro and cellular aging in vivo (Dimri et al., 1995). Replicative senescence is the acquisition of growth arrest with the serial passaging of cells in culture and may mirror cellular aging in vivo (Campisi, 2005). For many human cell types, such as fibroblasts, keratinocytes and endothelial cells, cultures start with little or no SA  $\beta$ -Gal activity, but as they continue to be passaged, the number of cells proliferating declines, while the number of cells staining strongly for SA  $\beta$ -Gal increases (Dimri et al., 1995; van der Loo). By contrast, immortal cell lines, such as HeLa, do not stain for SA  $\beta$ -Gal (Dimri et al., 1995), but can be induced to senesce and express SA  $\beta$ -Gal (Goodwin et al., 2001). Although SA  $\beta$ -Gal activity is extensively used as a biomarker of aged cells, the underlying biochemical and cellular basis for the correlation is still subject to question (Hwang et al., 2009; Lee et al., 2006; Severino et al., 2000).

For fish, SA  $\beta$ -Gal activity has only just begun to be used to characterize cell lines and to study aging and the relationship between SA  $\beta$ -Gal and cell proliferation is unclear. For the short-lived killifish *Nothobranchius furzeri*, no SA  $\beta$ -Gal staining was observed in primary cultures from the skin and fins and after the cultures had undergone several population doublings (Graf et al., 2013). The authors concluded that for this species SA  $\beta$ -Gal was not a suitable marker for cellular senescence in vitro (Graf et al., 2013). By contrast, the skin of older killifish and medaka had more SA  $\beta$ -Gal staining

than the skin of younger fish (Ding et al., 2010; Graf et al., 2013). SA  $\beta$ -Gal activity also was a good in vivo marker of aging in zebrafish, *Danio rerio* (Tsai et al., 2007). Yet few or no cells stained for SA  $\beta$ -Gal in cultures of zebrafish cell lines from embryos and spleen (Zing et al., 2008; 2009). For the walleye, *Sander vitreus*, SA  $\beta$ -Gal staining was different between heart and fin cell cultures: in early passage cultures (< 5), no staining was seen with caudal fin fibroblasts, whereas heart cell cultures stained strongly (Vo et al., 2014). Possibly the relationship between SA  $\beta$ -Gal activity and replicative senescence in vitro is more complex and differs more among teleosts than in mammals because they show indeterminate growth and novel patterns of senescence (Kishi, 2004). Senescence patterns have been described as rapid, gradual or negligible. Pacific salmon that live for a few years and die at first spawning exemplify rapid senescence, whereas rougheye rock fish that live for over two hundred years without increased mortality exemplify negligible senescence. Gradual senescence with some similarities to mammalian senescence has been described for the guppy and carp (Kishi, 2004). Categorizing fish into these patterns has been done for relatively few species and seems particularly difficult for gradual versus negligible senescence. Zebrafish is described as being very gradual or sub negligible (Kishi, 2004).

In this report a recently described endothelial cell line (WEBA) from the walleye bulbous arteriosus was found to stain for SA  $\beta$ -Gal through all stages of development. This led to an investigation of SA  $\beta$ -Gal staining in many existing cell lines from various tissues and species and during the course of development of new cell lines from walleye and rainbow trout, including for the first time cell lines from reproductive fluids, milt and coelomic or ovarian fluid. The presence of mainly SA  $\beta$ -Gal negative cells in cultures predicted on-going cell proliferation in the culture, whereas the presence of SA  $\beta$ -Gal positive cells had several possible interpretations and was associated with slow or no growth.

## **6.2. MATERIALS AND METHODS**

### **6.2.1. Cell lines**

The cell lines that were used and their basic properties and original citations are listed in Tables 6.1, 6.2 and 6.3 but can be considered as belonging to one of three groups. One group is the long-standing cell lines, CHSE-214, RTG-2 and EPC, that were originally obtained from the American Type Culture Collection (ATCC, Manassas, VA). The second group of cell lines has been developed from several fish species, but mostly rainbow trout, over the last 25 years from the labs of Drs. LEJ Lee and NC Bols. The third group contains cell lines from walleye and rainbow trout and they are being described here for the first time.

### **6.2.2. Culture medium and conditions**

All the cell lines and primary cultures were maintained under similar conditions, with the exceptions being noted where they arise. The basal medium was Leibovitz's L-15, which allowed the cultures to be kept in an atmosphere of 100 % air. Unless stated otherwise, L-15 and other culture supplies were from Sigma (St Louis, MO). The L-15 was supplemented with 10 % fetal bovine serum (FBS) and antibiotics (200 U mL<sup>-1</sup> penicillin and 200 µg mL<sup>-1</sup> streptomycin, P/S, Thermo Scientific) and after supplementation is referred to as the growth medium and designated L15/FBS. Slightly different FBS concentrations were sometimes used, as will be noted later. Usually cultures were subcultivated at a 1 to 2 split, which is referred to as a passage. Subcultivation was done with trypsin or TrypLE (Invitrogen). The salmonid cell lines, as well as those from the Pacific herring and haddock, were maintained at 20 to 22 °C, whereas all others were kept at 26 °C.

### **6.2.3. Cell line development from solid organs of walleye and rainbow trout**

The preparation from fish organs of primary cultures by explant outgrowth and subsequent development of these into cell lines has been described previously in general terms for rainbow trout (Ganassin & Bols, 1997) and for the walleye caudal fin specifically (Vo et al., 2014). For this report, explants for outgrowth were obtained from

ovaries and testes of sexually mature rainbow trout (see section below) and from anal fin, skin, brains and hearts of juvenile walleye (see Vo et al., 2014 for more details on the walleye). In a laminar flow hood, the organs were removed and cut into small fragments (explants). The explants were rinsed in several times in Dulbecco's phosphate-buffered saline (DPBS; Cellgro) with P/S. The explants were transferred into plastic tissue culture vessels, usually 25-cm<sup>2</sup> flasks, and incubated at room temperature in L15/FBS. When the tissue culture vessels became confluent, subcultivation or passaging was performed with TrypLE and usually involved transferring the contents of a confluent vessel into two new vessels (1:2 split) and was passage 1. These were grown again to confluency and subcultivated in the same manner. This cycle was repeated serially to obtain enough cells to cryopreserve them as described previously (Ganassin et al., 1997). The resulting cell lines are listed in Tables 6.1 and 6.2.

#### **6.2.4. Cell line development from rainbow trout ovarian fluid (OvF)**

Ovarian fluid was obtained from three-year-old sexually mature fish during the routine breeding program for rainbow trout at the Alma Aquaculture Research Station of the University of Guelph. Inasmuch as in salmonids the eggs after ovulation are held in fluid within the coelomic cavity, the fluid is often described as either coelomic or ovarian but to avoid overlapping abbreviations ovarian fluid or OvF will be used here. When rainbow trout were stripped, OvF with the eggs was collected in a bowl with a strainer. The eggs were removed with the strainer and the OvF immediately transported on ice to the University of Waterloo (UW). At this stage, most cells in the OvF appear under the phase contrast microscope as white blood cells with some red blood cells and the total number of cells varied between  $9.2 \times 10^5$  and  $5.3 \times 10^6$  cells per mL. The OvF was mixed 1 to 2 with L15/FBS and aliquots of varying volumes added to 25-cm<sup>2</sup> tissue culture flasks. By the next day, cells were attaching and spreading but on subsequent days many cultures were lost due to microbial contamination despite the presence of antibiotics. However, some cultures remained microbial free and after 1 to 2 weeks at room temperature the attached cells appeared predominantly epithelial-like and after 3-5 weeks some formed complete epithelial monolayers. These cultures were serially

subcultivated 1 to 2 to give rise to the RTovf cell lines one of which is referred to as RTovf1 and was stained for senescence-associated  $\beta$ -galactosidase (SA  $\beta$ -Gal).

#### **6.2.5. Cell line development from rainbow trout milt**

Milt was obtained from 3 year old sexually mature fish during the routine breeding program for rainbow trout at the Alma Aquaculture Research Station. Milt was transported on ice to UW where aliquots were plated into tissue culture flasks with L15/FBS. Most commonly the medium was changed 48 h later, which removed most the sperm, and left a small number of adherent somatic cells that grew slowly to form subconfluent primary cultures. Some of these were examined for SA  $\beta$ -Gal. Others were treated with trypsin to redistribute the cells more evenly within the flasks and these cells were allowed to proliferate at room temperature and become confluent monolayers. These cultures were serially subcultivated 1 to 2 to give rise to the RTmilt cell lines one of which is referred to as RTmilt5 and was stained for SA  $\beta$ -Gal.

#### **6.2.6. Senescence-associated $\beta$ -galactosidase (SA $\beta$ -Gal) staining**

The Senescence Cells Histochemical Staining Kit (CS0030) was purchased from the manufacturer, Sigma (St Louis, MO), and used throughout according to the company's instructions, with the exception that the fish cells were incubated in the staining solution for 20 h at either 20 or 26°C rather than at 37 °C. For each cell type, usually triplicate cultures in L15/FBS were initiated in 12 well plates. Commonly the cell lines were seeded so that the culture was nearly confluent and staining was done the next day. For some of the long standing cell lines, such as CHSE-214, cultures were initiated at a range of cell densities and maintained for up to 6 days prior to staining. For quantification, approximately 5 randomly chosen microscope fields in three independent cultures were examined at 20 x magnification so that at least 200 cells were scored as either being SA  $\beta$ -Gal positive or negative. Positive cells had cytoplasmic staining that appeared blue, green or greenish blue depending on the microscope filter. The results are presented as the percentage of cells being SA  $\beta$ -Gal positive.

### **6.2.7. Periodic Acid-Schiff (PAS) staining**

The Periodic Acid-Schiff (PAS) staining system was purchased from the manufacturer, Sigma (St Louis, MO), and used according to the company's instructions (Procedure N. 395) for standard Procedure I. Previously this staining system was used to demonstrate mucopolysaccharides in RTgill-W1 (Lee et al., 2009) and can indicate several classes of complex polysaccharides. Approximately  $7 \times 10^4$  WEBA or WE-cfin11f cells were seeded per well in 12-well plates and allowed to grow for 3 days in L-15/FBS at 26 °C prior to the cultures being exposed to periodic acid solution and Schiff's reagent, followed by counterstaining with hematoxylin.

### **6.2.8. Comparing cell proliferation in WE-cfin11f and WEBA cultures**

Proliferation in L-15 with 15 % FBS at 26 °C was compared in 6 well plastic tissue culture plates over 9 days, with one change of medium on day 5. The handheld automated cell counter Scepter (Millipore, Mississauga, ON, Canada) was used to count cells after they had been detached from the growth surface and resuspended in DPBS. The experiments were initiated with the seeding and attachment of approximately  $8 \times 10^4$  WE-cfin11f cells and  $1.2 \times 10^5$  WEBA cells into triplicate wells. The next day cells were counted in three wells for each cell line to give the initial or day zero value. Cell counts made on subsequent days were expressed as a percentage of the day zero values.

## **6.3. RESULTS**

### **6.3.1. SA $\beta$ -Gal staining during cell line development from walleye bulbus arteriosus**

During the development of the endothelial cell line, WEBA, from the walleye bulbus arteriosus, cultures stained strongly for SA  $\beta$ -Gal from the earliest passage examined, 6 to the latest, 40 (Fig 6.1A, Table 6.1). The staining was cytoplasmic and most intense around the nucleus. As the SA  $\beta$ -Gal staining at all passage levels was unexpected, the presence of this activity during the development of cell lines from other walleye organs was investigated.

### **6.3.2. SA $\beta$ -Gal staining during cell line development from other walleye solid organs**

For all walleye organs examined, explant outgrowth led to cultures that could be subcultivated several times but the proportion of SA  $\beta$ -Gal positive cells and the ease with which these early passage cultures could be continuously propagated differed. For the caudal fin and anal fin, few cells stained for SA  $\beta$ -Gal, and three cell lines, WE-cfin11e, WE-cfin11f and WE-afin8e, were obtained. These have been split 1 to 2 for up to at least 40 times and at all passage levels, few or no SA  $\beta$ -Gal positive cells were seen (Table 6.1). For the walleye skin and spleen cell lines, SA  $\beta$ -Gal staining status at early passages was not examined; however, after over 20 passages, these cell cultures exhibited little SA  $\beta$ -Gal activity (Table 6.1). By contrast, in early passage cultures from the brain and heart, most cells were SA  $\beta$ -Gal positive (Fig 6.2; Table 6.1). However, these cultures initially grew more slowly than the fin cultures, and although enough cells were obtained to cryopreserve them, their slow growth made them difficult to work with. However, one brain cell line, WE-brain5, was taken to passage 15. At this point, less than 10 % of the cells were SA  $\beta$ -Gal positive (Table 6.1).

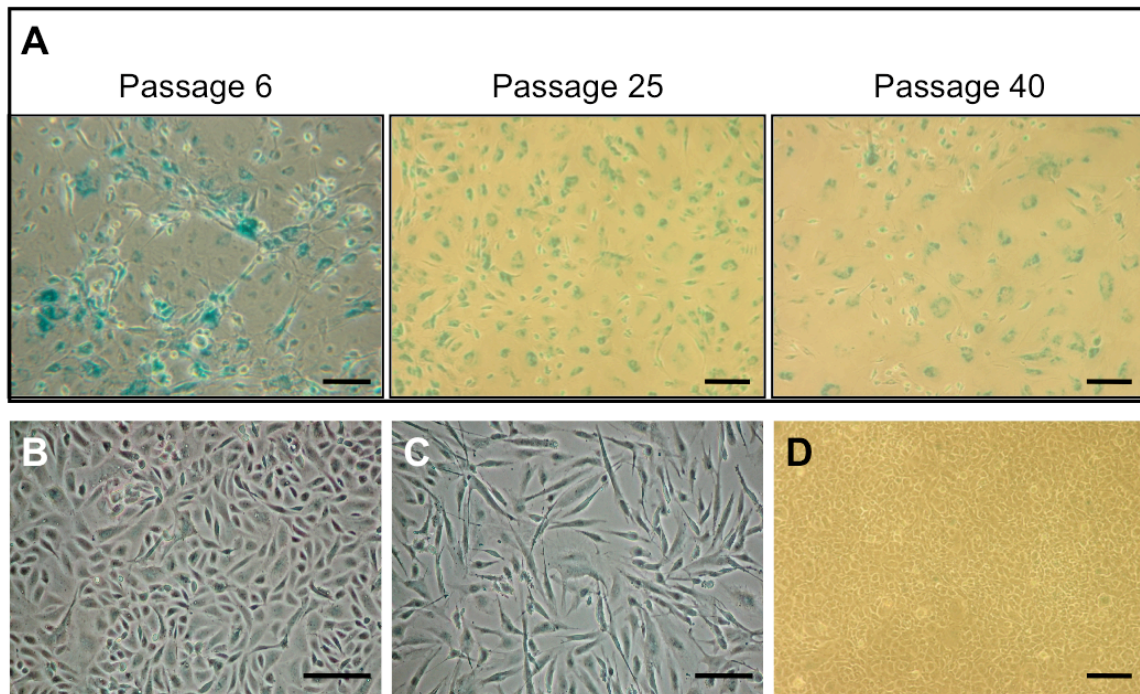


**Figure 6.1. Senescence-associated  $\beta$  galactosidase (SA  $\beta$ -Gal) staining of cultures of the endothelial cell line WEBA from walleye bulbus arteriosus (A) and of CHSE-214 from chinook salmon (B), RTG-2 from rainbow trout (C) and EPC from fathead minnow (D). In the top row (A) WEBA cultures were examined at passages 6, 25, and 40 and the majority of the cells stained positive for SA  $\beta$ -Gal at all passages. In contrast, very few cells if any cells are SA  $\beta$ -Gal positive in cultures of the long-standing immortal fish cell lines. Scale bar = 100  $\mu$ m.**

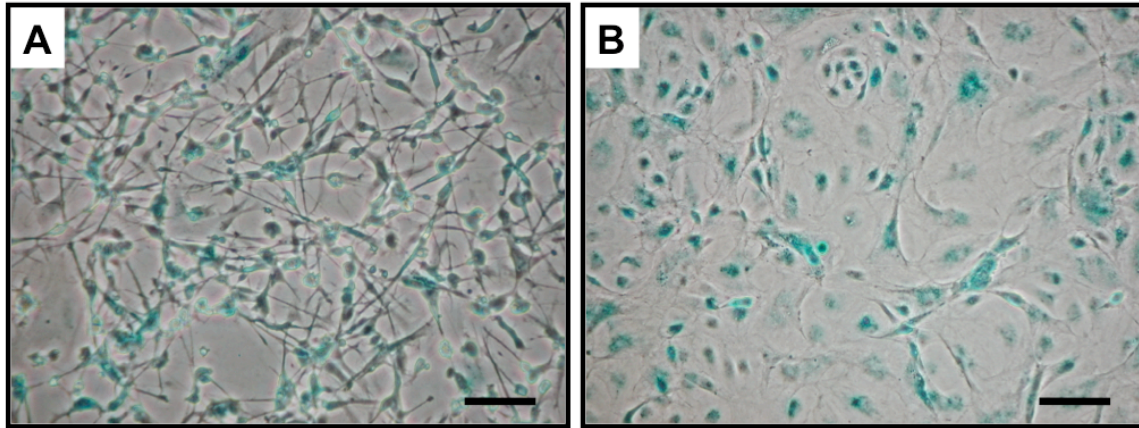


**Figure 6.2. SA  $\beta$ -Gal staining in early passage cultures of walleye brain (A) and heart (B). Most cells are SA  $\beta$ -Gal positive. Scale bar = 100  $\mu$ m.**

**Table 6.1. Senescence-associated  $\beta$ -Gal staining<sup>1</sup> in cultures<sup>2</sup> of cell lines from walleye, *Sander vitreus***

Tissue of origin	Cell line designation	Cellular Morphology	% of cells staining for SA $\beta$ -Gal <sup>3</sup>		
			Early passages (<5)	Middle passages (5-20)	Late passages (>20)
Caudal Fin	WE-cfin11f (Vo et al., 2014a)	fibroblastic	< 1 %	< 1%	< 1 % (passage 70)
	WE-cfin11e (Curtis et al., 2013, described in chapter 3)	epithelial	< 1 %	< 1 %	< 1 % (passage 24)
Anal Fin	WE-afin8e (this study)	epithelial	< 1 %	< 1 %	< 1 % (passage 20)
Brain	WE-brain3 (this study)	glial-like	92 %	n/a	n/a
	WE-brain5 (this study)	glial-like	86 %	8 %	n/a
Bulbus Arteriosus	WEBA (described in chapter 5)	endothelial	95 %	100 %	100 % (passage 40)
Heart	WE-heart1 (this study)	epithelial/ endothelial/ fibroblastic	95 %	n/a	n/a
	WE-heart6 (Vo et al., 2014a)	epithelial/ endothelial	95 %	98 %	n/a
Spleen	WE-spleen6 (described in chapter 4)	epithelial/ fibroblastic	n/a	n/a	< 1 %
Skin	WE-skin11f (this study)	fibroblastic	n/a	n/a	< 1 %

<sup>1</sup> The senescence cells histochemical staining kit (CS0030) from Sigma was used.

<sup>2</sup> Staining was done on cultures grown to near confluency in L-15 with 10% FBS, except for WE-cfin11f and WEBA at 15% FBS and WE-cfin11e at 5% FBS.

<sup>3</sup> At least 200 cells were observed and cells with blue coloring were scored positive.  
n/a = not available

### **6.3.3. Comparison of PAS staining and growth of two walleye cell lines**

Besides differing in how they stained for SA  $\beta$ -Gal, WEBA cells from the bulbus arteriosus differed in other ways from WE-cfin11f cells from the caudal fin. WEBA cells were positive for the PAS reaction (Fig 6.3), but WE-cfin11f cells were not. However WE-cfin11f cells grew significantly better than WEBA cells (Fig 6.4).

### **6.3.4. SA $\beta$ -Gal staining for rainbow trout cell lines**

Rainbow trout cell lines from several different solid organs examined after at least 12 passages were found to have 5 % or less of the cells staining for SA  $\beta$ -Gal (Table 6.2). When cultures of RTG-2 and RTgill-W1 cells were maintained for a week at different cell densities, from extremely low to very confluent, the percentage of SA  $\beta$ -Gal positive cells continued to be less than 1 %. Although after 12 passages less than 1 % of the cells stained for SA  $\beta$ -Gal, the testicular cell line (RT-testis) in early passage cultures did have 80 % of the cells being SA- $\beta$ -Gal positive. The other cell lines had not been examined during their development for SA- $\beta$ -Gal activity so the opportunity to do so had been lost. However, this was done for cell lines developed from rainbow trout reproductive fluids, ovarian fluid (OvF) and milt.

### **6.3.5. SA $\beta$ -Gal staining during cell line development from rainbow trout OvF**

In the first few days of initiation, the primary cell cultures of rainbow trout OvF were complex, with many floating and loosely attached white blood cells, which were not part of this study, but after several weeks areas of monolayer emerged with epithelial-like cells (Fig 6.5A) and these did not stain for SA  $\beta$ -Gal (Fig 6.5B). Although the epithelial like cells grew well, often forming complete monolayers, many OvF cultures were lost due to microbial contamination. However, a few monolayer cultures were split 1 to 2 and grown in L-15 with 10 % FBS at room temperature. After several weeks these could be serially subcultivated at a 1 to 2 split and over the course of approximately 3 months enough cells were obtained for cryopreservation. One of these cell lines is referred to as

RTovf1 and has undergone 30 passages. In cultures at approximately passages 5-15, less than 1 % of the cells stained positive for SA  $\beta$ -Gal (Table 6.2).

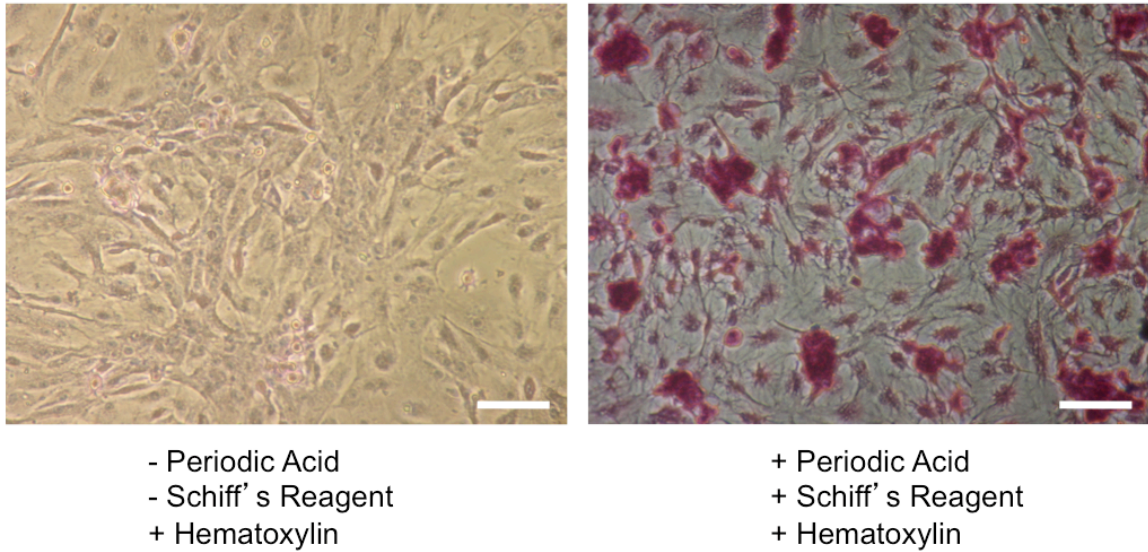


**Figure 6.3. Periodic acid Schiff (PAS) staining in WEBA cells.** The pink staining indicates PAS reactivity; the purple coloration is from hematoxylin counterstaining. In the left panel, cells without the prior application of PAS reagents were stained with hematoxylin. Scale bar = 100  $\mu$ m.

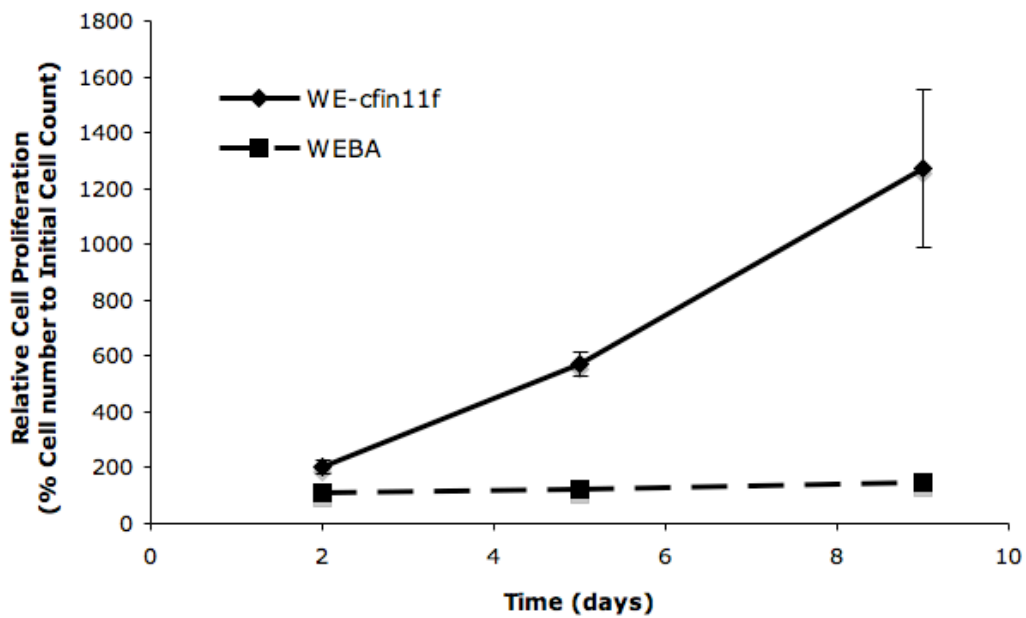


**Figure 6.4. Comparing cell proliferation in cultures of two walleye cell lines under similar growth conditions.** Growth was monitored in L-15 with 15 % FBS over 9 days at 26 °C for the fibroblast cell line, WE-cfin11f, from the caudal fin and for the endothelial cell line, WEBA, from bulbus arteriosus. Cell proliferation was expressed as percent of the cell numbers at the beginning of the cultures.

**Table 6.2. Senescence-associated  $\beta$ -Gal staining<sup>1</sup> in cultures<sup>2</sup> of cell lines<sup>3</sup> from different tissues of rainbow trout<sup>4</sup>**

<b>Tissue of origin</b>	<b>Cell line designation</b>	<b>Cellular Morphology</b>	<b>% of cells staining for SA <math>\beta</math>-Gal<sup>5</sup></b>
Mixed gonads	RTG-2 (Wolf & Quimby, 1962)	fibroblastic	< 1 %
Liver	RTL-W1 (Lee et al., 1993)	epithelial	< 1 %
Gill	RTgill-W1 (Bols et al., 1994)	epithelial	< 1 %
Intestine	RTgut-GC (Kawano et al., 2010)	epithelial	5 %
Brain	RTbrain (Vo et al., 2014b)	glial-like	5 %
Skin	RTHDF (Ossum et al., 2004)	fibroblastic	< 1 %
Testis	RT-Testis (described in this study)	epithelial	< 1 %*
Ovary	RTO-2 (described in this study)	fibroblastic	< 1 %
Ovarian Fluid	RT-ovf1 (described in this study)	epithelial	< 1 %
Milt	RTmilt5 (described in this study)	fibroblastic	< 1 %*

<sup>1</sup> The senescence cells histochemical staining kit (CS0030) from Sigma was used.

<sup>2</sup> Staining was done on cultures grown to near confluency in L-15 with 10% FBS.

<sup>3</sup> These cell lines have undergone at least 12 passages.

<sup>4</sup> *Oncorhynchus mykiss*.

<sup>5</sup> At least 200 cells were observed and cells with blue coloring were scored positive.

\* In early passage cultures greater than 80 % of the cells stained.

### **6.3.6. SA $\beta$ -Gal staining during cell line development from rainbow trout milt**

When tissue culture flasks (12.5 cm<sup>2</sup> or 25 cm<sup>2</sup>) with respectively 5 or 10 mL of L15 with 10% FBS received a small volume of milt and were incubated at room temperature or 12 °C, a few adherent cells were seen as early as 1 day later and are referred to as somatic cells. Every sample of milt examined this way yielded somatic cells. -The milt was obtained over a 4 year period from approximately 30 rainbow trout. The volume of milt put into a flask could be as low as 10  $\mu$ L and as high as 10 mL. However, the higher the volume the more likely microbial contamination would emerge and end the culture a week or two later. Higher volumes of milt usually increased the number of attached somatic cells only slightly because the enormous number of sperm in the culture appeared to physically interfere with the attachment and spreading of somatic cells. Therefore most often 100  $\mu$ L to 1 mL of milt was used and 48 h later the medium was aspirated off to remove sperm and fresh medium added to the culture. Adhered cells, single or in small clumps, slowly spread to reveal fibroblast-like and epithelial like cells (Fig 6.5C). Nearly all the cells in cultures at this stage stained for SA  $\beta$ -Gal (Fig 6.5D).

These primary cultures initially grew very slowly at room temperature but eventually led to cell lines. Over several months patches of cells began to appear on the flask surface but rarely grew to cover the whole surface. More commonly trypsin was used to detach the cell patches followed by the addition of L-15 with 10% FBS to allow single cells or clumps to reattach more evenly over the flask surface and eventually grow over a period of several months to form complete monolayers. These monolayers could be serially subcultivated at a 1 to 2 split over the course of 18 months to obtain enough cells for cryopreservation. One of these cell lines is referred to as RTmilt5 and has undergone 8 passages. In cultures at passage 5, less than 1 % of the cells stained positive for SA  $\beta$ -Gal (Table 6.2).

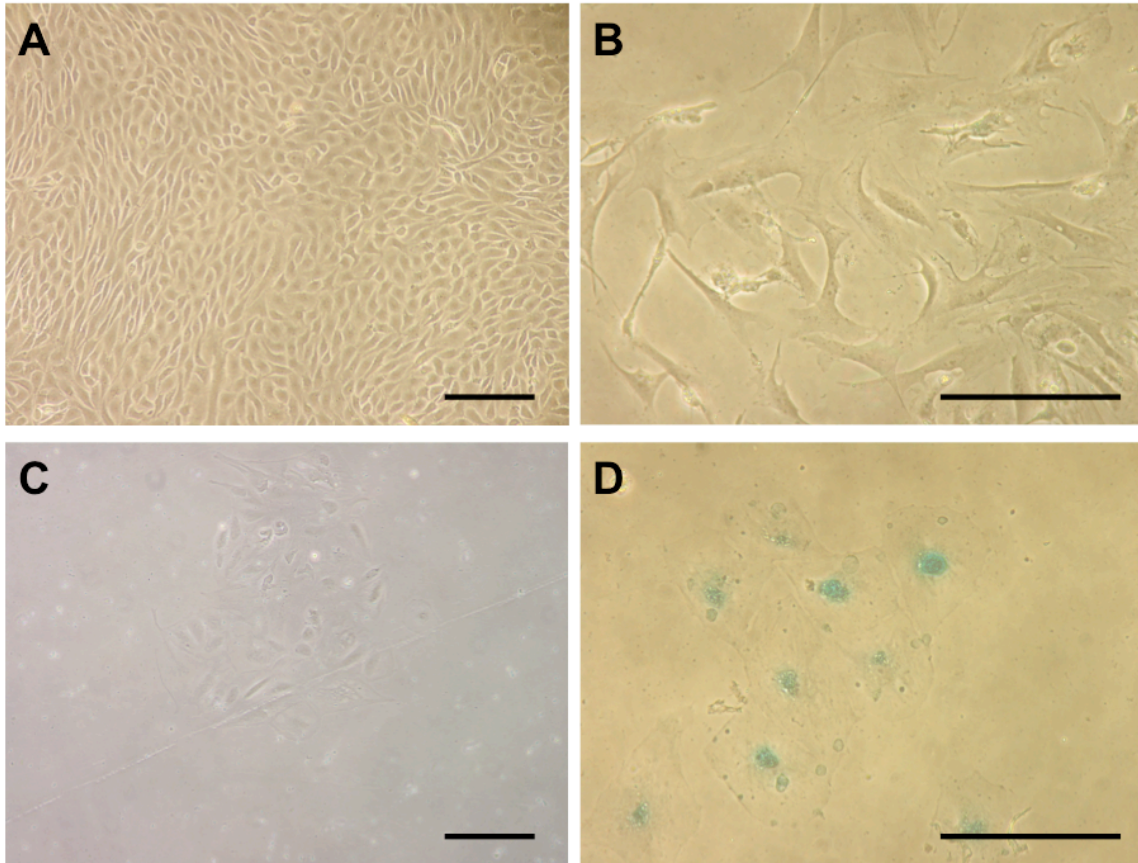


**Figure 6.5. Appearance and senescence-associated  $\beta$ -Gal staining of primary somatic cell cultures of ovarian fluid (OvF) and of milt from rainbow trout.** On the left, the phase contrast microscope appearance of OvF (A) and milt (C) cultures is shown, whereas on the right cultures have been stained for SA  $\beta$ -Gal, revealing no staining of the OvF epithelial cells (B), whereas milt fibroblastic-like and epithelial-like cells stained positive for SA  $\beta$ -Gal (D). Scale bar = 100  $\mu$ m.

### **6.3.7. Staining cultures of cell lines from a range of fish species for SA $\beta$ -Gal**

Cell lines from a wide range of species, encompassing fish undergoing rapid senescence (Chinook salmon) and very gradual senescence (zebrafish) were found to have very few cells staining for SA  $\beta$ -Gal (Table 6.3). This was true for long-standing fish cell lines, such as CHSE-214 and EPC (Fig 6.1C-D), which have been in use for approximately 50 and 30 years respectively without reports of cultures undergoing cellular senescence and would have to be considered immortal.

**Table 6.3. SA  $\beta$ -Gal staining<sup>1</sup> in cultures<sup>2</sup> of cell lines<sup>3</sup> from other fish species**

Cell line designation (original reference)	Species (common name)	Tissue of origin	Cellular Morphology	% of cells staining for SA $\beta$ -Gal <sup>4</sup>
CHSE-214 (Fryer et al., 1965)	<i>Oncorhynchus tshawytscha</i> (Chinook salmon)	embryo	epithelial	< 1 %
ZEB2J (Xing et al., 2008)	<i>Danio rerio</i> (zebrafish)	embryo	epithelial	< 1 %
ZSSJ (Xing et al., 2009)	<i>Danio rerio</i> (zebrafish)	spleen	epithelial	2%
GFSk-S1 (Lee et al., 1997)	<i>Carassius auratus auratus</i> (goldfish)	skin	fibroblastic	< 1 %
EPC (Fijan et al., 1983)	<i>Pimephales promelas</i> (fathead minnow)	skin	epithelial	< 1 %
FHMT (Vo et al., 2010)	<i>Pimephales promelas</i> (fathead minnow)	testis	epithelial	< 1 %
PHL (Ganassin et al., 1999)	<i>Clupea harengus</i> (Pacific herring)	larvae	epithelial	< 1 %
HEW (Bryson et al., 2006)	<i>Melanogrammus aeglefinus</i> (haddock)	embryo	fibroblastic	< 1 %

<sup>1</sup> The senescence cells histochemical staining kit (CS0030) from Sigma was used.

<sup>2</sup> Staining was done on cultures grown to near confluency in L-15 with 10% FBS.

<sup>3</sup> These cell lines have undergone at least 40 passages.

<sup>4</sup> At least 200 cells were observed and cells with blue coloring were scored positive.

#### 6.4. DISCUSSION

Various types of fish cell cultures have been stained for senescence-associated  $\beta$ -galactosidase (SA  $\beta$ -Gal). In cultures of a recently established endothelial cell line (WEBA) from the walleye bulbous arteriosus (BA) most cells stained during all stages of development, whereas during development of cell lines from the walleye caudal fin and from rainbow trout coelomic or ovarian fluid little or no SA  $\beta$ -Gal staining was ever seen. By contrast, most cells in early cultures of walleye brain and of rainbow trout milt were SA  $\beta$ -Gal positive but after their development into cell lines most cells were SA  $\beta$ -Gal negative. Cultures of long-standing fish cell lines from different tissues and species showed little or no SA  $\beta$ -Gal staining. As discussed below, these results suggest that SA  $\beta$ -Gal staining could have several meanings but the absence of cells staining in cultures predicts the continuous proliferation of cells.

##### SA $\beta$ -Gal staining throughout cell line development, WEBA

From early to late passage, most cells in WEBA cultures stained for SA  $\beta$ -Gal, suggesting that the SA  $\beta$ -Gal activity was not indicating cellular senescence but something characteristic of the cell line. The uniqueness of WEBA could revolve around lysosomes. In human cells SA  $\beta$ -Gal is not due to a distinct enzyme but due to lysosomal  $\beta$ -galactosidase that although optimally active at pH 4.0, can be detected at pH 6.0 in senescent cells (Kurz et al., 2000). The detection of SA  $\beta$ -Gal is considered a surrogate marker for an increase in lysosome number or activity (Lee et al., 2006). Thus the number of lysosomes or the lysosomal activity might always be high in WEBA cells, perhaps related to their BA origin.

WEBA mirrored some of the histochemistry of the BA endothelium and possibly because of this and /or unique BA endothelium organelles SA  $\beta$ -Gal activity is high. When the BA of 80 teleost species was examined histochemically by periodic acid-Schiff (PAS) reaction and ultrastructurally by transmission electron microscopy, the endothelial cells of most species, including a member of the family Percidae, were PAS positive and contained moderately-dense granules (Benjamin et al., 1983; 1984). PAS positivity was

attributed to polysaccharides and glycoproteins in the granules (Benjamin et al., 1984; Leknes, 2009). The granules were 100-600 nm in diameter and membrane bound (Benjamin et al., 1983), but in at least one species were not considered lysosomes (Leknes, 2009). WEBA but not the other walleye cell lines was PAS positive. This suggests that as well as having more SA  $\beta$ -Gal activity, WEBA has more potential substrates for the  $\beta$ -galactosidase, which cleaves  $\beta$ -linked terminal galactosyl residues from a wide range of naturally occurring substrates (Kurz et al., 2000). Whether WEBA SA  $\beta$ -Gal activity is in granules remains to be determined, but in at least case of the mouse visceral endoderm SA  $\beta$ -Gal staining was noted in apical vacuoles rather than lysosome (Huang & Rivera-Perez, 2014). In the future the BA could be examined *in vivo* to see if high SA  $\beta$ -Gal activity is a feature of the endothelium.

WEBA was an exceptional cell line in appearing to be immortal but still staining for SA  $\beta$ -Gal. The coexistence of cell proliferation and high SA  $\beta$ -Gal activity has been seen *in vivo* for some mammalian tissues. In the visceral endoderm of mouse embryos (Huang & Rivera-Perez, 2014) and in cells on the luminal surface of dysplastic glandular and squamous epithelia of the human upper gastrointestinal tract (Going et al., 2002), cell proliferation and SA  $\beta$ -Gal staining were observed together. Interestingly, although WEBA cells continuously grow and have SA  $\beta$ -Gal activity, WEBA cultures grew more slowly than cultures of other walleye cell lines under similar culture conditions.

#### Absence of SA $\beta$ -Gal staining during development of walleye caudal fin cell lines

Some fish cell lines appear to be established with few or no SA  $\beta$ -Gal staining cells being present in the cultures at any stage of development. This was illustrated for the walleye caudal fin cell lines (WE-cfin11f and e) where the earliest stage in cell line development was passage 5 and the latest was passage 75 (WE-cfin11f). Similar observations were made with primary cultures from the skin and fins from the short-lived killifish *Nothobranchius furzeri* (Graf et al., 2013). No SA  $\beta$ -Gal staining was observed in the primary cultures and after the cultures had undergone several population doublings (Graf et al., 2013). This absence of SA  $\beta$ -Gal staining through cell line development might have been a feature of the integumentary system, but as outlined below, cells from

another anatomical site and species were established into cell lines without SA  $\beta$ -Gal positive cells being seen during their development.

#### Absence of SA $\beta$ -Gal staining during development of rainbow trout OvF cell lines

Although initially complex, with many floating and loosely attached white blood cells, the primary cell cultures of rainbow trout OvF become after several weeks relatively uniform with large areas of epithelial cells that showed little or no staining for SA  $\beta$ -Gal. The origin of these epithelial cell monolayers is likely somatic cells that have entered OvF from follicles and/ or from the coelomic epithelial and mesovarial cells lining the peritoneum. Whether these somatic cells in the OvF lacked SA  $\beta$ -Gal activity or lost the activity with time in culture is difficult to distinguish because the primary cultures take several weeks to become uniformly epithelial. However the simplest explanation is that the somatic cells in the OvF that give rise to the epithelial cell cultures were negative for SA  $\beta$ -Gal. From within 3-4 months of initiation, cultures gave rise to confluent epithelial cell monolayers that could be subcultivated to yield OvF cell lines. These have been serially propagated for at least a year at a 1 to 2 split without the appearance of SA  $\beta$ -Gal positive cells. Thus although from chronologically old donors, somatic cells from OvF do not appear to undergo cellular senescence upon routine propagation in vitro.

#### The loss of SA $\beta$ -Gal staining through walleye brain cell line development

In the case of the walleye brain, cell lines appeared to begin from cultures in which most cells stained for SA  $\beta$ -Gal but as the cultures were serially passaged the SA  $\beta$ -Gal activity was lost. As the amount of brain tissue available to start cultures was small, early cultures were not sacrificed for SA  $\beta$ -Gal staining until passage 5 when most cells (> 85 %) were SA  $\beta$ -Gal positive. For cultures of mammalian brain neuronal cells, cellular senescence was thought to occur because the number of SA  $\beta$ -Gal positive cells increased from < 10% to over 90 % during 30 days of primary culture (Dong et al., 2011). Therefore, the high percentage of SA  $\beta$ -Gal positive cells in WE-brain5 cultures at passage 5 could have two different origins. The initial primary culture might have had a

low % of SA  $\beta$ -Gal but as the culture grew and was subcultivated the proportion of SA  $\beta$ -Gal positive cells increased, possibly due to cellular senescence in vitro. Alternatively the % might have been high in the initial primary culture because the many cells from the brain were either senescent or expressed high SA  $\beta$ -Gal activity for physiological reasons. Regardless of the SA  $\beta$ -Gal positive cell origins, the continued cultivation of WE-brain5 led to their numbers to drop, with less than 10 % of the cells staining at passage 13. The drop could have been due to either SA  $\beta$ -Gal positive cells losing activity or a few negative cells proliferating so that their progeny make up most of the culture. As human neural stem cells do not stain for SA  $\beta$ -Gal (Villa et al., 2004), WE-brain5 could possibly represent a population of brain progenitor cells.

#### The loss of SA $\beta$ -Gal staining through rainbow trout milt cell line development

Milt primary cultures began with a single cell or small cluster of cells attaching, spreading and growing into small islands with a mixture of cell shapes, from bipolar to cobblestone, but with nearly all staining for SA  $\beta$ -Gal. As the density of somatic cells in milt is very low and their attachment and spreading onto tissue culture plastic is slow, the primary milt cultures started at a very low density and were stained a week or later after initiation. These cells would have to condition a large volume of medium and might over time in culture have become metabolically stressed and acquired SA  $\beta$ -Gal activity. However, little or no staining was observed in low density cultures of immortal fish cell lines and of primary epithelial cell cultures from rainbow CF. Therefore, the simplest interpretation is that most somatic cells in rainbow trout milt were SA  $\beta$ -Gal positive, although a few negative cells still could have been present.

This appears to be the first observation of somatic cells in the milt of fish, and the first demonstration of SA  $\beta$ -Gal staining in somatic cells from the semen of vertebrates. Different somatic cell types, including macrophages/monocytes, lymphocytes, Sertoli cells and epithelial cells, have been found in mammalian semen, along with low levels of spermatogonia (Johanisson et al., 2000). These cells have an unclear origin, often described simply as being sloughed off from the luminal surface of the reproductive tract. The culturing of semen somatic cells was described first for humans and epithelial cells

were obtained (Phillips et al., 1978). Subsequently fibroblasts and epithelial cells have been cultured from the semen of farm animals, including sheep and chickens (Liu et al., 2009; Kjelland et al., 2013). In the case of human semen some of the primary epithelial cultures became confluent within 5 weeks and could be subcultivated (Phillips et al., 1978).

Primary cell cultures of milt were developed into cell lines that were continuously propagated for at least a year at a 1 to 2 split and were SA  $\beta$ -Gal negative, but the time course for cell line development was very slow. Milt cell lines were developed by detaching cells from the small areas of growth in the primary cultures and allowing them to reattach and grow more evenly over the culture surface. Ultimately confluent monolayers were formed that could be subcultivated. The time between first few passages was on the order of months but eventually the time to reach confluency shortened to a few weeks and the cells could be cryopreserved. When thawed and grown, less than 1 % of these cells stained for SA  $\beta$ -Gal. Thus during milt cell line development either cells lost SA  $\beta$ -Gal activity or only the few SA  $\beta$ -Gal negative cells went onto grow into a cell line.

#### Absence of SA $\beta$ -Gal staining in most immortal cell lines

As with mammalian cell lines, the fish cell lines considered to be immortal or continuous failed to stain for senescence associated  $\beta$ -galactosidase (SA  $\beta$ -Gal). For immortal mammalian cell lines that were demonstrated not to stain for SA  $\beta$ -Gal, most were derived from tumors, including HeLa and HT1080 (Dimri et al., 1995), or from deliberately immortalized rodent cells (Grendron et al., 2001). By contrast, the immortal fish cell lines that were negative for SA- $\beta$ -Gal were spontaneously derived from several different normal tissues from a wide range of species. Immortal mammalian cell lines usually have telomerase or the alternative lengthening of telomeres (ALT) pathways for maintaining telomeres (Cerone et al., 2005; Lee et al., 2013). Of the fish cell lines found to be negative for SA  $\beta$ -Gal staining, telomerase activity was clearly present in RTHDF, ZEB2 and HEW but very low in PHL (Bryson et al., 2006; Ossum et al., 2004; Xing et al., 2008). Whether all immortal fish cell lines maintain telomere length and do so

through telomerase activity or other mechanisms would be interesting to examine in the future.

### Summary

Long-standing immortal fish cell lines did not stain for SA  $\beta$ -Gal. Yet a recent endothelial cell line from the walleye bulbous arteriosus (BA) stained through all stages of development. Cell lines were obtained for the first time from fish reproductive fluids, rainbow trout milt and coelomic fluid (CF). Although the donor fish had similar chronological ages, most milt somatic cells were SA  $\beta$ -Gal positive and developed very slowly into cell lines, whereas for CF, most epithelial cells were SA  $\beta$ -Gal negative and developed more rapidly into cell lines. Progression of rainbow trout milt and walleye brain cell cultures into cell lines was accompanied by a decline in the number of SA  $\beta$ -Gal positive cells.

The concomitant acquisition of SA  $\beta$ -Gal positive cells and stopping of proliferation, which would have suggested the occurrence of replicative senescence as described in mammalian cell cultures, was not observed in any fish cell culture. On the other hand, possibly this occurred very early upon the initiation of the brain and milt somatic cell cultures and was missed. If this were the case, cellular senescence of fish cells in vitro would appear to be much more rapid than in mammalian cells. In conclusion whether fish cells undergo cellular senescence in vitro and SA  $\beta$ -Gal staining can be used as marker of the process is still unclear, but staining is a useful in vitro marker, with the absence of SA  $\beta$ -Gal activity predicting the continuous proliferation of cultures.

## **CHAPTER 7.**

**Immunocytochemical demonstration of acetylated  $\alpha$ -tubulin and primary cilia in cell lines from different species, life stages, and organs of fish**

## 7.1. INTRODUCTION

Acetylated  $\alpha$ -tubulin is widely distributed in nature, postulated to have various functions, and enriched in specific cellular structures, most notably primary cilia. The microtubules of the eukaryotic cytoskeleton are assembled from dimers of  $\alpha$ - and  $\beta$ -tubulin. In some  $\alpha$ -tubulins within microtubules, the lysine 40 is acetylated, but the precise acetyl transferases responsible and the significance of this posttranslational modification are still being investigated (Sadoul et al., 2011). Acetylation has been thought to be responsible for microtubule stabilization, although another view is that acetylation could be a consequence of stabilization. Recently, acetylated  $\alpha$ -tubulin has been shown to participate in intracellular protein trafficking (Reed et al., 2006) including to the nucleus (Zhong et al., 2014). The monoclonal antibody (mAb) 6-11B-1 is specific for the acetylated lysine 40 in  $\alpha$ -tubulin and has been used to localize  $\alpha$ -tubulin in cells, with primary cilia appearing as intensely stained rod-like structures of varying length (Piperno & Fuller, 1985; Piperno et al., 1987).

Primary cilia occur singly on most cells in the vertebrate body (Alieva et al., 1999; Satir et al., 2010; Wheatley et al., 1996). They have a 9 + 0 axoneme, are immotile, and contain acetylated  $\alpha$ -tubulin. Primary cilia are often referred to as the cell's sensor antenna and coordinate signaling pathways during development and in tissue homeostasis (Satir et al., 2010). Increasing numbers of normal cellular and physiological processes are being shown to have primary cilia involved (Cianfanelli & Cecconi, 2013), and primary cilia abnormalities are central to several human diseases (Bergmann, 2012). However, studies on primary cilia in fish are few, although a few model species have provided invaluable insights (Miyamoto et al., 2011). Inasmuch as primary cilia are present on some mammalian cell lines (Alieva et al., 1999; Wheatley et al., 1996), fish cell lines might be suitable for studying primary cilia in teleosts. Yet, to date, only one fish cell line, SBP from the brain of the subnose pompano, has been shown to have primary cilia (Wen et al., 2010).

Therefore, in this chapter, mAb 6-11B-1 has been used to identify acetylated  $\alpha$ -tubulin containing structures in cell lines from seven species of fish, including eight cell lines from walleye (*Sander vitreus*) and ten from rainbow trout (*Onchorhynchus mykiss*).

Seven out of eight walleye cell lines commonly contained primary cilia, whereas, surprisingly, rainbow cell lines appeared to lack them.

## **7.2. MATERIALS AND METHODS**

### **7.2.1. Fish cell lines**

Twenty three fish cell lines were used in this study. Descriptions of these fish cell lines with their original references are summarized in Table 1. CHSE-214 (CRL-1681), EPC (CRL-2872), and RTG-2 (CCL-55) were originally obtained from the American Type Culture Collection (ATCC, Manassas, VA). The other fish cell lines were developed in the laboratory of Dr. Niels Bols at the University of Waterloo (Waterloo, ON, Canada) in the last 25 years, including two available from ATCC, RTgill-W1 (CRL-2523) and PHL (CRL-2750). Unless otherwise specified, Leibovitz's L-15 medium (Hyclone) with 10 % fetal bovine serum (FBS, Hyclone), 100 U/mL penicillin and 100 µg/mL streptomycin (ThermoFisher) was used to maintain most of the fish cell lines used in this study. Exceptions include WEBA, WE-brain5, RTbrain and RTS11 being kept at 15% FBS and WE-cfin11e being kept at 5% FBS. All lines (except for RTS11 being known as semi-adherent due to their monocyte/macrophage characteristics) were adherent cell lines grown in 75-cm<sup>2</sup> polystyrene tissue culture flasks (BD Biosciences); routine subcultivation was done in 1 to 2 splitting with Trypsin-Versene solution (0.05 % (w/v) trypsin, 0.02 % (w/v) EDTA) (Lonza). For RTS11, cell splitting was done in 1 to 2 ratio by transferring half of the culture medium from the original 25-cm<sup>2</sup> flask to a new flask and equal volumes of fresh medium was added into both flasks. The cell lines derived from salmonids, haddock and Pacific herring were kept at 20-22 °C; the other cell lines were kept at 26 °C.

### **7.2.2. Mammalian cell lines**

Four mammalian cell lines used in this study were HeLa (ATCC CCL-2), HepG2 (ATCC HB-8065), Caco-2 (ATCC HTB-37) and H4IIE (ATCC CRL-1548). They were originally obtained from ATCC. Brief descriptions of these cell lines were provided in Table 2. HeLa cells were maintained in Dulbecco's Modified Eagle's Medium (DMEM, Sigma) with 10% heat inactivated FBS, 4.5 g/L glucose, 0.11 g/L sodium pyruvate, 2.5 mM L-glutamine, 100 U/mL penicillin and 100 µg/mL streptomycin (ThermoFisher). The other three cell lines were maintained in RPMI-1640 medium (Hyclone) with 10%

heat inactivated FBS, 100 U/mL penicillin, 100 µg/mL streptomycin and 2.05 mM L-glutamine. For routine maintenance, these cell lines were subcultured with Trypsin-Versene solution and kept at 37 °C in 5% CO<sub>2</sub> atmosphere.

### **7.2.3. Immunofluorescence of acetylated alpha tubulin**

For most of the cell lines, cells were seeded to 80 % confluent level in four-chamber tissue culture-treated glass slides (BD Biosciences). Exceptions include WE-eye, WEBA and RTbrain, which were loosely attached and easily detached on the BD chamber glass slides after multiple solution changes and PBS washing steps during the immunocytochemistry procedures. For these three cell lines, they were seeded to 80 % confluent level in polystyrene slide flasks (Nunc). All cell lines were plated in their normal growth media and growth conditions as described above. Unless otherwise stated, all the following reagents were purchased from Sigma Aldrich. Briefly, cells were fixed in 3 % (w/v) paraformaldehyde in phosphate buffered saline (PBS, Lonza) for 20 minutes at 4 °C, permeabilized with 0.1 % (v/v) Triton X-100 in PBS for 10 minutes and then were incubated with the blocking solution (3 % (w/v) bovine serum albumin, 10 % (v/v) goat serum and 0.1 % (v/v) Triton X-100) for an hour at room temperature. Mouse monoclonal anti-acetylated  $\alpha$ -tubulin primary antibody (clone 6-11B-1) was applied to the fixed cultures in 1:1000 in blocking buffer for an hour at room temperature and then overnight at 4 °C. Three PBS washes were followed. Alexa Fluor 488-conjugated goat anti-mouse IgG secondary antibody (Invitrogen) was used at 1:1000 in PBS and applied to the cultures for an hour. As a control for specific binding, slide flask cultures received the secondary antibody without previous incubation with the primary antibody. Another three PBS washes were followed. Cultures were allowed to air-dry and then Fluorshield mounting medium with DAPI (to counterstain the cell nuclei) was applied. Samples were examined with the Zeiss LSM 510 laser scanning microscope and confocal images were acquired and analyzed using a ZEN lite 2011 software. Fluorescence staining was never observed in flask cultures to which only secondary antibody had been applied.

#### 7.2.4. $\alpha$ -tubulin sequence alignment

The mAb 6-11B-1 recognizes the four-residue epitope where the lysine 40 is situated and acetylated in the aa25-50 region of  $\alpha$ -tubulin (LeDizet and Piperno, 1987). To demonstrate that  $\alpha$ -tubulin of several salmonid species including rainbow trout have an almost identical aa25-50 sequence,  $\alpha$ -tubulin sequences were obtained from the National Center of Biotechnology Information (NCBI) database (<http://www.ncbi.nlm.nih.gov>). The aa25-50 region sequences of  $\alpha$ -tubulin sequences from human (*H. sapiens*) (Accession No. AAA91576.1), rainbow trout (*O. mykiss*) (Accession No. NP\_001118163), chum salmon (*O. keta*) (Accession No. P30436), sockeye salmon (*O. nerka*) (Accession No. AAK11715), Atlantic salmon (*S. salar*) (Accession No. ACN10896) and zebrafish (*D. rerio*) (Accession No. AAB84143.1) were compared using the multiple sequence alignment program Clustal Omega (<http://www.ebi.ac.uk/Tools/msa/clustalo/>). The aa25-50 region of  $\alpha$ -tubulin sequences from human (*H. sapiens*) (Accession No. AAA91576.1), rainbow trout (*O. mykiss*) (Accession No. NP\_001118163), chum salmon (*O. keta*) (Accession No. P30436), sockeye salmon (*O. nerka*) (Accession No. AAK11715), Atlantic salmon (*S. salar*) (Accession No. ACN10896) and zebrafish (*D. rerio*) (Accession No. AAB84143.1) shared the almost same sequence identity with the conserved Lysine 40 that was known to be subject to the post-translational acetylation.

### **7.3. RESULTS**

When cultures were examined immunocytochemically with mAb 6-11B-1 to acetylated  $\alpha$ -tubulin, examples of midbodies, mitotic spindles and centrioles staining strongly were seen in cultures of all the cell lines (Fig 7.1). The staining of other structures varied with the cell line. The results for the fish cell lines are summarized in Table 7.1 and the mammalian cell lines in Table 7.2. Observations focussed on the staining of primary cilium, cytoplasm and nucleus.

#### **7.3.1. Primary cilia**

Primary cilia were seen as short brightly stained rods that appeared only one to a cell (Figs 7.2-7.3). In cultures of some cell lines, cells with a primary cilium were seen, whereas for other cell lines no cells with a primary cilium were detected. Of eight walleye cell lines examined, seven cell lines had primary cilia (Table 7.1; Figs 7.2-7.3). In one examined cell line from each of the following fish species: fathead minnow, zebrafish and Pacific herring, primary cilia were also detected (Table 7.1; Fig 7.3). Primary cilia were absent in cultures of all ten rainbow trout cell lines, one Chinook salmon embryo cell line and one haddock embryo cell line (Table 7.1, Figs 7.3-7.4). Primary cilia were not detected in the four mammalian cell lines (Table 7.2). This agrees with previous reports in the case of HeLa and Caco-2 (Piperno et al., 1987; Overgaard et al., 2009).

#### **7.3.2. Cytoplasmic staining**

In general, there were three cytoplasmic staining patterns: microtubule network, diffuse staining and no staining. Of eight walleye cell lines, the staining of microtubule networks was apparent and very strong in the cytoplasm of most cells in cultures of four cell lines (Table 7.1, Fig 7.3). In the other three walleye cell lines and seven rainbow trout cell lines the staining was absent (Table 7.1, Fig 7.3). For the remaining fish cell lines, weak and diffuse staining occurred in the cytoplasm of some cells (Figs 7.2-7.4). Some level of cytoplasmic staining was observed in all four mammalian cell lines (Table 7.2); HeLa and H4IIE cell lines had strong microtubule network staining. In the original

characterization of mAB 6-11B-1 a subset of the HeLa cell microtubules stained strongly (Piperno et al., 1987).

### **7.3.3. Nuclear staining**

In all salmonid cell lines and one haddock embryo cell line, uniformly weak nuclear staining was seen (Table 7.1, Figs 7.3-7.4); however, the nuclear staining was almost always absent in mitotic figures (Figs 7.1, 7.3, 7.4). Interestingly, in cultures of five of these cell lines (CHSE-214, RTG-2, RTgut-GC, RTeeb and HEW), there were two distinct populations of cells: one with nuclear staining and the other with no nuclear staining (Table 7.1, Fig 7.4). Except for RTG-2 cell line, the cell population with no nuclear staining usually had weak diffuse cytoplasmic staining (Fig 7.4). In all cell lines from walleye, fathead minnow, zebrafish and Pacific herring, no nuclear staining was detected (Table 7.1, Fig 7.3). No nuclear staining was seen in one rat and three human epithelial cell lines (Table 7.2).

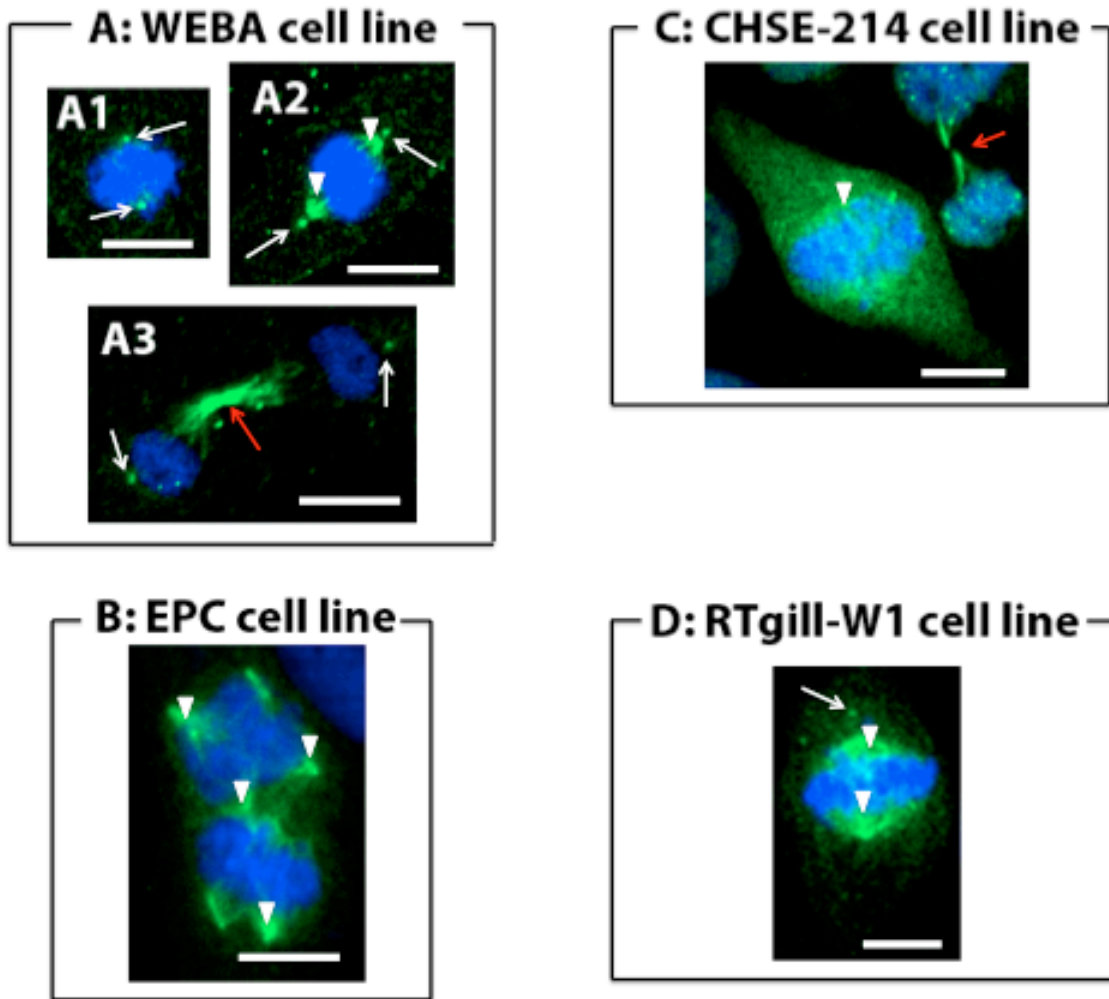


**Figure 7.1. Examples of mitotic spindles, midbodies and centrioles being stained for acetylated  $\alpha$ -tubulin by mAb 6-11B-1 in fish cell lines.** Four fish cell lines were shown here as examples: (A) walleye-derived WEBA cell line, (B) fathead minnow-derived EPC cell line, (C) Chinook salmon-derived from CHSE-214 cell line and (D) rainbow trout-derived RTgill-W1 cell line. White arrows indicate centrioles; white arrowheads indicate mitotic spindles; red arrows indicate midbodies. In panel A, A1 refers to a prophase; A2 refers to a prometaphase; A3 refers to a telophase. In panel B, two EPC cells underwent abnormal mitosis with multipolar spindles. In panel C, the white arrowhead points to a prophase/prometaphase and the red arrow points to cytokinesis. In panel D, a cell in prometaphase/metaphase is shown. Scale bar = 10  $\mu$ m.

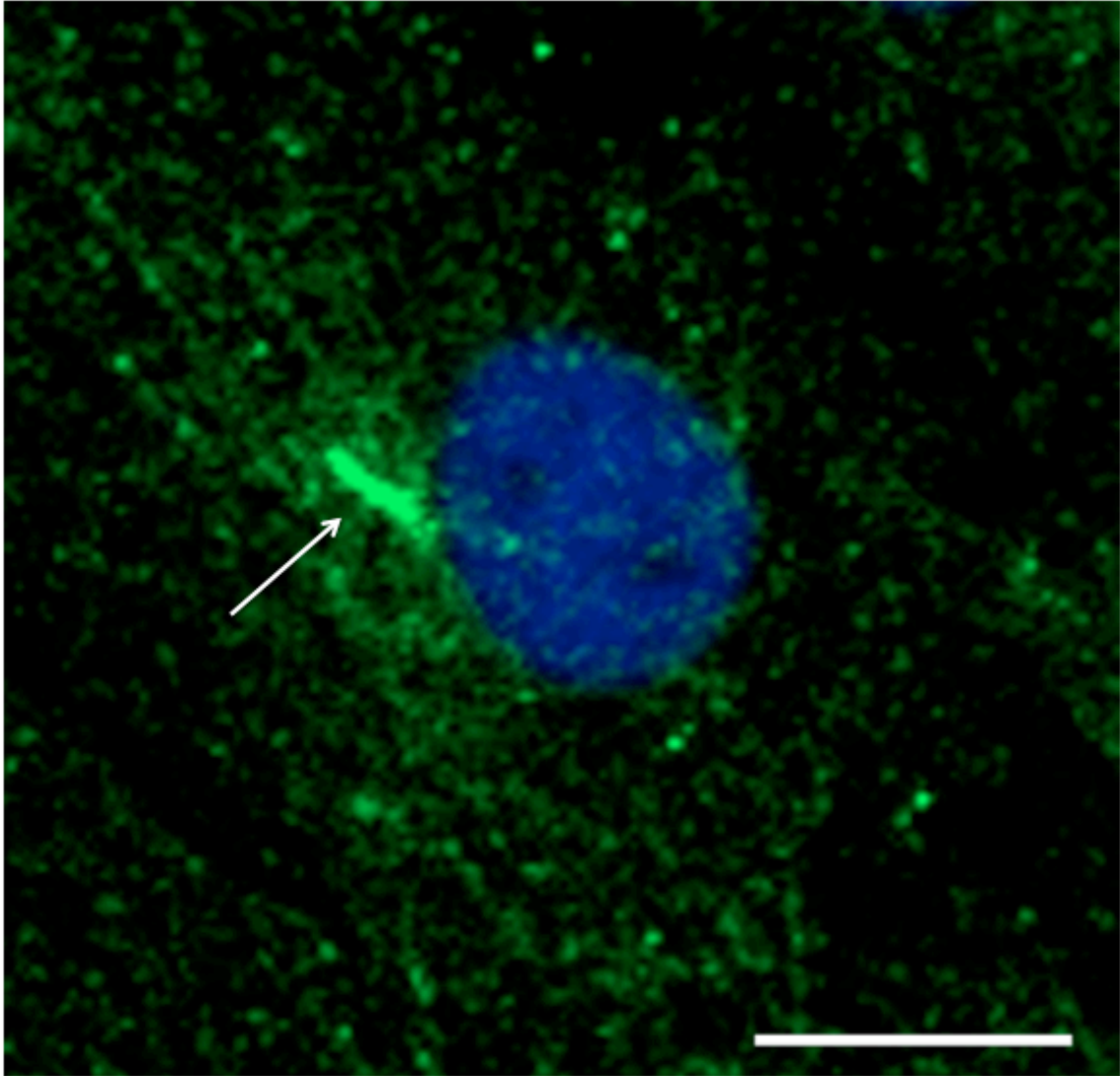


**Figure 7.2. Demonstration by mAb 6-11B-1 for primary cilia and cytoplasmic staining in the walleye caudal fin fibroblast WE-cfin11f cell line.** In most cases, there was one single primary cilium per cell (white arrow). Weak diffuse-like cytoplasmic staining was also detected in WE-cfin11f. Acetylated  $\alpha$ -tubulin is shown in green (Alexa Fluor 488) and cell nuclei are shown in blue (DAPI). Scale bar = 10  $\mu$ m.

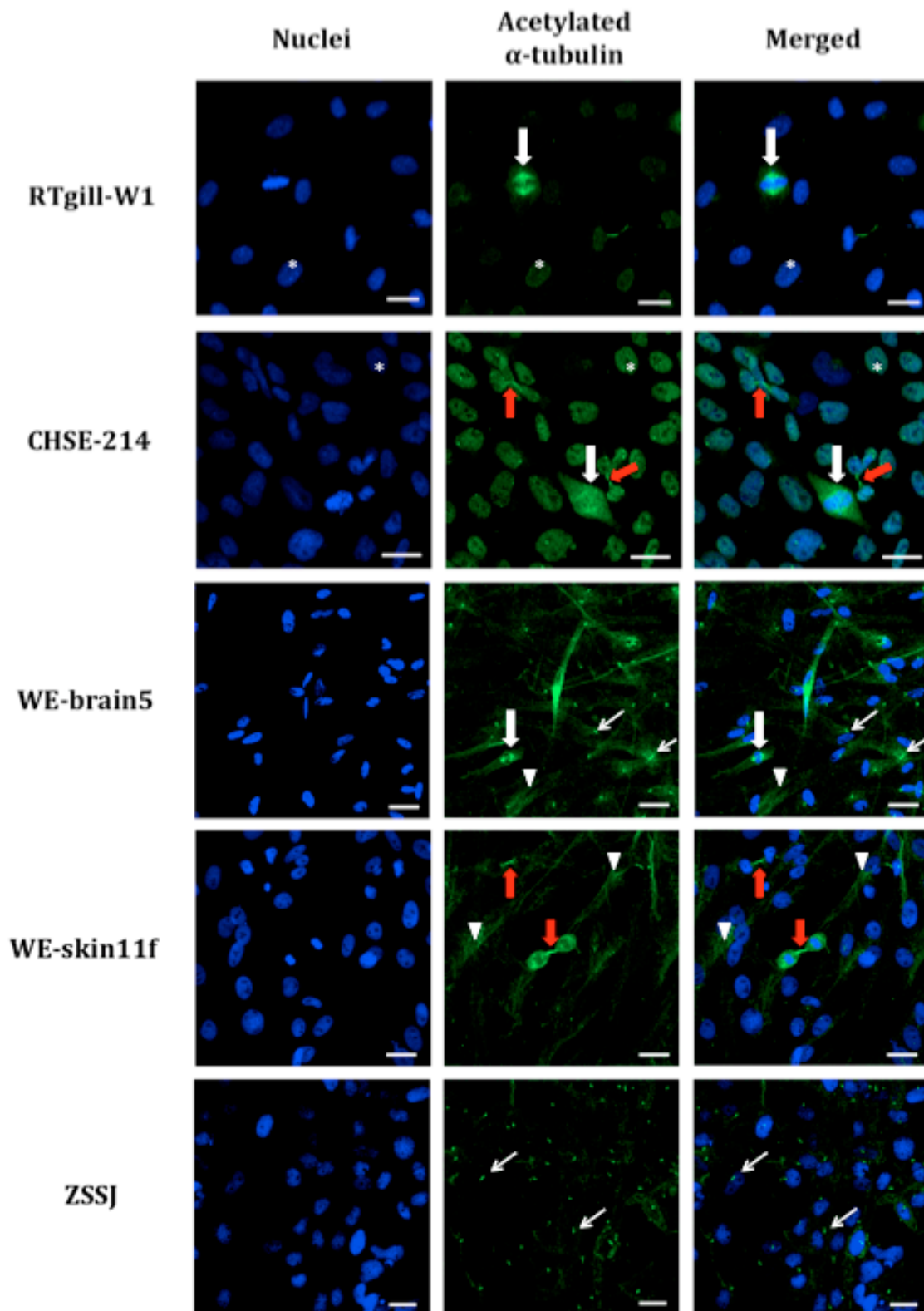


**Figure 7.3. Immunocytochemical staining by mAb 6-11B-1 in cell lines from rainbow trout gill (RTgill-W1), Chinook salmon embryo (CHSE-214), walleye brain (WE-brain5), walleye skin (WE-skin11f) and zebrafish spleen (ZSSJ).** Acetylated  $\alpha$ -tubulin is shown in green (Alexa Fluor 488) and cell nuclei are shown in blue (DAPI). White thick arrows indicate mitotic spindles; red thick arrows indicate midbodies; stars indicate nuclear signal detectable by mAb 6-11B-1; arrows indicate primary cilia; arrowheads indicate cytoplasmic microtubules. Scale bar = 20  $\mu$ m.

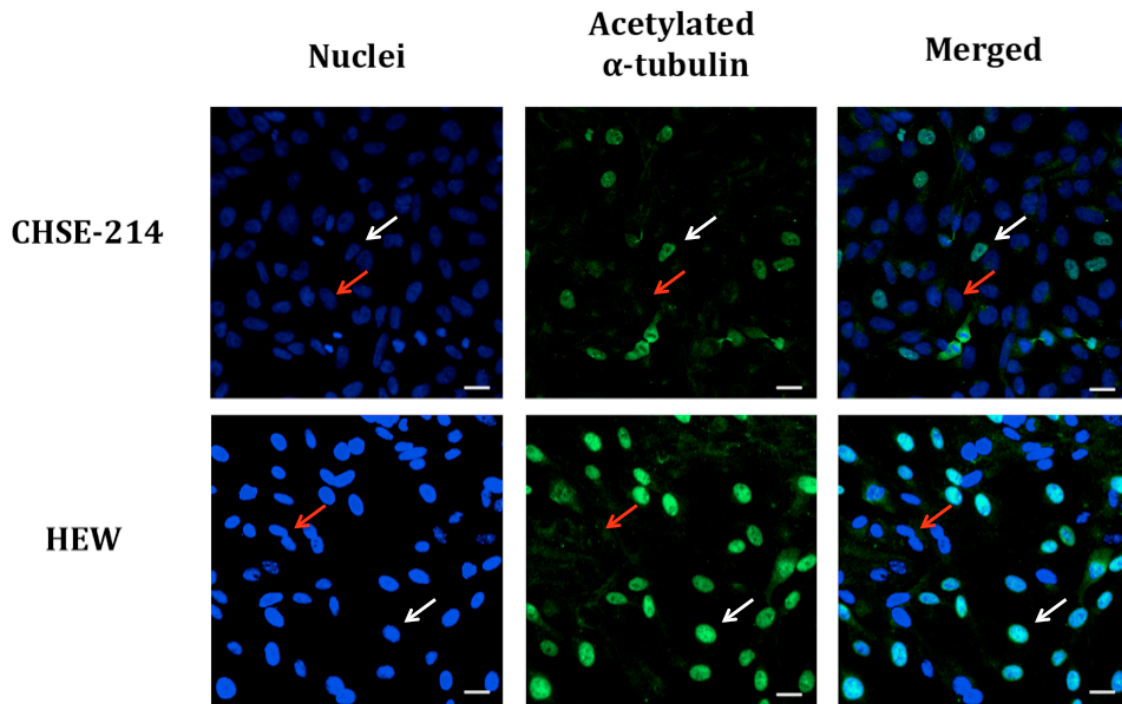


**Figure 7.4. Nuclear staining by mAb 6-11B-1 in cell lines from Chinook salmon embryo (CHSE-214) and haddock embryo (HEW).** Some cells in the cultures had detectable nuclear signals for acetylated  $\alpha$ -tubulin (white arrows) whereas others did not (red arrows). When cells had no detectable nuclear signals by mAb 6-11B-1, weak cytoplasmic staining was observed. Scale bar = 20  $\mu$ m.

↓

H.sapiens	clehgiqpdgqmpsdktigggddsfn
O.mykiss	clehgiqpdgqmpsdktigggddsfn
O.nerka	clehgiqpdgqmpsdktigggddsfn
D.rerio	clehgiqpdgqmpsdktigggddsfn
O.keta	clehgiqpdgqmpsdktcgggddsfn
S.salar	clehgiqpdgqmpsdktrgggddsfn
	*****

**Figure 7.5. Sequence alignment of amino acids 25-50 of  $\alpha$ -tubulin from human, salmonids and zebrafish.** This aa25-50 region contains the antigenic determinant with a single acetylated lysine 40 (arrow) of mAb 6-11B1. From National Center of Biotechnology Information (NCBI) database (<http://www.ncbi.nlm.nih.gov>), the aa25-50 region sequence was extracted from the full length  $\alpha$ -tubulin sequences from human (*H. sapiens*) (Accession No. AAA91576.1), rainbow trout (*O. mykiss*) (Accession No. NP\_001118163), chum salmon (*O. keta*) (Accession No. P30436), sockeye salmon (*O. nerka*) (Accession No. AAK11715), Atlantic salmon (*S. salar*) (Accession No. ACN10896) and zebrafish (*D. rerio*) (Accession No. AAB84143.1). The Clustal Omega program tool from the European Bioinformatics Institute (<http://www.ebi.ac.uk/Tools/msa/clustalo/>) was used to perform the sequence alignment. Stars indicate conserved amino acid among compared sequences.

**Table 7.1. Immunocytochemical staining pattern of acetylated  $\alpha$ -tubulin<sup>1</sup> in cell lines from seven fish species.**

Species (common name)	Cell line designation (original reference)	Tissue of origin	Cell shape	Acetylated $\alpha$ -tubulin Localization		
				Nuclear staining	Cytoplasmic staining	Primary Cilia
<i>Oncorhynchus tshawytscha</i> (Chinook salmon)	CHSE-214 (Fryer et al., 1965)	embryo	epithelial	Yes <sup>a</sup>	Yes <sup>b</sup>	No
<i>Oncorhynchus mykiss</i> (rainbow trout)	RTG-2 (Wolf & Quimby, 1962)	mixed gonads	fibroblastic	Yes <sup>a</sup>	No	No
	RTL-W1 (Lee et al., 1993)	liver	epithelial	Yes	No	No
	RTgill-W1 (Bols et al., 1994)	gills	epithelial	Yes	No	No
	RTgut-GC (Kawano et al., 2010)	intestine	epithelial	Yes <sup>a</sup>	Yes <sup>b</sup>	No
	RTbrain (Vo et al., 2014b)	brain	glial-like	Yes	No	No
	RTHDF (Ossum et al., 2004)	skin	fibroblastic	Yes	No	No
	RTS11 (Ganassin and Bols, 1998)	spleen	Monocyte/ macrophage	Yes	Yes <sup>c</sup>	No
	RT-Testis (described in chapter 6)	testis	epithelial	Yes	No	No
	RTO-2 (described in chapter 6)	ovary	fibroblastic	Yes	No	No
	RTeeb (Bols et al., 2004)	early embryo	fibroblastic	Yes <sup>a</sup>	Yes <sup>b</sup>	No
<i>Melanogrammus aeglefinus</i> (haddock)	HEW (Bryson et al., 2006)	embryo	fibroblastic	Yes <sup>a</sup>	Yes <sup>b</sup>	No
<i>Pimephales promelas</i> (fathead minnow)	EPC (Fijan et al., 1983)	skin	epithelial	No	Yes <sup>d</sup>	Yes
<i>Danio rerio</i>	ZSSJ	spleen	epithelial	No	Yes <sup>c</sup>	Yes

(zebrafish)	(Xing et al., 2009)					
<i>Clupea harengus</i> (Pacific herring)	PHL (Ganassin et al., 1999)	larvae	epithelial	No	Yes <sup>c</sup>	Yes
<i>Sander vitreus</i> (Walleye)	WE-cfin11f (Vo et al., 2014)	caudal fin	fibroblastic	No	Yes <sup>c</sup>	Yes
	WE-cfin11e (described in chapter 3; Curtis et al., 2013)	caudal fin	epithelial	No	No	Yes
	WE-skin11f (described in chapter 6)	skin	fibroblastic	No	Yes	No
	WE-liver3 (unpublished)	liver	fibroblastic	No	Yes <sup>e</sup>	Yes
	WE-brain5 (described in chapter 6)	brain	glial-like	No	Yes <sup>e</sup>	Yes
	WE-spleen6 (described in chapter 4)	spleen	epithelial	No	Yes <sup>e</sup>	Yes
	WEBA (described in chapter 5)	bulbus arteriosu s	endothelial	No	No	Yes
WE-Eye (unpublished)	eye/retin a	epithelial	No	No	Yes	

<sup>1</sup> Immunocytochemistry was performed with affinity-purified mouse monoclonal antibody clone 6-11B-1 that could identify acetylated  $\alpha$ -tubulin from a wide spectrum of species.

<sup>a</sup> A portion of the cultures were negative for this staining pattern

<sup>b</sup> Cells that don't have nuclear staining tended to have weak cytoplasmic staining

<sup>c</sup> Weak fluorescence staining

<sup>d</sup> Weak fluorescence staining; cytoplasmic staining was more strong in senescent-like multinucleated cells)

<sup>e</sup> Very strong fluorescence staining with fibrous pattern

**Table 7.2. Immunocytochemical staining pattern of acetylated  $\alpha$ -tubulin<sup>1</sup> in mammalian cell lines.**

Species (common name)	Cell line designation (original reference)	Tissue of origin	Cell shape	Acetylated $\alpha$ -tubulin Localization		
				Nuclear staining	Cytoplasmic staining	Primary Cilia
<i>Homo sapiens</i> (Human)	HeLa (Gey et al., 1952)	cervical adenocarcinoma	epithelial	No	Yes <sup>a</sup>	No
	HepG2 (Aden et al., 1979; Lopez-Terrada et al., 2009)	hepatoblastoma	epithelial	No	Yes	No
	CaCo-2 (Fogh et al., 1977)	colorectal adenocarcinoma	epithelial	No	Yes	No
<i>Rattus norvegicus</i> (Rat)	H4IIE (Pitot et al., 1964)	hepatoma	epithelial	No	Yes <sup>a</sup>	No

<sup>1</sup> Immunocytochemistry was performed with affinity-purified mouse monoclonal antibody clone 6-11B-1 that could identify acetylated  $\alpha$ -tubulin from a wide spectrum of species.

<sup>a</sup> Very strong fluorescence staining with fibrous pattern

#### 7.4. DISCUSSION

Acetylated  $\alpha$ -tubulin was found in all the fish cell lines, which were from multiple anatomical sites and from seven species. This was demonstrated by immunocytochemistry with the commercially available monoclonal antibody (mAb), 6-11B-1, which was raised against tubulin from the axonemes of sea urchin sperm flagella, is specific for acetylated  $\alpha$ -tubulin (Piperno & Fuller, 1985), and has been used to detect acetylated  $\alpha$ -tubulin from a wide range of animal and plant species (Wolf 1996; Nakagawa et al., 2013). For fish, this mAb was shown previously to label axon tracts in whole mounts of zebrafish embryos (Chitnis & Kuwada, 1990) and to demonstrate acetylated  $\alpha$ -tubulin in western blots of extracts from trout, eelpout, wrasse, and cod (Billger et al., 1991; Modig et al., 1994) but not from a goldfish cell line (Lessman et al., 1995). For mammalian cell lines, immunocytochemical staining with 6-11B-1 has been commonly observed. Frequently primary cilia have been revealed (Alieva et al., 1999), but mitotic spindles, midbodies, and subsets of cytoplasmic microtubules also have been found to stain in some cell lines (Alieva et al., 1999; Alieva & Vorobjev, 2004; Piperno et al., 1987). Collectively, similar structures were found to stain in fish cells, but cell lines from different species varied considerably, especially for primary cilia, which appeared to be absent in salmonid cell lines.

##### Primary cilia

This study extends the number of fish cell lines that express primary cilia from one, SBP from the subnose pompano (Wen et al., 2010), to cell lines from walleye (WE-cfin11f, WE-cfin11e, WE-liver3, WE-brain, WE-spleen, WEBA, and WE-eye), fathead minnow (EPC, ATCC CRL-2872), Pacific herring (PHL, ATCC CRL2750) and zebrafish (ZSSJ). Previously, in a histochemical study, the mAb was used to demonstrate primary cilia in zebrafish (Kim et al., 2010), but this would appear to be the first demonstration of primary cilia in the other species. Generally, mammalian cell lines vary in the proportion of cells with primary cilia and in primary cilia length (Alieva & Vorbojev, 2004, Wheatley et al., 1996; Wheatley & Bowser, 2000; Ou et al., 2009). Although requiring further analysis, including SEM examination, the frequency and perhaps the length of primary cilia appeared to vary among eight walleye cell lines. The one walleye cell line

that had very few or no primary cilia was the skin fibroblast, WE-skin11f. Yet, human skin fibroblasts have been reported to have a very high cilium incidence (Wheatley et al., 1996). By contrast, most cells in cultures of the caudal fin fibroblast (WE-cfin11f) and liver fibroblast (WE-liver3) cell lines had primary cilia. Mammalian fibroblasts from different anatomical sites are known to have different properties (Nolte et al., 2008). Whether the frequency of primary cilium consistently varies among fibroblasts from different anatomical sites in vertebrates remains to be explored in the future. Nevertheless, staining fish fibroblasts for primary cilia by mAb 6-11B-1 could become part of the routine characterization of new cell lines. Overall, the spectrum of walleye cell lines might be useful for studying how primary cilia formation and function varies between organs and tissues. For instance, the presence of primary cilia on the walleye endothelial cell line, WEBA, is of particular interest because primary cilia might have a mechanosensory role in the endothelium (Egorova et al., 2012).

In contrast to being present in most cell lines from walleye, primary cilia appeared to be absent in all eleven salmonid cell lines. Three general lines of thought can be advanced to explain why no or few primary cilia were detected in the salmonid cell lines. One is that the cells from this family of fish lack primary cilia. However, this seems unlikely as primary cilia seem to be present in all vertebrates (Pazour & Whitman, 2003) and have been identified ultrastructurally in at least some salmonids (Buckland-Nicks et al., 2012). A second line of reasoning is that acetylation of  $\alpha$ -tubulin in the primary cilia of salmonids either does not take place or is not recognized by mAb 6-11B-1. This seems unlikely because (1)  $\alpha$ -tubulin from several salmonids contain the almost identical aa25-50 peptide with lysine 40 that was determined to be the antigenic region of this mAb (LeDizet and Piperno, 1987) (2) this mAb stained the mitotic spindle and midbodies of salmonid cells, but could be ruled in the future by examining salmonid tissues through immunohistochemistry and/or immuno-electron microscopy. Finally, and most likely, salmonid cells might have little or no ability to assemble and/or maintain primary cilia in vitro.

The inability of salmonid cells in culture to maintain primary cilia could have several explanations. One is the inadvertent loss of function in one or more genes essential for cilia formation during cell line development. This might explain the lack of primary cilia

for some cell lines. For example, few or no primary cilia were reported on HeLa cells (Alieva et al., 1999) and this was confirmed here. However, chance events seem an unsatisfactory explanation for why primary cilia were absent or reduced on all twelve salmonid cell lines. Another explanation could be the lack of cells in G<sub>0</sub> and G<sub>1</sub> in the salmonid cell cultures because for many mammalian cell types, primary cilia are resorbed as cells undergo the G<sub>1</sub>/S transition (Goto et al., 2013; Li et al., 2011). However, rainbow trout cell cultures usually have all cycle stages present, unless efforts are made to synchronize them (Lee et al., 1988). Possibly, the development of salmonid cell lines selects for cells that do not express primary cilia. Interestingly, although present before culturing, primary cilia were rarely seen in human keratinocyte cultures (Wheatley et al., 1996). Additionally, for some human cancers and cancer cell lines, the primary cilia are decreased dramatically or missing (Yuan et al., 2010), suggesting that few or no primary cilia favoured cell proliferation. In prostate cancer cell lines, disturbed lipogenesis impaired the formation of primary cilia and blocking fatty acid synthesis restored the appearance of primary cilia (Willemarck et al., 2010; Schmidt et al., 2007). Lipid metabolism in cultures of cells from different groups of fish is known to differ (Ghioni et al., 1999) and possibly this could contribute to the presence of cilia in cells from some species, like walleye, and not in others, like salmon. In the future, these two groups of cell lines should be useful tools for investigating ciliogenesis in teleosts.

#### Staining for acetylated $\alpha$ -tubulin in the cytoplasm of fish cell lines

Examination of twenty three fish cell lines with the mAb 6-11B-1 revealed three cytoplasmic staining patterns. In cultures of four walleye cell lines, microtubule networks stained strongly in the cytoplasm of most cells. In ten cell lines from walleye and rainbow trout staining was absent. For the remaining nine cell lines, weak, diffuse staining occurred in the cytoplasm of some cells.

The cytoplasmic fibrillar staining in cell lines from some organs and not others fits observations made to date for mammals and fish that suggest the tissue and organ distribution of acetylated  $\alpha$ -tubulin is restricted. For mammals, cytoplasmic staining of acetylated microtubules was seen in neurons and megakaryocytes but generally not for most cells in culture, including cell lines (Sadhoul et al., 2011). However, 3T3 and HeLa

cells showed some staining (Piperno et al., 1987). A limited amount of western blotting data on cell and tissue extracts found that microtubule acetylation was uniquely abundant in the fish brain (Billger et al., 1991; Modig et al., 1994; Rutberg et al., 1995). However, among the fish cell lines a walleye brain cell line stained but one from the rainbow trout brain did not. Some functions proposed for acetylated  $\alpha$ -tubulin are the stabilization of microtubules by bundling them and the enhancement of protein trafficking (Sadoul et al., 2011; Zhong et al., 2014). Therefore, the cytoplasmic staining of walleye cell lines from skin, liver, brain and spleen might reflect a need for these actions in at least some of the cells in these organs.

The diffuse cytoplasmic staining was nearly always seen in cultures of cell lines with few or no primary cilia. Cytoplasmic staining for acetylated  $\alpha$ -tubulin has been reported to increase after deciliation of the Madin-Darby kidney cell line with chloral hydrate (Overgaard et al., 2009) and of human renal proximal tubular epithelial cells with two chemical carcinogens (Radford et al., 2012). These observations suggested that in the absence of ciliary axoneme,  $\alpha$ -tubulin was still acetylated and with no site in which to be incorporated accumulated in the cytoplasm. Thus possibly a reduced ability to form stable axoneme contributes to absence of primary cilia in salmonid cell cultures. However, this pattern of weak cytoplasmic staining also correlated with cultures that showed diffuse nuclear staining and so a different explanation, as discussed below, is that this staining represents  $\alpha$ -tubulin from mitotic spindles undergoing deacetylation.

#### Staining for acetylated $\alpha$ -tubulin in the nuclei of fish cell lines

This appears to be the first observation of acetylated  $\alpha$ -tubulin in the nuclei of cells that have not been genetically modified. For mammalian cells in culture, reports of nuclear tubulin have been slowly increasing over the last 35 years (Akoumianaki et al., 2009; Menko & Tan, 1980; Walss-Bass et al., 2002; Yeh & Luduena, 2004), but acetylated  $\alpha$ -tubulin has yet to be reported in the nuclei of wild type cells. However, in a mouse neuroblastoma cell line that had been engineered to overexpress collapsing response mediator protein 2 (CRMP-2), acetylated  $\alpha$ -tubulin was found in intra-nuclear inclusions (Gu & Ihara, 2000). Inasmuch as the mitotic spindle of mammalian cells in culture stained strongly for acetylated  $\alpha$ -tubulin (Piperno et al., 1987), the intra-nuclear

inclusions were attributed to the failure of spindle microtubules to completely disassemble at the end of mitosis (Gu & Ihara, 2000). In mammals acetylation is thought to occur not on free  $\alpha$ -tubulin but on microtubules and disassembly of microtubules leads to rapid deacetylation (Gu & Ihara, 2000). The mitotic spindle of fish cell lines also stained strongly for acetylated  $\alpha$ -tubulin. Therefore, the diffuse staining of interphase nuclei in some fish cell lines might be due to acetylated  $\alpha$ -tubulin that arose from disassembled mitotic spindles but that had yet to be deacetylated or was being deacetylated slowly.

The nuclear staining for acetylated  $\alpha$ -tubulin was found in all eleven salmonid cell lines and in the only haddock cell line but not in the all eight cell lines from walleye or the only cell line from each of fathead minnow, zebrafish and Pacific herring. These two groups of fish might differ in how efficiently they deacetylate  $\alpha$ -tubulin from the mitotic spindle. Histone deacetylases (HDACs) are responsible for tubulin deacetylation in mammals (Liu et al., 2002) and possibly their effectiveness and regulation in these fish groups is different. The temperatures at which the cell lines are maintained might enhance differences. All the cell lines with nuclear staining were from cold water species and were maintained at 20 to 22 °C, which would be in the upper region of the temperature tolerance zone for these fish (Bols et al., 1992), whereas all the cell lines without nuclear staining might be considered cool water or warm water species and were maintained at 26 °C, which would be in the middle of the tolerance zone for these fish (Vo et al., 2014). Thus for the cell lines from warm water fish, the deacetylation process might be acting optimally, eliminating acetylated  $\alpha$ - tubulin from the nucleus.

In cultures of five fish cell lines, staining for acetylated  $\alpha$ - tubulin was solely nuclear in some cells whereas in other cells only weak, diffuse cytoplasmic staining was seen. Possibly the diffuse cytoplasmic staining represents nuclear acetylated  $\alpha$ - tubulin that has been shuttled to the cytoplasm for deacetylation but has yet to be completely deacetylated. In HeLa cells,  $\alpha$ - and  $\beta$ -tubulin have been reported to shuttle between nuclear and cytoplasmic compartments (Akoumianaki et al., 2009) and HDACs are found in the cytoplasm (Liu et al., 2012).

## **Chapter 8.**

# **General Summary and Future Research**

## **General Summary**

This thesis has developed cell lines from the walleye, *Sander vitreus*. These have been used to study viral haemorrhagic septicaemia virus (VHSV IVb), which is the causative agent for viral haemorrhagic septicaemia (VHS), and to contribute to the comparative cellular biology and physiology of fish. The major outcomes for these two research directions are summarized below.

### **A. Cell lines and information for studying the impact of viral hemorrhagic septicaemia (VHS) on walleye**

In the last decade VHSV IVb has emerged in the Great Lakes region of North America causing fish kills and raising concerns about stocking practices and aquaculture of several freshwater species but the most important of these are walleye. Like other fish rhabdoviruses, VHSV IVb is a negative-sense single-stranded RNA virus that contains six protein coding genes: nucleocapsid (N), polymerase-associated phosphoprotein (P), matrix protein (M), surface glycoprotein (G), non-virion protein (NV) and RNA-dependent RNA polymerase (L). The cell lines and information of this thesis that can be used to address the general problem of VHSV IVB in walleye biology and management can be summarized by the following 4 points.

1. Twelve walleye cell lines have been developed, cryopreserved and shown to be susceptible to VHSV IVb, although viral susceptibility has been fully studied and presented in this thesis for only three, WE-cfin11f, WE-cfin11e, and WE-spleen6. Previous walleye cell lines that have been described in the literature appear to be lost or unavailable so this thesis has provided a cell line resource for studying walleye. The cell line, WE-spleen6, was particularly sensitive to VHSV IVb and should prove useful for detecting VHSV IVb in cell extracts.

2. For the first time, VHSV IVb infectious cycle has been studied at temperature extremes, 4 °C and 26 °C, as well as the optimal temperature 14 °C. At 26°C infection could possibly be initiated but not completed. At 4 °C, the VHSV IVb infectious cycle

could be initiated and slowly completed in the fibroblast cell line, WE-cfin11f, but in the epithelial cell line WE-cfin11e, infection could be initiated but not completed. This is the first hint that low temperature can alter the cellular tropism of a virus. The preferential replication of VHSV IVb in the fibroblasts might be away for the virus to overwinter in fish. Upon warming in spring, the virus would undergo vigorous replication and cause fish kills. Thus at low temperatures VHSV IVb would appear to 'hit and stay', whereas at 14 °C the virus would 'hit and run'. Thus if managers in charge of stocking walleye were worried about fish being infected with VHSV IVb, fish that had been held for a period at high temperatures (20 to 26°C) would appear to offer over wintering cold persistence.

3. A stromal cell line, WE-spleen6, has been established from the spleen, which is an organ that commonly shows pathological lesions during VHSV IVb infections of fish. The cell line is tentatively identified as being composed of fibroblastic reticular cells (FRCs). In vivo FRCs modulate the quality and intensity of immune responses. The greater susceptibility WE-spleen6 might reflect a cellular tropism that allows the virus to avoid the adaptive immune response of fish. Having this cell line should allow the study of stromal/immune cell interactions and how VHSV IVb modulates them.

4. With the stromal cell line, a potential antiviral therapeutic, the synthetic dsRNA, polyinosinic: polycytidylic acid (pIC), was shown to be effective at delaying the VHSV IVb infectious cycle. Although pIC induced the antiviral protein Mx in WE-spleen6, the precise mechanism behind the delay still needs investigation. Yet a unique observation was made. The pIC treatment caused the disappearance of the polymerase-associated phosphoprotein (P) at 2 days post infection. Such a focussed action of pIC on the rhabdovirus life cycle has not been observed previously, and this system could be an interesting one for dissecting novel actions of pIC on rhabdoviruses. With the demonstration of pIC inhibiting the VHSV IVb infectious cycle, pIC might be considered for further study in walleye. This could lead to an antiviral treatment for walleye aquaculture.

## **B. Contributions of the cell lines to comparative cellular biology and physiology**

Fundamentally the cells of vertebrates are expected to be very similar but in this thesis fish cell lines are found to behave in ways similar to mammalian cells but in other ways quite different. This is summarized in the following three points.

1. One of the first fish endothelial cell lines, WEBA, was established from the bulbus arteriosus of the walleye. The bulbus arteriosus is a dilated part of the aorta in front of the heart and modulates the pressure of blood being pumped to gills and rarely has been a source of cell lines. WEBA expressed many of the properties that are characteristic of mammalian cell lines that are described as endothelial. These include the ability to spontaneously form capillary-like structures and expression of von Willebrand factor (vWF). Additionally WEBA constitutively produced nitric oxide, the only fish cell line reported to do so to date. WEBA should be useful for investigating the cell biology of the fish cardiovascular system.

2. All fish cell lines lacked senescence-associated  $\beta$ -galactosidase (SA  $\beta$ -Gal) except for endothelial cell line, WEBA. The lack of SA  $\beta$ -Gal was true for cell lines from species that undergo rapid senescence, like Chinook salmon, and for cell lines from species that have gradual senescence, like zebrafish. These results suggest that repeated passaging does not lead fish cell lines to undergo cellular senescence. By contrast, even after 40 passages, most cells in the cultures of WEBA stained strongly for SA  $\beta$ -Gal. In this case SA  $\beta$ -Gal activity would appear to represent something unique to the cell line and be unrelated to senescence. For example the level of lysosomes in these cells might be higher than in the other cell lines. Overall the absence of cellular senescence in the fish cell lines might reflect the indeterminate growth of fish.

3. Immunocytochemical staining with a monoclonal antibody to acetylated  $\alpha$ -tubulin of the walleye cell lines together with many salmonid cell lines revealed several unprecedented observations about the distribution of this tubulin covalently modified on lysine at position 40. Firstly, primary cilia, which contain acetylated  $\alpha$ -tubulin, were demonstrated in seven of eight walleye cell lines but not in any of eleven salmonid cell

lines. This was the first demonstration of primary cilia on a large group of cell lines from several fish species and was expected because primary cilia are observed on each cell of most cell types in the vertebrate body. However, the absence of primary cilia on the cell lines from one group of fish was unanticipated and is an observation that should be followed up in future research. A second surprising observation was that weak, diffuse nuclear staining was seen in all the salmonid cell lines. Nuclear staining for acetylated  $\alpha$ -tubulin has not previously been observed in any cells of vertebrates. Finally in a few cell lines acetylated  $\alpha$ -tubulin was seen in a network of cytoplasmic fibres. This has been observed in mammalian cell lines but is not common.

## **Future Research Directions**

Cell lines are a resource for research into applied problems and into basic curiosity driven questions and in this thesis walleye cell lines have been developed and used for both. The discoveries of an applied nature were made on the interactions between walleye cells and the rhabdovirus, VHSV IVb, a pathogen of fish. Three discoveries of more fundamental interest were made on the walleye cardiovascular system, cellular senescence in fish, and a unique cellular localization in fish cells of a eukaryote structural protein, acetylated  $\alpha$ -tubulin. How these basic research discoveries can be applied to the virology of VHSV IVb would be an overarching direction for the future. Three specific examples of what might be explored are outlined below.

### **1. Explore possible antiviral roles for nitric oxide (NO) in vertebrates**

For the first time, the production of nitric oxide (NO) was demonstrated in a fish cell line, WEBA, from the bulbus arteriosus. The involvement of NO in the virus infections of mammals has been studied for over a decade (Akaike & Maeda, 2000) but much less is known about this topic in fish. Future research would involve using existing tools, such as drugs, but developing new ones such as antibodies and gene probes for the walleye genes for the enzymes involved in NO production. The existing tools would be NO donors, such as S-nitrosoglutathione (GSNO), and NO scavengers, such as N-acetyl-L-cysteine (NAC). The effect of these on the development of the VHSV IVb infectious cycle in WEBA and other walleye cell lines could be examined. The antibodies and gene probes could be used to determine in vitro and in vivo whether VHSV IVb modulates the expression of the enzymes in NO metabolism. The research could reveal whether localized levels of NO are a fundamental focus of struggle between host and virus.

### **2. Explore possible antiviral roles for cellular senescence in vertebrates**

In mammals cellular senescence recently has been considered an antiviral defense (Reddel, 2010), and although none of the fish cell lines of this thesis showed cellular senescence, they might be interesting tools to explore the importance of cellular senescence as an antiviral defense among vertebrates. Senescent cells can be defined as

irreversible non-dividing cells that cannot be triggered to divided even with mitogenic stimuli (Rodier & Campisi, 2011). For mammalian cell lines a wide variety of agents have been found to induce cellular senescence, including lipopolysaccharide and hydrogen peroxide (Ohtaini & Hara, 2013). Thus whether fish cell lines can be induce to senesce by applying a variety of treatments will be interesting to explore. If cellular senescence can be induced in the fish cell lines, then their ability to be infected with viruses, such as VHSV, can be compared with normal cultures to reveal possible protective effects of senescence.

### **3. Explore possible roles in acetylated $\alpha$ -tubulin in virus infections**

Inasmuch as some viruses have been shown to modulate the acetylation of microtubules and acetylated  $\alpha$ -tubulin appeared to participate in the intracellular transport of viral proteins (Husain & Harrod, 2011), the unique distribution of acetylated  $\alpha$ -tubulin in the fish cell lines of this thesis might make them generally useful for investigating the involvement of acetylated  $\alpha$ -tubulin in viral infections. VHSV IVb infection of cell lines with little cytoplasmic staining for acetylated  $\alpha$ -tubulin could be compared with those that have staining, and likewise those cell lines that have nuclear acetylated  $\alpha$ -tubulin versus those that do not could be compared. The endpoints to be examined would be changes in the amount and distribution of acetylated  $\alpha$ -tubulin in cells, the movement of viral proteins within the cells, and the production of virus. A particularly interesting situation to investigate would be low temperatures because acetylated  $\alpha$ -tubulin has been associated with microtubule stability and for mammals microtubules disassemble in low temperatures.

## REFERENCES

### Chapter 1 References

- Ades WE, Candal FJ, Swerlick RA, George VG, Summers S, Bosse DC, Lawley TJ (1992) HMEC-1: Establishment of an immortalized human microvascular endothelial cell line. *J Invest Dermatol* 99:683-690.
- Al-Hussinee L, Huber P, Russell S, LePage V, Reid A, Young KM, Nagy E, Stevenson RMW, Lumsden JS (2010) Viral haemorrhagic septicaemia virus IVb experimental infection of rainbow trout, *Oncorhynchus mykiss* (Walbaum), and fathead minnow, *Pimephales promelas* (Rafinesque). *J Fish Dis* 33:347-360.
- Alonso M, Kim CH, Johnson MC, Pressley M, Leong JA (2004) The NV gene of snakehead rhabdovirus (SHRV) is not required for pathogenesis, and a heterologous glycoprotein can be incorporated into the SHRV envelope. *J Virol* 78:5875-5882.
- Ammayappan A, Vakharia VN (2009) Molecular characterization of the Great Lakes viral hemorrhagic septicemia virus (VHSV) isolate from USA. *Virology* 6:171-187.
- Blecharz KG, Burek M, Bauersachs J, Thum T, Tsikas D, Widder J, Roewer J, Forster CY (2014) Inhibition of proteasome-mediated glucocorticoid receptor degradation restores nitric oxide bioavailability in myocardial endothelial cells in vitro. *Biol Cell* 106:219-235.
- Bols, NC, Dayeh VR, Lee LEJ, Schirmer K (2005) Use of fish cell lines in toxicology of fish. In: *Biochemistry and Molecular Biology of Fishes-Environmental Toxicology*. Vol. 6. Edited by T.W. Moon and T. P. Mommsen. Amsterdam: Elsevier Science. pp. 43-84.
- Bowser PR, Wooster GA, Earnest-Koons K (1997) Effects of fish age and challenge route in experimental transmission of walleye dermal sarcoma in walleyes by cell-free tumor filtrates. *J Aquat Anim Health* 9:274-278.
- Brudeseth BE, Raynard RS, King JA, Evensen O (2005) Sequential pathology after experimental infection with marine viral haemorrhagic septicemia virus isolates of low and high virulence in turbot, *Scophthalmus maximus* (L). *Vet Pathol* 42:9-18.

- Canadian Aquaculture Industry Alliance (2012). The Canadian aquaculture industry – A success story. <http://www.aquaculture.ca/files/CanAquacultureFacts-08.pdf>. Retrieved on July 6, 2014.
- Canada's Department of Fisheries and Oceans (2007) Survey of recreational angling in Canada, 2005. Ottawa: Economic Analysis and Statistics.
- Cines DB, Pollack ES, Buck CA, Loscalzo J, Zimmerman GA, McEver RP, Pober JS, Wick TM, Konkle BA, Schwartz BD, Barnathan ES, McCrae KR, Hug BA, Schmidt AM, Stern DM (1998) Endothelial cells in physiology and in the pathophysiology of vascular disorders. *Blood* 91:3527-3561.
- Clayton RD, Summerfelt RC (1996) Toxicity of hydrogen peroxide to fingerling walleyes. *J Appl Aquacult* 6:39-49.
- Cornwell ER, Bellmund CA, Groocock GH, Wong PT, Hambury KL, Getchell RG, Bowser PR (2013a). Fin and gill biopsies are effective nonlethal samples for detection of viral hemorrhagic septicemia virus genotype IVb. *J Vet. Diagn. Invest.* 25:203-209.
- Cornwell ER, Labuda SL, Groocock GH, Getchell RG, Bowser PR (2013b). Experimental infection of koi carp with viral hemorrhagic septicemia virus type IVb. *J Aquat Anim Health* 25:36-41.
- Debacq-Chainiaux F, Erusalimsky JD, Campisi J, Toussaint O (2009) Protocols to detect senescence-associated beta-galactosidase (SA-beta-gal) activity, a biomarker of senescent cells in culture and in vivo. *Nat Protoc* 4: 1798-1806.
- Desjardins F, Balligand JL (2006) Nitric oxide-dependent endothelial function and cardiovascular disease. *Acta Clinica Belgica* 61:326-334.
- Dimri GP, Lee X, Basile, G, Acosta M, Scott G, Roskelley C, Medrano EE, Linskens M, Rubelj I, Pereira-Smith O, Peacocke M, Campisi J (1995) A biomarker that identifies senescent human-cells in culture and in aging skin in vivo. *Proc Natl Acad Sci USA* 92:9363-9367.
- Einer-Jensen K, Ahrens P, Forsberg R, Lorenzen N (2004) Evolution of the fish rhabdovirus viral haemorrhagic septicaemia virus. *J Gen Virol* 85:1167-1179.
- Elsayed E, Faisal M, Thomas M, Whelan G, Batts W, Winton J (2006) Isolation of viral haemorrhagic septicaemia virus from muskellunge, *Esox masquinongy* (Mitchill), in

- Lake St Clair, Michigan, USA reveals a new sublineage of the North American genotype. *J Fish Dis* 29:611–619.
- Emmenegger EJ, Moon CH, Hershberger PK, Kurath G (2013) Virulence of viral hemorrhagic septicemia virus (VHSV) genotype Ia, IVa, IVb, and IVc in five fish species. *Dis Aquat Org* 107:99-111.
- Evensen O, Meier W, Wahli T, Olense NJ, Jorgensen PEV, Hastein T (1994) Comparison of immunohistochemistry and virus cultivation for detection of viral hemorrhagic septicemia virus in experimentally infected rainbow trout *Onchorhynchus mykiss*. *Dis Aquat Org* 20:101–109.
- Finke S, Conzelmann KK (2005) Replication strategies of rabies virus. *Virus Res* 111:120-131.
- Fisheries and Ocean Canada (FOC) (2008). Aquaculture in Canada. <http://www.dfo-mpo.gc.ca/aquaculture/ref/aqua-can2008-eng.pdf>. Retrieved on July 6, 2014.
- Gagné N, Mackinnon AM, Boston L, Souter B, Cook-Versloot M, Griffiths S, Olivier G (2007) Isolation of viral haemorrhagic septicaemia virus from mummichog, stickleback, striped bass and brown trout in eastern Canada. *J Fish Dis* 30:213-223.
- Graf M, Hartmann N, Reichwald K, Englert C (2013) Absence of replicative senescence in cultured cells from the short-lived killifish *Nothobranchius furzeri*. *Exp Gerontol* 48:17-28.
- Grice J (2012) Pathogenicity of viral hemorrhagic septicemia virus IV in walleye (*Sander vitreus*). MSc Thesis. University of Guelph.
- Grice J, Reid A, Peterson A, Blackburn K, Tubbs L, Huber LS, Dixon B, Bols NC, Lumsden JS (2014) Walleye (*Sander vitreus* Mitchill) are relatively resistant to experimental infections with viral hemorrhagic septicaemia virus IVb. *J Fish Dis* (In Press).
- Guemez-Gamboa A, Coufal NG, Gleeson JG (2014) Primary cilia in the developing and mature brain. *Neuron* 82:511-521.
- Hamlin A, Harford CG (1952) Effect of influenza virus on cilia and epithelial cells in the bronchi of mice. *J Exp Med* 95: 173-189.

- Harmache A, LeBerre M, Droineau S, Giovannini M, Brémont M (2006). Bioluminescence Imaging of Live Infected Salmonids Reveals that the Fin Bases Are the Major Portal of Entry for *Novirhabdovirus*. *J Virol* 80:3655-3659.
- Hayflick L (1965) The limited in vitro lifetime of human diploid cell strains. *Exp Cell Res* 47: 614-636.
- Heppell J, Lorenzen N, Armstrong NK, Wu T, Lorenzen E, Einer-Jensen K, Schorr J, Davis HL (1997) Development of DNA vaccines for fish: vector design, intramuscular injection and antigen expression using viral haemorrhagic septicaemia virus genes as model. *Fish Shellfish Immunol* 8:271-286.
- Hope KM, Bowser PR, Casey JW (2009) A Zebrafish Model To Investigate the Pathogenicity and Persistence of Viral Hemorrhagic Septicemia Virus IVb. *Aquaculture America*, Seattle, Washington.
- Hope KM, Casey RN, Groocock GH, Getchell RG, Bowser PR, Casey JW (2010). Comparison of quantitative RT-PCR with cell culture to detect viral hemorrhagic septicemia virus (VHSV) IVb infections in the Great Lakes. *J Aquat Anim Health* 22:50-61.
- Husain M, Harrod KS (2011) Enhanced acetylation of alpha-tubulin in influenza A virus infected epithelial cells. *FEBS Lett* 585: 128-132.
- Ito T, Olesen NJ (2013) Susceptibility of various Japanese freshwater fish species to an isolate of viral haemorrhagic septicaemia virus (VHSV) genotype IVb. *Dis Aquat Org* 107:1-8.
- Jayakar HR, Jeetendra E, Whitt MA (2004) Rhabdovirus assembly and budding. *Virus Res* 106:117-132.
- Kassis R, Larrous F, Estaquier J, Bourhy H (2004) Lyssavirus matrix protein induces apoptosis by a TRAIL-dependent mechanism involving caspase-8 activation. *J Virol* 78:6543-6555.
- Kelly RK, Miller HR, Nielsen O, Clayton JW (1980) Fish cell culture: characteristics of a continuous fibroblastic cell line from Walleye (*Stizostedion vitreum vitreum*). *Can J Fish Aquat Sci* 37:1070–1075.

- Kelly RK, Nielsen O, Mitchell SC, Yamamoto T (1983) Characterization of Herpes virus vitreum isolated from hyperplastic epidermal tissue of walleye, *Stizostedion vitreum vitreum* (Mitchill). *J Fish Dis* 6:249-260.
- Kim R, Faisal M (2010a) Comparative susceptibility of representative Great Lakes fish species to the North American viral hemorrhagic septicemia virus Sublineage IVb. *Dis Aquat Organ* 91:23-34.
- Kim R, Faisal M (2010b) Experimental studies confirm the wide host range of the Great Lakes viral haemorrhagic septicaemia virus genotype IVb. *J Fish Dis* 33:83-88.
- Kim RK, Faisal M (2010c) The Laurentian Great Lakes strain (MI03) of the viral haemorrhagic septicaemia virus is highly pathogenic for juvenile muskellunge, *Esox masquinongy* (Mitchill). *J Fish Dis* 33:513-527.
- Kerr SJ (2008) A survey of walleye stocking activities in North America. Fish and Wildlife Branch. Ontario Ministry of Natural Resources. Peterborough, Ontario.
- Kopecky SA, Lyles DS (2003) Contrasting the effects of matrix protein on apoptosis in HeLa and BHK cells infected with vesicular stomatitis virus are due to inhibition of host gene expression. *J Virol* 77:4658-4669.
- Kurath G, Emmenegger E, Moon CH (2009) Susceptibility of Pacific salmonids, yellow perch, and koi to viral hemorrhagic septicemia virus strains from the Great Lakes, Pacific and Atlantic coasts of Canada, and Europe. *Aquaculture America*, Seattle, Washington.
- Kuzmin IV, Novella IS, Dietzgen RG, Padhi A, Rupprecht CE (2009) The rhabdoviruses: Biodiversity, phylogenetics, and evolution. *Infect Genet Evol* 9:541-553.
- Lee BY, Han JA, Im JS, Morrone A, Johung K, Goodwin ED, Kleijer WJ, DiMaio D, Hwang ES (2006) Senescence-associated  $\beta$ -galactosidase is lysosomal  $\beta$ -galactosidase. *Aging Cell* 5:187-195.
- Licata JM, Harty RN (2003) Rhabdoviruses and apoptosis. *Int Rev Immunol* 22:451-476.
- Lumsden JS, Morrison B, Yason C, Russell S, Young K, Yazdanpanah A, Huber P, Al-Hussinee L, Stone D, Way K (2007) Mortality event in freshwater drum *Aplodinotus grunniens* from Lake Ontario, Canada, associated with viral haemorrhagic septicemia virus, type IV. *Dis Aquat Org* 76:99-111.

- Madison BN, Wang YS (2006) Haematological responses of acute nitrite exposure in walleye (*Sander vitreus*). *Aquat Toxicol* 79:16–23.
- Ohtani N, Hara E (2013) Roles and mechanisms of cellular senescence. *Cancer Sci* 104:525-530.
- Olson W, Emmenegger E, Glenn J, Simchick C, Winton J, Goetz F (2013) Expression kinetics of key genes in the early innate immune response to Great Lakes viral hemorrhagic septicemia virus IVb infection in yellow perch (*Perca flavescens*). *Dev Comp Immunol* 41:11-19.
- Phillips TA, Summerfelt RC, Wu J, Laird DA (2003) Toxicity of chlorpyrifos adsorbed on humic colloids to larval walleye (*Stizostedion vitreum*). *Arch Environ Contam Toxicol* 45:258-263.
- Piperno G, LeDizet M, Chang X-J (1987) Microtubules containing acetylated  $\alpha$ -tubulin in mammalian cells in culture. *J Cell Biol* 104:289-302.
- Reddel RR (2010) Senescence: an antiviral defense that is tumor suppressive? *Carcinogenesis* 31:19-26.
- Rodier F, Campisi J (2011) Four faces of cellular senescence. *J Cell Biol* 192:547-556.
- Rovnak J, Casey RN, Brewster CD, Casey JW, Quackenbush SL (2007) Establishment of productively infected walleye dermal sarcoma explant cells. *J Gen Virol* 88:2583–2589.
- Sadoul K, Wang J, Diagouraga B, Khochbin S (2011) The tale of protein lysine acetylation in the cytoplasm. *J Biomed Biotech* 2011:970382.
- Satir P, Pedersen LB, Christensen ST (2010) The primary cilium at a glance. *J Cell Sci* 123:499-503.
- Severino J, Allen RG, Balin S, Balin A, Christofalo VJ (2000) Is beta-galactosidase staining a marker of senescence in vitro and in vivo? *Exp Cell Res* 257:162-172.
- Scott WB, Crossman EJ (1973) *Freshwater Fishes of Canada*. Bulletin 184, Fisheries Research Board of Canada, Ottawa.
- Srikiatkachorn A, Spiropoulou CF (2014) Vascular events in viral hemorrhagic fevers: a comparative study of dengue and hantaviruses. *Cell Tissue Res* 355:621-633.
- Summerfelt RC (2000) A white paper on the status and needs of walleye aquaculture in the North Central region. North Central Regional Aquaculture Center.

<http://aquanic.org/species/walleye/documents/walleyeaquacultureNCRAC.pdf>.

Retrieved on October 13, 2010)

- Summerfelt RC (2006) Intensive culture of walleye. Pages 173-182 in Proceedings of the Canadian Freshwater Aquaculture Symposium - Aquaculture Canada 2004. Aquaculture Association of Canada Special Publication No. 11.
- Summerfelt RC, Clayton RD, Johnson JA, Kinnunen RE (2010) Production of walleye as a food fish. North Central Regional Aquaculture Center, Fact Sheet No. 116.
- Sutherland DR, Cooper S, Stelzig P, Marcquenski S, Marcino J, Lom J, Dyková I, Nilsen F, Hsu H-M, Jahns W, Hoyle J, Penney R (2004) *Heterosporis* sp. (Microspora): a new parasite from yellow perch (*Perca flavescens*) and walleye (*Stizostedion vitreum*) in Minnesota, Wisconsin and Lake Ontario, North America. 13<sup>th</sup> International Conference on Aquatic Invasive Species, Ennis, County Clare, Ireland.
- Takahashi K, Sawasaki Y, Hata JI, Mukai K, Goto T (1990) Spontaneous transformation and immortalization of human endothelial cells. *In Vitro Cell Dev Biol* 25:265-274.
- Thoulouze MI, Bouguyon E, Carpentier C, Bremont M (2004) Essential role of the NV protein of Novirhabdovirus for pathogenicity in rainbow trout. *J Virol* 78:4098-4107.
- Tordo N, Benmansour A, Calisher C, Dietzgen RG, Fang RX, Jackson AO, Kurath G, Nadin-Davis S, Tesh RB, Walker P (2004). Family Rhabdoviridae. In The eighth report of the international committee for taxonomy of viruses Academic Press, San Diego.
- Tort MJ, Pasnik DJ, Fernandez-Cobas C, Wooster GA, Bowser PR (2002). Quantitative Scoring of Gill Pathology of Walleyes Exposed to Hydrogen Peroxide. *J Aquat Anim Health* 14:154–159.
- Unger RE, Krump-Konvalinkova V, Peters K, Kirkpatrick CJ (2002) In vitro expression of the endothelial phenotype: comparative study of primary isolated cells and cell lines, the novel cell line HPMEC-ST1.6R. *Micro Res* 64:384-397.
- U.S. Office of the Federal Register (2008) Federal order: viral hemorrhagic septicemia (VHS) interim rule 9. Code of Federal Regulations, Parts 83.1–83.7, 93.900, and 93.910–93.916. U.S. Government Printing Office, Washington, D.C.

- Wagner DD, Olmsted JB, Marder VJ (1982) Immunolocalization of von Willebrand protein in Weibel-Palade bodies of human endothelial cells. *J Cell Biol* 95:355-360.
- Weeks C, Kim R, Wolgamot M, Whelan G, Faisal M (2011) Experimental infection studies demonstrate the high susceptibility of the salmonid, lake herring, *Coregonus artedii* (Le Sueur), to the Great Lakes strain of viral haemorrhagic septicaemia virus (genotype IVb). *J Fish Dis* 34:887-891.
- Western Fisheries Research Center (WFRC), U.S. Department of the Interior, U.S. Geological Survey (2008). Molecular epidemiology of viral hemorrhagic septicemia virus in the Great Lakes region. <http://wfrc.usgs.gov/products/fs20083003.pdf>. Retrieved on December 29, 2010.
- Wilensky CS, Bowser PR (2005). Growth characteristics of the WF2 cell cultures. *J World Aquacult Soc* 36:538-541.
- Wolf K, Quimby MC (1962). Established eurythermic line of fish cells in vitro. *Science* 135:1065-1066.
- Wolf K, Mann JA (1980) Poikilotherm vertebrate cell lines and viruses: a current listing for fishes. *In vitro* 16:168-179.
- Wolf K (1988) Fish viruses and fish viral diseases. Cornell University Press.
- Yosef N, Ubogu EE (2013) An immortalized human blood-nerve barrier endothelial cell line for in vitro permeability studies. *Cell Mol Neurobiol* 33:75-186.
- Zhang Z, Martineau D (1999) Walleye dermal sarcoma virus: OrfA N-terminal end inhibits the activity of a reporter gene directed by eukaryotic promoters and has a negative effect on the growth of fish and mammalian cells. *J Virol* 73:8884-8889.
- Zhong M, Zheng K, Chen M, Xiang Y, Jin F, Ma K, Qiu X, Wang Q, Peng T, Kitazato K, Wang Y (2014) Heat-shock protein 90 promotes nuclear transport of herpes simplex virus 1 capsid protein by interacting with acetylated tubulin. *PLoS ONE* 9 (6):e99425.

## Chapter 2 References

- Al-Hussinee L, Huber P, Russell S, LePage V, Reid A, Young KM, Nagy E, Stevenson RMW, Lumsden JS (2010) Viral haemorrhagic septicaemia virus IVb experimental infection of rainbow trout, *Oncorhynchus mykiss* (Walbaum), and fathead minnow, *Pimephales promelas* (Rafinesque). *J Fish Dis* 33:347-360.
- Al-Hussinee L, Lord S, Stevenson RMW, Casey RN, Groocock GH, Britt KL, Kohler KH, Wooster GA, Getchell RG, Bowser PR, Lumsden JS (2011) Immunohistochemistry and pathology of multiple Great Lakes fish from mortality events associated with viral hemorrhagic septicemia virus type IVb. *Dis Aquat Org* 93:117-127.
- Alvarez-Torres D, Garcia-Rosado E, Fernandez-Trujillo MA, Bejar J, Alvarez MC, Borrego JJ, Alonso MC (2013) Antiviral specificity of the *Solea senegalensis* Mx protein constitutively expressed in CHSE-214. *Marine Biotechnol* 15:125-132.
- Araki N, Wada Y, Yamaguchi M, Hasobe M, Nakano H (1994) A fish cell-line CHSE-SP exposed to long-term cold temperature retains viability and ability to support viral replication. *In Vitro Cell Dev Biol - Anim* 30:148-150.
- Avunje S, Oh MJ, Jung SJ (2013) Impaired TLR2 and TLR7 response in olive flounder infected with viral haemorrhagic septicaemia virus at host susceptible 15 °C but high at non-susceptible 20 °C. *Fish Shellfish Immunol* 34:1236-1243.
- Beitinger TL, Bennett WA, McCauley RW (2000) Temperature tolerances of North American freshwater fishes exposed to dynamic changes in temperature. *Environ Biol Fishes* 58:237-275.
- Björklund HV, Johansson TR, Rinne A (1997) Rhabdovirus-induced apoptosis in a fish cell line is inhibited by a human endogenous acid cysteine proteinase inhibitor. *J Virol* 71:5658-5662.
- Bols NC, Dayeh VR, Lee LEJ, Schirmer K (2005) Use of fish cell lines in toxicology of fish. In: *Biochemistry and Molecular Biology of Fishes-Environmental Toxicology*. Vol. 6. Edited by T.W. Moon and T. P. Mommsen. Amsterdam: Elsevier Science. pp. 43-84.

- Bols NC, Lee LEJ (1994) Cell lines: availability, propagation and isolation. In: Hochachka P.W.; Mommsen T.P. (eds) *Biochemistry and molecular biology of fishes*. vol. 3. Elsevier Science, Amsterdam, pp 145-149.
- Bols NC, Mosser DD, Steels GB (1992) Temperature studies and recent advances with fish cells in vitro. *Comp Biochem Physiol* 103A:1-14.
- Brubacher JL, Secombes CJ, Zou L, Bols NC (2000) Constitutive and LPS-induced gene expression in a macrophage-like cell line from the rainbow trout (*Oncorhynchus mykiss*). *Dev Comp Immunol* 24:565-574.
- Cain KD, Byrne KM, Brassfield AL, LaPatra SE, Ristow SS (1999) Temperature dependent characteristics of a recombinant infectious hematopoietic necrosis virus glycoprotein produced in insect cells. *Dis Aquat Organ* 36:1-10.
- Colby PJ, McNicol RE, Ryder RA (1979) Synopsis of biological data on the walleye. Fisheries Synopsis No. 119, Food and Agriculture Organization, Rome, Italy. 139 p.
- Cooper JK, Sykes G, King S, Cottrill K, Ivanova NV, Hanner R, Ikonomi P (2007) Species identification in cell culture: a two-pronged molecular approach. *In Vitro Cell Dev Biol - Anim* 43:344-351.
- Dayeh VR, Bols NC, Tanneberger K, Schirmer K, Lee LEJ (2013) The use of fish-derived cell lines for investigation of environmental contaminants: an update following OECD's fish toxicity testing Framework No. 171. *Current Protocols Toxicol* 1.5.1-1.5.20.
- Dayeh VR, Bols NC, Schirmer K, Lee LEJ (2003) The use of fish-derived cell lines for investigation of environmental contaminants. *Current Protocols Toxicol* 1.5.1-1.5.17.
- DeWitte-Orr SJ, Leong JA, Bols NC (2007) Induction of antiviral genes, Mx and vig-1, by dsRNA and Chum salmon reovirus in rainbow trout monocyte/macrophage and fibroblast cell lines. *Fish Shellfish Immunol* 23:670-82.
- Eckerlin GE, Farrell JM, Casey RN, Hope KM, Grooncock GH, Bowser PR, Casey J (2011) Temporal variation in prevalence of viral hemorrhagic septicaemia virus type IVb among upper St Lawrence River smallmouth bass. *Trans Am Fish Soc* 140:529-536.

- Fenton R, Mathias JA, Moodie GEE (1996) Recent and future demand for Walleye in North America. *Fisheries* 21:6-12.
- Goodwin AE, Merry GE (2011) Mortality and carrier status of bluegills exposed to viral hemorrhagic septicaemia virus genotype IVb at different temperatures. *J Aquat Anim Health* 23:85-91.
- Goodwin AE, Merry GE, Noyes AD (2012) Persistence of viral RNA in fish infected with VHSV-IVb at 15 °C and then moved to warmer temperatures after the onset of disease. *J Fish Dis* 35:523-528.
- Graf M, Hartmann N, Reichwald K, Englert C (2013) Absence of replicative senescence in cultured cells from the short-lived killfish *Nothobranchius furzeri*. *Exp Gerontol* 48:17-28.
- Hawley L, Garver K (2008) Stability of viral hemorrhagic septicemia virus (VHSV) in freshwater and seawater at various temperatures. *Dis Aquat Organ* 82:171-178.
- Hokanson KEF (1977) Temperature requirements of some percids and adaptations to seasonal temperature cycle. *J Fisher Res Board Can* 34:1524-1550.
- Ivanova NV, Zemplak TS, Hanner RH, Hebert PDN (2007) Universal primer cocktails for fish DNA barcoding. *Mol Ecol Notes* 7:544–548.
- Kawano A, Haiduk C, Schirmer K, Hanner R, Lee LEJ, Dixon B, Bols NC (2010) Development of a rainbow trout intestinal epithelial cell line and its response to lipopolysaccharide. *Aquacult Nutr* 17:e241-e252.
- Kelly RK, Miller HR, Nielsen O, Clayton JW (1980) Fish cell culture: characteristics of a continuous fibroblastic cell line from walleye (*Stizostedion vitreum vitreum*). *Can J Fisher Aquat Sci* 37:1070-1075.
- Kelly RK, Nielsen O, Mitchell SC (1983) Characterization of *Herpesvirus vitreum* isolated from hyperplastic epidermal tissue of walleye, *Stizostedion vitreum vitreum* (Mitchill). *J Fish Dis* 6:249-260.
- Kerr SJ, Corbett BW, Hutchinson NJ, Kinsman D, Leach JH, Puddister D, Standfield L, Ward N (1997) Walleye habitat: A synthesis of current knowledge with guidelines for conservation. Percid Community Synthesis, Walleye Habitat Working Group, Ontario Ministry of Natural Resources, Peterborough, Ontario. 98 p.

- Kim R, Faisal M (2011) Emergence and resurgence of the viral hemorrhagic septicaemia virus (*Novirhabdovirus*, *Rhabdoviridae*, *Mononegavirales*). *J Adv Res* 2:9-23.
- de Kinkelin P, Bearzotti-Le Berre M, Bernard J (1980) Viral hemorrhagic septicaemia of rainbow trout: selection of a thermoresistant virus variant and comparison of polypeptide synthesis with the wild-type virus strain. *J Virol* 36:652-658.
- Lorenzen N, Olesen NJ, Jorgensen PE. (1988) Production and characterization of monoclonal antibodies to four Egtved virus structural proteins. *Dis Aquat Org* 4:35–42.
- Lumsden JS, Morrison B, Yason C, Russell S, Young K, Yazdanpanah A, Huber P, Al-Hussinee L, Stone D, Way K (2007) Mortality event in freshwater drum *Aplodinotus grunniens* from Lake Ontario, Canada, associated with viral haemorrhagic septicemia virus, Type IV. *Dis Aquat Org* 76:99-111.
- McAllister PE, Wagner RR (1977) Virion RNA polymerases of two salmonid rhabdoviruses. *J Virol* 22:839-843.
- Mosser DD, Heikkila JJ, Bols NC (1986) Temperature ranges over which rainbow trout fibroblasts survive and synthesize heat-shock proteins. *J Cell Physiol* 128:432-440.
- Pham PH, Jung J, Bols NC (2011) Using 96-well tissue culture polystyrene plates and fluorescence plate reader as tools to study the survival and inactivation of viruses on surfaces. *Cytotechnology* 63:385-397.
- Pham PH, Lumsden JS, Tafalla C, Dixon B, Bols NC (2013) Differential effects of viral hemorrhagic septicemia virus (VHSV) genotypes IVa and IVb on gill epithelial and spleen macrophage cell lines from rainbow trout (*Onchorhynchus mykiss*). *Fish Shellfish Immunol* 34:632-640.
- Purcell MK, Laing KJ & Winton JR (2012) Immunity to fish rhabdoviruses. *Viruses* 4:140-166.
- Ratnasingham S, Hebert PDN (2007) BOLD, the Barcode of Life Data System (<http://www.barcodinglife.org>). *Mol Ecol Notes* 7:355–364.
- Sansom B, Vo NTK, Kavanagh R, Hanner R, MacKinnon M, Dixon DG, Lee LEJ (2013) Rapid assessment of the toxicity of oil sands process-affected waters using fish cell lines. *In Vitro Cell Dev Biol – Anim* 49:52-65.

- Shimizu A, Nakatani Y, Nakamura T, Jinno-Oue A, Ishikawa O, Boeke JD, Takeuchi Y, Hoshino H (2014) Characterization of cytoplasmic DNA complementary to non-retroviral RNA viruses in human cells. *Sci. Rep.* 4:5074.
- Summerfelt R.C. (2005) The culture of walleye. In *Aquaculture in the 21<sup>st</sup> Century* (Ed: Kelly A, Silverstein J), American Fisheries Society.
- Tafalla C, Sanchez E, Lorenzen N, DeWitte-Orr SJ, Bols NC (2008) Effects of viral hemorrhagic septicemia virus (VHSV) on the rainbow trout (*Oncorhynchus mykiss*) monocyte cell line RTS-11. *Mol Immunol* 45:1439-1448.
- VHSV Expert Panel and Working Group (2010) Viral hemorrhagic septicaemia virus (VHSV IVb) risk factors and association measures derived by expert panel. *Prev Vet Med* 94:128-139.
- Villena AJ (2003) Applications and needs of fish and shellfish cell culture for disease control in aquaculture. *Rev Fish Biol Fisher* 13:111-140.
- Ward RD, Hanner R, Herbert PDN (2009) The campaign to DNA barcode all fishes, FISH-BIOL. *J Fish Biol* 74:329-356.
- Wilensky CS, Bowser PR (2005) Growth characteristics of the WF2 cell cultures. *J World Aquacult Soc* 36:538-541.
- Wilson SM, Nagler JJ (2006) Age, but not salinity, affects the upper lethal temperature limits for juvenile walleye (*Sander vitreus*). *Aquaculture* 257:187-193.
- Winton J, Batts W, deKinkelin P, LeBerre M, Bremont M, Fijan N (2010) Current lineages of the Epithelioma papulosum cyprini (EPC) cell line are contaminated with fathead minnow, *Pimephales promelas*, cells. *J Fish Dis* 33:701-704.
- Winton J, Kurath G, Batts W (2007) Detection of viral hemorrhagic septicemia virus. US Geological Survey, Fact Sheet 2007-3055. Available: [biology.usgs.gov/documents/USGS\\_Fact-Sheet-1-on-VHS.pdf](http://biology.usgs.gov/documents/USGS_Fact-Sheet-1-on-VHS.pdf). (March 2011).
- Wisner DA, Christie AE (1987) Temperature Relationships of Great Lakes Fishes: A Data Compilation. Great Lakes Fisheries Commission Special Publication 87-3. 165 p.
- Wolf K, Mann JA (1980) Poikilotherm vertebrate cell lines and viruses: a current listing for fishes. *In Vitro* 16:168-179.

### Chapter 3 References

- Albertini AAV, Baquero E, Ferlin A, Gaudin Y (2012) Molecular and cellular aspects of rhabdovirus entry. *Viruses* 4:117-139.
- Bauer H, Zweimueller-Mayer J, Steinbacher P, Lamestchwandtner A, Bauer HC (2010) The dual role of zonula occludens (ZO) proteins. *J Biomed Biotechnol* 402593:1-11.
- Bearzotti M, Delmas B, Lamoureux A, Loustau AM, Chilmonczyk S, Bremont M (1999) Fish rhabdovirus cell entry is mediated by fibronectin. *J Virol* 73:7703-7709.
- Becerra J, Montes GS, Bexiga SRR, Junqueira LCU (1983) Structure of the tail fin in teleosts. *Cell Tissue Res* 230:127-137.
- Benezra M, Greenberg RS, Masur SK (2007) Localization of ZO-1 in the nucleolus of corneal fibroblasts. *Ophthalmol Vis Sci* 48:2043-2049.
- Caipang CMA, Hirono I, Aoki T (2003) In vitro inhibition of fish rhabdoviruses by Japanese flounder, *Paralichthys olivaceus* Mx. *Virology* 317:373-382.
- Chan D, Lamande SR, Cole WG, Bateman JF (1990) Regulation of procollagen synthesis and processing during ascorbate-induced extracellular matrix accumulation in vitro. *Biochem J* 269:175-181.
- Cornwell ER, Bellmund CA, Grocock GH, Wong PT, Hambury KL, Getchell RG, Bowser PR (2013) Fin and gill biopsies are effective nonlethal samples for detection of viral hemorrhagic septicaemia virus genotype IVb. *J Vet Dis INv* 25:203-209.
- Curtis TM, Howard A, Gerlach B, Brennan LM, Widder MW, van der Schalie WH, Vo NTK, Bols NC (2013) Suitability of invertebrate and vertebrate cells in a portable impedance-based toxicity sensor : temperature mediated impacts on long-term survival. *Toxicol In Vitro* 27:2061-2066.
- Dorson M, Torhy C (1993) Viral haemorrhagic septicaemia virus replication in external tissue excised from rainbow trout, *Oncorhynchus mykiss* (Walbaum), and hybrids of different susceptibilities. *J Fish Dis* 16:403-408.
- Dzamba BJ, Wu H, Jaenisch R, Peters DM (1993) Fibronectin binding sites in type I collagen regulates fibronectin fibril formation. *J Cell Biol* 121:1165-1172.

- Ellencrona K, Syed A, Johansson M (2009) Flavivirus NS associates with host-cell proteins zonula occludens-1 (ZO)-1 and regulating synaptic membrane exocytosis-2 (RIMS2) via an internal PDZ binding mechanism. *Biol Chem* 390:390-323.
- Fenton R., Mathias J.A. & Moodie G.E.E. (1996) Recent and future demand for Walleye in North America. *Fisheries* 21:6-12.
- Garcia DM, Bauer H, Dietz T, Schubert T, Markl J, Schaffeld M (2005) Identification of keratins and analysis of their expression in carp and goldfish: comparison with the zebrafish and trout keratin catalog. *Cell Tissue Res* 322:245-256.
- Gignac SJ, Vo NTK, Mikhaeil MS, Alexander JAN, MacLatchy DL, Schulte PM, Lee LEJ (2014) Derivation of a continuous myogenic cell culture from embryos of common killifish, *Fundulus heteroclitus*. *Comp Biochem Physiol Part A* 175:15-27.
- Goodwin AE, Merry GE (2011) Mortality and carrier status of bluegills exposed to viral hemorrhagic septicaemia virus genotype IVb at different temperatures. *J Aquat Anim Health* 23:85-91.
- Grice J, Reid A, Peterson A, Blackburn K, Tubbs L, Huber LS, Dixon B, Bols NC, Lumsden JS (2014) Walleye (*Sander vitreus* Mitchill) are relatively resistant to experimental infections with viral hemorrhagic septicaemia virus IVb. *J Fish Dis* (in press).
- Harmache A, LeBerge M, Droineau S, Giovannini M, Bremont M (2006) Bioluminescence imaging of live infected salmonids reveals that fin bases are the major portal of entry for Novirhabdovirus. *J Virol* 80:3655-3659.
- Higaki S, Koyama Y, Shirai E, Yokota T, Fujioka Y, Sakai N, Takada T (2013) Establishment of testicular and ovarian cell lines from Honmoroko (*Gnathopogon caeruleus*). *Fish Physiol Biochem* 39:701-711.
- Jensen PKA, Therkelsen AJ (1981) Cultivation at low temperature as a measure to prevent contamination with fibroblasts in epithelial cultures from human skin. *J Invest Derm* 77:210-212.
- Krenning G, Zeisberg EM, Kalluri R (2010) The origin of fibroblasts and mechanisms of cardiac fibrosis. *J Cell Physiol* 225:631-637.
- Lal-Nag M, Morin PJ (2009) The claudins. *Genome Biology* 10 (8):235.

- Lee LEJ, Caldwell SJ, Gibbons J (1997) Development of a cell line from skin of goldfish, *Carassius auratus*, and effects of ascorbic acid on collagen deposition. *Histochem J* 29:31-43.
- Lovy J, Lewis NL, Hershberger PK, Bennett W, Meyers TR, Garver KA (2012) Viral tropism and pathology associated with viral hemorrhagic septicaemia in larval and juvenile Pacific herring. *Vet Microbiol* 161:66-76.
- Lumsden JS, Morrison B, Yason C, Russell S, Young K, Yazdanpanah A, Huber P, Al-Hussinee L, Stone D, Way K (2007) Mortality event in freshwater drum *Aplodinotus grunniens* from Lake Ontario, Canada, associated with viral haemorrhagic septicemia virus, Type IV. *Dis Aquat Org* 76:99-111.
- Mas V, Rocha A, Perez L, Coll JM, Estepa A (2004) Reversible inhibition of spreading of in vitro infection and imbalance of viral protein accumulation at low pH in viral hemorrhagic septicaemia Rhabdovirus, a Salmonid Rhabdovirus. *J Virol* 78:1936-1944.
- Mauger PE, Labbe C, Bobe J, Cauty C, Leguen I, Baffet G, Le Bail PY (2009) Characterization of goldfish fin cells in culture: some evidence of an epithelial cell profile. *Comp Biochem Physiol Part B* 152:205-215.
- Montero J, Garcia J, Ordas MC, Casanova I, Gonzalez A, Villena A, Coll J, Tafalla C (2011). Specific regulation of the chemokine response to viral hemorrhagic septicemia virus at the entry site. *J Virol* 85:4046-4056.
- Quillet E, Dorson M, Aubard G, Torhy C (2001) In vitro viral haemorrhagic septicaemia virus replication in excised fins of rainbow trout: correlation with resistance to waterborne challenge and genetic variation. *Dis Aquatic Org* 45:171-182.
- Pham PH, Jung J, Bols NC (2011) Using 96-well tissue culture polystyrene plates and fluorescence plate reader as tools to study the survival and inactivation of viruses on surfaces. *Cytotechnology* 63:385-397.
- Pham PH, Lumsden JS, Tafalla C, Dixon B, Bols NC (2013) Differential effects of viral hemorrhagic septicemia virus (VHSV) genotypes IVa and IVb on gill epithelial and spleen macrophage cell lines from rainbow trout (*Oncorhynchus mykiss*). *Fish Shellfish Immunol* 34:632-640.

- Trobridge GD, Chiou PP and Leong JC (1997) Cloning of the Rainbow Trout (*Oncorhynchus mykiss*) Mx2 and Mx3 cDNAs and characterization of trout Mx protein expression in Salmon cells. *J Virol* 71:5304-5311.
- Vo NTK, Bender AW, Lee LEJ, Lumsden JS, Lorenzen N, Dixon B, Bols NC (2014) Development of a walleye cell line and use to study the effects of temperature on infection by viral haemorrhagic septicemia virus group IVb. *J Fish Dis* (In Press)
- Wilkins C, Woodward J, Lau DTY, Barnes A, Joyce M, McFarlane N, McKeating JA, Tyrrell DL, Gale M (2013) IFITM1 is a tight junction protein that inhibits Hepatitis C virus entry. *Hepatology* 57:461-469.
- Wilkins C, Woodward J, Lau DTY, Barnes A, Joyce M, McFarlane N, McKeating JA, Tyrell JA, Tyrrell DL, Gale M (2013). IFITMI is a tight junction protein that inhibits hepatitis C virus entry. *Hepatology* 57:461-469.
- Winton J, Kurath G, Batts W (2007) Detection of viral hemorrhagic septicemia virus. US Geological Survey, Fact Shee 2007-3055. Available: [biology.usgs.gov/documents/USGS\\_Fact-Sheet-1-on-VHS.pdf](http://biology.usgs.gov/documents/USGS_Fact-Sheet-1-on-VHS.pdf). (March 2011).
- Winton J, Batts W, deKinkelin P, LeBerre M, Bremont M, Fijan N (2010) Current lineages of the Epithelioma papulosum cyprini (EPC) cell line are contaminated with fathead minnow, *Pimephales promelas*, cells. *J Fish Dis* 33:701-4.

## Chapter 4 References

- Alvarenga HG, Marti L (2014) Multifunctional roles of reticular fibroblastic cells: more than meets the eye? *J Immunol Res* 2014:402038.
- Balogh P, Fisi V, Szakal AK (2008) Fibroblastic reticular cells of the peripheral lymphoid organs: unique features of a ubiquitous cell type. *Mol Immunol* 46:1-7.
- Bergan V, Robertsen B (2004) Characterization of Atlantic halibut (*Hippoglossus hippoglossus*) Mx protein expression. *Dev Comp Immunol* 28:1037-1047.
- Bouis D, Hospers GAP, Meijer C, Molema G, Mulder NH (2001) Endothelium in vitro: a review of human vascular endothelial cell lines for blood vessel-related research. *Angiogenesis* 4:91-102.
- Briard D, Azzarone B, Brouty-Boye D (2005) Importance of stromal determinants in the generation of dendritic and natural killer cells in the human spleen. *Clin Exp Immunol* 140:265-273.
- Brouland JG, Gilbert M, Bonneau M, Pignaud G, Solier CBD, Droulet L (1999) Macro and microheterogeneity in normal endothelial cells: differential composition of luminal glycocalyx and functional implications. *Endothelium* 6:251-262.
- Caipang CMA, Hirono I, Aoki T (2003) In vitro inhibition of fish rhabdoviruses by Japanese flounder, *Paralichthys olivaceus* Mx. *Virology* 317:373-382.
- Charbord P, Oostendorp R, Pang W, Herault O, Noel F, Tsuji T, Dzierzak E, Peault (2002) Comparative study of stromal cell lines derived from embryonic, fetal, and postnatal mouse blood-forming tissues. *Exp Hemat* 30:1202-1210.
- Dayeh VR, Bols NC, Tanneberger K, Schirmer K, Lee LEJ (2013) The use of fish-derived cell lines for investigation of environmental contaminants: an update following OECD's fish toxicity testing Framework No. 171. *Current Protocols Toxicol* 1.5.1-1.5.20.
- Despars G, O'Neill HC (2006) Heterogeneity amongst splenic stromal cell lines which support dendritic cell hematopoiesis. *In Vitro Cell Dev Biol* 42:208-215.
- DeWitte-Orr SJ, Leong JA, Bols NC (2007) Induction of antiviral genes, Mx and vig-1, by dsRNA and chum salmon reovirus in rainbow trout monocyte/macrophage and fibroblast cell lines. *Fish Shellfish Immunol* 22:670-682.

- Eaton WD (1990) Anti-viral activity in four species of salmonids following exposure to poly inosinic: cytidylic acid. *Dis Aquat Org* 9:193-198.
- El-Helou V, Gosselin H, Villeneuve L, Calderone A (2012) The plating of rat scar myofibroblasts on matrigel unsmasks a novel phenotype: the self assembly of lumen-like structures. *J Cell Biochem* 113:2442-2450.
- Fenton R, Mathias JA, Moodie GEE (1996) Recent and future demand for Walleye in North America. *Fisheries* 21:6-12.
- Fletcher AI, Malhotra D, Acton SE, Lukacs-Kornek V, Bellemare-Pelletier A, Curry M, Armant M, Turley SJ (2011) Reproducible isolation of lymph node stromal cells reveals site-dependent differences in fibroblastic reticular cells. *Front Immunol* 2(35):1.
- Ganassin RC, Bols NC (1996) Development of long-term rainbow trout spleen cultures that are haemopoietic and produce dendritic cells *Fish Shellfish Immunol* 6:17-34.
- Ganassin RC, Bols NC (1999) A stromal cell line from rainbow trout spleen, RTS34st, that supports the growth of rainbow trout macrophages and produces conditioned medium with mitogenic effects on leukocytes. *In Vitro Cell Dev Biol* 35:80-86.
- Garnett HM, Harigaya K, Cronkite EP (1982) Characterization of a murine cell-line derived from cultured bone marrow stromal cells. *Stem Cells* 2:11-23.
- Gignac SJ, Vo NTK, Mikhaeil MS, Alexander JAN, MacLatchy DL, Schulte PM, Lee LEJ (2014) Derivation of a continuous myogenic cell culture from an embryo of common killifish, *Fundulus heteroclitus*. *Comp Biochem Physiol A* 175:15-27.
- Green TJ, MacPherson S, Qiu S, Lebowitz J, Wertz GW, Luo M (2000) Study of the assembly of vesicular stomatitis virus N protein: role of the P protein. *J Virol* 74:9519-9524.
- Grice J, Reid A, Peterson A, Blackburn K, Tubbs L, Huber LS, Dixon B, Bols NC, Lumsden JS (2014) Walleye (*Sander vitreus* Mitchill) are relatively resistant to experimental infections with viral hemorrhagic septicaemia virus IVb. *J Fish Dis* (in press).
- Guleria A, Kiranmayi M, Sreejith R, Kumar K, Sharma SK, Gupta S (2011) Reviewing host proteins of Rhabdoviridae: possible leads for lesser studied viruses. *J Biosci* 36:929-937.

- Haller O, Stertz S, Kochs G (2007) The Mx GTPase family of interferon-induced antiviral proteins. *Microb Infect* 9:1636-1643.
- Issaad C, Croisille L, Katz A, Vainchenker W, Coulombel L (1993) A murine stromal cell-line allows the proliferation of very primitive human CD34<sup>++</sup>/CD38-progenitor cells in long-term cultures and semisolid assays. *Blood* 81: 2916-2924.
- Jensen I, Albuquerque A, Sommer AI, Robertsen B (2002) Effect of poly I:C on the expression of Mx proteins and resistance against infection by infectious salmon anaemia virus in Atlantic salmon. *Fish Shellfish Immunol* 13:311-326.
- Jensen I, Robertsen B (2002) Effect of double-stranded RNA and interferon on the antiviral activity of Atlantic salmon cells against infectious salmon anemia virus and infectious pancreatic necrosis virus. *Fish Shellfish Immunol* 13:221-241.
- Kain MJW, Owens BMJ (2013) Stroma cell regulation of homeostatic and inflammatory lymphoid organogenesis. *Immunology* 140:12-21.
- Kibenge MJT, Munir K, Kibenge FSB (2005) Constitutive expression of Atlantic salmon Mx1 protein in CHSE-214 cells confers resistance to infectious Salmon Anemia virus. *Virology* 2:75.
- Kim WS, Kim JO, Cho JK, Oh MJ (2014) Changes of viral hemorrhagic septicaemia virus (VHSV) titer in olive flounder (*Paralichthys olivaceus*) following Poly(I:C) administration. *Aquacult Int* 22:1175-1179.
- Kleinman HK, Martin GR (2005) Matrigel: basement membrane matrix with biological activity. *Seminars Cancer Biol* 15:378-386.
- Lester K, Hall M, Urquhart K, Gahlawat S, Collet B (2012) Development of an in vitro system to measure the sensitivity to the antiviral Mx protein of fish viruses. *J Virol Methods* 182:1-8.
- Lin OE, Ohira T, Hirono I, Saito-Taki T, Aoki T (2005) Immunoanalysis of antiviral Mx protein expression in Japanese flounder (*Paralichthys olivaceus*) cells. *Dev Comp Immunol* 29:443-455.
- Lockhart K, Bowden TJ, Ellis AE (2004) Poly I:C-induced Mx response in Atlantic salmon parr, post-smolts and growers. *Fish Shellfish Immunol* 17:245-254.

- Lorenzen N, Olesen NJ, Jorgensen PEV (1988) Production and characterization of monoclonal antibodies to four Egtved virus structural proteins. *Dis Aquat Org* 4:35–42.
- Lumsden JS, Morrison B, Yason C, Russell S, Young K, Yazdanpanah A, Huber P, Al-Hussinee L, Stone D, Way K (2007) Mortality event in freshwater drum *Aplodinotus grunniens* from Lake Ontario, Canada, associated with viral haemorrhagic septicemia virus, Type IV. *Dis Aquat Organ* 76:99-111.
- Markl M, Franke WW (1988) Localization of cytokeratins in tissues of the rainbow trout: fundamental differences in expression pattern between fish and higher vertebrates. *Differentiation* 39:97-122.
- Mas V, Rocha A, Perez L, Coll JM, Estepa A (2004) Reversible inhibition of spreading of in vitro infection and imbalance of viral protein accumulation at low pH in viral hemorrhagic septicaemia Rhabdovirus, a Salmonid Rhabdovirus. *J Virol* 78:1936-1944.
- Mondal A, Roy A, Sarkar S, Mukherjee J, Ganguly T, Chattopadhyaya D (2012) Interaction of Chandipura virus N and P proteins: identification of two mutually exclusive domains of N involved in interaction with P. *PLoS One* 7(4):e34623.
- Mueller SN, Germain RN (2009) Stromal cell contributions to the homeostasis and functionality of the immune system. *Nat Rev Immunol* 9:618-629.
- Ng CT, Nayak BP, Schmedt C, Oldstone MBA (2012) Immortalized clones of fibroblastic reticular cells activate virus-specific T cells during virus infection. *PNAS* 109:7823-7828.
- Nygaard R, Husgard S, Sommer AL, Leong JAC, Robertsen B (2000) Induction of Mx by interferon and double-stranded RNA in salmonid cells. *Fish Shellfish Immunol* 10:435-450.
- Pevsner-Fischer M, Levin S, Zipori D (2011) The origins of mesenchymal stromal cell heterogeneity. *Stem Cell Rev Rep* 7:560-568.
- Pham PH, Jung J, Bols NC (2011) Using 96-well tissue culture polystyrene plates and fluorescence plate reader as tools to study the survival and inactivation of viruses on surfaces. *Cytotechnology* 63:385-397.

- Pham PH, Lumsden JS, Tafalla C, Dixon B, Bols NC (2013) Differential effects of viral hemorrhagic septicemia virus (VHSV) genotypes IVa and IVb on gill epithelial and spleen macrophage cell lines from rainbow trout (*Oncorhynchus mykiss*). *Fish Shellfish Immunol* 34:632-640.
- Piersma AH, Brockbank KGM, Ploemacher RE (1984) Regulation of an in vitro myelopoiesis by a hemopoietic stromal fibroblast cell line. *Exp Hematol* 12:617-623.
- Pietrangeli CE, Hayashi SI, Kincade PW (1988) Stromal cell lines which support lymphocyte growth: characterization, sensitivity to radiation and responsiveness to growth factors. *Eur J Immunol* 18:863-872.
- Polak S, Galfiova P, Varga I (2009) Ultrastructure of human spleen in transmission and scanning electron microscope. *Biologia* 64:402-408.
- Press CM, Dannevig BH, Landsverk T (1994) Immune and enzyme histochemical phenotypes of lymphoid and nonlymphoid cells within the spleen and head kidney of Atlantic salmon (*Salmo salar* L.). *Fish Shellfish Immunol* 4:79-93.
- Sadler AJ, Williams BRG (2008) Interferon-inducible antiviral effectors. *Nature Rev Immunol* 8:559-568.
- Sagi B, Maraghechi P, Urban VS, Hegyi B, Szigeti A, Fajka-Boja R, Kudlik G, Nemet K, Monostori E, Gocza E, Uher F (2012) Positional identification of mesenchymal stem cells resident in different organs is determined in the postsegmentation mesoderm. *Stem Cells Devel* 21:814-828.
- Smail DA, Snow M (2011) Viral haemorrhagic septicaemia. In *Fish Diseases and Disorders* eds. Publisher 3:110-142.
- Sorensen KK, McCourt P, Berg T, Crossley C, Le Couteur D (2012) The scavenger endothelial cell: a new player in homeostasis and immunity. *Am J Physiol Regul Integr Comp Physiol* 303:R1217-R1230.
- Strakova Z, Livak M, Krezalek M, Ihnatovych I (2008) Multipotent properties of myofibroblast cells derived from human placenta. *Cell Tiss Res* 332:479-488.
- Stain-Jean SR, Perez-Prieto SI (2006) Interferon mediated antiviral activity against salmonid fish viruses in BF-2 and other cell lines. *Vet Immunol Immunopath* 110:1-10.

- Steiniger B, Barth P, Hellinger A (2001) The perifollicular and marginal zone of the human splenic white pulp – Do fibroblasts guide lymphocyte migration? *Am J Pathol* 159:37-46.
- Summerfelt R.C. (2005) The culture of walleye. In *Aquaculture in the 21<sup>st</sup> Century* (Ed: Kelly A, Silverstein J), American Fisheries Society.
- Suzuki J, Fujita J, Taniguchi S, Sugimoto K, Mori KJ (1992) Characterization of murine hematopoietic-supportive (MS-1 and MS-5) and nonsupportive (MS-K) cell lines. *Leukemia* 6:452-458.
- Tang DD (2008) Intermediate filaments in smooth muscle. *Am J Physiol* 294:C869-C878.
- Trobridge GD, Chiou PP and Leong JC (1997) Cloning of the rainbow trout (*Oncorhynchus mykiss*) Mx2 and Mx3 cDNAs and characterization of trout Mx protein expression in salmon cells. *J Virol* 71:5304-5311.
- Tschiyama J, Mori M, Okaka S (1995) Murine spleen stromal cell line SPY3-2 maintains long-term hematopoiesis in vitro. *Blood* 85:3107-3116.
- Verhelst J, Hulpiau P, Saelems X (2013) Mx proteins: antiviral gatekeepers that restrain the uninvited. *Micro Mol Biol Rev* 77:551-566.
- Vo NTK, Bender AW, Lee LEJ, Lumsden JS, Lorenzen N, Dixon B, Bols NC (2014) Development of a walleye cell line and use to study the effects of temperature on infection by viral haemorrhagic septicemia virus group IVb. *J Fish Dis* (in press)
- Weiss L (1991) Barrier cells in the spleen. *Immunol Today* 24:24-29.
- Winton J, Batts W, deKinkelin P, LeBerre M, Bremont M, Fijan N (2010) Current lineages of the Epithelioma papulosum cyprini (EPC) cell line are contaminated with fathead minnow, *Pimephales promelas*, cells. *J Fish Dis* 33:701-704.
- Xing JG, El-Sweisi W, Lee LEJ, Collodi P, Seymour C, Mothersill C, Bols NC (2009) Development of a zebrafish spleen line, ZSSJ, and its growth-arrest by gamma irradiation and capacity to act as feeder cells. *In Vitro Cell Dev Biol* 45:163-174.
- Yanai N, Satoh T, Obinata M (1991) Endothelial-cells create a hematopoietic inductive microenvironment preferential to erythropoiesis in the mouse spleen. *Cell Structure Function* 16:87-93.

- Zhen T, Mustafaa MZ, Flavell SJ, Barrington F, Jenkinson EJ, Anderson G, Lane PJJ, Withers DR, Buckley CD (2010) Splenic stromal cells mediate IL-7 independent adult lymphoid tissue inducer cell survival. *Eur J Immunol* 40:359-365.
- Zipori D, Duksin D, Tamir M, Argaman A, Toledo J, Malk Z (1985) Cultured mouse stromal cell lines. II Distinct subtypes differing in morphology, collagen types, myelopoietic factors, and leukemic cell growth modulating activities. *J Cell Physiol* 122:81-90.

## Chapter 5 References

- Aamelfot M, Weli SC, Dale OB, Koppang EO, Falk K (2013) Characterization of a monoclonal antibody detecting Atlantic salmon endothelial and red blood cells, and its association with the infectious salmon anaemia virus cell receptor. *J Anat* 222:547-557.
- Ades WE, Candal FJ, Swerlick RA, George VG, Summers S, Bosse DC, Lawley TJ (1992) HMEC-1: Establishment of an immortalized human microvascular endothelial cell line. *J Invest Dermatol* 99:683-690.
- Aird WC (2007) Phenotypic heterogeneity of the endothelium II. Representative vascular beds. *Circ Res* 100:174-190.
- Arenas MI, Braile B, De Miguel M, Paniagua R (1995) Intermediate filaments in the testis of the teleost mosquito fish *Gambusia affinis holbrooki*: a light and electron microscope immunocytochemical study and western blotting analysis. *Histochem J* 27:329-337.
- Baltzegar DA, Reading BJ, Brune ES, Borski RJ (2013) Phylogenetic revision of the claudin gene family. *Mar Genomics* 11:17-26.
- Bayless KJ, Davis GE (2004) Microtubule depolymerisation rapidly collapses capillary tube networks in vitro and angiogenic vessels in vivo through the small GTPase Rho. *J Biol Chem* 279:11686-11695.
- Benjamin M, Norman D, Santer RM, Scarborough D (1983) Histological, histochemical and ultrastructural studies on the bulbus arteriosus of the sticklebacks, *Gasterosteus aculeatus* and *Pungitius pungitius* (Pisces: Teleostei). *J Zool* 200:325-346.
- Bols NC, Lee LEJ (1991) Technology and uses of cell cultures from the tissues and organs of bony fish. *Cytotechnology* 6:163-187.
- Bols NC, Schirmer K, Joyce EM, Dixon DG, Greenberg BM, Whyte JJ (1999) Ability of polycyclic aromatic hydrocarbons to induce 7-ethoxyresorufin-o-deethylase activity in a trout liver cell line. *Ecotoxicol Environ Saf* 44:118-128.
- Boyd RB, DeVries AL, Eastman JT, Pietra GG (1980) The secondary lamellae of the gills of cold water (high latitude) teleosts. *Cell Tissue Res* 213:361-367.

- Davis GE, Senger DR (2005) Endothelial extracellular matrix: biosynthesis, remodelling, and functions during vascular morphogenesis and neovessel stabilization. *Circ Res* 97:1093-1107.
- Diago ML, Lopez-Fierro P, Razquin B, Villena A (2000) Spontaneous in vitro angiogenesis in a trout pronephric stromal cell line (TPS) and in TPS-haemopoietic co-cultures. *Fish Shellfish Immunol* 10:21-31.
- Carrillo M, Kim S, Rajpurohit SK, Kulkarni V, Jagadeeswaran P (2010) Zebrafish von Willebrand factor. *Blood Cells Mol Dis* 45:326-333.
- Camalxaman SN, Zeenathul NA, Quah YW, Loh HS, Zuridah H, Hani H, Sheikh-Omar AR, Mohd-Azmi ML (2013) Establishment of rat brain endothelial cells susceptible to rat cytomegalovirus ALL-03 infection. *In Vitro Cell Dev Biol* 49:238-244.
- Chen Y, Lu Q, Schneeberger EE, Goodenough DA(2000) Restoration of tight junction structure and barrier function by down-regulation of the mitogen-activated protein kinase pathway in Ras-transformed Madin-Darby canine kidney cells. *Mol Biol Cell* 11:849-862.
- Cines DB, Pollak ES, Buck CA, Loscalzo J, Zimmerman GA, McEver RP, Pober JS, Wick TM, Konkle BA, Schwartz BS, Barnathan ES, McCrae KR, Hug BA, Schmidt AM, Stern DM (1998) Endothelial cells in physiology and in the pathophysiology of vascular disorders. *Blood* 91:3527-3561.
- Cotta-Pereira G, Sage H, Bornstein P, Ross R, Schwartz S (1980) Studies of morphologically atypical (“sprouting”) cultures of bovine endothelial cells. Growth characteristics and connective tissue protein synthesis. *J Cell Physiol* 102:183-191.
- Craig LE, Spelman JP, Stranberg JD, Zink MC (1998) Endothelial cells from diverse tissues exhibit differences in growth and morphology. *Microvascular Res* 55:65-76.
- Curtis TM, Howard A, Gerlach B, Brennan LM, Widder MW, van der Schalie WH, Vo NTK & Bols NC (2013) Suitability of invertebrate and vertebrate cells in a portable impedance-based toxicity sensor: temperature mediated impacts on long-term survival. *Tox In Vitro* 27:2061-2066.
- Donald JA, Broughton BR (2005) Nitric oxide control of lower vertebrate blood vessels by vasomotor nerves. *Comp Biochem Physiol A* 142:188-197.

- Dorovini-Zis K, Huynh HK (1992) Ultrastructural localization of Factor VIII-related antigen in cultured human brain microvessel endothelial cells. *J Histochem Cytochem* 40:689-696.
- Elonen GE, Spehar RL, Holcombe GW, Johnson RD, Fernandez JD, Erickson RJ, Tietge JE, Cook PM (1998) Comparative toxicity of 2,3,7,8-tetrachlorodibenzo-p-dioxin to seven freshwater species during early life-stage development. *Environ Toxicol Chem* 17:472-483.
- Farrell AP, Saunders RL, Freeman HC, Mommsen TP (1986) Arteriosclerosis in Atlantic salmon-effects of dietary-cholesterol and maturation. *Arteriosclerosis* 6:453-461.
- Fenton R, Mathias JA, Moodie GEE (1996) Recent and future demand for Walleye in North America. *Fisheries* 21:6-12.
- Ferri S, A. Sesso A (1983) Tubulated bodies in teleost (*Pimelodus maculatus*) endothelial cells, *Arch. Anat. Microsc. Morphol. Exp.* 72:19-22.
- Findley MK, Koval M (2009) Regulation and roles for claudin-family tight junction proteins. *IUBMB Life* 61:431-437.
- Gan N, Hondou T, Miyata H (2012) Spontaneous increases in the fluorescence of 4,5-daminofluorescein and its analogs: their impact on the fluorometry of nitric oxide production in endothelial cells. *Biol Pharm Bull* 35:1454-1459.
- Gardell AM, Qin Q, Rice RH, Li J, Kultz D (2014) Derivation and osmotolerance of three immortalized Tilapia (*Oreochromis mossambicus*) cell lines. *PLOS One* 9 (5):e95519.
- Garrick RA (2000) Isolation and culture of capillary endothelial cells from the eel, *Anguilla rostrata*. *Microvasc Res* 59:377-385.
- Garrick RA, Woodin BR, Stegeman JJ (2005) Cytochrome P4501A induced differentially in endothelial cells cultured from *Anguilla rostrata*. *In Vitro Cell Dev Biol Anim* 41:57-63.
- Garrick RA, Woodin BR, Wilson JY, Middlebrooks BL, Stegeman JJ (2006) Cytochrome P4501A is induced in endothelial cell lines from the kidney and lung of the bottlenose dolphin, *Tursiops truncatus*. *Aquatic Toxicol* 76:295-305.

- Gignac SJ, Vo NTK, Mikhaeil MS, Alexander JAN, MacLatchy DL, Schulte PM & Lee LEJ (2014) Derivation of a continuous myogenic cell culture from embryos of common killifish, *Fundulus heteroclitus*. *Comp Biochem Physiol Part A* 175:15-27.
- Grimes AC, Stadt HA, Shepherd IT, Kirby ML (2006) Solving an enigma: arterial pole development in the zebrafish heart. *Dev Biol* 290:265-276.
- Guiney PD, Smolowitz RM, Peterson RE, Stegeman JJ (1997) Correlation of 2,3,7,8-tetrachlorodibenzo-p-dioxin induction of cytochrome P4501A in vascular endothelium with toxicity in early life stages of Lake Trout. *Toxicol Appl Pharmacol* 143: 256-273.
- Helbo S, Weber RE, Fago A (2013) Expression patterns and adaptive functional diversity of vertebrate myoglobins. *Biochim Biophysica Acta –Proteins and Proteomics* 1834:1832-1839.
- Hendegen-Cotta UB, Merx MW, Shiva S, Schmitz J, Becher S, Klare JP, Steinhoff HJ, Goedecke A, Schrader J, Gladwin MT, Kelm M, Rassaf T (2014) Myoglobin's novel role in nitrite-induced hypoxic vasodilation. *Trends Card Med* 24:69-74.
- Hirase T, Node K (2011) Endothelial dysfunction as a cellular mechanism for vascular failure. *Am J Physiol Heart Circ Physiol* 302:H499-H505.
- Hormia M, Lehto VP, Virtanen I (1983) Identification of UEA-I binding surface glycoproteins of cultured human endothelial cells. *Cell Biol Intern Reports* 7:467-475.
- Humblet O, Birnbaum L, Rimm E, Mittleman MA, Hauser R (2008) Dioxins and cardiovascular disease mortality. *Env Hlth Persp* 116:1443-1448.
- Huang Y-S, Huang W-L, Lin W-F, Chen M-C, Jeng S-R (2006) An endothelial-cell-enriched primary culture system to study vascular endothelial growth factor (VEGF A) expression in a teleost, the Japanese eel (*Anguilla japonica*). *Comp Biochem Physiol A* 145:33-46.
- Icardo JM (2013) Collagen and elastin histochemistry of the teleost bulbus arteriosus: false positives. *Acta Histochemica* 115:185-189.
- Icardo JM, Colvee E, Cerra MC, Tota B (2000) The bulbus arteriosus of stenothermal and temperate teleosts: a morphological approach. *J Fish Biol* 57:121-135.

- Jeong JY, Kwon HB, Ahn JC, Kang D, Jeong A, Kim KW (2008) Functional and developmental analysis of the blood-brain barrier in zebrafish. *Brain Res Bull* 75:619-628.
- Kim DJ, Martinez-Lemus LA, Davis GE (2013) EB1, p150<sup>Glued</sup>, and Clasp1 control endothelial tubulogenesis through microtubule assembly, acetylation, and apical polarization. *Blood* 121:3521-3530.
- Kojima H, Nakatsubo N, Kikuchi K, Urano Y, Higuchi T, Tanaka J, Kudo Y, Nagano T (1998) Direct evidence of NO production in rat hippocampus and cortex using a new fluorescent indicator: DAF-2DA. *Neuroreport* 9:3345-3348.
- Kopf PG, Scott JA, Agbor LN, Boberg JR, Elased KM, Huwe JK, Walker MK (2010) Cytochrome P4501A1 is required for vascular dysfunction and hypertension induced by 2,3,7,8-tetrachlordibenzo-p-dioxin. *Toxicol Sci* 117:537-546.
- Kuruvilla L, Santhoshkumar TR, Kartha CC (2007) immortalization and characterization of porcine ventricular endocardial endothelial cells. *Endothelium* 14:35-43.
- Kwak HI, Kang J, Dave JM, Mendoza EA, Su SC, Maxwell SA, Bayless KJ (2012) Calpain-mediated vimentin cleavage occurs upstream of MT1-MMP membrane translocation to facilitate endothelial sprout initiation. *Angiogenesis* 15:287-303.
- Jackson CJ, Garbett PK, Nissen B, Schrieber L (1990) Binding of human endothelium to *Ulex europaeus* I-coated dynabeads: application to the isolation of microvascular endothelium. *J Cell Sci* 96:257-262.
- Leknes IL (2009) Structural and histochemical studies on the teleostean bulbus arteriosus. *Anat Histol Embryol* 38:424-428.
- Lepiller S, Laurens V, Bouchot A, Herbomel P, Solary E, Chluba J (2007) Imaging of nitric oxide in a living vertebrate using a diaminofluorescein probe. *Free Radical Biol Med* 43:619-627.
- Lewis DH, Marks JE (1985) Microcultures of *Sarotherodon massambicus* (Peters) cells: their use in detecting fish viruses. *J Fish Dis* 8:477-478.
- Luque A, Granja AG, Gonzalez L, Tafalla C (2014) Establishment and characterization of a rainbow trout heart endothelial cell line with susceptibility to viral hemorrhagic septicemia virus (VHSV). *Fish Shellfish Immunol* 3:255-264.

- Markl J (1991) Cytokeratins in mesenchymal cells: impact on functional concepts of the diversity of intermediate filament proteins. *J Cell Sci* 98:261-264.
- Nakamura H, Shimozawa A (1994) Phagocytotic cells in the fish heart. *Arch Histol Cytol* 57:415-425.
- Neuhaus W, Wirth M, Plattner VE, Germann B, Gabor F, Noe CR (2008) Expression of claudin-1, claudin-3 and claudin-5 in human blood-brain barrier mimicking cell line ECV304 is inducible by glioma-conditioned media. *Neuroscience Lett* 446:59-64.
- Nitta T, Hata M, Gotoh S, Seo Y, Sasaki H, Tsukita S (2003) Size-selective loosening of the blood-brain barrier in Claudin-5 deficient mice. *J Cell Biol* 161:653-660.
- Omar SA, Webb AJ (2014) Nitrite reduction and cardiovascular protection. *J Mol Cell Cardiology* in press.
- Pombo A, Blasco M, Climent V (2012) The status of farmed fish hearts: an alert to improve health and production in three Mediterranean species. *Rev Fish Biol Fisheries* 22:779-789.
- PrabhuDas M, Bowdish D, Drickamer K, Febbraio M, Herz J, Kobzik L, Kreiger M, Loik J, Means TK, Moestrup SK, Post S, Sawamura T, Silverstein S, Wang XY, Il Khoury K (2014) Standardizing scavenger receptor nomenclature. *J Immunol* 192:1997-2006.
- Ryan US (1988) Phagocytic properties of endothelial cells. Chapter 30. *Endothelial Cells*, Vol 3 pp 33-48.
- Reidy MA, Chopek M, Chao S, McDonald T, Schwartz SM (1989) Injury induces increase of von Willebrand factor in rat endothelial cells. *Am J Pathol* 134:857-864.
- Runkle EA, Mu D (2014) Tight junction proteins: from barrier to tumorigenesis. *Cancer Lett* 337:41-48.
- Sahm M, Seifert p (2000) Light and electron microscopic examination of endothelial cells from bovine retinal vessels in long-term cultures. *Virchows Arch* 436:249-256.
- Sandvik GK, Nilsson GE, Jensen FB (2012) Dramatic increase of nitrite levels in hearts of anoxia-exposed crucian carp supporting a role in cardioprotection. *Am J Physiol Regul Integ Comp Physiol* 302:R468-R477.
- Sansom B, Vo NTK, Kavanagh R, Hanner R, MacKinnon M, Dixon DG & Lee LEJ (2013) Rapid assessment of the toxicity of oil sands process-affected waters using fish

- cell lines. *In Vitro Cell Dev Biol – Anim* 49:52–65.
- Schnittler HJ, Schmandra T, Drenckhahn D (1998) Correlation of endothelial vimentin content with hemodynamic parameters. *Histochem Cell Biol* 110:161-167.
- Schnittler H, Taha M, Schnittler MO, Taha AA, Lindemann N, Seebach J (2014) Actin filament dynamics and endothelial cell junctions: the Ying and Yang between stabilization and motion. *Cell Tissue Res* 355:529-543.
- Song L, Pachter JS (2003) Culture of brain microvascular endothelial cells that maintain expression and cytoskeletal association of tight junction-associated proteins. *In Vitro Cell Dev Biol* 39:313-320.
- Sorensen KK, McCourt P, Berg T, Crossley C, De Couteur D, Wake K, Smedsrod B (2012) The scavenger endothelial cell: a new player in homeostasis and immunity. *Am J Physiol Regul Integr Comp Physiol* 303:R1217-R1230.
- Sorensen KK, Melkko J, Smedsrod B (1998) Scavenger-receptor-mediated endocytosis in endocardial endothelial cells of Atlantic cod *Gadus morhua*. *J Exp Biol* 20:1707-1718.
- Sugimoto K, Fujii S, Takemasa T, Yamashita K (2000) Detection of intracellular nitric oxide using a combination of aldehyde fixatives with 4, 5-diaminofluorescein diacetate. *Histochem Cell Biol* 113:341-347.
- Summerfelt RC (2005) The culture of walleye. In *Aquaculture in the 21st Century* (Ed: Kelly A, Silverstein J), American Fisheries Society.
- Takahashi K, Sawasaki Y, Hata JI, Mukai K, Goto T (1990) Spontaneous transformation and immortalization of human endothelial cells. *In Vitro Cell Dev Biol* 25:265-274.
- Tom DJ, Lee LEJ, Lew J, Bols NC (2001) Induction of 7-ethoxyresorufin-o-deethylase activity by planar chlorinated hydrocarbons and polycyclic aromatic hydrocarbons in cell lines from the rainbow trout pituitary. *Comp Biochem Physiol* 128:185-198.
- Tota B, Amelio D, Pellegrino D, Ip YK, Cerra MC (2005) NO modulation of myocardial performance in fish hearts. *Comp Biochem Physiol Part A* 142:164-177.
- Unger RE, Krump-Konvalinkova V, Peters K, Kirkpatrick CJ (2002) In vitro expression of the endothelial phenotype: comparative study of primary isolated cells and cell lines, the novel cell line HPMEC-ST1.6R. *Micro Res* 64:384-397.

- Vernon RB, Lara SL, Drake CJ, Iruela-Arispe ML, Angello JC, Little CD, Wight TN, Sage EH (1995) Organized type I collagen influences endothelial patterns during “spontaneous angiogenesis in vitro”: planar cultures as models of vascular development. *In Vitro Cell Dev Biol* 31:120-131.
- Vo NTK, Bender AW, Lee LEJ, Lumsden JS, Lorenzen N, Dixon B, Bols NC (2014) Development of a walleye cell line and use to study the effects of temperature on infection by viral haemorrhagic septicemia virus group IVb. *J Fish Dis* (In Press)
- Voyta JC, Via DP, Butterfield CE, Zettrier BR (1984) Identification and isolation of endothelial cells based on their increased uptake of acetylated-low density lipoprotein. *J Cell Biol* 88:2034-2040.
- Wagner DD, Olmsted JB, Marder VJ (1982) Immunolocalization of von Willebrand protein in Weibel-Palade bodies of human endothelial cells. *J Cell Biol* 95:355-360.
- Ward RD, Hanner R, Herbert PDN (2009) The campaign to DNA barcode all fishes, FISH-BIOL. *J Fish Biol* 74:329-356.
- Watanabe T, Dohgu S, Takata F, Nishioku T, Nakashima A, Futagami K, Yamauchi A, Kataoka Y (2013) Paracellular barrier and tight junction protein expression in the immortalized brain endothelial cell lines bEND.3, bEND.5 and mouse brain endothelial cell 4. *Biol Pharm Bull* 3:492-495.
- Zauner W, Farrow NA, Haines AMR (2001) In vitro uptake of polystyrene microspheres: effect of particle size, cell line and cell density. *J Controlled Res* 71:39-51.
- Zhang J, Liss M, Wolburg H, Blasig IE, Abedlilah-Seyfried S (2012) Involvement of claudins in zebrafish brain ventricle morphogenesis. *Ann NY Acad Sci* 1257:193-198.

## Chapter 6 References

- Benjamin M, Norman D, Santer RM, Scarborough D (1983) Histological, histochemical and ultrastructural studies on the bulbus arteriosus of the sticklebacks, *Gasterosteus aculeatus* and *Pungitius pungitius* (Pisces: Teleostei). *J Zool* 200:325-346.
- Benjamin M, Norman D, Scarborough D, Santer RM (1984) Carbohydrate-containing endothelial cells lining the bulbus arteriosus of teleosts and the conus arteriosus of elasmobranchs (Pisces). *J Zool* 202:383-392.
- Campisi J (2005) Senescent cells, tumor suppression, and organismal aging: good citizens, bad neighbors. *Cell* 120:513-522.
- Cerone MA, Autexier C, London-Vallejo JA, Bacchettie S (2005) A human cell line that maintain telomeres in the absence of telomerase and of key markers of ALT. *Oncogene* 24:7893-7901.
- Cho S, Hwang ES (2012) Status of mTOR activity may phenotypically differentiate senescence and quiescence. *Mol Cells* 33:597-604.
- Curtis TM, Howard A, Gerlach B, Brennan LM, Widder MW, van der Schalie WH, Vo NTK, Bols NC (2013) Suitability of invertebrate and vertebrate cells in a portable impedance-based toxicity sensor : temperature mediated impacts on long-term survival. *Toxicol In Vitro* 27:2061-2066.
- Debacq-Chainiaux F, Erusalimsky JD, Campisi J, Toussaint O (2009) Protocols to detect senescence-associated beta-galactosidase (SA-beta-gal) activity, a biomarker of senescent cells in culture and in vivo. *Nat Protoc* 4 (12):1798-1806.
- Dimri GP, Lee X, Basile, G, Acosta M, Scott G, Roskelley C, Medrano EE, Linskens M, Rubelj I, Pereira-Smith O, Peacocke M, Campisi J (1995) A biomarker that identifies senescent human-cells in culture and in aging skin in vivo. *Proc Natl Acad Sci USA* 92:9363-9367.
- Ding L, Kukne WW, Hinton DE, Song J, Dynan WS (2010) Quantifiable biomarkers of normal aging in the Japanese medaka fish (*Oryzias latipes*). *PLoS one* 5 (10):e13287.
- Donnini S, Giachetti A, Ziche M (2013) Assessing vascular senescence in zebrafish. *Methods Mol Biol* 965:517-531.
- Frippiat C, Chen QM, Zdanov S, Magalhaes JP, Remacle J, Toussaint O (2001) Subcytotoxic H<sub>2</sub>O<sub>2</sub> stress triggers a release of transforming growth factor-  $\beta$ 1, which

- induces biomarkers of cellular senescence of human diploid fibroblasts. *J Biol Chem* 276:2531-2537.
- Ganassin, R.C. and N.C. Bols. 1997. Development and growth of cell lines from fish: rainbow trout *Oncorhynchus mykiss*. In: *Cell & Tissue Culture: Laboratory Procedures*. (Griffiths, J.J., A. Doyle and D.G. Newell eds) (John Wiley & Sons Limited, Wiltshire, UK). 23A:1.1-23A:1.9.
- Gendron RL, Liu C-Y, Paradis H, Adams LC, Kao WW (2001) MK/T-1, an immortalized fibroblast cell line derived using cultures of mouse corneal stroma. *Mol Vision* 7:107-113.
- Goodwin EC, DiMaio D (2001) Induced senescence in HeLa cervical carcinoma cells containing elevated telomerase activity and extended telomeres. *Cell Growth Diff* 12:525-534.
- Going JJ, Stuart RC, Downie M, Fletcher-Monaghan AJ, Keith WN (2002) 'Senescence-associated  $\beta$ -galactosidase activity in the upper gastrointestinal tract. *J Pathol* 196:394-400.
- Graf M, Hartmann N, Reichwald K, Englert C (2013) Absence of replicative senescence in cultured cells from the short-lived killifish *Nothobranchius furzeri*. *Exp Geront* 48:17-28.
- Huang T, Rivera-Perez JA (2014) Senescence-associated  $\beta$ -galactosidase activity marks visceral endoderm of mouse embryos but is not indicative of senescence. *Genesis* 52:300-308.
- Hwang ES, Yoon G, Kang HT (2009) A comparative analysis of the cell biology of senescence and aging. *Cell Mol Life Sci* 66:2503-2524.
- Johanisson E, Campana A, Luthi R, de Agostini A (2000) Evaluation of 'round cells' in semen analysis: a comparative study. *Human Reprod Update* 6:404-412.
- Kjelland ME, Liu J, Hyatt D, Kraemer D (2013) Collection, isolation, and culture of somatic cells from avian semen. *Avian Biol Res* 6:255-260.
- Kurz DJ, Decary S, Hong Y, Erusalimsky JD (2000) Senescence-associated  $\beta$ -galactosidase reflects an increase in lysosomal mass during replicative ageing of human endothelial cells. *J Cell Sci* 113:3613-3622.

- Leknes IL (2009) Structural and histochemical studies on the teleostean bulbus arteriosus. *Anat Histol Embryol* 38:424-428.
- Lee BY, Han JA, Im JS, Morrone A, Johung K, Goodwin ED, Kleijer WJ, DiMaio D, Hwang ES (2006) Senescence-associated  $\beta$ -galactosidase is lysosomal  $\beta$ -galactosidase. *Aging Cell* 5:187-195.
- Lee LEJ, Dayeh VR, Schirmer K, Bols NC (2009) Applications and potential uses of fish gill cell lines: examples with RTgill-W1. *In Vitro Cell Dev Biol – Anim* 45:127-134.
- Lee M, Hills M, Conomos D, Stutz MD, Dagg RA, Lau LMS, Reddel RR, Pickett HA (2013) Telomerase extension by telomerase and ALT generates variants by mechanistically distinct processes. *Nucleic Acids Res* 42:1733-1746.
- Liu J, Westhusin M, Johnson G, Raudsepp T, Chowdhary B, Burghardt R, Long C, Kraemer D (2009) Evaluation of culture systems for attachment and proliferation of epithelial cells cultured from ovine semen. *Anim Reprod Sci* 115:49-57.
- Ossum CG, Hoffmann EK, Vijayan MM, Holt SE, Bols NC (2004) Isolation and characterization of a novel fibroblast-like cell line from the rainbow trout (*Oncorhynchus mykiss*) and a study of p38<sup>MAPK</sup> activation and induction of HSP70 in response to chemically induced ischemia. *J Fish Biol* 64:1103-1116.
- Phillips SG, Phillips DM, Kabat EA, Miller OJ (1978) Human semen as a source of epithelial cells for culture. *In Vitro* 14:639-650.
- Severino J, Allen RG, Balin S, Balin A, Christofalo VJ (2000) Is beta-galactosidase staining a marker of senescence in vitro and in vivo? *Exp Cell Res* 257:162-172.
- Tsai SB, Tucci V, Uchiyama J, Fabian NJ, Lin MC, Bayliss PE, Neuberg DS, Zhdanova IV, Kishi S (2007) Differential effects of genotoxic stress on both concurrent body growth and gradual senescence in the adult zebrafish. *Aging Cell* 6:209-224.
- Van der Loo B, Fenton MJ, Erusalimsky JD (1998) Cytochemical detection of a senescence-associated  $\beta$ -galactosidase in endothelial and smooth muscle cells from human and rabbit blood vessels. *Exp Cell Res* 241:309-315.
- Villa A, Navarro-Galve B, Beuno C, Franco S, Bllasco MA, Martinez-Serrano A (2004) Long-term molecular and cellular stability of human neural stem cell lines. *Exp Cell Res* 294:559-570.

- Vo NTK, Bender AW, Lee LEJ, Lumsden JS, Lorenzen N, Dixon B, Bols NC (2014)  
Development of a walleye cell line and use to study the effects of temperature on  
infection by viral haemorrhagic septicemia virus group IVb. *J Fish Dis* (in press)
- Xing JG, Lee LEJ, Fan L, Collodi P, Holt SE & NC Bols (2008) Initiation of a  
zebrafish blastula stem cell line on rainbow trout stromal cells and subsequent  
development under feeder-free conditions into a cell line, ZEB2J. *Zebrafish* 5:49-  
63.
- Xing JG, El-Sweisi W, Lee LEJ, Collodi P, Seymour C, Mothersill C & NC Bols (2009)  
Development of a zebrafish spleen line, ZSSJ, and its growth-arrest by gamma  
irradiation and capacity to act as feeder cells. *In Vitro Cell Dev Biol* 45:163-174.

## Chapter 7 References

- Aden DP, Fogel A, Plotkin S, Damjanov I, Knowles BB (1979) Controlled synthesis of HbsAg in a differentiated human liver carcinoma-derived cell line. *Nature* 282:615-617.
- Akoumianaki T, Kardassis D, Polioudaki H, Georgatos SD, Theodoropoulos PA (2008) Nucleocytoplasmic shuttling of soluble tubulin in mammalian cells. *J Cell Sci* 122:1111-1118.
- Alieva IB, Gorgidze LA, Komarova YA, Chernobelskaya OA, Vorobjev IA (1999) Experimental model for studying the primary cilia in tissue culture cells. *Membr Cell Biol* 12:895-905.
- Alieva IB, Vorobjev IA (2004) Vertebrate primary cilia: a sensory part of centrosomal complex in tissue cells, but a “sleeping beauty” in cultured cells? *Cell Biol Int* 28:139-150.
- Bergmann C (2012) Ciliopathies. *Eur J Pediatr* 171:1285-1300.
- Billger M, Stromberg E, Wallin M (1991) Microtubule-associated proteins-dependent colchicine stability of acetylated cold-labile brain microtubules from the Atlantic cod, *Gadus morhua*. *J Cell Biol* 113:331-338.
- Bols NC, Brubacher JL, Fujiki K, Dixon B, Collodi R (2004). Development and characterization of a cell line from a blastula stage rainbow trout embryo. *In Vitro Cell Dev Biol* 40:80A.
- Bols N.C., Mosser D.D. & Steels G.B. (1992) Temperature studies and recent advances with fish cells in vitro. *Comparative Biochem Physiol* 103A:1-14.
- Buckland-Nicks JA, Gillis M, Reimchen TE (2012) Neural network detected in a presumed vestigial trait: ultrastructure of the adipose fin. *Proc Royal Soc B Biol Sci* 279:553-563.
- Chitnis AB, Kuwada JY (1990) Axonogenesis in the brain of zebrafish embryos. *J Neurosci* 10:1892-1905.
- Cianfanelli V, Cecconi F (2013) Molecular clearance at the cell’s antenna. *Nature* 502:180-181.

- Egorova AD, van der Heiden K, Poelmann RE, Hierck BP (2012) Primary cilia as a biomechanical sensors in regulating endothelial function. *Differentiation* 83:S56-S61.
- Fogh J, Fogh JM, Orfeo T (1977) One hundred and twenty seven cultured human tumor cell lines producing tumors in nude mice. *J Natl Cancer Inst* 59:221-226.
- Gey GO, Coffman WD, Kubicek MT (1952). Tissue culture studies of the proliferative capacity of cervical carcinoma and normal epithelium. *Cancer Res* 12:264-265.
- Ghioni C, Tocher DR, Bell MV, Dick JR, Sargent JR (1999) Low C-18 to C-20 fatty acid elongase activity and limited conversion of steraridonic acid, 18: 4(n-3), to eicosapentaenoic acid, 20:5(n-3), in a cell line from the turbot, *Scophthalmus maximus*. *Biochim Biophys Acta Mol Cell Biol Lipids* 1437:170-181.
- Gignac SJ, Vo NTK, Mikhaeil MS, Alexander JAN, MacLatchy DL, Schulte PM, Lee LEJ (2014) Derivation of a continuous myogenic cell culture from embryos of common killifish, *Fundulus heteroclitus*. *Comp Biochem Physiol Part A* 175:15-27.
- Goto H, Inoko A, Inagaki M (2013) A cell cycle progression by the repression of primary cilia formation in proliferating cells. *Cell Mol Life Sci* 70:3893-3905.
- Gu Y, Ihara Y (2000) Evidence that collapsing response mediator protein-2 is involved in the dynamics of microtubules. *J Biol Chem* 275: 17917-17920.
- Kim HR, Richardson J, van Eden F, Ingham PW (2010) Gli2a protein localization reveals a role for Iguana/DZIP1 in primary ciliogenesis and a dependence of Hedgehog signal transduction on primary cilia in the zebrafish. *BMC Biol* 8:65.
- LeDizet M, Piperno G (1987). Identification of an acetylation site of *Chlamydomonas*  $\alpha$ -tubulin. *Proc. Natl Acad. Sci. USA* 84:5720-5724.
- Lee LEJ, Martinez A, Bols NC (1988) Culture conditions for arresting and stimulating the proliferation of a rainbow trout fibroblast cell line, RTG-2. *In Vitro Cell Dev Biol* 24:795-802.
- Lessman CA, Zhang J, MacRae TH (1993) Posttranslational modifications and assembly characteristics of goldfish tubulin. *Biol Cell* 79:63-70.
- Liu Y, Peng L, Seto E, Huang S, Qiu Y (2012) Modulation of histone deacetylase 6 (HDAC6) nuclear import and tubulin deacetylase activity through acetylation. *J Biol Chem* 287:29168-29174.

- Lopez-Terrada D, Cheung SW, Finegold MJ, Knowles BB (2009) Hep G2 is a hepatoblastoma-derived cell line. *Human Pathol* 40:1512-1515.
- Menko AS, Tan KB (1980) Nuclear tubulin of tissue culture cells. *Biochim Bio Acta* 629:359-370.
- Miyamoto T, Porazinski S, Wang H, Borovina A, Ciruna B, Shimizu A, Kajii T, Kikuchi A, Furutani-Seiki M, Matsuura S (2010) Insufficiency of BUBR1, a mitotic spindle checkpoint regulator, causes impaired ciliogenesis in vertebrates. *Human Mol Genetics* 20:2058-2070.
- Modig C, Stromberg E, Wallin M (1994) Different stability of posttranslationally modified brain microtubules isolated from cold-temperate fish. *Mol Cell Biochem* 130:137-147.
- Nakagawa U, Suzuki D, Ishikawa M, Sato H, Kamemura K, Imamura A (2013) Acetylation of  $\alpha$ -tubulin on Lys<sup>40</sup> is a widespread post-translational modification in angiosperms. *Biosci Biotechnol Biochem* 77:1602-1605.
- Nolte SV, Xu W, Rennekampff HO, Rodemann HP (2008) Diversity of fibroblasts- A review on implications for skin tissue engineering. *Cells Tissues Organs* 187:165-176.
- Ou Y, Ruan Y, Cheng M, Moser JJ, Rattner JB, van der Hoorn FA (2009) Adenylate cyclase regulates elongation of mammalian primary cilia. *Exp Cell Res* 315:2802-2817.
- Overgaard CE, Sanzone KM, Spiczka KS, Sheff DR, Sandra A, Yeaman C (2009) Deciliation is associated with dramatic remodeling of epithelial cell junctions and surface domains. *Mol Biol Cell* 20:102-113.
- Pazour GJ, Witman GB (2003) The vertebrate cilium is a sensory organelle. *Curr Opin Cell Biol* 15:105-110.
- Piperno G, Fuller MT (1985) Monoclonal antibodies specific for an acetylated form of  $\alpha$ -tubulin recognize the antigen in cilia and flagella from a variety of organisms. *J Cell Biol* 101:2085-2094.
- Piperno G, LeDizet M, Chang X-J (1987) Microtubules containing acetylated  $\alpha$ -tubulin in mammalian cells in culture. *J Cell Biol* 104:289-302.

- Pitot HC, Peraino C, Morse PA Jr, Potter VR (1964) Hepatomas in tissue cultures compared with adapting liver in vivo. *Natl Cancer Inst Monogr* 13:229-245.
- Radford R, Slattery C, Jennings P, Blacque O, Pfaller W, Gmuender H, van Delft J, Ryan MP, McMorrow T (2012) Carcinogens induce loss of the primary cilium in human renal proximal tubular epithelial cells independently of effects on the cell cycle. *Am J Physiol Renal Physiol* 302:F905-F916.
- Reed NA, Cai D, Blasius L, Jih GT, Meyhofer E, Gaertig J, Verhey KJ (2006) Microtubule acetylation promotes kinesin-1 binding and transport. *Current Biol* 16:2166-2172.
- Rutberg M, Billger M, Modig C, Wallin M (1995) Distribution of acetylated tubulin in cultured cells and tissues from the Atlantic cod (*Gadus morhua*). Role of acetylation in cold adaptation and drug stability. *Cell Biol Int* 19:749-758.
- Sadoul K, Wang J, Diagouraga B, Khochbin S (2011) The tale of protein lysine acetylation in the cytoplasm. *J Biomed Biotech* 2011:970382.
- Satir P, Pedersen LB, Christensen ST (2010) The primary cilium at a glance. *J Cell Sci* 123:499-503.
- Schmidt LJ, Ballman KV, Tindall DJ (2007) Inhibition of fatty acid synthase activity in prostate cancer cells by dutasteride. *Prostate* 67:1111-1120.
- Vo NTK, Bender AW, Lee LEJ, Lumsden JS, Lorenzen N, Dixon B, Bols NC (2014) Development of a walleye cell line and use to study the effects of temperature on infection by viral haemorrhagic septicemia virus group IVb. *J Fish Dis* (in press)
- Walss-Bass C, Xi L, David S, Fellous A, Luduena RF (2002) Occurrence of nuclear  $\beta$ -tubulin in cultured cells. *Cell Tissue Res* 308:215-223.
- Ou Y, Ruan Y, Cheng M, Moser JJ, Rattner JB, van der Hoorn FA (2009) Adenylate cyclase regulates elongation of mammalian primary cilia. *Exp Cell Res* 315:2802-2817.
- Wen CM, Wang CS, Chin TC, Cheng ST, Nan FH (2010). Immunochemical and molecular characterization of a novel cell line derived from the brain of *Trachinotus blochii* (Teleostei, Perciformes): A fish cell line with oligodendrocyte progenitor cell and tanyocyte characteristics. *Comp Biochem Physiol A* 156(2):224-31.

- Wheatley DN, Bowser SS (2000) Length control of primary cilia: analysis of monociliate and multiciliate PtK1 cells. *Biol Cell* 92:573-582.
- Wheatley DN, Wang AM, Strugnell GE (1996) Expression of primary cilia in mammalian cells. *Cell Biol Internat* 20:73-81.
- Willemarck N, Rysman E, Brusselmans K, Imschoot GV, Vanherhoydonc F, Moerloose K, Lerut E, Verhoeven G, van Roy F, Vleminckx K, Swinnen JV (2010) Aberrant activation of fatty acid synthesis suppresses primary cilium formation and distorts tissue development. *Cancer Res* 70:9453-9462.
- Wolf KW (1996) Acetylation of  $\alpha$ -tubulin in male meiotic spindles of *Pyrrhocoris apterus*, an insect with holokinetic chromosomes. *Protoplasma* 191:148-157.
- Yuan K, Frolova N, Xie Y, Wang D, Cook L, Kwon YJ, Steg AD, Serra R, Frost AR (2010) Primary cilia are decreased in breast cancer: analysis of a collection of human breast cancer cell lines and tissues. *J Histochem Cytochem* 58:857-870.
- Yeh IT, Luduena RF (2004) The  $\beta_{II}$  isotype of tubulin is present in the cell nuclei of a variety of cancers. *Cell Motility Cytoskel* 57:96-106.
- Zhong M, Zheng K, Chen M, Xiang Y, Jin F, Ma K, Qiu X, Wang Q, Peng T, Kitazato K, Wang Y (2014) Heat-shock protein 90 promotes nuclear transport of herpes simplex virus 1 capsid protein by interacting with acetylated tubulin. *PLOS* 9:e99425.

## **Chapter 8 References**

- Akaike T, Maeda H (2000) Nitric oxide and virus infection. *Immunology* 101:300-308.
- Husain M, Harrod KS (2011) Enhanced acetylation of alpha-tubulin in influenza A virus infected epithelial cells. *FEBS Lett* 585:128-132.
- Reddel RR (2010) Senescence: an antiviral defense that is tumor suppressive? *Carcinogenesis* 31:19-26.
- Ohtani N, Hara E (2013) Roles and mechanisms of cellular senescence. *Cancer Sci* 104:525-530.
- Rodier F, Campisi J (2011) Four faces of cellular senescence. *J Cell Biol* 192:547-556.